ABSTRACT

Title of Document: USE OF DRINKING WATER TREATMENT RESIDUALS AS A SOIL AMENDMENT FOR STORMWATER NUTRIENT TREATMENT

Sean William O'Neill, Master of Science, 2010

Directed By: Professor Allen P. Davis
Department of Civil and Environmental Engineering

Stormwater runoff has been implicated as a major source of excess nutrients to surface waters, contributing to the development of eutrophic conditions. Bioretention, a promising technology for urban stormwater pollution treatment, was investigated to determine if an aluminum-based water treatment residual (WTR) amended bioretention soil media (BSM) could adsorb phosphorus to produce discharge concentrations below 25 μg/L.

Batch, small column, and vegetated column studies were employed to determine both the optimal BSM mixture and media performance. Media tests demonstrated P adsorption proportional to WTR addition. Final selected experimental media consisted of 75% sand, 10% silt, 5.8% clay, 5.2% WTR, and 3.4% bark mulch (air dry mass basis).This media showed excellent P removal relative to a non-WTR-amended media. Whereas the control media leached P (71.1% increase in mass), the experimental media adsorbed 85.7% of the P mass applied, displaying a cumulative effluent EMC of 16.1 μg/L, below the 25 μg/L goal.

USE OF DRINKING WATER TREATMENT RESIDUALS AS A SOIL AMENDMENT FOR STORMWATER NUTRIENT TREATMENT

By

Sean William O'Neill

Thesis submitted to the Faculty of the Graduate School of the
University of Maryland, College Park, in partial fulfillment
of the requirements for the degree of
Master of Science
2010

Advisory Committee:
Professor Allen P. Davis, Chair
Professor Alba Torrents
Assistant Professor Joshua McGrath

For my wife Kristin, without whose love and support

none of this would have been possible

Acknowledgements

Thanks to the Maryland State Highway Administration for their financial support of this project, and a special thanks to Ms. Karen Coffman and Ms. Christie Minami for their input and direction.

I am indebted and ever grateful to my advisor, Dr. Allen Davis, for his guidance and mentorship.

Thanks as well to my other committee members, Drs. Alba Torrents and Joshua McGrath, for their input into this work. I would also like to thank my labmates Dr. Hunho Kim, Jason Becker, Carmen Franks, Poornima Natarajan, and Jennifer Olszewski for their help and for fostering an atmosphere of mutual learning.

Table of Contents

List of Tables

List of Figures

Chapter 1: Introduction

Non-point source pollution continues today to be a challenge that needs addressing by engineers, scientists, and regulators. As land development continues and the size of urban conurbations continues to increase, so do the associated impervious areas such as roads, parking lots, and roofs. Urban stormwater runoff from such areas, and the concomitant flux of pollutants to surface water bodies, is an especially pressing issue that requires attention because of the negative impact pollution from such sources has on receiving water bodies. Low Impact Development (LID) is a development ideology whereby these increases in impervious areas are counterbalanced by providing for on-site green spaces and other areas that attempt to maintain the pre-development hydrology of an area. One LID technology, which also happens to be an EPA Best Management Practice (BMP), that is implemented as a means to reduce runoff pollution discharges is bioretention. Also known as biofiltration or rain gardens, these facilities are effectively shallow depressions filled with sandy media into which runoff is directed (Figure 1-1). This interception of runoff prevents direct stormwater migration to surface waterways, increases groundwater infiltration, and improves water quality.

Although ongoing research concerning the design and performance of bioretention facilities leads to continued improvement, bioretention remains an immature technology with a number of concerns and issues still to be resolved. Prominent among these is the development of a bioretention soil medium (BSM) locally optimized to reach treatment goals, as specifications are inconsistent jurisdictionally. Even within the state of Maryland there is little consensus.

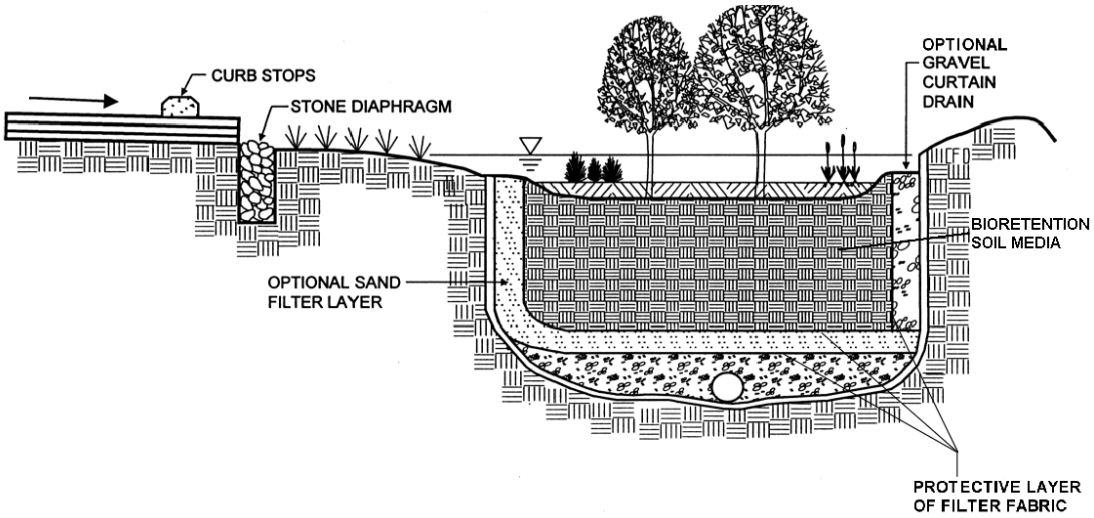

Figure 1-1. Schematic representation of a typical bioretention facility. Adapted from MDE, 2000.

Regardless of the medium employed, previous bioretention research has shown effective removal of suspended solids, oil and grease, and particulate metal species (e.g., Davis et al., 2001; Bratieres et al., 2008). While some work has already been undertaken, a means of improving the highly variable removal of dissolved phosphorus and nitrogen species is still necessary. This is because these nutrients lead to the development of eutrophic conditions in surface waters; when excess nutrients produce explosive growth of photoautotrophic organisms such algae, the death and decomposition of which leads to dissolved oxygen depletion with concomitant negative ecosystem impacts. Eutrophication is estimated to cost the United States over $2.2 billion every year from recreational and drinking water losses, decreased waterfront property values, and expenses related to threatened/endangered species habitat recovery (Dodds et al., 2009).

1.1. Research Goals

In many surface water ecosystems, P is the limiting nutrient (Schindler et al., 2008; Smolders et al., 2010). Therefore, it is believed that eutrophication may be reduced or even eliminated in some systems by effective control of this nutrient. Bioretention may be used as one means of reducing the P load to urban runoff-impacted waters through the development of a BSM to efficiently capture P. Research has shown that traditional BSM performs adequate to poor for P removal from incoming stormwater (Hunt et al., 2006; Bratieres et al., 2008; Li and Davis, 2009). Because P mobility is controlled by Al and Fe species in acidic soils (McGechan and Lewis, 2002), the addition of sufficient Al or Fe to the BSM is expected to produce a media with the ability to adequately remove P from stormwater. This BSM will be a sandy loam, loam, or loamy sand amended with aluminum-based drinking water treatment residual (Al-WTR) and possibly an appropriate organic amendment.

It is hypothesized that Al-WTR will perform ideally in the relatively acidic soil environment of the east coast of the United States (Elliott et al., 2002). Greatly improved P retention capacity in BSM may be provided without compromising media hydraulic conductivity by augmentation with WTR, a byproduct of drinking water treatment. Al-WTR is generated when alum (aluminum sulfate) or a similar compound is added to drinking water as a coagulant. The sulfate and aluminum dissociate in solution and the aluminum forms aluminum (hydr)oxide. Aluminum (hydr)oxide interacts with suspended colloidal material to alter particle net surface charge and mitigate repulsive forces, leading to the formation of flocs which

precipitate from the water column. This settled material, upon removal from the settling tank and dewatering, is classified as WTR. It has a very high potential for P adsorption because of its large amorphous (i.e., poorly crystalline) aluminum (hydr)oxide content.

Many other materials were reviewed as potential BSM amendments, including coal combustion fly ash and steel slag, but were decided to be inappropriate because they operate mainly through Ca-P complexation, which performs optimally in an alkaline environment. Also, iron-based WTR was considered, but rejected because of the scarcity of use in the Baltimore-Washington corridor, as well as the potential for iron to release all adsorbed P under subsurface reducing conditions.

An organic amendment is also necessary as such organic matter imparts important qualities to the medium. While some organic materials may mineralize and release P, others have been noted in the literature to enhance P adsorption (Borggaard et al., 2005; Guan et al., 2006; Kang et al., 2009), probably by serving to retain moisture and prevent crystallization of amorphous metal oxides (i.e., aluminum hydroxide). An organic matter with high carbon content and relatively small amounts of N and P is hypothesized to be ideal for moisture retention without ultimately leading to increased nutrient leaching. Additionally, this material will provide a carbon source for microbiological activity within the bioretention cell, further enhancing stormwater nutrient treatment.

A small but carefully selected group of organic materials including shredded hardwood bark mulch, wood chips, leaf compost, and newspaper was reviewed with respect to their ability to retain soil moisture and the effect of their addition on P

adsorption. Bark mulch was selected as an ideal organic amendment as it was expected to minimally affect P adsorption due to its high C:N:P ratio (see Section 2.4.1). Leaf compost, conversely, should have a very low C:N:P ratio, ultimately causing reduced phosphorus adsorption, and was chosen for investigation to provide a negative control for the effect of organic matter amendments on the P adsorption capacity of BSM.

Development of the enhanced-P BSM progressed in three phases. Initially, P sorption isotherms for mixtures containing various amounts of WTR, sand, and differing organic amendments were derived to determine the optimal component ratio for P capture. Pure aluminum hydroxide was also used as an amendment for comparison purposes. The specific focus for all isotherms was on equilibrium with P at low solution concentration (120 μg/L), because of the low P concentrations typically found in urban stormwater. This differs from the main body of published research in the field of stormwater P capture using soil amendments, which primarily are focused on situations in agriculture subject to much higher P concentrations. These concentrations depend on fertilizer types and application rates, but may be upwards of 3 mg P/L (Sharpley et al., 2003).

Based on the results of the phase 1 isotherm studies, selected mixtures were investigated in small-scale (15.2 cm) sealed upflow columns undergoing continuous flow or intermittent (wet/dry) cycling. The third and final phase involved the selection of an optimal BSM mixture based on Phase 2 results. Performance of this mixture was evaluated in a vegetated mesoscale (0.9 m) gravity-flow column fed a suite of nutrients. Additionally, in an effort to develop BSM performance criteria

with respect to P adsorption capacity, operationally defined amorphous Al and Fe extracts of all media were taken and analyzed for Al, Fe, and P.

Chapter 2: Literature Review

Much work already exists concerning the evaluation of hydrologic and pollutant treatment capabilities of bioretention facilities. Additionally, a large body of work has been published concerned with improving these capabilities through media and configuration adjustments.

2.1. Hydrologic Performance

Contributing toward maintaining or returning a site's hydrology to a predevelopment state through increased infiltration of stormwater is one of bioretention's major advantages. Accordingly, this necessitates media which provides a high hydraulic conductivity (Hsieh and Davis, 2005). Storage is also a benefit of bioretention. Storm events of sufficiently small size may produce no outflow from the system, leading to reduced loading of the receiving waterbodies (Davis, 2008). Through increased infiltration and reduced surface runoff, bioretention as a technology helps to mitigate waterway peak flows by delaying the peak and redistributing the stormwater volume more equally over a given time period. This more closely mimics the behavior of undeveloped land, where water flows are slowed by natural meandering, infiltration, and vegetation, leading to reductions in stream erosion (Davis, 2008).

2.2. Pollutant Removal

2.2.1. Particulates

Excellent removal of particulate and particulate-bound pollutants has been shown, including total suspended solids (TSS); metals such as Pb, Cu, Zn, and Cd; particulate organic nitrogen (PON), and phosphorus (P). TSS has been shown to be

removed predominantly in the surface mulch layer and upper soil profile of bioretention cells (Li and Davis, 2008a; 2008b). Both metals and P, when particulate associated, are captured via the filtration mechanism of the soil and mulch much the same as TSS. In fact, work has shown that effective removal of particulate contaminants takes place in approximately the top 20 cm (8 in) of the bioretention media (Li and Davis, 2008a; 2008b). In this same research, Li and Davis (2008a) recommend a media depth of only 20 to 40 cm (8 to 16 in) to effectively remove particulate-associated pollutants.

2.2.2. Dissolved Species

Capture of dissolved species within bioretention media often depends on adsorption and complexation mechanisms to immobilize pollutants. Dissolved metals are often captured within a bioretention cell when they bind to organic material such as the mulch top dressing and organics within the BSM (Davis et al., 2001).

Dissolved organic nitrogen (DON) and ammonium (NH_4^+) may be removed by adsorption to charged soil particles. However, these compounds are microbially degraded in aerobic environments to the oxidized nitrogen (NOx) species nitrite (NO_2^-) and nitrate (NO_3^-), and may even be produced through breakdown of the organic portion of the BSM. These NOx species are soluble and readily leach through soils (Dietz and Clausen, 2005; Hsieh et al., 2007b; Bratieres et al., 2008). NOx leaching has been prevented through the establishment of effective vegetative cover (Bratieres et al., 2008; Read et al., 2008), and by installing saturated anoxic zones in the media to promote denitrification of NOx to nitrogen gas (Kim et al., 2003; Hunt et al., 2006; Zinger et al., 2007). Additionally, research has shown that

such saturated zones contribute to improved metals retention. They maintain a higher soil moisture content, thereby lessening organic matter (OM) mineralization and soil aggregate drying. This leads to reduced metal loss by preventing the generation and washout of particulate OM and fine soil particle associated metals (Blecken et al., 2009).

Dissolved P, similarly, is often not just uncaptured but may be produced through the degradation of organic material associated with the bioretention media (Hsieh et al., 2007a; Bratieres et al., 2008), leading to inconsistent removal among different facilities. Additional variables may also impact bioretention media performance such as the available media capacity to adsorb P (see Section 2.4.2). Davis et al. (2006) reported effluent TP concentration reductions for two field sites in MD of 65 and 87%. Hunt et al. (2006) reported TP mass loading reductions of 65 and -240% for two field sites in NC. For two sites in Melbourne, Victoria, Australia and McDowell, Queensland, Australia, Hatt et al. (2008) reported TP mass loading reductions by the facilities of -398 and 86%, respectively. These results exemplify the extreme variability in P removal from stormwater by bioretention facilities.

Sufficient vegetative coverage and the selection of appropriate plant species have been found to greatly control P and N mobility through uptake. Significant differences in nutrient uptake have been found among plant species, making selection of utmost importance (Lucas and Greenway, 2007; Read et al., 2008). For instance, Lucas and Greenway observed unvegetated bioretention mesocosoms retaining 14 to 56% of the applied P mass, depending on the media employed. The same experiments conducted with vegetated media displayed P mass retention of 44 to

92%, an increase in retention relative to the unvegetated media of 28 to 36%. Media amendments also have been investigated to promote P capture within facilities. Zhang et al. (2008) investigated the incorporation of coal combustion fly ash into a sand-based BSM (98% sand) for P immobilization. They reported mass load reductions of 66 and 85% for BSM amended with 2.5 and 5% fly ash (air dry mass).

2.3. Pollutant Concentrations

The U.S. EPA Nationwide Urban Runoff Program reported an average urban stormwater concentration of 0.33 mg/L phosphorus (TP), of which 120 μg/L is soluble (SP). This equates to 64% of phosphorus in stormwater being in particulate form (US EPA, 1983). They also reported that stormwater, on average, contains 1.5 mg/L total Kjeldahl nitrogen (TKN) and 0.68 mg/L oxidized nitrogen species (NOx). The Metropolitan Washington Council of Governments (MWCOG) reported ranges for total P and N of 0.10 – 0.66 mg/L and 0.25 – 1.4 mg/L, respectively, in urban stormwater runoff in the Washington area (MWCOG, 1983). Average concentrations of the most commonly found stormwater contaminants are given in Table 2-1.

2.4. Soil-Phosphorus Interactions

Effective P removal within soil systems is a complicated challenge, as there is conflicting evidence of which factors promote and diminish P retention. The primary mechanisms of P capture involve interactions with iron (Fe), aluminum (Al), and calcium (Ca), and these interactions are highly pH dependent. Immobilization in calcareous environments is primarily through (co)precipitation reactions with Ca and Ca-containing compounds like $CaCO_3$ and hydroxyapatite. Primary mechanisms in acidic environments are sorption to Fe and Al (hydr)oxides such as goethite,

Table 2-1. Commonly found urban stormwater contaminants and their average concentrations. Adapted from US EPA, 1983 (U.S. national average) and Duncan, 1999 (Global average).

Contaminant	Average Concentration	
	US EPA, 1983	Duncan, 1999
Total Suspended Solids (mg/L)	80	330
Total P (mg/L)	0.3	0.5
Total N (mg/L)	2.1	2.6
Zinc (Zn; µg/L)	60	430
Copper (Cu; µg/L)	5	100
Nickel (Ni; µg/L)	30	40
Lead (Pb; µg/L)	15	260
Cadmium (Cd; µg/L)	1	7

ferrihydrite, gibbsite, as well as phyllosilicates and other hydroxylated mineral surfaces (Ann et al., 2000; Arai and Sparks, 2007; Zhao et al., 2007). Ann et al. (2000) reported that adsorption to Fe and Al (hydr)oxides is optimal at pH 5.6 to 7.7, while for Ca phosphate precipitation the optimal pH range is 6 to 8.5.

2.4.1. Organic Matter

2.4.1.1. Organophosphorus Release

As mentioned above, OM contains P, the concentration of which varies depending on the specific source. Breakdown of OM is implicated in reduced bioretention performance through increases in leaching of the soluble organic fraction of P (Hsieh et al., 2007a; Bratieres et al., 2008). This occurs as soil microorganisms, plant roots, and mycorrhizae release phosphohydrolase, enzymes that mobilize P to allow for uptake by the organisms. Significant release of organic P (P_o) from soil organic matter (SOM) has been observed to only occur when inorganic P (P_i), such as the predominant orthophosphate [PO_4(-III)] found in runoff, is limited in supply (McGill and Cole, 1981). A very coarse means of determining whether P_o will mineralize from OM or remain immobilized is through the ratio of organic carbon

(org-C) to P_o. When org-C:$P_o \leq 200$, mineralization will occur; when org-C:$P_o \geq 300$, it will not (Dalal, 1977). While this is an imprecise measure, it does allow some quantification for the potential of P_o release from OM in soil and bioretention media.

2.4.2. Competition for and Contribution of Sorption Sites

Dissolved organic matter has been shown to possibly compete with P for sorption sites on Fe and Al compounds in acidic environments, and in this way may reduce P capture in bioretention. Borggaard et al. (2005) observed that P will outcompete OM for $Al(OH)_3$ adsorption sites (as well those of iron (oxyhydr)oxides) if provided with sufficient contact time. Unfortunately, sufficient time was show to be at least 2 days (Borggaard et al., 2005), well beyond the time permitted in bioretention systems. Because of this, mixing order is important. P will control the sorption sites when OM is not present, while if OM and the sorption sites are associated first, it will take time for P to exchange with the OM and become sorbed to the media active sites (Borggaard et al., 2005).

Other research has shown increased rather than competitive P sorption in OM rich soils (Kang et al., 2009). This has been attributed to the formation of metal-OM complexes (Figure 2-1) in the soil that can provide sites for increased P retention. Obviously these results are contradictory with those above, and the matter is still under investigation. Ultimately, evidence suggests that if sorption sites are present in sufficient abundance, there will be no competition and both organic material and P will sorb (Guan et al., 2006).

A statistical path analysis was conducted on soils from North Carolina by Kang et al. (2009). The interactions between P adsorption in the soils and various

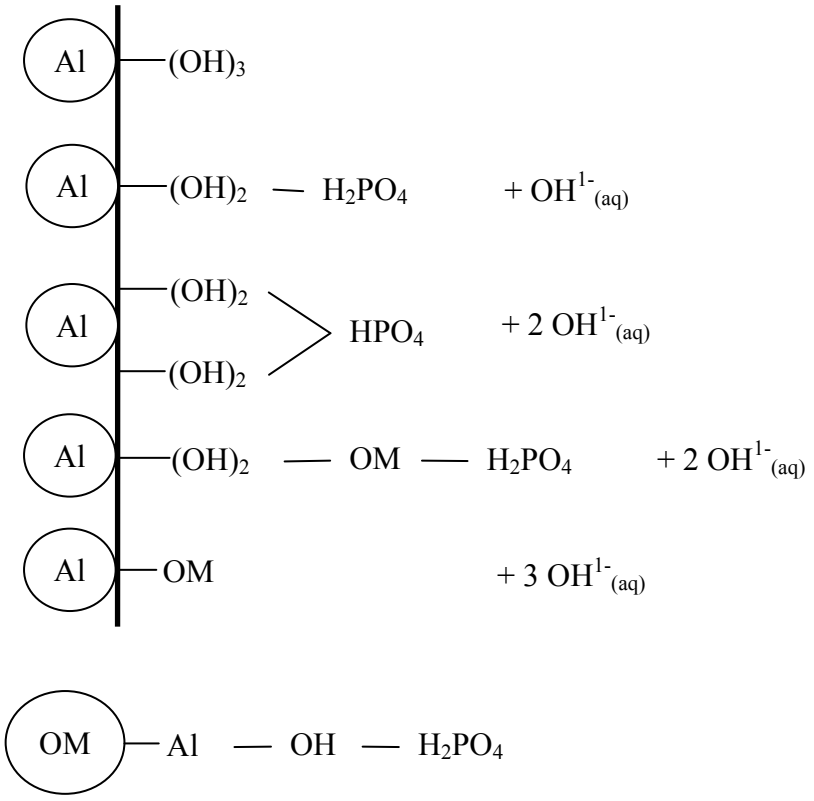

Figure 2-1. Schematic of potential interactions between the Al-WTR surface and inorganic P species in solution. Additionally, interactions may also potentially occur on the surface of OM.

soil parameters, including oxalate-extractable Al (Al_{ox}) and OM contents, were analyzed. Results show a direct effect of Al_{ox} content on P adsorption, and an indirect effect of OM content on P adsorption via Al content. This suggests there is some manner of interaction between Al_{ox} and SOM, resulting in soil P adsorption. Furthermore, their findings show a steep positive correlation between increasing OM content and P adsorption, up to a certain point deemed the change point (Figure 2-2). This change point was observed at approximately 5% OM content. The correlation between P adsorption and OM had a slope one order of magnitude lower when SOM

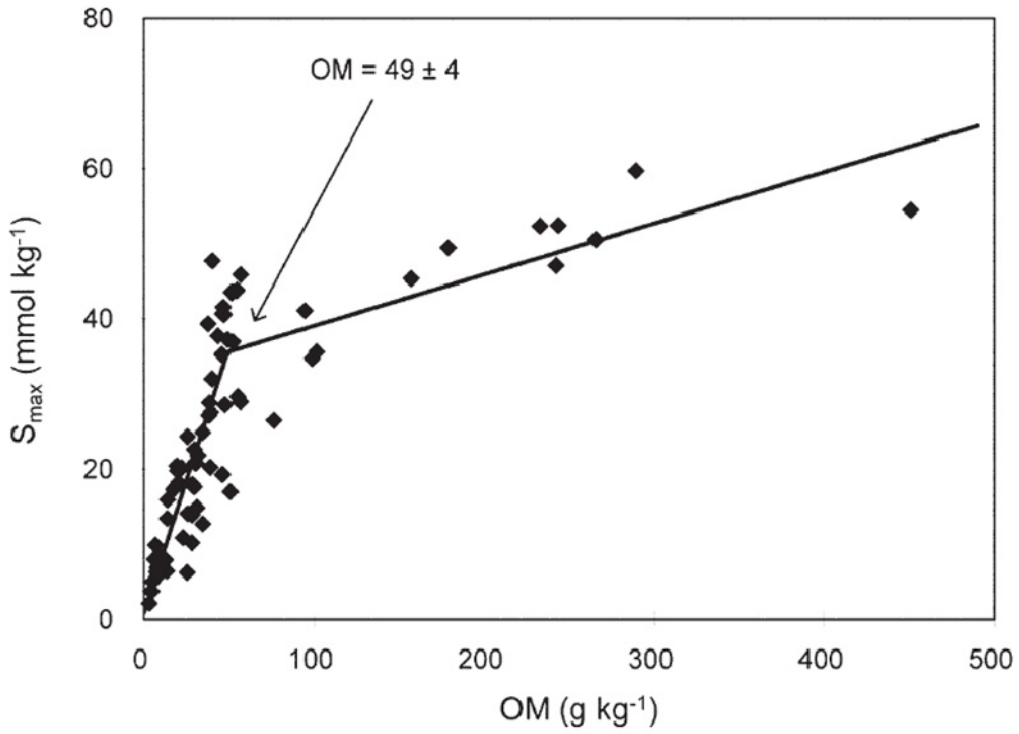

Figure 2-2. Depiction of experimentally determined relationship between soil OM content and S_{max}, the fitted Langmuir isotherm maximum media P adsorption capacity. A change point is evident at approximately 5% OM content. Adapted from Kang et al., 2009.

content was above this change point (greater than 5%), suggesting that beyond this change point the benefit of increased P adsorption provided by increasing OM content is greatly reduced.

2.4.3. Wetting and Drying

Soil drying is another important mechanism for P mobilization. Even minor drying of soils has been shown to dramatically increase the amount of soluble P that may readily leach because of the resultant crystallization of mineral compounds, soil aggregate breakdown, and disruption of clay OM coatings (Worsfold et al. 2005; Styles and Coxon, 2006). However, OM may also play an important role in minimizing P loss through retention of soil moisture. This prevents soil drying and

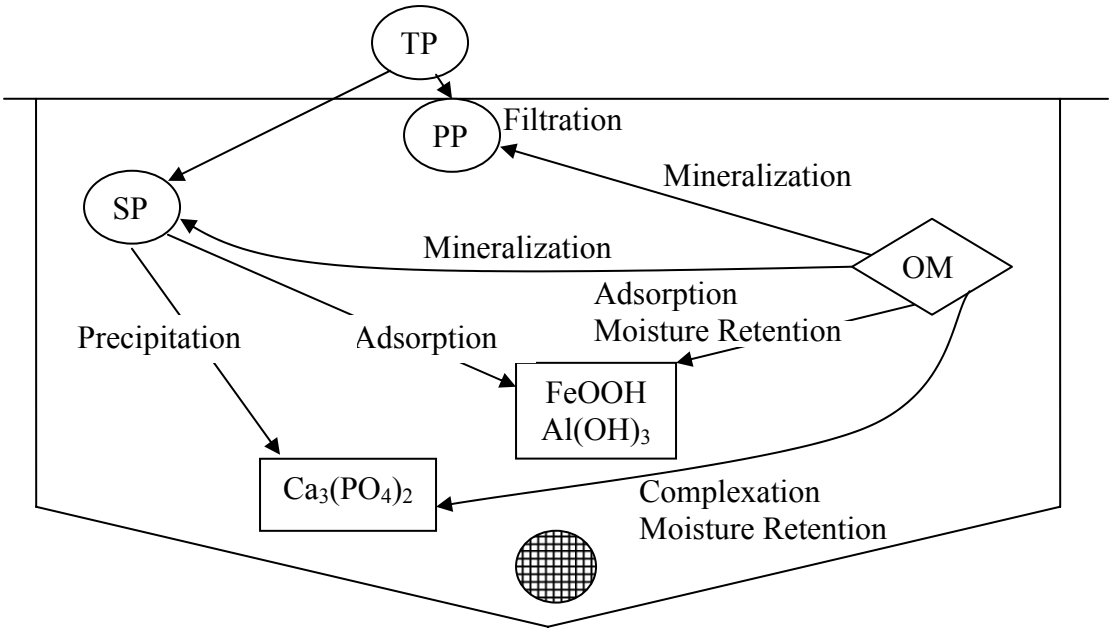

Figure 2-3. Phosphorus interactions in a bioretention cell. TP – total phosphorus, SP – soluble phosphorus, PP – particulate phosphorus, OM – organic matter. $Ca_3(PO_4)_2$, FeOOH, and $Al(OH)_3$ exemplify calcium phosphates, iron (oxyhydr)oxides, and aluminum (hydr)oxides, respectively.

the concomitant crystallization of P-sorbing metal compounds (Borggaard et al., 1990). Amorphous (i.e., poorly crystalline) compounds have a vastly superior ability to bind phosphorus compared to crystallized, attributed to their appreciably larger surface area (Darke and Walbridge, 2000). Therefore OM such as that found within bioretention media and as the surface mulch layer may ultimately lead to greater P retention through increased sorption capacity, brought about by maintaining P complexing compounds in an amorphous state. This OM will also provide a carbon source in the event of saturated conditions, ideally resulting in biological denitrification reactions in the subsurface. A graphical representation of P interactions in a bioretention cell is presented in Figure 2-3.

2.5. Bioretention Soil Media Amendments

2.5.1. Organic Matter

Numerous organic amendments have been used in bioretention facilities, including bark, wood or woodchips, sawdust, peat moss, and leaf mulch/yard waste compost. An important parameter to consider for evaluation of organic matter amendments is the C:N:P ratios of their constituents. These ratios vary greatly among components and depend on the specific species of plant or tree from which the material is derived, as well as the conditions under which it was grown. A compilation of such ratios from relevant literature (Byard et al., 1996; Yarie and Van Cleve, 1996; Antikainen et al., 2004; Beauchamp et al., 2006; Sardans et al., 2008) may be found in Table 2-2. In addition to potentially high labile nutrient content, concerns have been raised regarding the input to soils of toxic pollutants which are incorporated into the OM amendments. For example, some research has shown increased bark heavy metal content from trees grown in areas subject to increased air or soil metal content, such as near metal smelters (Saarela et al., 2005; Baptista et al., 2008). However, the small proportion of OM amended to the total BSM makes the contribution of significant amounts of toxics from such sources highly unlikely.

In general, wood based organics such as bark have a higher C:N:P ratio than that of many other organic materials as they contain less N and P per unit of C, as shown in Table 2-2. A high C:N:P ratio for an organic amendment is theorized to be desirable, as it will minimize the mass of added N and P and reduce the potential for their mineralization and possible leaching from the organic matter. Making the assumption that 50% of the total C reported in Table 2-2 is organic, and all of the P is organic, org-C:P_o ratios can be determined. Only one material, birch leaves, reported

Table 2-2. C:N:P ratios of various organic amendments on a molar basis. All reported C contents ranged from 45.0 – 50.4% (w/w). Therefore, C content was estimated to be 47% (w/w) and ratio calculated accordingly when not reported in the references. †: C content estimated as 47% (w/w), ×: Data not reported. References: [1] Beauchamp et al., 2006; [2] Antikainen et al., 2004; [3] Sardans et al., 2008; [4] Byard et al., 1996; [5] Yarie and Van Cleve, 1996. Data from [5] calculated from the average of all control samples across all sample years.

Bark	C	N	P
Fresh [1]	6587 †	26.5	1
Young [1]	6771 †	29.8	1
Light brown [1]	5611 †	36.9	1
Brown [1]	7215 †	49.3	1
Black [1]	12243 †	77.7	1
Pine [2]	2020 †	14.7	1
Spruce [2]	2204 †	19.3	1
Birch [2]	2424 †	20.8	1
Aspen [2]	2020 †	34.6	1
Eucalyptus [2]	404 †	3.17	1
Wood			
Pine [2]	22037 †	24.1	1
Spruce [2]	12121 †	17.7	1
Birch [2]	12121 †	17.7	1
Aspen [2]	13467 †	4.91	1
Eucalyptus [2]	3910 †	7.85	1
Quercus ilex L. [3]	611	6.53	1
Phillyrea latifolia [3]	3022	13.7	1
Arbutus unedo L. [3]	2112	10.7	1
Sawdust [5]	4198	10	×

Leaves	C	N	P
Quercus ilex L. [3]	1145	26.3	1
Phillyrea latifolia [3]	1029	21.6	1
Arbutus unedo L. [3]	949	19.8	1
Strypnodendron microstachyum [4]	577 †	20.4	1
Callophylum brasiliense [4]	1347 †	26.8	1
Jacaranda copaia [4]	673 †	20.9	1
Vochysia guatemalensis [4]	866 †	22.6	1
Birch [5]	362	12.3	1
Aspen [5]	557	18.8	1
Poplar [5]	725	20.3	1
Alder [5]	869	38.1	1
White Spruce [5]	871	14.4	1
Leaf Litter			
Quercus ilex L. [3]	1576	28.0	1
Phillyrea latifolia [3]	1573	23.4	1
Arbutus unedo L. [3]	2058	22.2	1

an org-C:P_o ratio < 200 (org-C:P_o 181). Three others reported indeterminate ratios between 200 and 300. *Strypnodendron microstachyum* leaves had a ratio of 289, aspen leaves had a ratio of 278, and eucalyptus bark had a ratio of 202. This gives

some indication that OM amendments produced from sources like leaves, such as leaf and yard waste compost, may be at greater risk for mineralization of P_o compared to those make from bark or wood, such as bark mulch.

2.5.2. Aluminum-based Drinking Water Treatment Residual

2.5.2.1. Mechanisms of Action

Al-WTR is a byproduct of alum addition for the removal of colloidal material during the drinking water treatment process (see Section 1.1). Because of this, Al-WTR contains large amounts of Al (hydr)oxides, adsorbing P through mono and/or bidentate ligand exchange mechanisms (Figure 2-1; Goldberg and Sposito, 1985; Stumm and Morgan, 1996). This has been verified through measured release of hydroxide and other ions after P adsorption (Goldberg and Sposito, 1985; Yang et al., 2006). Yang et al. (2006), upon investigating an Al-WTR, observed ligand exchange between P and OH^-, Cl^-, SO_4^{2-}, and humic substances (OM); as well as additional releases of Cl^-, SO_4^{2-}, and OM due to dissolution and hydrolysis.

As stated in Section 2, such sorption mechanisms with Al predominate in acidic environments and are dependent on pH. Results from Agyin-Birikorang and O'Connor (2007) indicate that soil amended with Al-WTR show maximized P adsorption at pH 4 within an investigated range of 3 through 9. Yang et al. (2006) investigated the effects of pH on P adsorption to an Al-WTR in the range of 4.3 to 9 and found a decline in adsorption as pH increased, with this decline greatly increasing above pH 6. These studies correspond well with the known zero point of charge (pH_{zpc}) and solubility of $Al(OH)_3$, whereby surface charge becomes positive at approximately pH 9 and shows a continued positive increase with decreasing pH until approximately pH 4.0, below which hydroxylated Al is no longer the

thermodynamically preferential form but rather free Al (Al^{3+}) is (Stumm and Morgan, 1996).

2.5.2.2. Al Toxicity

Al is a heavy metal toxic to both aquatic and terrestrial organisms in sufficient quantities. As such, there is reasonable concern over potential leaching of elemental Al from Al-WTR when used as a BSM amendment. $Al(OH)_3$, the dominant Al species in Al-WTR is sparingly soluble at approximately $4 \leq pH \leq 11$, with greatly increasing solubility beyond these pH values (Figure 2-4). Natural soils tend to maintain $pH \geq 5$ because of their buffering capacity, and urban stormwater has a circumneutral pH due to the buffering capacity of impervious surfaces such as concrete. Because of this, the pH of any bioretention system is expected to maintain a pH well within the pH range of $Al(OH)_3$ insolubility, and significant Al(III) will not be released to solution except under very extreme conditions.

Numerous studies have investigated the impacts of Al-WTR application on crops, which gives an indication of the impact of Al-WTR on a bioretention system. Many have reported increased soil Al concentrations, and some have reported increased plant Al concentrations, although this appears to depend on the plant species (e.g., Mahdy et al., 2009; Oladeji et al., 2009). Mahdy et al. (2009) reported increased plant Al concentrations, but noted they remained well below the level which could be harmful if ingested (200 – 1000 mg/kg). No indications of Al

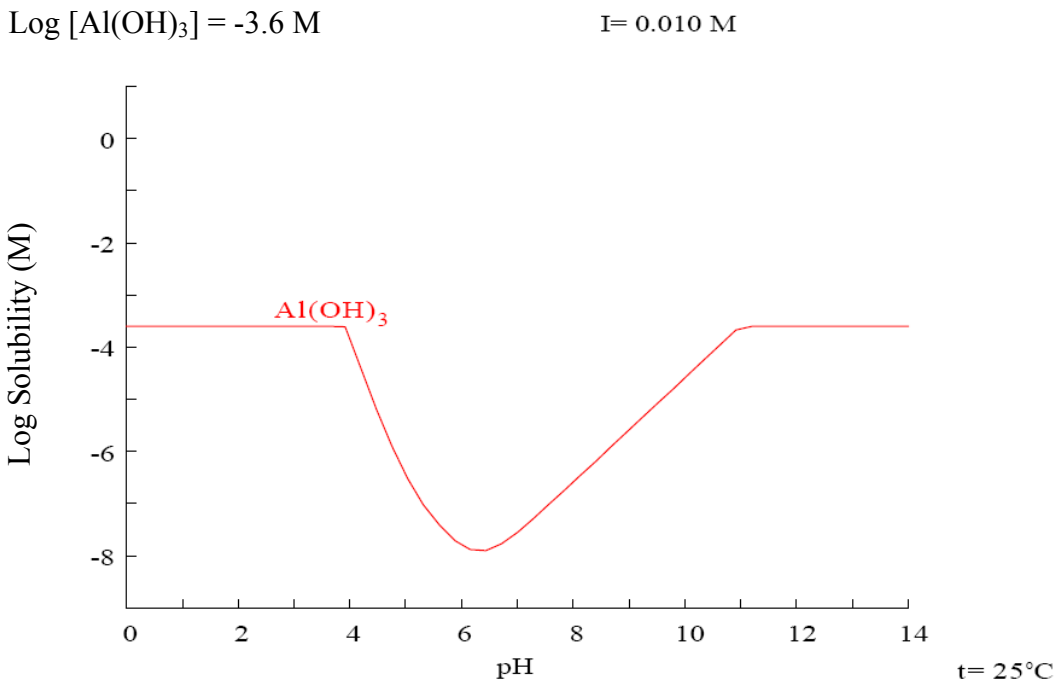

Figure 2-4. Solubility diagram of aluminum hydroxide. Generated using HYDRA/MEDUSA, KTH Royal Institute of Technology, Stockholm, Sweden.

phytotoxicity were reported, but in many cases crop yields were negatively correlated with increasing WTR application rates (Oladeji et al., 2007; Mahdy et al., 2009; Oladeji et al., 2009). This is likely the result of a plant available P deficiency (Lombi et al., 2010). Additionally, Sotero-Santos et al. (2005) investigated the toxicity of Al-WTR using *Daphnia similis* as a bioassay. They found no acute toxicity and minimal impacts on *Daphnia* fecundity, suggesting little Al toxicity of WTR at the investigated pH (7.0-7.3).

While soils applied with Al-WTR have been observed with slightly elevated Al contents, the greatest concern involved mobilization of elemental Al from the WTR. Agyin-Birikorang et al. (2009) investigated Al leaching from Al-WTR treated field plots at various depths. While measurable concentrations of Al were found in

the groundwater, they were not significantly different between control and experimental (Al-WTR applied) plots. Summarily, the reported Al concentrations in experimental plots were 70 – 120 μg/L in shallow wells and 140 – 250 μg/L in deep wells, vis-à-vis concentrations in control plots of 70 – 110 μg /L in shallow wells and 170 – 210 μg/L in deep wells.

Chapter 3: Materials and Methodology

Initial P batch studies for determination of adsorption isotherms were conducted to determine adsorption properties of various BSM mixtures, which allowed prediction of adsorption behavior under various conditions and were ultimately used to determine the best performing BSM at this stage. The most promising mixtures investigated were then used in small column studies receiving a P solution to determine their adsorption behavior under dynamic flow conditions. Mixture performance could be verified with these studies and adequate hydraulic conductivity of the media estimated. Performance under wet/dry cycling (i.e., intermittent flow) was also investigated at this stage in an attempt to better simulate actual bioretention conditions. Larger, vegetated columns were then studied using a mixture based on that which was the best performing to date. These larger columns received a complete suite of pollutants, including orthophosphate, ammonium, nitrogen oxides, and organic nitrogen as glycine to determine BSM performance for nutrient pollutant removal. Plant survival was observed to determine possible toxicity or other negative effects of WTR addition. Effluent samples were also analyzed for potential leaching of free aluminum, as this metal is toxic to many aquatic and terrestrial organisms in sufficient concentrations. All mixtures and BSM components were subjected to acid ammonium oxalate extraction and analyzed for oxalate-extractable P, Al, and Fe content. These data were compiled for use as a measure to determine P adsorption potential for BSM mixtures.

3.1. Media Performance Benchmark

Performances of all media were measured against a target adsorption of 34 mg/kg (oven dry mass basis) soluble P. This adsorption benchmark was calculated as:

$$\frac{V_{P,1} \cdot C_{SP} \cdot t}{V_C \cdot \rho} \tag{3-1}$$

where $V_{P,1}$ is the volume of precipitation per annum, C_{SP} is the concentration of soluble P, t is time, V_C is the volume of the bioretention cell, and ρ is the bioretention media bulk density. The Washington Metropolitan Area receives approximately 102 cm (40 in) of rain per year, and the average stormwater soluble P concentration is 120 µg P/L (US EPA, 1983; Bratieres et al., 2008). The media adsorption benchmark was determined for a bioretention facility sized at 5% of catchment area and having 20 years capacity. Therefore, a BSM mixture must be able to adsorb at least 34 mg_P/kg_{media} at 120 µg/L soluble P to provide the necessary stormwater treatment.

3.2. Media Characterization

3.2.1. Bioretention Soil Media and Al-WTR

BSM was obtained pre-mixed from a local landscape supplier and passed through a 2-mm sieve. A sample was sent to the University of Delaware Soil Testing Program for particle size analysis. The media contained 77% sand, 14% silt, and 8% clay, and was classified as a sandy loam per USDA soil texture classification. The media was stored in water tight containers, and before use was air dried for at least 1 week. Loss on ignition at 550°C (LOI), a measure of OM content, measured 2.1%. pH was measured with a pH meter (Mettler Toledo MA235) using a glass electrode probe. A mixture of air dried BSM and deionized water (1:2 w/v) resulted in a pH measured as 6.0. A conductance probe (YSI Model 35) measured the electrical

Table 3-1. Media component characteristics. EC: electrical conductance; WC: water content; OM: Organic matter; BSM: bioretention soil media; WTR: water treatment residual; HBM: hardwood bark mulch; LC: leaf compost; †: Data reported by manufacturer; ×: Data not collected.

	pH		EC (mmohs/cm)		WC [moist] (%)		WC [air dry] (%)		OM (%)	
	Avg.	**S.D.**	**Avg.**	**S.D.**	**Avg.**	**S.D.**	**Avg.**	**S.D.**	**Avg.**	**S.D.**
BSM	**6.03**	**(0.20)**	**0.79**	**(0.04)**	**8.19**	**(0.28)**	**0.64**	**(0.11)**	**2.11**	**(0.32)**
WTR	**7.53**	**(0.04)**	**1.35**	**(0.05)**	**85.9**	**(0.24)**	**42.6**	**(0.44)**	**36.4**	**(3.35)**
HBM	**6.90**	**(0.03)**	**0.20**	**(0.02)**	**49.9**	**(6.33)**	**6.22**	**(0.93)**	**74.5**	**(6.90)**
LC	×	×	×	×	**57.1**	**(0.93)**	×	×	**47.1**	**(1.79)**
Sand	**6.5** †	×	×	×	**0**	**(0)**	×	×	**0.19**	**(0.04)**

conductance (EC) of a deionized water saturated media paste (1:1 w/v) as 0.8 mmohs/cm (Table 3-1).

Al-WTR was secured from the Rockville Drinking Water Treatment Plant in Potomac, MD. Until use it was stored in water tight covered containers to retain moisture. The work of Yang et al. (2008) showed that the phosphorus adsorption capacity of Al-WTR stored in such containers is not affected by ageing for at least 18 months, and so the material used is expected to be representative of fresh Al-WTR. Agyin-Birikorang and O'Connor (2009) came to a similar conclusion with regard to the effect of ageing on WTR 0.2 M acid ammonium oxalate extractable P, Fe, and Al contents. Prior to use as a BSM amendment, the WTR was crushed by hand, sieved < 2 mm, and then air dried for at least 1 week. WTR LOI was measured 36.4%. The high organic matter content of the WTR is somewhat misleading, as this is not representative of typical surface water OM content. It is believed to have two causes: additionally released water from hydrous oxides upon ignition (Elliott et al., 2002); and the use of a nonionic organic polymer (Praestol N3100 LTR; Ashland, Inc.) in the drinking water coagulation process (Vern Simmons, Rockville Drinking Water

Treatment Plant, personal communication). The pH of a 1:2 (w/v) water:media mixture measured was 7.5. EC of a saturated paste (1:2 w/v) measured 1.4 mmohs/cm (Table 3-1).

3.2.2. Low-fines BSM

Influence of clay content on P adsorption was investigated by the addition of sand to the BSM to reduce the net fines (silt and clay) content. Concurrently, this also provided an estimation of the performance of a media mixture of a different textural class. The BSM was amended with angular, white quartz sand (Mystic White® II, U.S. Silica Co.). This produced a media textural profile of 85% sand, 10% silt, and 5% clay; rated as a loamy sand per the USDA soil textural classification. Organic content was measured via LOI as 1.6%, and the pH was 6.2 as calculated from a mass weighted average of the sand and BSM pH values. Henceforth, this media mixture is referred to as low-fines bioretention soil media (LFBSM).

3.2.3. Organic Matter Amendments

The WTR amended BSM was further amended with organic material to investigate its effects on media P adsorption capacity. The investigated materials were triple-shredded hardwood bark mulch (HBM) and leaf and yard waste compost (LC). The HBM was purchased from a local landscaping supply company in the Washington, DC area, and the LC was obtained from the College Park, MD Department of Public Works and is their screened Smartleaf® Compost. The pH (1:4 w/v) and EC (1:4 w/v saturated paste) of HBM was found to be 6.9 and 0.2 mmohs/cm, respectively. HBM was 74.5% OM and LC was 47.1% OM as measured by LOI (Table 3-1).

3.2.4. Aluminum Hydroxide

Aluminum hydroxide [$Al(OH)_3$] was synthesized and used as an amendment to provide a comparison between the effectiveness of Al-WTR and pure $Al(OH)_3$ in terms of P adsorption. $Al(OH)_3$ was synthesized by mixing aluminum sulfate ($Al_2(SO_4)_3 \cdot 14\ H_2O$; Fisher Scientific) and NaOH (Fisher Scientific) in a molar ratio of 1:3 Al:OH. Both compounds were mixed in deionized water under vigorous stirring for 1 hour, allowed to settle for 1 hour, and then the pH was adjusted to approximately 7 with HCl. After pH adjustment, the solution was centrifuged at 4200 rpm for 10 minutes. The supernatant was than decanted and the pellet filtered and collected on a glass fiber filter (Whatman No. 40) under vacuum. It was washed three times with ethanol and once with acetone to remove excess sulfate and sodium ions, and air dried overnight (Borggaard et al., 2005).

3.3. Phosphorus Adsorption Isotherms

P isotherms were determined for unamended BSM as well as BSM amended with Al-WTR, triple-shredded hardwood bark mulch (HBM), yard and leaf waste compost (LC), quartz sand, and/or pure aluminum hydroxide ($Al(OH)_3$), using a modified method based on that reported by Nair et al. (1984). In this study, NaH_2PO_4 was used to make 0.3, 0.9, 3.0, and 9.0 mg/L P solutions with a 0.01 M KCl background electrolyte concentration. Isotherms were prepared as follows: 1.8 g of media mixture was weighed and placed in each of 5 centrifuge tubes of 50 mL volume. To these was added 45 mL P solution, for a media:solution ratio of 1:25 (w/v). A sixth centrifuge tube containing no media, but 45 mL of appropriate P solution was carried through all procedures with the samples as a control. Each media mixture had phosphorus solution addition at concentrations of 0.3, 0.9, and 3.0

mg P/L as NaH_2PO_4. In addition, any mixture containing 10% WTR (air dry mass basis) underwent addition of 9.0 mg P/L as NaH_2PO_4, and these data were included in the isotherm. Due to the high adsorption capacity of the mixture, this was necessary to extend the isotherm and provide for comparison of all treatments.

For each treatment and P solution addition, investigation was then undertaken to observe the effects of varying pH on P adsorption. Three samples were acidified to approximately pH 4.00, 4.25, and 4.50 using 0.05 – 0.2 mL 0.1 M HCl, and to one sample 0.05 – 0.1 mL 0.1 M NaOH was added to produce a pH of approximately 7.5 to 8.5. The final sample as well as the control underwent no pH adjustment. Samples were then shaken on an end-over-end shaker for 24 hours, after which they were centrifuged at 2000 rpm for 13 minutes and the supernatant decanted and filtered through a 0.22 μm membrane filter. Final pH was measured and then the samples were analyzed for soluble reactive phosphorus (SRP) by the ascorbic acid molybdenum blue method (4500-P E) as presented in Standard Methods (APHA, 1992). A 5 cm pathlength cuvette was employed to provide a detection limit of 0.01 mg/L P. The final data were fitted with Freundlich isotherms using nonlinear regression in Microsoft® Excel®. Freundlich isotherms are of the form:

$$q = K \cdot C^{1/n} \tag{3-2}$$

where C is the equilibrium P concentration in solution (mg/L), q is the equilibrium media adsorption capacity (mg/kg), and both K and n are fitting constants. The value of q is calculated as the difference between the initial and final P solution concentrations normalized by the media mass (oven dry mass).

Adjustments to the method proposed by Nair et al. (1984) include the use of KCl as the background electrolyte, as well as the decision to use a media mass of 1.8 g and 45 mL P solution instead of 1 g and 25 mL, respectively. It was decided not to use $CaCl_2$ as a background electrolyte as the method recommends because at the higher pH values encountered in these analyses the precipitation of calcium phosphates may result, which would misrepresent the phosphorus adsorption capacity of the media. Also, alterations in the sample mass, solution volume, and consequently the equilibration vessel headspace, stemmed from the use of a 5 cm pathlength cuvette for spectrophotometric P concentration determination. It was desired to maximize sorption characterization ability, and so the lowest detection limit was necessary. Because of the large volume of the cuvette, a larger volume of solution (45 mL) was necessary. To maintain the desired soil:solution ratio, 1.8 g media was used.

Phosphorus adsorption isotherms were determined for BSM and BSM amended with 2, 4, and 10% Al-WTR on an air dried mass basis (1.2, 2.4, and 6.0% WTR on an oven dried mass basis, respectively; Tables 3-2 and 3-3). Amended BSM mixtures were prepared by weighing the necessary amounts of BSM, WTR, and any other amendments, placing together in a sealed bag, and homogenizing through vigorous shaking**.**

LFBSM P adsorption isotherms were also determined. LFBSM, in contrast to BSM, was amended with Al-WTR at rates of 0 (unamended), 3, 6, and 10% WTR on an air dried mass basis (0, 1.8, 3.5, and 6.0% WTR on an oven dried mass basis, respectively; Table 3-2).

Table 3-2. Composition of investigated bioretention media. BSM: bioretention soil media; WTR: water treatment residual; HBM: hardwood bark mulch; LC: leaf compost; LFBSM: low-fines BSM; AH: aluminum hydroxide; †: Air dry mass; ‡: Field moist weight; *: Percent weight of $Al(OH)_3$, analogous to 0.5% WTR with respect to amorphous Al content.

Media	BSM † (%)			WTR † (%)	HBM/LC ‡ (%)
	Sand	Silt	Clay		
BSM	100			0	0
	77.3	14.4	8.30		
BSM + 2% WTR	98.0			2	0
	75.8	14.1	8.13		
BSM + 4% WTR	96.0			4	0
	74.2	13.8	7.97		
BSM + 10% WTR	90.0			10	0
	69.6	13.0	7.47		
LFBSM	100			0	0
	85.2	9.40	5.40		
LFBSM + 3% WTR	97.0			3	0
	82.6	9.12	5.24		
LFBSM + 4% WTR	96.0			4	0
	81.8	9.02	5.18		
LFBSM + 6% WTR	94.0			6	0
	80.1	8.84	5.08		
LFBSM + 10% WTR	90.0			10	0
	76.7	8.46	4.86		
BSM + HBM	94.2			0	5.84
	72.8	13.6	7.82		
BSM + 2% WTR + HBM	92.3			1.88	5.84
	71.3	13.3	7.66		
BSM + 4% WTR + HBM	90.4			3.77	5.84
	69.9	13.0	7.50		
BSM + LC	88.5			0	11.5
	68.4	12.7	7.35		
BSM + 4% WTR + LC	85.6			2.95	11.5
	66.1	12.3	7.10		
BSM + 4% WTR + LC [OM+]	71.0			2.95	26.1
	54.8	10.2	5.89		
Sand + 4% WTR	96.0			4	0
	96.0	0	0		
BSM + 0.5% AH	99.9			0.12*	0
	77.2	14.4	8.29		

HBM was amended to media containing 0, 2, and 4% WTR (air dry mass; Table 3-2). For LC, amendments were made only to 0 and 4% WTR media (Table 3-2). Additionally, 4% WTR amended BSM was augmented with an increased mass of LC to further investigate the negative effects of LC on P adsorption, termed the OM+ treatment (Table 3-2).

The organic amendments provided increased OM to the BSM, as did the WTR. Because of the high measured OM content of the WTR, noticeable increases in BSM OM content were observed with increasing WTR content. Therefore, it was decided to amend all media treatments with an equal proportion of organic material (either mulch or compost). In accordance with the findings of Kang et al. (2009) who showed greatly diminished improvement in soil P adsorption when SOM exceeded 5%, it was decided to amend treatments with the mass necessary to produce 5% OM content in the 2% WTR amended treatment. The organic amendments were mechanically shredded and sieved < 2 mm, then added at field moisture (49.9% and 56.5% water content for HBM and LC, respectively) to air dried WTR amended BSM (BSM+WTR) at a ratio of 1:16.1 (w/w) HBM:(WTR+BSM) and 1:7.7 (w/w) LC:(WTR+BSM). For the LC OM+ mixture, LC addition occurred at approximately 2.5 times the mass with which other mixtures were amended, having a ratio of addition of 1:2.8 (w/w) LC:(WTR+BSM).. Organic amendments were added at field moisture vis-à-vis air dried mass to prevent uncharacteristic P leaching that would result upon rewetting, similar to the release of additional P from the mineralization of SOM upon rewetting (Worsfold et al., 2005; Styles and Coxon, 2006). The addition of the organic amendments to WTR-amended BSM resulted in a net reduction in

Table 3-3. Aluminum based water treatment residual (WTR) and organic matter (OM) content of investigated BSM mixtures during batch studies. † : Per air dry mass basis; ‡ : Per oven dry mass basis; * : Measured by loss on ignition at 550°C.

Organic Material Amendment	**WTR Content (%)†**				
	0	2	4	4 [OM+]	10
None					
% WTR‡	-	1.2	2.4	×	6.0
% OM*	2.2	2.7	3.1	×	4.5
Hardwood Bark Mulch					
% WTR‡	-	1.1	2.3	×	×
% Bark Mulch‡	3.2	3.2	3.2	×	×
% OM*	5.6	4.0	5.7	×	×
Leaf Compost					
% WTR‡	-	×	1.9	1.9	×
% Leaf Compost‡	5.2	×	5.3	12.0	×
% OM*	4.6	×	5.4	8.8	×

WTR content, but this was minimal (≤ 0.5% gross change in WTR content of the mixtures on an oven dry mass basis). Tables 3-2 and 3-3 detail the proportions of constituents in the majority of mixtures investigated in this study on an air dry mass and oven dry mass basis, respectively.

For $Al(OH)_3$-amended mixtures, the oxalate-extractable (i.e., amorphous) aluminum content of the constituents and mixes were investigated, as described in Section 3.6. With this information, $Al(OH)_3$ was amended to BSM at a rate analogous to the amorphous Al content of 0.5%, 2% and 4% WTR, utilizing the assumptions that the $Al(OH)_3$ did not include any significant impurities, and was completely amorphous. These mixes are referred to hereafter as 0.5%, 2%, and 4% AH, respectively. In actuality, the mixes were 0.12%, 0.50%, and 0.98% $Al(OH)_3$ on an air dry mass basis, respectively.

3.4. Minicolumn Adsorption Experiment

Adsorption studies using small sealed upflow columns were conducted to investigate the behavior and P adsorption capabilities of the various media mixes.

3.4.1. Column Setup

Columns were constructed as detailed in Figure 3-1. A 15.2 cm (6 in.) tall, 2.5 cm (1 in.) inner diameter (5.07 cm^2 cross-sectional area) Plexiglass cylinder was attached to a base chamber. The cylinder and base chamber were separated by a base plate containing drilled holes, and was overlaid with a metal screen intended to prevent media movement into the base chamber. Influent was pumped horizontally into the base chamber and redirected vertically through the base plate to evenly distribute flow radially throughout the column.

During installation, the media was allowed to naturally settle within the column by slowly filling the column with deionized water as the media was being placed. This allowed the particles to settle before sealing the column and helped to remove possible air bubbles. Prior to placement in the column, media was manually homogenized through vigorous shaking and stirring with a laboratory spatula. Media was placed in the column to a height of 12.0 cm (4.73 in.) and then a 1.0 cm (0.39 in.) washed quartz sand layer was placed on top to prevent washout of fines. This provided for a total bed volume of 66.0 mL. A rubber stopper with an outlet port was inserted 2.22 cm (0.88 in.) into the top of the column and sealed using silicone and epoxy. A small metal mesh screen was installed in the column stopper to further prevent the washout of material.

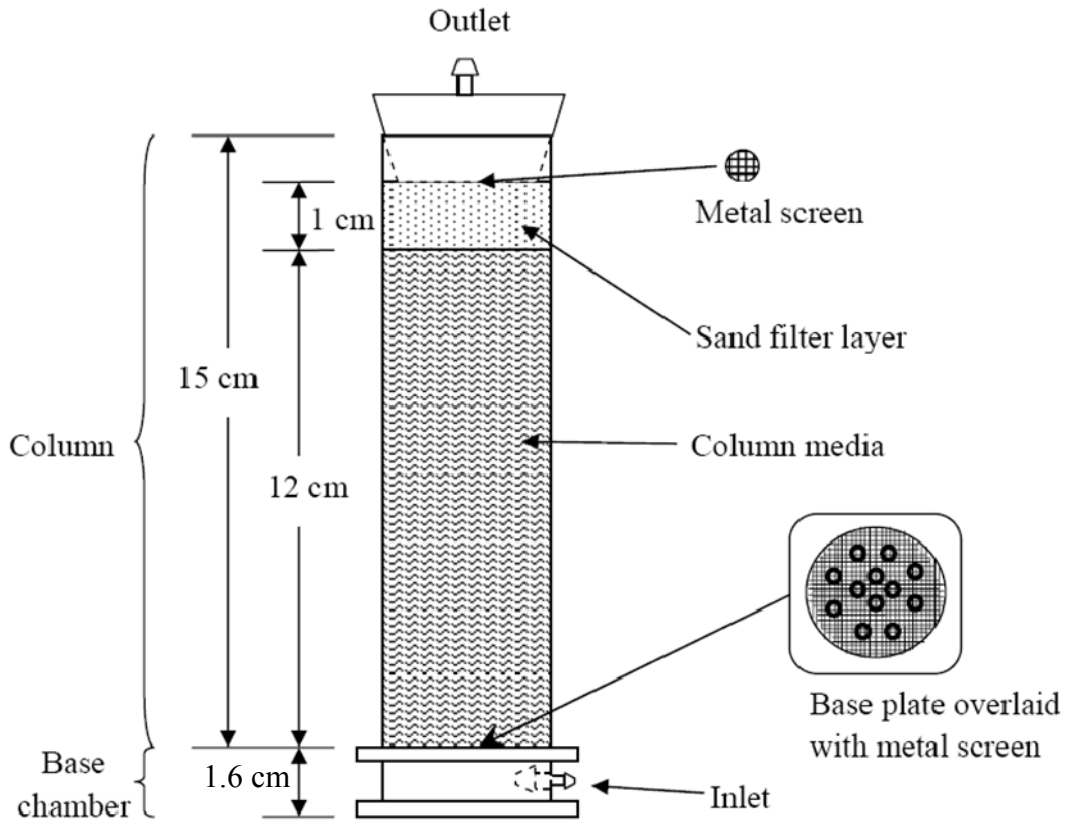

Figure 3-1. Upflow column schematic for minicolumns.

3.4.2. Media, Influent, and Flow Characteristics

Column experiments were initiated with six different media or flow characteristics at a time (Table 3-4). All media had been previously investigated to determine batch adsorption isotherms with the exception of the LFBSM + 4% WTR and Sand + 4% WTR mixes. 4% WTR was chosen in both cases to maintain a constant proportion of WTR among all columns. After LFBSM amended with WTR produced greater P adsorption in both batch and column studies, a column of the same washed quartz sand used as a filter layer was amended with WTR to further investigate the effect of reduced fines content on WTR P adsorption.

Table 3-4. Media and flow regimes for minicolumn experimental groups I and II. BSM: bioretention soil media; WTR: water treatment residual; HBM: hardwood bark mulch; LFBSM: low-fines BSM

Experimental Group	Column Media	Flow Regime
1	Unamended BSM	Continuous
	BSM + 2% WTR	Continuous
	BSM + 4% WTR	Continuous
	BSM + HBM + 2% WTR	Continuous
	BSM + HBM + 4% WTR	Continuous
	LFBSM + 4% WTR	Continuous
2	Unamended BSM	Continuous
	BSM + 4% WTR	Continuous
	Sand + 4% WTR	Continuous
	BSM + HBM + 4% WTR	Intermittent
	BSM + 4% WTR	Intermittent
	LFBSM + 4% WTR	Intermittent

Two experimental groups of six columns each were tested, for a total of twelve column experiments. Select experiments were duplicated to verify results. Influent solution was pumped into each column via a peristaltic pump from a continuously stirred influent batch to assure homogeneity. Two continuously stirred influent tanks were used and connected in series through a siphon, providing at total batch volume of 38 L when full. Column flowrates were calibrated by using a stopwatch to time the duration to fill a 5 mL volumetric flask. Each column was individually calibrated to within 5% of the desired flowrate. Figure 3-2 depicts the experimental setup.

Influent for the experiment was a solution of 120 μg/L dissolved P, using NaH_2PO_4, and 0.01 M KCl as a background electrolyte. 1 N NaOH was added to the solution to adjust the pH to approximately 7. Over the course of the column experiments, column flowrates were systematically increased in an attempt to force

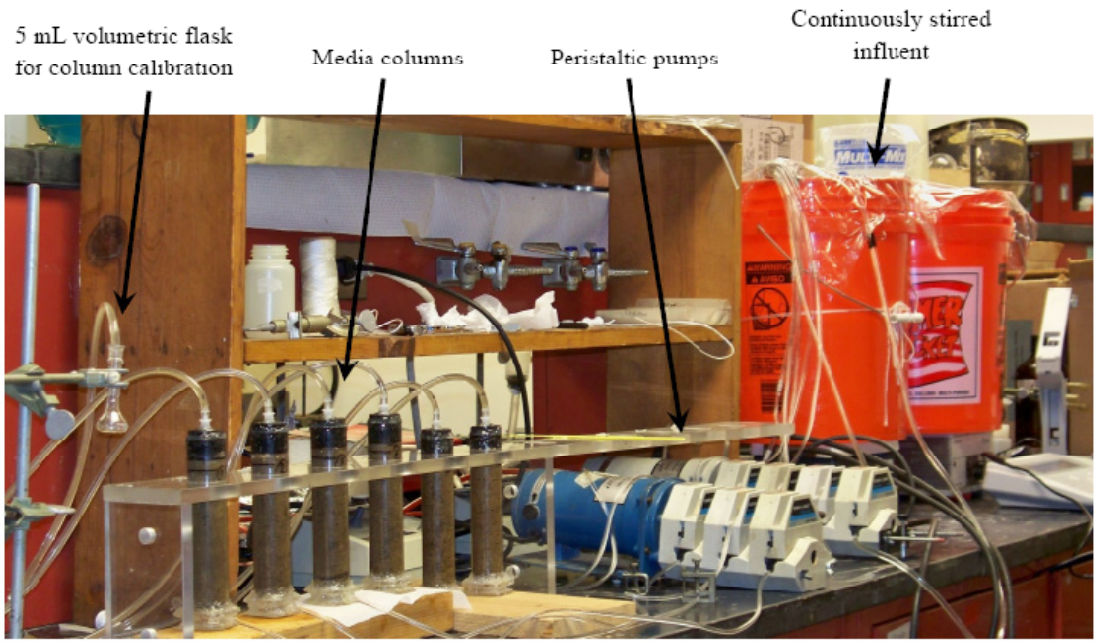

Figure 3-2. Column experimental setup. Influent is continually drawn from the stirred influent batches and pushed through the columns. Column effluent was sampled daily for pH, turbidity, and total phosphorus (TP).

breakthrough. All columns began at an inflow rate of 1.29 mL/min (6 in/hr), at which they were run for exactly 28 days. After that time, flow was doubled to 2.57 mL/min (12 in/hr) and run for an additional 21 days. Finally, after 49 days of total run time, flow was again doubled to 5.15 mL/min (24 in/hr) at which rate the columns were run until completion of the experiment. While flow greater than 6 in/hr is not representative of that seen in actual, gravity driven bioretention cells in the field, such high flows were needed to provide the mass loading necessary to force column breakthrough.

Within both experimental sets, nine columns were operated under continuous flow for at least eight weeks. Samples were collected from all columns primarily daily, except when this was logistically infeasible. In all instances continuously running columns were never unsampled for more than two consecutive days, and

samples were collected on four out of every seven days at a minimum. The percent of sampled days on a number-of-days-run weighted average basis was 89% for set I and 73% for set II.

Three columns from experimental set II were operated intermittently to simulate a rain-induced wetting/drying regime. These columns underwent throughflow for approximately 24 to 36 hours, during which time two sets of samples were collected: one for initial performance and one to analyze for performance immediately prior to shutdown. After shutdown, columns were disconnected from the influent tanks and the column pumps slowly operated in reverse to drain the columns and continuously pull ambient air through the media. Columns were operated dry for four days in between flow events on average.

3.5. Mesoscale Vegetated Column Experiments

Larger (0.9 m) columns were constructed with the final selected BSM mixture and periodically subjected to 6-hour synthetic storms. These storm events allowed measurement of media performance with regard to the removal of PO_4(-III), NH_4^+, NO_3^-, and DON.

3.5.1. Column Setup

The large vegetated columns were constructed of 1.1 m (3.6 ft.) of clear Plexiglas pipe affixed to a base plate which was bolted to a stand. The column had a cross-sectional area of 284 cm^2. The column drained vertically through an outlet valve and outflow was redirected horizontally via Tygon® tubing (Saint-Gobain Corp.). A fiberglass filter (1 mm mesh) was placed inside the columns at the base to prevent media washout. Atop the filter was a 5 cm (2 in.) angular quartz sand layer to

further minimize media washout. The majority of the remaining column space (86 cm, 2.8 ft.) contained the final BSM mixture. Ultimately both the sand and BSM were 0.9 m (3 ft.) in height, characteristic of a bioretention cell. This resulted in a bed volume of 26 L. The columns were left with 15 cm (6.0 in.) of freeboard to allow for ponding, above which the ponded water would drain through an overflow structure. Figure 3-3 details the column schematic and experimental setup.

3.5.2. Column Vegetation

Vegetation for column planting was selected based on species status as a native to the Chesapeake Bay region, tolerance to drought and anaerobic conditions, moisture use, minimum root depth, and local availability. Based on these constraints (largely due to availability upon commencing the experiment in January) Narrowleaf Blue-eyed grass (*Sisyrinchium angustifolium*) was purchased for use. Planting media was gently washed from the plants roots as completely as possible before transplantation to columns. Four mature plants were installed along with the column media, two plants per column. Total plant mass was approximately equal between each columns. Each planted column was illuminated by a grow light (Phillips 50 W 120 V Agro-lite plant light), which were placed on a timer set to provide the plants with a 12 hour light period.

3.5.3. Media, Influent, and Flow Characteristics

Media composition was selected based on the results of minicolumn studies; initially determined to be 5% Al-WTR (air dry w/w), 3.3% HBM (air dry w/w), and the remainder BSM. HBM was amended at a rate of 3.3% as this was the mass necessary to produce a 5% OM content in a 2% WTR amended mixture. All non-

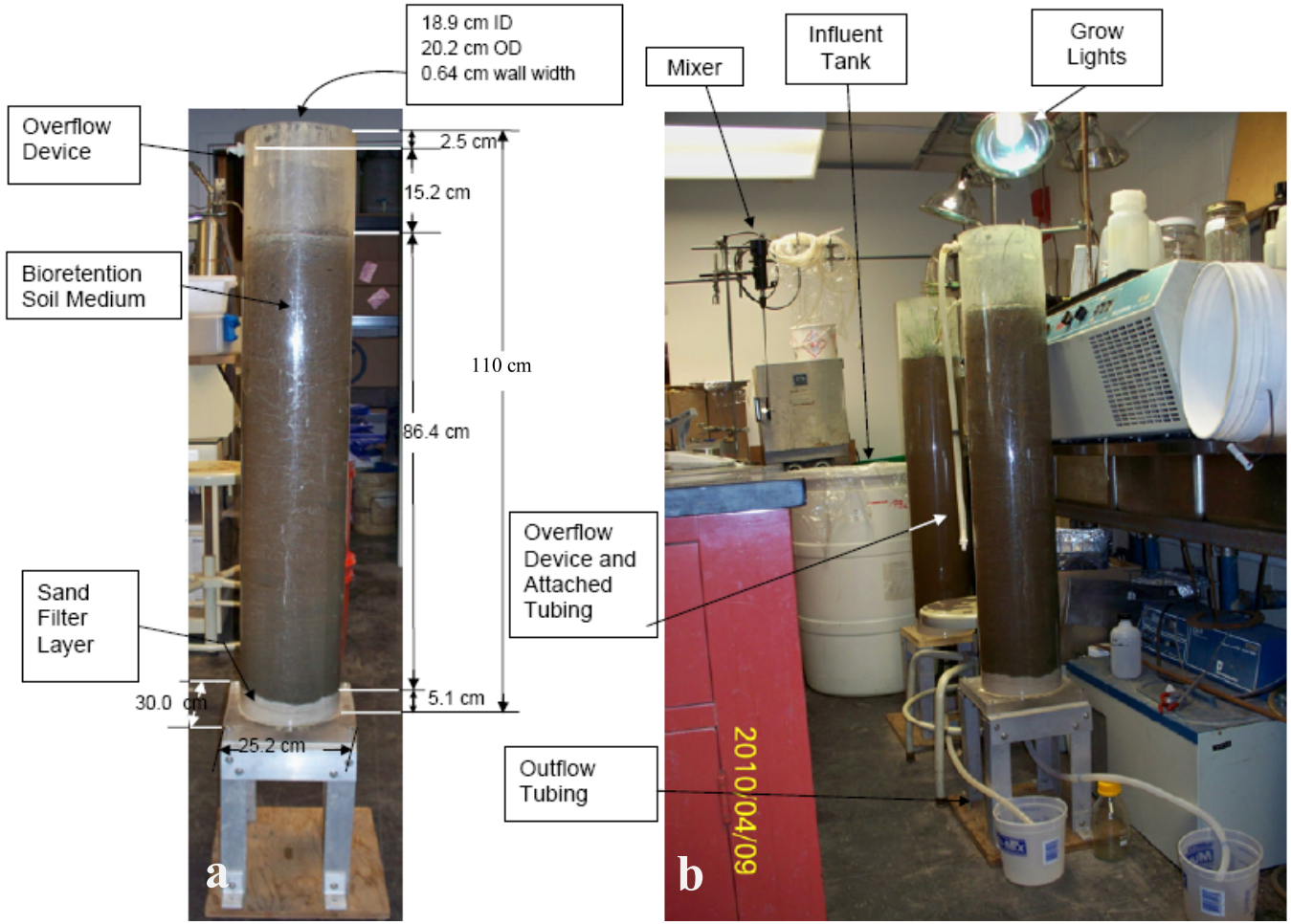

Figure 3-3. Detail of (a) gravity driven vegetated column schematic and (b) experimental setup.

Table 3-5. Relative proportions of vegetated column BSM mixture media constituents. BSM: bioretention soil media; WTR: water treatment residual; HBM: hardwood bark mulch.

	Experimental			Control		
	Moist	Air Dry	Oven Dry	Moist	Air Dry	Oven Dry
BSM	59.8%	69.2%	70.7%	73.7%	74.4%	74.4%
WTR	17.3%	5.15%	3.12%	0.00%	0%	0%
HBM	5.04%	3.30%	3.18%	5.79%	3.30%	3.12%
Sand	17.8%	22.3%	23.0%	20.5%	22.3%	22.5%

organic media was sieved < 2 mm, HBM was shredded and sieved < 2.36 mm, and the components were combined at field moist water content. However, upon setup of the columns the measured infiltration rate, while sufficient for the majority of specifications (≥ 1.33 cm/hr, ≥ 0.52 in/hr), did not meet the Prince George's County requirement of ≥ 2.0 in/hr (≥ 5.1 cm/hr). Consequently, media was removed from the columns, air dried for 1 week, and amended with sand as well as additional WTR and HBM (both field moist) to maintain the desired concentrations of each. After the decision to amend the media with sand, the media OM content was reduced because of the low sand OM content. Therefore, the amount of HBM necessary to produce 5% OM in a 2% WTR amended media was altered. Ultimately, the experimental BSM consisted, on an air dry mass basis, of 69% BSM, 5% WTR, 22% additional sand, and 3% HBM. Control BSM consisted of 74% BSM, 22% additional sand, and 3% HBM on an air dry mass basis. Final media composition may be seen in Table 3-5.

Influent composition was based on average stormwater concentrations (US EPA, 1983; Maestre and Pitt, 2005; Bratieres et al., 2008). All pollutants were applied as dissolved species, as particulate species are treated well through the filtration mechanism of the BSM and so were deemed unnecessary to include (Li and

Table 3-6. Concentration (μg/L) and source compounds for vegetated column synthetic stormwater influent solution. TP: total phosphorus; TDP: total dissolved phosphorus; TN: total nitrogen; NO_3^--N: nitrate nitrogen; TKN: total Kjeldahl nitrogen; NH_4^+-N: ammonium nitrogen; DON: dissolved organic nitrogen; †: Contaminant; ‡: Concentration (μg/L).

Contam.†	Conc.‡	Contam.†	Conc.‡	Contam.†	Conc.‡	Source
TP/TDP	120					NaH_2PO_4
TN	1700	NO_3^--N	700			NH_4NO_3 $NaNO_3$
		TKN	1000	NH_4^+-N	300	NH_4NO_3
				DON	700	Glycine

Davis, 2008b). Summarily, pollutant concentrations were 120 μg/L PO_4^{3-}-P, 700 μg/L NO_3^--N, 300 μg/L NH_4^+-N, and 700 μg/L DON. This resulted in total N (TN) input of 1.3 mg/L, and TKN of 1.0 mg/L. Table 3-6 details pollutant concentrations and species source compounds.

Both columns were subjected primarily to a standard hydrologic regime, being a constant inflow rate (i.e., uniform distribution) of approximately 182 mL/min (38.5 cm/hr) for a continuous 6 hour period, providing a total storm volume of 65 L (17.2 gal.) per column. This flowrate is equivalent to a rainfall rate of 1.91 cm/hr (0.75 in/hr) over the entire catchment area, assuming a bioretention cell sized at 5% of catchment. Such a storm duration and flowrate is a typical medium-to-large sized storm for that duration in the Washington, DC region (Kreeb, 2003). These synthetic storms were applied to the columns once per week, providing an antecedent dry period of 6 days.

Table 3-7. Testing regime for vegetated bioretention columns. Uniform hydrologic regime influent P concentration was 120 µg/L. Log-normal hydrologic regime influent P concentration ranged from 69 to 175 µg/L. Standard antecedent dry period was 6 days.

Test No.	Hydrologic Distribution	Influent Concentration	Antecedent Dry Period
1 - 5	Uniform	100%	Standard
6	Log-normal	100%	Standard
7	Uniform	250%	Standard
8	Uniform	100%	Standard
9	Log-normal	250%	2x
10	Uniform	60%	Standard
11	Uniform	100%	Standard
12	Uniform	100%	1/2x
13	Uniform	100%	Standard

Periodically, the columns were subjected to variations in influent hydrologic regime, pollutant loading, and antecedent dry period. This testing regime is outlined in Tables 3-7 and 3-8. Test 6 subjected the columns to an altered hydrologic regime, consisting of 6 "steps" of varying flowrate and pollutant concentration to more closely simulate actual rainfall. The flowrate followed an approximate log-normal distribution, being typical for stormwater runoff. It must be noted that the influent was not statistically log-normally distributed as it failed the Kolmogorov–Smirnov one sample test for a log-normal distribution. The applied pollutant concentration decreased step-wise with time. The applied flowrate and pollutant concentration were calculated to provide each column over the course of the 6 hour test with the same total influent volume and pollutant mass as the standard tests (65 L/column, 7.8 mg P). It should be noted that across all tests, all pollutants were applied at a constant ratio relative to P. Figure 3-4 provides a graphic representation of the flowrate and pollutant concentration for test 6.

Table 3-8. Vegetated column study detail of test flowrates and applied *o*-phosphate phosphorus [PO_4(-III)-P] concentrations.

	Flow				PO_4^{3-}
	Step No.	Duration (min)	Rate (mL/min)	Rate (cm/hr)	Concentration (µg/L)
Standard Test	-	360	182	38.5	120
Test 6	1	16	65	13.7	175
	2	24	233	49.3	153
	3	57	333	70.4	131
	4	80	250	52.8	109
	5	90	150	31.7	88.5
	6	93	65	13.7	68.5
Test 7	-	360	182	38.5	313
Test 9	1	16	65	13.7	476
	2	24	233	49.3	437
	3	57	333	70.4	373
	4	80	250	52.8	329
	5	90	150	31.7	250
	6	93	65	13.7	201
Test 10	-	360	182	38.5	68.4
Tests 11 & 12	-	180	182	38.5	120

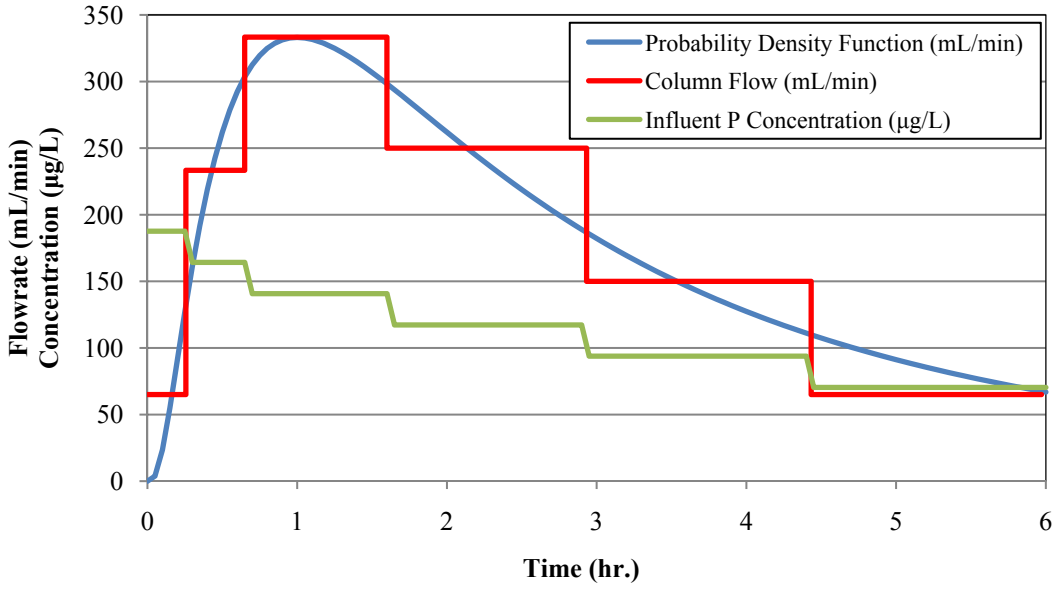

Figure 3-4. Hydrologic and pollutant concentration regime for Test 6, as well as the hydrologic regime for Test 9.

Test 7 subjected the columns to a standard uniformly-distributed hydrologic regime with a 2.5-fold increase in the influent pollutant concentration. Test 9 again subjected the columns to a log-normally distributed hydrologic regime with a 2.5-fold increase in the concentration of each "step". Additionally, the antecedent dry period for this test was doubled to 13 days. Test 10 had a standard hydrologic regime with a reduced influent concentration of approximately 60% of standard. Tests 11 and 12 subjected the columns to a reduced antecedent dry period. Test 11 was a standard experiment run for only 3 hours instead of 6. Test 12 was a replicate of test 11 run 4 days later, providing an antecedent dry period of 3 days. It was chosen to run both tests at ½ duration (3 hours) due to the logistical impossibility of analyzing all samples from a full duration test provided the reduced time period between runs.

3.6. Analytical Procedures

Numerous analytical procedures were performed on the column effluents and batch study solutions. The batch study solution was analyzed for SRP per Standard Method 4500-P E. Additionally, pH was determined using a glass electrode pH meter (Mettler Toledo MA235). Total phosphorus (TP) was determined using potassium persulfate digestion (4500-P B.5) and colorimetric determination by the ascorbic acid method (4500-P E) at 880 nm as described in Standard Methods (APHA, 1992). Samples were also analyzed for turbidity using a turbidimeter (Hach 2100N). Electrical conductance was measured using a conductance meter (YSI Model 35). Total dissolved phosphorus (TDP) samples were filtered through a 0.22 μm membrane filter and analyzed using methods identical to TP analysis. Samples for NO_3^- determination were filtered (0.22 μm membrane) and analyzed by ion

chromatograph (Dionex DX-100) per Standard Method 4110 (APHA, 1992). TKN was analyzed using 300 mL sample volume and the macro-Kjeldhal digestion method and titration per Standard Method techniques 4500-N_{org} B and 4500-NH_3 C, respectively (APHA, 1992). Samples for SO_4^{2-} were filtered (0.22 μm membrane) and analyzed by ion chromatograph (Dionex DX-100) per Standard Method 4110 (APHA, 1992). NO_2^- was analyzed colorimetrically in compliance with Standard Method 4500- NO_2^- B. Summarily, 2 mL of color reagent was added to 50 mL filtered sample (0.22 μm) and analyzed after 10 minutes via spectrophotometer (Shimadzu, UV-160) at 543 nm.

Water extraction of various media and media components was performed per the method outlined in *Methods of Soil Analysis* (Kovar and Pierzynski, 2009). 4 g of media (oven dry mass basis) were placed in a 50 mL centrifuge tube along with 40 mL deionized water, to provide a 1:10 media:solution ratio. A tube containing solely deionized water was also carried through all analyses as a blank. Centrifuge tubes were then placed on an end-over-end shaker for 1 hour. After shaking, all samples were centrifuged at 4000 rpm for 13 minutes and then filtered through a 0.22 μm membrane filter. Water-extractable phosphorus (WEP) was determined by the ascorbic acid method (4500-P E; APHA, 1995). Anions such as NO_3^- and SO_4^{2-} were determined by ion chromatography per Standard Method 4110 (APHA, 1992).

Both BSM and WTR were digested per EPA Method 3050B (Acid Digestion of Sediments, Sludges, and Soils) and analyzed by atomic absorption spectrophotometry (AAS) (Perkin-Elmer 5100PC) for total content of metals, including: Al, Fe, Ca, and Mg. This method releases most elements that may become

environmentally available. By design, this method generally does not release those elements bound by silicates, as these are predominantly non-mobile in the environment. In brief, Method 3050B involved digesting 1 g (oven dry mass) of sieved media (< 2 mm) with concentrated HNO_3 for two hours or until a final volume of 5 mL was reached, with HNO_3 addition sufficient for all organic material to be oxidized as evidenced by the cessation of brown fume generation (an indicator of oxidation of organic material). Then, 2 mL water and 2-10 mL H_2O_2 was added, 1 mL at a time, until effervescence was minimal or the maximum 10 mL added. Again, the mixture was digested for 2 hours or to a final volume of 5 mL. Finally, 10 mL concentrated HCl was added and the mixture heated for 15 minutes. It was then filtered through a glass fiber filter (Whatman No. 40), diluted to 100 mL, and analyzed by AAS.

Effluent total metals content was determined by AAS after digestion per Standard Method 3030 E (APHA, 1992). 5 mL of concentrated HNO_3 was added to 50 mL of column effluent in an erlenmeyer flask, which was heated until the total solution volume was reduced to approximately 10 mL. The flask was then removed from the heat, allowed to cool, and rediluted to 50 mL. This solution was then analyzed by AAS. Prior to analysis, collected samples were acidified < pH 2 with HNO_3 and stored at 4°C. Digestion and analysis was conducted within 6 months of sample collection.

Determination of oxalate extractable elements; namely iron (Fe), aluminum (Al), and phosphorus (P), was also undertaken. An acid ammonium oxalate solution was used as an extractant to selectively dissolve the amorphous (non-crystalline)

fraction of certain soil compounds; namely (hydr)oxides of Al and Fe (McKeague and Day, 1966; 1993). A number of studies have shown a strong correlation between oxalate-extractable aluminum and iron (Al_{ox} + Fe_{ox}) and P sorption capacity or, conversely, risk of soil P leaching (Dayton and Basta, 2005). Specifically, the Phosphorus Saturation Index (PSI) is often used as a measure of P adsorption/leaching potential, and is defined as:

$$\text{PSI} = \frac{P_{ox}}{(Al_{ox} + Fe_{ox})} \quad (3\text{-}3)$$

where P_{ox}, Al_{ox}, and Fe_{ox} are oxalate-extractable P, Al, and Fe in mmol/kg, respectively. Work has shown that in general, a PSI above 0.1 greatly increases the risk for P leaching from a soil (Agyin-Birikorang and O'Connor, 2007, Kleinman et al., 2000).

In this research, a modified method of McKeague and Day (1993) was utilized, with a 0.275 M acid ammonium oxalate (0.175 M Ammonium Oxalate + 0.1 M Oxalic Acid) solution used as an extractant, this solution having a pH of approximately 3.4. The pH was adjusted to 3.0 ± 0.1 using 1 M HCl. A 1:40 w/v ratio of media to oxalate solution was used. The single exception to this was the determination of the oxalate-extractable content for WTR alone, for which was used a 1:100 w/v ratio per the recommendation of Dayton and Basta (2005), who showed that a greater ratio is necessary to accurately characterize WTRs because of their much greater amorphous aluminum content.

The oxalate solution was both added to the media and shaken on an orbital shaker for 2 hours in the dark. Samples were centrifuged for 13 minutes at 2000 rpm after shaking and filtered through a 0.22 μm membrane filter. This filtrate was then analyzed by AAS for Fe and Al within 1 week.

P was analyzed using the method of Wolf and Baker (1990), a modification of the method of Murphy and Riley (1962), with the addition of excess ammonium molybdate. This addition is necessary as oxalate binds molybdate, resulting in insufficient concentration in solution to react with P to form the phosphomolybdic acid which is ultimately measured. This method calls for the use of 0.275 M acid ammonium oxalate solution, and is the impetus behind the use of this higher-than-standard concentration in this work. As with Fe and Al, oxalate extraction samples were analyzed colorimetrically for P within 1 week.

3.7. Statistical and Numerical Analyses

3.7.1. Media Adsorption Capacity

Media adsorption capacity for column studies was calculated by the equation:

$$q = \frac{T_{P,in} - T_{P,out}}{M_{media}} \tag{3-4}$$

where q is the total media P adsorption capacity (mg_P/kg_{media}), $T_{P,in}$ is the total mass of P which entered the column (mg P), $T_{P,out}$ is the total mass of P which exited the column (mg P), and M_{media} is the oven-dried mass of media within the column at the outset of the experiment (kg media). $T_{P,in}$ and $T_{P,out}$ were calculated as:

$$T_P = \int_{t_0}^{t_i} C \cdot Q \, dt \tag{3-5}$$

where T_p is the total mass of P either entering or exiting the column (mg P). C is the concentration of P (mg/L) and Q the volumetric flowrate (L/min), integrated with

respect to time from the beginning of column flow (t = 0 min) to the cessation of the experiment (t = i min). The media adsorption capacity, q, defines the mass of a pollutant that can be adsorbed or otherwise immobilized per unit of treatment media under specific environmental conditions (i.e., pH, pollutant concentration, ionic strength, temperature, etc.).

Predominantly, TP and TDP were used independently to calculate media adsorption of total and dissolved P species. However, when TDP measured greater than TP for a given sample (one occurrence for the vegetated control column), the result was rejected as irrational and erroneous, and TP used for all calculations.

3.7.2. Event Mean Concentration

Synthetic storm event mean concentrations (EMCs) were calculated for a number of tests and pollutants, specifically during the vegetated column experiments. The EMC is calculated from a composite of discrete samples, and used to estimate the flow-weighted mean outflow concentration for the entire storm. The EMC may be visualized as the concentration of the outflow if the entire runoff volume could be captured in a single container. It is calculated by using integration to determine the entire influent pollutant mass divided by the entire flow volume, or:

$$\mathrm{EMC} = \frac{\int_{t_0}^{t_i} C \cdot Q \, dt}{\int_{t_0}^{t_i} Q \, dt} \tag{3-6}$$

where C is the concentration, Q is the flowrate, and t_0 and t_i are the initial and final times, respectively. The EMC is used as a means to compare mean pollutant concentrations between events and to compare average influent and effluent pollutant concentrations.

3.7.3. The Kolmogorov-Smirnov One Sample Test

The Kolmogorov-Smirnov one sample test is a hypothesis test to analyze for the probability density function (PDF) of a sample population. The test involves calculation of the test statistic, |D|, which is the absolute maximum difference between the cumulative probability distribution of the sample and that of the hypothesized PDF. The analysis tests the null hypothesis (H_0) that the sample population has the given PDF against the alternative hypothesis (H_A) that is does not. A critical value (D_α) is calculated at the 5% level of significance, and if $|D| > D_\alpha$, H_0 is rejected and sample population does not have the hypothesized PDF.

3.7.4. The Dixon-Thompson Test

The Dixon-Thompson Test is an analysis for the determination of outliers from a given sample population. The test assumes that the sample data are independent measurements from a normal population, and that a datum that tests positive as an outlier is in fact from another population having either a different mean or a larger variance. The analysis tests the null hypothesis (H_0) that all data point are from the same population, against the alternative hypothesis (H_A) that the most extreme point in the sample is not from the same normal population as all other sample points.

The test is only valid for the analysis of a single outlier of either extreme (i.e., upper or lower outlier). All data are sorted in descending order and the most extreme value is used in the calculation of the test statistic (R). The calculation for R is dependent on sample size. R is evaluated against the critical value (R_α) at the 5% level of significance, and the null hypothesis is rejected if $R > R_\alpha$. Upon rejection of the null hypothesis, the potential outlying point was assessed to determine if there

was an empirical reason for the extreme value (e.g., excessive release of particulate matter from the media after flowrate increase). If there was such an identifiable cause for the event, the outlier was removed from further calculations.

3.7.5. T-test

The t-test was used as means of determining if two sample means are statistically the same. A test statistic, t, is calculated to analyze the degree of variation between each sample relative to that within a sample. The value of t is calculated as:

$$t = \frac{x_1 - x_2}{S_p \cdot (\frac{1}{n_1} + \frac{1}{n_2})^{0.5}} \quad (3\text{-}7)$$

where x_i is a sample mean, n_i is the number of data points within a sample, and S_p is the standard deviation of the paired means, calculated as:

$$S_p^2 = \frac{(n_1 - 1) \cdot S_1^2 + (n_2 - 1) \cdot S_2^2}{n_1 + n_2 - 2} \quad (3\text{-}8)$$

where S_i is the standard deviation of a given the sample. It was assumed that all sample populations were normally distributed and had equal variances. This analysis was used to test the null hypothesis (H_0: $\mu_1 = \mu_2$) that the two sample population means compared are equal, against the alternate hypothesis that they are not (H_A: $\mu_1 \neq \mu_2$). The calculated t value was compared against a critical value, t_α, at a 1% level of significance.

Chapter 4:Batch and Column Experiments

Phosphorus adsorption batch studies were undertaken to investigate the impact of various media amendments on BSM and their effectiveness on the removal of P from solution. These studies provided an initial estimate of the proportion of these amendments in the BSM, as well as gave evidence of the impact of certain environmental variables on media performance, such as pH.

4.1. Media Characterization

Characterization of the materials used in this study was necessary to provide insight on the nature of these components. The results of 0.275 M acid ammonium oxalate extraction and WEP for BSM, WTR, HBM, and LC are found in Table 4-1. Additionally, the results of a 3050B digestion and metal analysis for BSM and WTR are also included. From Table 4-1, it is seen that LC contains 11.7 mg WEP/kg, followed by HBM with 2.85 mg WEP/kg, BSM with 0.358 mg WEP/kg, and WTR which measured below the detection limit of 0.1 mg WEP/kg. Clearly the organic amendments, and LC in particular, contain the largest amount of very labile WEP.

Interestingly, P_{ox} does not follow a similar order of increasing P content. WTR contains by far the largest P_{ox} content with 1.81 g P_{ox}/kg. LC contains the second largest amount with 0.492 g P_{ox}/kg, followed by BSM with 0.125 g P_{ox}/kg, and HBM with 0.116 g P_{ox}/kg. Therefore the percent fraction of very labile P (WEP/P_{ox}) is 2.46% for HBM, 2.37% for LC, 0.286% for BSM, and < 0.006% for WTR. This ratio shows the proportion of a component's P which is in the most labile state. The strong adsorption of P by the WTR is clear as effectively none of its P is

Table 4-1. Media component characterization. BSM: bioretention soil media; WTR: water treatment residual; HBM: hardwood bark mulch; LC: leaf compost; WEP: water-extractable phosphorus; ×: Data not collected.

	Oxalate Extractable (g/kg)			WEP	3050B Digestion (g/kg)			
	P	Fe	Al	(mg/kg)	Ca	Mg	Fe	Al
BSM	0.125	0.871	0.286	0.358	2.24	2.58	20.4	21.9
WTR	1.81	3.67	155	< 0.1	0.038	0.778	8.80	169
HBM	0.116	3.04	0.343	2.85	×	×	×	×
LC	0.492	2.20	0.369	11.7	×	×	×	×

labile. Similarly, the inherent P in the BSM appears to be predominantly adsorbed to Fe and Al species and not released until dissolution by oxalate. Both organic amendments show similar proportions of very labile P, however the magnitude of P in each material is different, which may partly explain their different P adsorption behavior.

Among the four materials, Fe_{ox} content is fairly consistent. WTR contains the most with 3.67 g Fe_{ox}/kg, HBM contains 3.04 g Fe_{ox}/kg, LC contains 2.20 g Feox/kg, and BSM contains the least with only 0.871 g Fe_{ox}/kg. Additionally, total Fe was determined for both the BSM and WTR, which showed 20.4 g Fe_{Tot}/kg and 8.80 g Fe_{Tot}/kg, respectively. This indicates that of the Fe in the BSM, 4.27% is amorphous, while the WTR Fe is 41.7% amorphous. A much larger proportion of the Fe in the BSM is crystalline.

For Al_{ox}, the WTR shows a clearly larger amount compared to the other materials with 155 g Al_{ox}/kg. The LC contains 0.369 g Al_{ox}/kg, HBM contains 0.343 g Al_{ox}/kg, and BSM contains 0.286 g Al_{ox}/kg. The total Al content for the BSM and WTR are 21.9 g Al_{Tot}/kg and 169 g Al_{Tot}/kg, respectively. This equates to 1.30 and 91.8% of the Al being amorphous in the BSM and WTR, respectively. Again, this

indicates that the majority of Al in the BSM is crystalline, while nearly the entire Al contained in the WTR is amorphous.

Having analyzed all four materials for oxalate-extractable P, Fe, and Al, the media PSI may be determined. Each media PSI measures 1.00, 5.58, 15.4, and 29.9% for the WTR, HBM, WTR, and LC, respectively. Research has shown that media P leaching greatly increases with a PSI > 10% (Agyin-Birikorang and O'Connor, 2007). This indicates that, as expected, the WTR has a very large capacity for P adsorption. The HBM also shows some capacity on account of its low P_{ox} content relative to its $(Al+Fe)_{ox}$ content, which may explain the improved P adsorption capacity of the BSM when amended with both HBM and WTR (see Sections 4.3 and 4.4.3). Conversely, the LC PSI indicates it is as risk for P leaching, which may again explain its poor P adsorption performance. The BSM also indicates it is at risk for P leaching. This is because it has low $(Al+Fe)_{ox}$ content, which appears to be nearly or completely saturated with P as suggested by its relatively high P_{ox} content.

Aluminum-based WTR can be a highly variable material, and the implications this has on its use as a BSM amendment requires addressing. The physical and chemical characteristics of WTR will conceivably be affected by a number of parameters. For instance, the amount of alum added to remove colloidal material in the flocculation basin during drinking water treatment will have some impact on the resulting mass of aluminum hydroxide in the WTR, and likely affect its P adsorption capabilities.

A number of references have discussed WTR Al_{ox} content. Elliott et al. (2002) reported 71.9 g Al_{ox}/kg in a WTR used in a column study as a soil amendment to measure its impact on soil P leachability. In a field study in Florida to assess the impact of surface-applied WTR and manure on soil P leaching, Agyin-Birikorang et al. (2009) reported a WTR Al_{ox} content of 84.3 ± 6.2 g Al_{ox}/kg. Dayton and Basta (2005) reported on 18 WTRs from Pennsylvania and Oklahoma, having a mean Al_{ox} content of 73.1 ± 44.2 g Al_{ox}/kg, and a median content of 58.8 g Al_{ox}/kg. The WTR used in the present study measured 155 ± 7.45 g Al_{ox}/kg (Table 4-1).

These data show quite a large amount of variation in WTR characteristics. The WTR used in this work trends toward the high end in terms of typical Al_{ox} content, and this must be taken into account when considering P adsorption results. However, this should have no effect on the use of Al-WTR as a BSM amendment. Ultimately, recommendations in Sections 6.4 and 7.1 are based on the measure of P_{ox}, Al_{ox}, and Fe_{ox} in a BSM mixture, not by percent mass of WTR. This should adequately account for the variability seen in the oxalate-extractable contents of WTRs.

4.2. Media Adsorption pH Effects

Results of investigation into pH effects on WTR adsorption capacity were encouraging. WTR acted as a buffer upon pH adjustment, which should be expected because of the chemicals routinely added to drinking water during treatment. This resulted in approximately neutral pH after equilibration in most instances. The final pH of solutions containing WTR ranged from approximately 5.9 to 7.4, trending higher with increasing WTR content. Mixtures unamended with WTR had a range of

final pH values that was shifted somewhat lower, as these did not benefit from the buffering capacity provided by the WTR, ranging from 4.6 to 7.2. Minimal pH effect on P adsorption capacity was observed in this pH range, as exemplified in Figures 4-1 and 4-2 (note the variations in both the ordinate and abscissa axes between the plots). Therefore, changes in pH within this range are not expected to produce large differences in media P adsorption and minor fluctuations in pH are not expected to significantly impact results.

4.3. Media P Adsorption Isotherms

Sorption isotherms for each amendment mixture were plotted as the P concentration remaining in solution after equilibration and the mass of adsorbed P per mass of media. Table 4-2 shows the Freundlich equation constants for each isotherm, and details each media's P adsorption capacity at equilibrium with a 120 μg/L P solution as calculated from the isotherms. The effect of WTR content on BSM sorption capacity is summarized in Figure 4-3, and its effect on LFBSM is seen in Figure 4-4. BSM and LFBSM media having the same WTR content are compared in Figure 4-5. These data clearly show that increasing the WTR content of the media increases its P adsorption capabilities, as does the estimated media adsorption capacities predicted utilizing the fitted Freundlich isotherms, seen in Table 4-1.

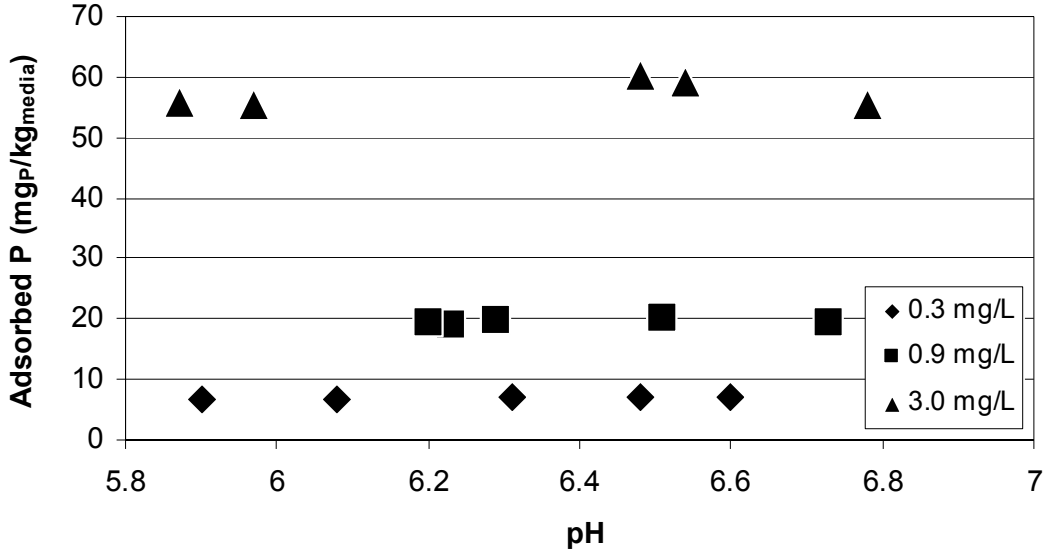

Figure 4-1. P sorption capacity of BSM + 2% WTR as affected by variation in pH after equilibration with P solutions of 0.3, 0.9, and 3.0 mg/L initial concentration.

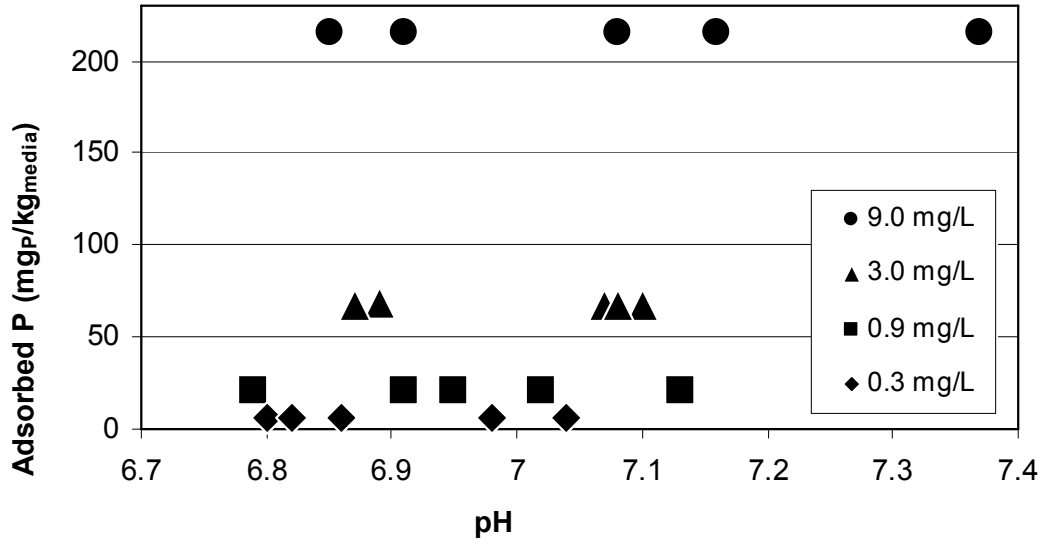

Figure 4-2. P sorption capacity of BSM + 10% WTR as affected by variation in pH after equilibration with P solutions of 0.3, 0.9, 3.0, and 9.0 mg/L initial concentration.

Table 4-2. Freundlich equation constants for the investigated BSM mixtures. 0.3, 0.9, 3.0, and 9.0 mg P/L solution additions were used containing 0.01 M KCl as a background electrolyte and at pH 4.6 to 7.4. A media to solution ratio of 1:25 was used. BSM: bioretention soil media; WTR: water treatment residual; HBM: hardwood bark mulch; LC: leaf compost; LFBSM: low-fines BSM; AH: aluminum hydroxide.

Mixture	K	n	Adsorption Capacity at 120 µg P/L (mg/kg)
BSM	46.0	1.69	13.1
2% WTR	69.3	1.61	18.6
4% WTR	106	1.50	25.6
10% WTR	361	1.49	81.9
LFBSM	21.0	1.37	4.49
3% WTR	90.4	1.62	24.4
6% WTR	271	1.35	56.1
10% WTR	1786	1.02	225
BSM + HBM	61.0	1.36	12.8
2% WTR + HBM	183	1.25	33.4
4% WTR + HBM	256	1.22	45.0
BSM + LC	17.5	0.778	1.14
4% WTR + LC	326	0.857	27.4
4% WTR + LC [OM+]	273	0.580	7.07
0.5% AH	244	1.23	43.7

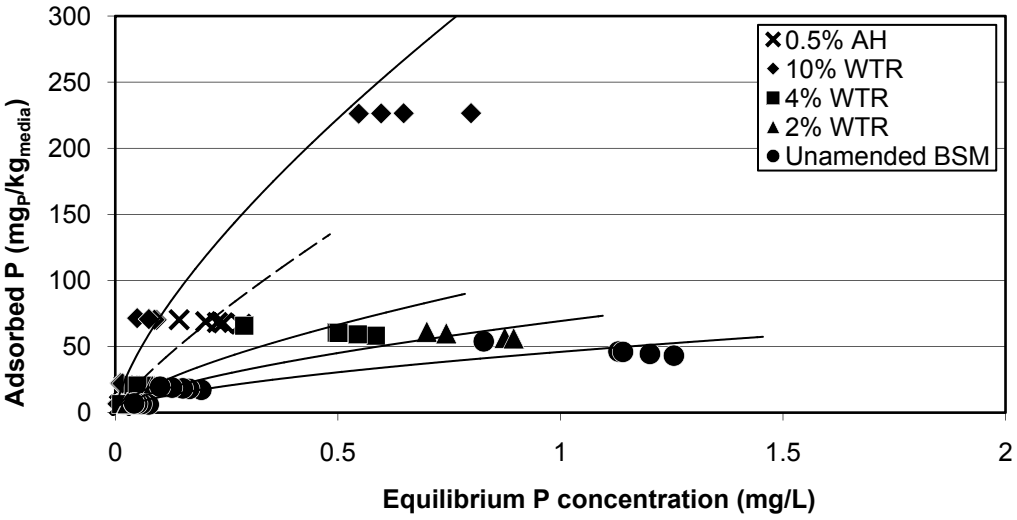

Figure 4-3. Comparison of P adsorption isotherms for BSM amended with various amounts of Al-WTR as well as 0.5% Al_{ox} WTR-equivalent as $Al(OH)_3$ at a pH range of approximately 4.2 to 7.4. Data produced using 0.01 M KCl as a background electrolyte and a media to solution ratio of 1:25. Lines are fitted Freundlich isotherms.

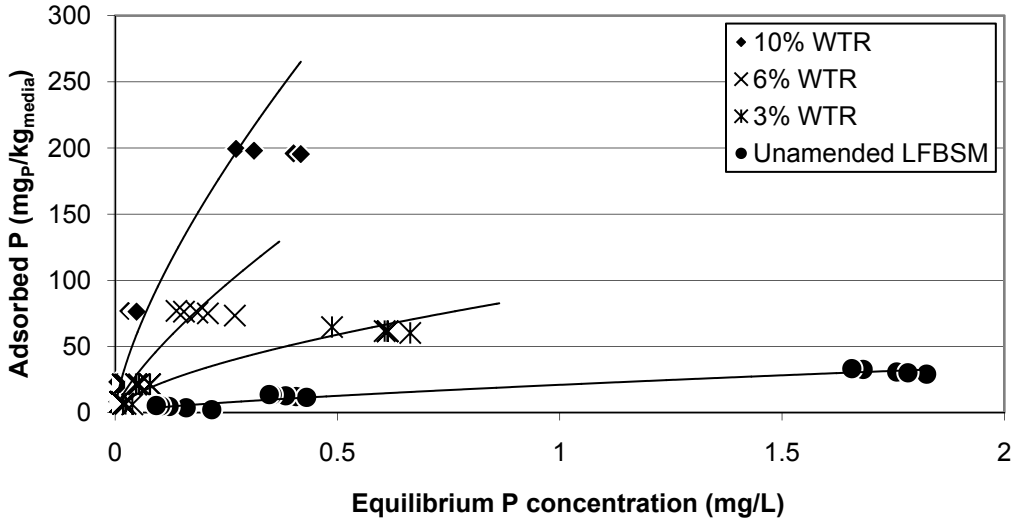

Figure 4-4. Comparison of P adsorption isotherms for LFBSM amended with various amounts of Al-WTR at a pH range of approximately 4.6 to 7.3. Data produced using 0.01 M KCl as a background electrolyte and a media to solution ratio of 1:25. Lines are fitted Freundlich isotherms.

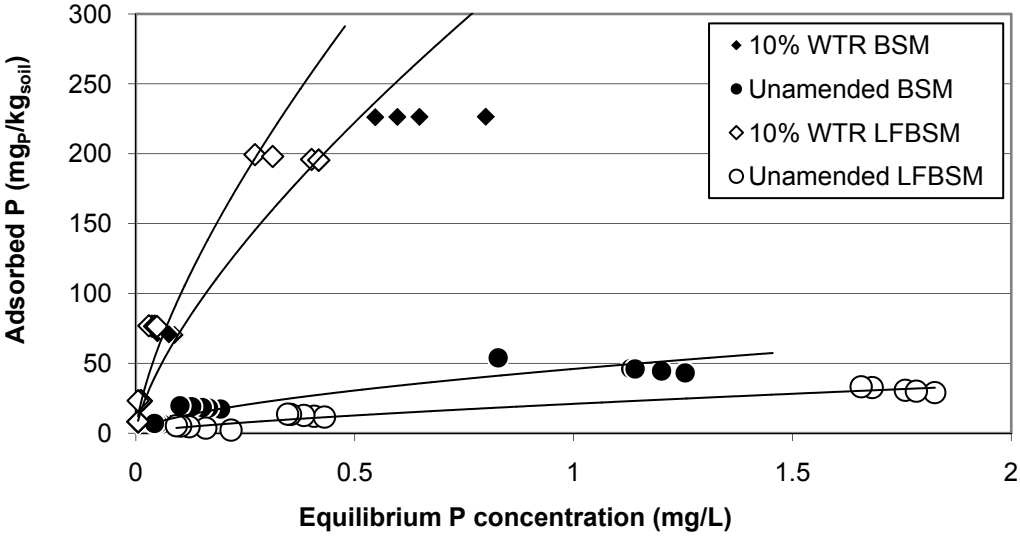

Figure 4-5. Comparison of P adsorption isotherms for BSM and LFBSM both unamended and amended with 10% Al-WTR (air dry wt.) at a pH range of approximately 4.6 to 7.4. Data produced using 0.01 M KCl as a background electrolyte and a media to solution ratio of 1:25. Lines are fitted Freundlich isotherms.

The unamended LFBSM media clearly shows a decreased adsorption capacity compared to the BSM, which is attributed to the lower clay content (and associated Al and Fe (hydr)oxides). However, increased adsorption for the low-fines media was observed when comparing the LFBSM and BSM amended with an equal proportion of WTR. The reason for this behavior is unknown, but may be explained by occlusion of WTR surfaces by fines in the media. As many soil minerals and especially clays have negative surface charges (Sposito et al., 1999), upon mixing with WTR the complementary surface charges of the clays and WTR may lead to surficial interactions (Goldberg, 1990). This results in decreased exposed surface area available for P adsorption. This phenomenon was further investigated through scanning electron microscopy (SEM) analysis of various media, but differences between mixtures were not overtly apparent. Fines addition may also improve adsorption because BSM is nearly saturated with P, as indicated by its 15.4% PSI. Addition of BSM adds significantly to the P_{ox} of the mixture, while the addition of sand reduces this source of P while maintaining a high Al_{ox} content as the proportional mass of WTR in the mixture is unchanged. This results in a greater P adsorption capacity. It is believed that both mechanisms account for the increased adsorption of low-fines media.

The addition of fines may only improve sorption capacity where BSM is no longer a sink for P. Consequently, use of BSM containing higher contents of clay not saturated with P may show decreasing P adsorption with addition of sand. However, electrostatic interactions between the complementarily charged clay and WTR surfaces are believed to be possible, and clays with a high net negative surface charge

may compete with P for available adsorptive surface sites based on evidence of competition between P and other anionic compounds (Goldberg and Sposito, 1985).

Effects of organic amendments on P adsorption may be seen in Figures 4-6 and 4-7. HBM improved adsorption, shown in Figure 4-6. This may possibly be due to the formation of metal-OM complexes which provide additional reactive sites for P adsorption (Darke and Walbridge, 2000; Kang et al., 2009; Figure 2-2).

As hypothesized, LC addition to the BSM resulted in decreased P adsorption, as seen in Figure 4-7. BSM + LC performed worse than BSM when unamended in all respects. When amended with WTR, though, this was not necessarily the case. The media amended with both WTR and LC performed better than without LC at higher P concentrations. This held true even for the 4% WTR amended BSM mixture with additional LC, referred to hereafter as the OM+ mix. However, the 4% WTR + LC performed better only above 0.1 mg P/L, and the OM+ mix performed better only above 0.5 mg P/L when utilizing the fitted trend lines. Therefore, at the concentrations of P found in most urban stormwater, it is expected that LC will have a detrimental effect on adsorption. It is believed that this loss of adsorptive capacity is caused by leachable P inherent in the LC, which may be released into solution and adversely affect adsorption to the WTR. By its nature, LC is in a greater state of decomposition than HBM and so is expected to have greater labile P content. This is supported by Gressel et al. (1996), who found that the extent of P mineralization and P_i content is positively correlated with the breakdown of OM (leaf litter) in forest soils. By corollary, the advanced state of decomposition of LC is reason to expect a

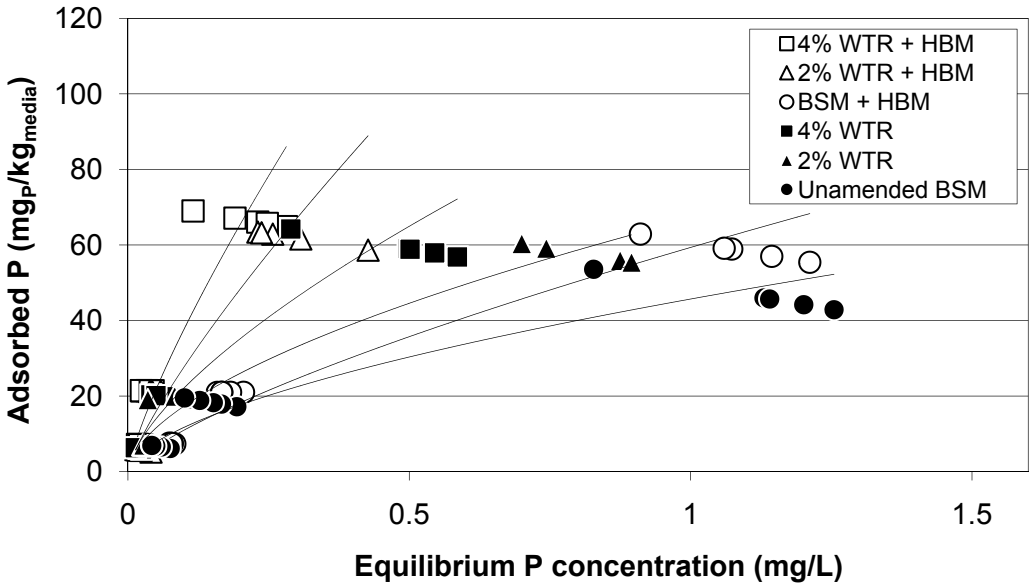

Figure 4-6. Comparison of P adsorption isotherms for BSM and BSM + HBM, both unamended and amended with 2% and 4% Al-WTR (air dry wt.) at a pH range of approximately 4.8 to 7.4. Data produced using 0.01 M KCl as a background electrolyte and a media to solution ratio of 1:25. Lines are fitted Freundlich isotherms.

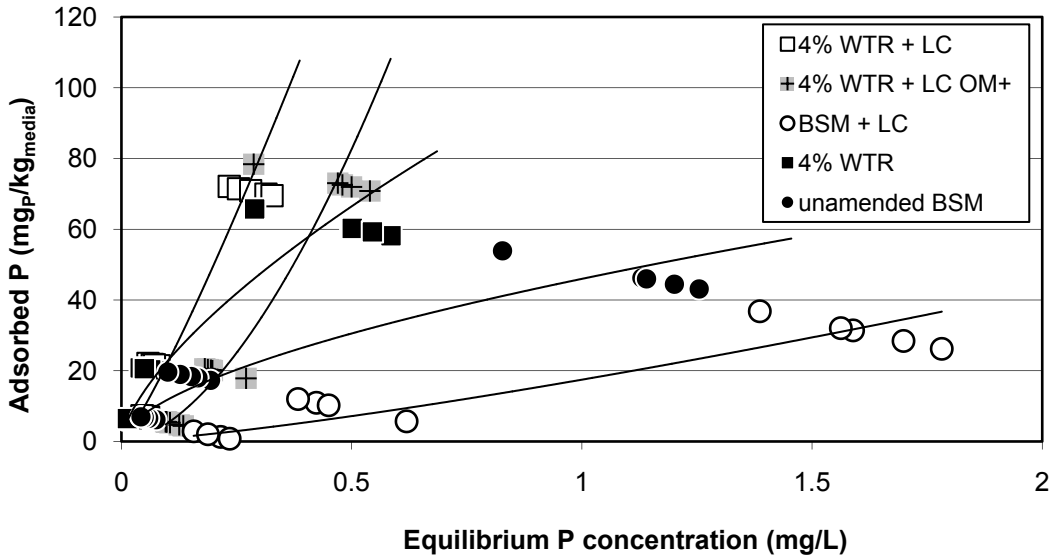

Figure 4-7. Comparison of P adsorption isotherms for BSM and BSM + LC, both unamended and amended with 4% Al-WTR (air dry wt.), plus 4% WTR with additional LC content (OM+ treatment). The pH range of the data is approximately 4.8 to 7.4., and was produced using 0.01 M KCl as a background electrolyte and a media to solution ratio of 1:25. Lines are fitted Freundlich isotherms.

high labile P_i content, which may explain the reduced media P adsorption capacity when LC is used as an amendment.

Pure $Al(OH)_3$ was also amended to the BSM to allow comparison with WTR. As explained in Section 4.4, $Al(OH)_3$ was amended on an amorphous Al basis analogous to 0.5%, 2% and 4% WTR. Both 2% AH and 4% AH additions completely or nearly completely removed all added phosphate, resulting in P concentrations after equilibration below the method detection limit (10 μg/L). In both instances an adsorption isotherm could not accurately be constructed because of this.

The 0.5% AH addition produced adsorption results from which an isotherm could be constructed. In comparison with BSM amended solely with WTR, it performed between the 4% and 10% mixtures (Figure 4-3). Although the WTR and AH amendments contain the same amount of amorphous $Al(OH)_3$, the AH amendment adsorbs P much more efficiently. A number of possibilities exist that may explain this phenomena. It may be that the AH amendment possesses a much greater surface area compared to the WTR, as it is a powder. Also, oxalate extraction is operationally defined as a measure of amorphous metals content. It may therefore be that some portion of the extracted Al is not actually amorphous, as oxalate extraction is only an operational definition of amorphous content. This would again cause the WTR to possess less surface area relative to the AH when compared on the basis of measured oxalate-extractable Al content.

It may also be that the fresh AH contains a greater percentage of highly reactive Al (hydr)oxides. Agyin-Birikorang and O'Connor (2009) investigated the effect of aging on extractable Al content of WTR using 0.2 M acid ammonium

oxalate and 0.005 M acid ammonium oxalate. The former is intended to be a measure of complete oxalate-extractable content, while the latter is a measure of the most reactive oxalate-extractable Al forms. They concluded that over the course of 2 years the total oxalate Al content did not significantly change, while the highly reactive oxalate-extractable Al content steadily decreased over the first 6 months after WTR generation, stabilizing thereafter. The freshly generated AH may contain a greater highly-reactive oxalate-extractable Al content than the WTR, resulting in the disparate P adsorption capacity. It should be noted, however, that Agyin-Birikorang and O'Connor (2009) did not correlate 0.005 M oxalate-extractable Al with P adsorption capacity of the WTR, and other studies (Yang et al., 2008) showed no aging effect on WTR P adsorption capacity when stored in a watertight container as was the WTR used in this study.

The strong positive correlation between % WTR (air dry weight) and media P adsorption for these batch tests is clearly seen in Figure 4-8. It is evident that as WTR content increases, so does the media adsorption capacity. Additional amendments may enhance or reduce mixture P adsorption. HBM increases adsorption, apparently because it contains a relatively low P content in relation to its Fe_{ox} content. Conversely, the addition of LC results in lower media P adsorption relative to media without LC addition. This appears to stem from its high P and low $(Al+Fe)_{ox}$ content. The addition of quartz sand to create low-fines media

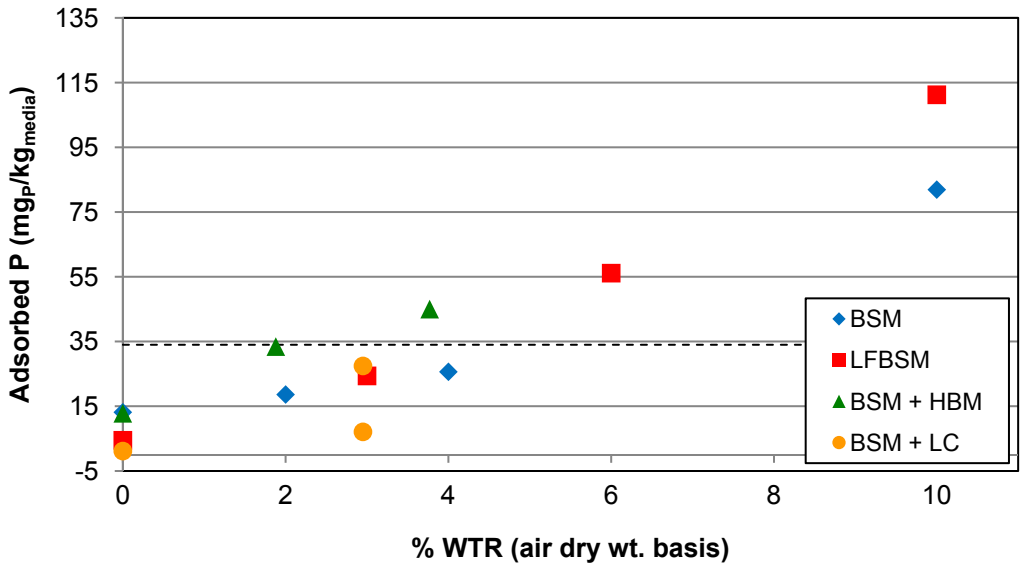

Figure 4-8. Batch data detailing increased P adsorption (at equilibrium with 120 µg/L P) with increasing WTR content (air dry weight basis). Batch adsorption data calculated from Freundlich isotherms. The dotted line represents the media adsorption benchmark of 34 mg P/kg.

also improved P adsorption. This may be due in part because the addition of sand reduces the overall media fines content. Fines, including clays, often have a net negative surface charge because of isomorphically substituted elements within the mineral lattice structure, which may undergo interactions with the positively charged WTR surface, thereby competing with P in solution for adsorption sites. It is also feasible that these small particulates are blocking WTR micropores, preventing P interactions was large portions of the WTR surface. Thirdly, the BSM used is nearly saturated with respect to P, and is at risk for P leaching as indicated by its PSI > 10%. So while reducing fines content in this media increases overall P adsorption, other media which are not saturated with P and contain significant Fe and Al (hydr)oxides may present increasing adsorption with increasing fines content. Also, these batch investigations only characterized the system under static conditions. Shorter

reactions times and the removal of any formed complexes or leached ions in solution will occur under dynamic flow conditions, which are expected to present a different indication of media adsorption capabilities.

4.4. Minicolumn P Adsorption Study

Small (approximately 15.2 cm length) column studies were undertaken to determine amended BSM P adsorption capacity under flow conditions. Experiments were set up and run as described in Section 3.7, including the calculation of media P adsorption capacity by Equation 3-4. Influent P concentration for set I averaged 124 ± 8.9 μg/L (± SD), and pH average 6.57 ± 0.29 (± SD). For set II, influent P concentration averaged 122 ± 2.2 μg/L and pH averaged 6.60 ± 0.55. Table 3-3 details the media and flow regimes investigated.

Ideally, exhaustion of the media was desired during the course of these experiments to determine total media adsorption capacity when in equilibrium with the influent P solution. Exhaustion was defined as two consecutive days where the TDP concentration was at or above the influent P concentration. However, column capacity was generally depleted very slowly over time and due to constraints on allowable run time, columns were taken offline prior to complete exhaustion occurring. However, in every case media capability to remove P from the influent solution significantly diminished with time. The only media to show true exhaustion was the unamended BSM after 4.41 and 5.08 m of inflow for sets I and II, respectively (Figure 4-9). This is equivalent to 22.1 and 25.4 cm over the entire catchment assuming a cell sized at 5%, or approximately 0.23 years of rain in Maryland.

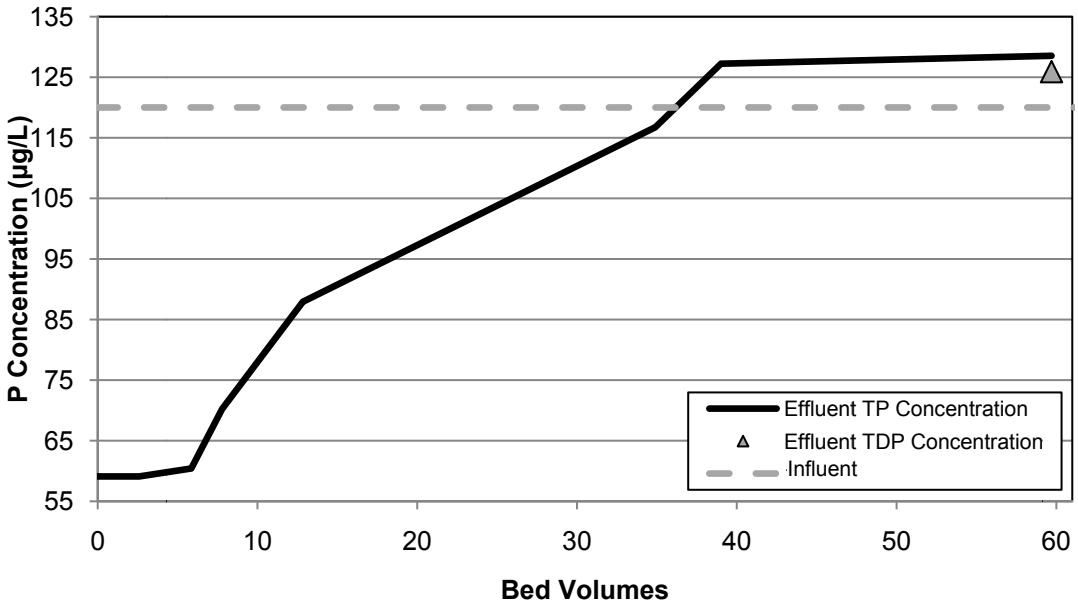

Figure 4-9. Breakthrough curve for continuously run unamended BSM media from set II. Mean influent TP concentration was 124 µg/L and pH was 5.58. The column ran for a total of 2 days at an inflow rate of 15.2 cm/hr. Total inflow was equivalent to 25.4 cm of rain over the entire catchment.

In terms of P adsorption, media were expected to perform approximately as well as during batch studies, and so column results were compared against batch results to evaluate performance. As seen with the batch tests, increasing the proportion of WTR in the media was expected to yield increasing media P adsorption capacity. Based on the results of the batch studies, the addition of HBM at approximately 3% oven dry weight along with WTR was expected to increase the adsorptive capacity of the media. Additional sand was expected to increase media adsorption as well by reducing the amount of fines which occlude WTR surfaces.

Intermittent flow studies were also conducted on three different media, as detailed in Tables 3-3 and 4-3, to more accurately replicate bioretention field conditions. The addition of HBM under such conditions was expected to yield further increases in media P adsorption over the long term as such organic material retains

Table 4-3. Media adsorption capacity at equilibrium with 120 µg P/L, in mg P/kg. Set I and Set II are experimental column results for media adsorption. Expected capacity is the calculated media adsorption with 120 µg P/L based on batch adsorption isotherms (Table 4-2). BSM: bioretention soil media; WTR: water treatment residual; HBM: hardwood bark mulch; LFBSM: low-fines BSM; ×: Data not collected; ‡: Outlier excluded; †: Intermittent flow regime.

	Set I		Set II		Expected
Media	Total	Dissolved	Total	Dissolved	Capacity
BSM	-1.00	0.422	0.706	×	13.1
BSM + 2% WTR	13.2	57.7	×	×	18.6
BSM + 4% WTR	‡ 14.4	84.0	43.7	62.2	25.6
BSM + 4% WTR †	×	×	† 8.14	† 27.2	25.6
BSM + 2% WTR + HBM	10.6	43.0	×	×	33.4
BSM + 4% WTR + HBM	57.5	62.3	† 37.6	† 52.7	45.0
LFBSM + 4% WTR	124	133	† 52.2	† 65.4	×
Sand + 4% WTR	×	×	132	×	×

water and reduced media drying (Borggaard et al., 2005). As media dries, P adsorbing amorphous metal (hydr)oxides crystallize, reducing their surface area and limiting the sites available for P adsorption (Borggaard et al., 2005). It was also expected that under intermittent flow, media would show temporary improvements in adsorption upon the reestablishment of flow following dry periods (Hsieh et al., 2007a). This is because of the biphasic nature of WTR and specifically Al (hydr)oxides; whereby after the cessation of flow, "fast" adsorption reactions no longer occur and "slow" reactions continue. During these "slow" reactions P molecules diffuse deeper into the WTR particles via pores (McGechan and Lewis, 2002; Makris et al., 2004), providing increased available adsorptive surfaces for P capture upon the recommencement of flow.

4.4.1. WTR-amended BSM

Column breakthrough curves show column effluent P concentration (μg/L) as a function of the cumulative number of bed volumes (BV) treated, which is the ratio of cumulative influent to the column media volume of 66.0 mL (L influent/L column media). The reduction in media P treatment can clearly be seen by the increasing effluent P concentrations as the experiments progress, such as for the unamended BSM from set II (Figure 4-9). Additionally, sharp increases in particulate P (PP) can be seen at points when there are large differences between TP and TDP, most notably after flowrate increases, for example with 4% WTR + BSM (4% BSM) in Figure 4-10. This is due to the migration of media from the column, which is discussed in greater detail below. In all instances, data tended to have a large amount of interdiurnal variability, attributed to particulate release and the combined impact of minor changes in influent P concentration and flowrate from day to day. Table 4-3 details the calculated media P adsorption capacity based on equations 3-4 and 3-5. The P adsorption capacity was calculated based on both column effluent TP measurements, as well as TDP measurements for columns that exhibited significant effluent turbidity. In many cases, media TDP adsorption capacity was significantly greater than that found for TP (Table 4-3). While this is predominantly because of PP losses from the column media, it must be noted that calculations based on TDP are a much more coarse measure of adsorption as TDP was analyzed for less consistently.

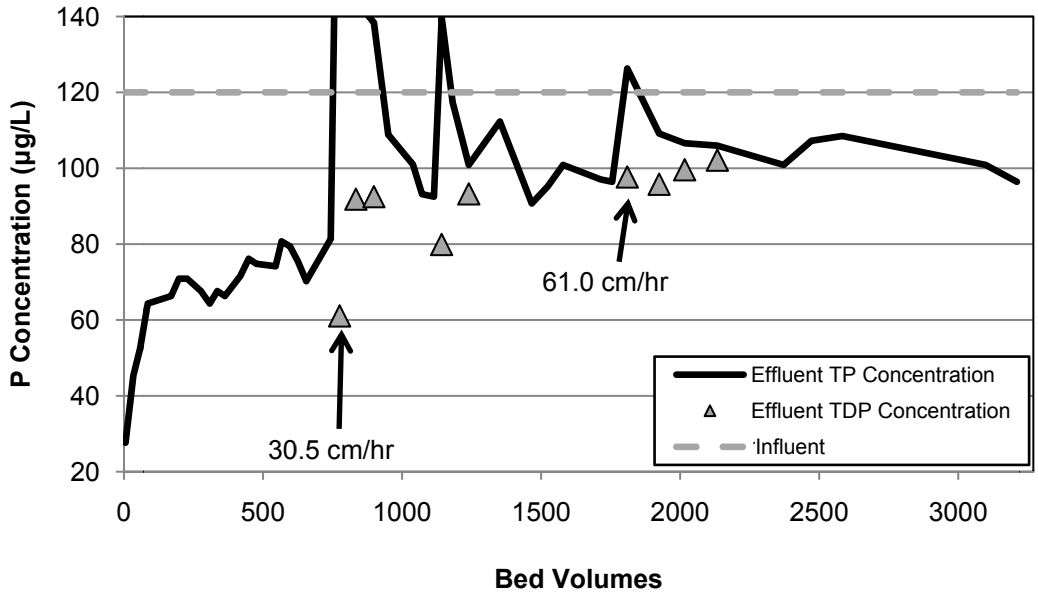

Figure 4-10. Breakthrough curve for continuously run BSM + 4% WTR from set II. Mean influent TP concentration was 122 µg/L and mean pH was 6.60. The column ran for a total of 64 days. Labeled arrows indicate increases in column flowrate from an initial rate of 15.2 cm/hr. Total inflow was equivalent to 20.9 m of rain over the entire catchment.

As stated previously, increasing WTR content produced increasing P adsorption capacity. However, column results were more mixed in terms of the magnitude of expected adsorption compared to batch studies. Subject to continuous flow, both unamended BSM and 2% WTR amended media (2% BSM) adsorbed less P to varying degrees relative to what was expected based on Freundlich isotherms (Table 4-2) from the batch studies. For instance, unamended BSM was expected to adsorb 13.1 mg P/kg based on batch study Freundlich isotherms (Table 4-2), but instead exported 1.00 mg P/kg. 2% BSM displayed adsorption of only 13.2 mg P/kg, which is somewhat lower than the predicted P adsorption capacity of 18.8 mg P/kg based on Freundlich isotherms. 4% BSM showed adsorption capacity of 43.7 mg P/kg during set II, better than the Freundlich isotherm-based expectation of 25.6 mg

P/kg. Conversely, TP adsorption for 4% BSM from set I performed significantly worse (Table 4-3), with equilibrium P adsorption of only 14.4 mg P/kg. This may likely be explained by PP releases, which reflected poorly in calculating media adsorption capacity. As a result of flowrate increases, column effluents often experienced an increase, in some cases a very significant increase, in turbidity and a concomitant release of PP. For example, the 2% BSM column from set I saw a turbidity increase of 6.27 to 61.4 NTU and a concomitant TP increase of 117 to 271 µg P/L upon flowrate increase to 61.0 cm/hr from 30.5 cm/hr. The 4% BSM under continuous flow from set II experienced an increase in turbidity from 5.47 to 85.4 NTU along with an increase from 81.4 to 233 µg P/L in TP after increasing the

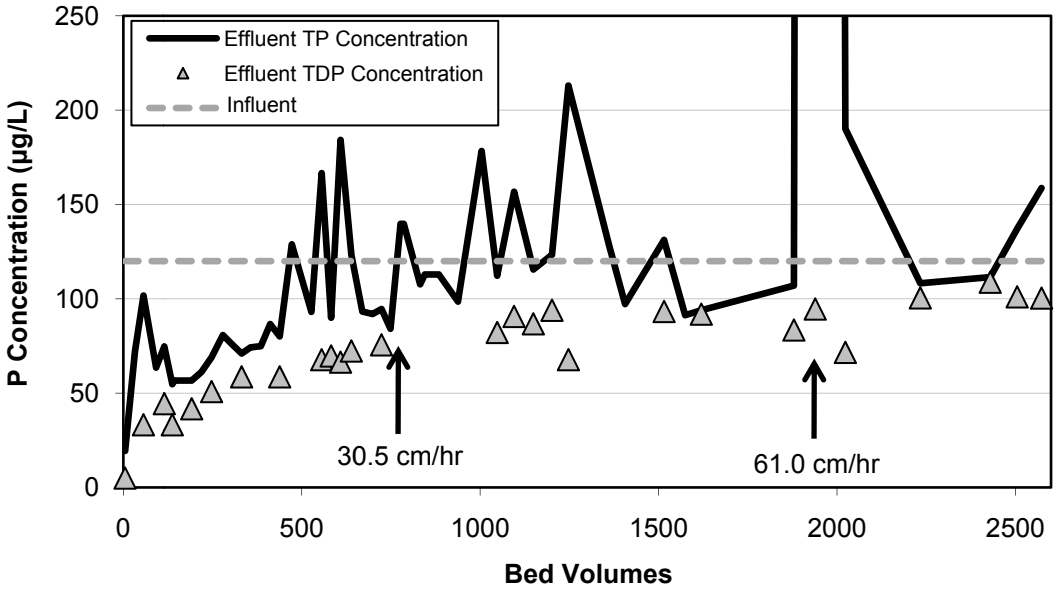

Figure 4-11. Breakthrough curve for continuously run BSM + 4% WTR from set I. Mean influent TP concentration was 124 µg/L and mean pH was 6.57. The column ran for a total of 57 days. Labeled arrows indicate increases in column flowrate from an initial rate of 15.2 cm/hr. Total inflow was equivalent to 16.7 m of rain over the entire catchment.

flowrate from 15.2 cm/hr to 30.5 cm.hr. In the majority of cases these increases did not have excessive influence on the calculated media adsorption capacity. The 4% BSM from set I, seen in Figure 4-11, was an exception to this. When the flowrate was increase to 61.0 cm/hr, sample turbidity increased to 3357 NTU. TP measured 5.20 mg/L, more than 40 times the influent P concentration. TDP at the same time, however, measured only 71.6 μg/L.

To account for this extreme event, the Dixon-Thompson test was performed, confirming that this sample point measuring 5.20 mg P/L was an outlier ($p < 0.05$) of the population of all column effluent samples. PP and turbidity levels did not return to normal, stable levels until the fourth day of increased flow. However, as only this single point was statistically an outlier, no additional data were excluded from media adsorption calculations. When all results were included in the media P adsorption calculations, TP capacity of -255 mg P/kg resulted. Excluding the outlier, TP capacity was 14.4 mg P/kg. It is believed that this estimated capacity is still negatively impacted by the elevated PP losses from the column because of the aforementioned continued residual PP losses after this event, leading to this low measure of capacity compared to batch and other column studies (Table 4-3).

In addition to continuous flow, 4% BSM was investigated under an intermittent flow regime (Figure 4-12). Over the course of the experiment, media P adsorption was only 8.14 mg P/kg, much worse compared to aforementioned batch or continuous flow studies (Table 4-3). This is believed to be the result of media drying during periods without inflow (Borggaard et al., 2005), which is assumed to have occurred as air was actively pumped through the column. As hypothesized, a

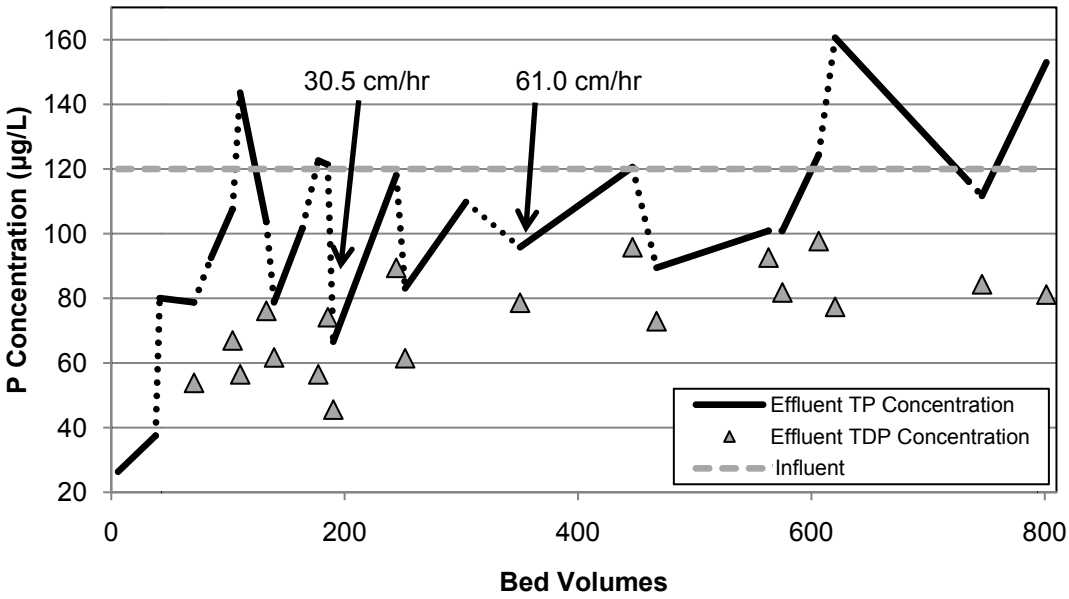

Figure 4-12. Breakthrough curve for intermittently run BSM + 4% WTR from set II. Mean influent TP concentration was 120 µg/L and mean pH was 6.63. The column ran 13 cycles (approx. 24 hours each) over a total of 86 days. Labeled arrows indicate increases in column flowrate from an initial rate of 15.2 cm/hr. Total inflow was equivalent to 5.21 m of rain over the entire catchment.

localized renewal or improvement in adsorption was observed after flow was reestablished following dry periods. This improvement was short lived and the media showed rapid decline in P adsorption, creating a sawtooth pattern for the effluent concentration. This supports the theory that during dry periods, secondary "slow" reactions are occurring, which free reactive surface sites for sorptive interactions with P. As flow continues, these newly re-exposed sites are quickly occupied, leading to the rapid decline in P adsorption.

4.4.2. Low-fines Media

LFBSM + 4% WTR (4% LFBSM) is presented to exemplify a LFBSM media breakthrough curve (Figure 4-13). Similar to BSM media, temporarily increased particulate release and turbidity were observed for LFBSM media after the flowrate

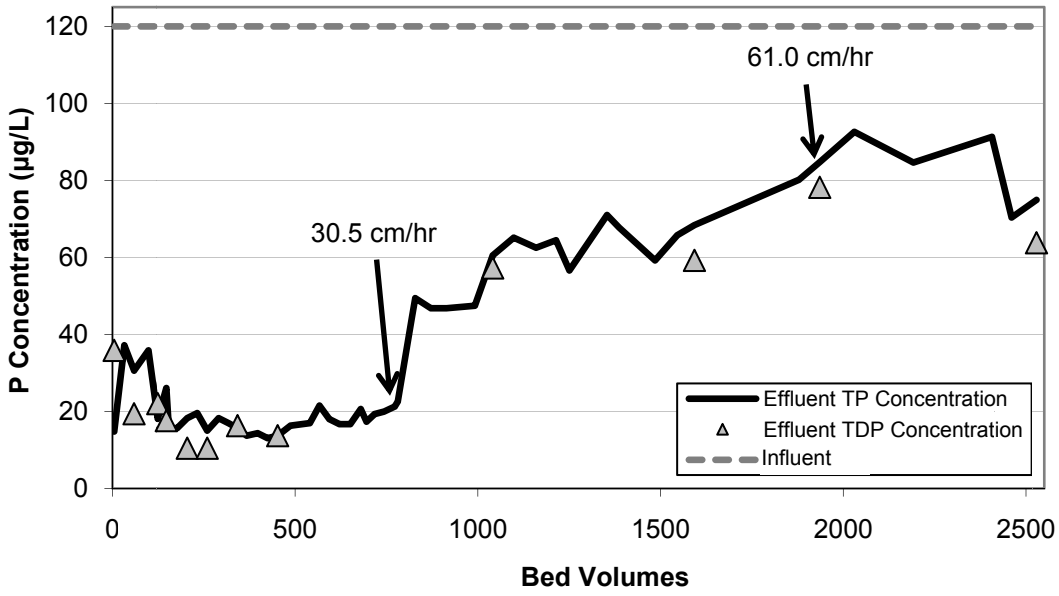

Figure 4-13. Breakthrough curve for continuously run LFBSM + 4% WTR from set I. Mean influent TP concentration was 124 µg/L and mean pH was 6.57. The column ran for a total of 57 days. Labeled arrows indicate increases in column flowrate from an initial rate of 15.2 cm/hr. Total inflow was equivalent to 16.5 m of rain over the entire catchment.

was increased, although to a lesser extent. By the second day after increasing the inflow rate from 15.2 cm/hr to 30.5 cm/hr, the 4% LFBSM media experienced an increase in turbidity from 7.39 to 15.3 NTU, along with an effluent TP increase of 20.0 to 49.4 µg P/L. This behavior was not observed for the 4% WTR amended sand media, although rapid increases in effluent P concentrations did occur. For instance, while turbidity dropped from 0.9 to 0.5 NTU after increasing the inflow rate from 15.2 cm/hr to 30.5 cm/hr, within two days after the flowrate increase, the effluent TP concentration had increased from 29.0 to 59.8 µg P/L. Similar to the reduced performance of media during column studies compared to batch, this increase in effluent P concentration from the amended sand column is attributed to further reduced contact time between the media and influent solution. The jump in effluent

concentration was followed by periods of leveling off as a steady state was reestablished.

Neither low fines media (4% LFBSM, Sand + 4% WTR) had batch isotherms determined to allow for a direct comparison with column studies. However, batch isotherms for LFBSM + 10% WTR and LFBSM + 3% WTR were determined and those media were expected to have adsorption capacities of 111 and 24.4 mg P/kg, respectively. Comparatively, both of the low fines column media far outperformed these batch results under continuous flow, with adsorption capacities of 124 and 132 mg P/kg for amended LFBSM and Sand, respectively (Table 4-3). Comparing the low-fines media results to the 4% BSM results, the low-fines media performed well, with the 4% BSM subject to continuous flow during set II displaying adsorption of only 43.7 mg P/kg. It is interesting that the low-fines media continued to display greater media P adsorption relative to analogous BSM mixtures for both batch and column experiments. For instance, WTR-amended LFBSM batch media unexpectedly showed higher P adsorption compared to WTR-amended BSM, contrary to initial hypotheses. Similarly, WTR-amended low-fines media exhibited greater media P adsorption than amended BSM under flow conditions as just detailed (Table 4-3). This suggests that decreases in fines content lead to further increases in media P adsorption in the presence of WTR, implying the need for increased WTR application to agricultural fields and bioretention media containing higher fines contents.

4% LFBSM was also investigated under intermittent flow to evaluate the performance of the media compared to BSM under more realistic bioretention conditions. Media adsorption dropped under intermittent flow compared to continuous from 124 to 52.2 mg P/kg, but maintained greater media adsorption relative to 4% BSM also subjected to intermittent flow, which showed adsorption of 8.14 mg P/L. In fact, intermittent 4% LFBSM showed greater adsorption than continuous flow 4% BSM, which had measured P adsorption capacity of 43.7 mg P/kg during set II (Table 4-3). This further supports the conclusion that decreases in media fines content yield increases in P adsorption.

4.4.3. Hardwood Bark Mulch Amended BSM

BSM amended with both WTR and HBM showed increased P adsorption under batch conditions. Under column conditions results were not as consistent. BSM amended with HBM and 2% WTR (2% HBM) adsorbed only 13.2 mg P/kg compared to the 18.6 mg P/kg expected media P adsorption capacity calculated from Freundlich isotherms conducted during batch studies (Table 4-3). The media also showed worse P adsorption than 2% BSM during column experiments, as 2% BSM measured adsorption of 13.2 mg P/kg and 2% HBM demonstrated an adsorption capacity of only 10.6 mg P/kg (Table 4-4). This was not expected as batch study Freundlich isotherms predicted 2% BSM to have a media P adsorption capacity of only 18.6 mg P/kg, while 2% HBM was predicted by Freundlich isotherms to have a greater P adsorption capacity of 33.4 mg P/kg. In contrast, BSM + HBM + 4% WTR (4% HBM) showed greater media P adsorption than it had during batch studies or compared to 4% BSM column studies (Table 4-4). 4% HBM had a measured P

adsorption capacity of 57.5 mg P/kg, while the batch study Freundlich isotherm predicted an adsorption capacity of only 45.0 mg P/kg, and 4% BSM media under continuous flow conditions measured adsorption of 43.7 mg P/kg during set II.

The increased adsorption of 4% HBM and decreased adsorption of 2% HBM relative to batch studies cannot be attributed to a direct release of P from the HBM. Because both media (2% and 4% HBM) were amended with the same proportion of mulch, a release of P would have caused a unified increase or decrease in adsorption relative to media unamended with HBM, not the divergent behavior observed. It is believed that this observed behavior is the result of the formation of an insoluble, possibly colloidal, Al-OM-P complex. Conceivably, some portion of the Al contained in the WTR, dissolved or colloidal OM that contains P_o (OM_P), and P in solution may have resulted in the formation of this complex when all three components were present in the same system (Figures 4-14 and 4-15). The formation of such complexes in soil systems have been reported by numerous authors (e.g., Sinha, 1971; Gerke and Hermann, 1992; Dolfing et al., 1999; Hens and Merckx, 2001). The formation of such a complex may have resulted in increased measured adsorption by providing additional reaction sites for the adsorption of P from solution.

The disparate behavior of the HBM media relative to the non-HBM is believed to be caused by a limitation in reaction time and available surface adsorption reactive sites in the 2% HBM column system. The longer reaction time in the batch studies (24 hrs) may have allowed Al to complex with both P and OM_P, preventing the solubilization of OM_P as well as removing a significant portion of P from solution

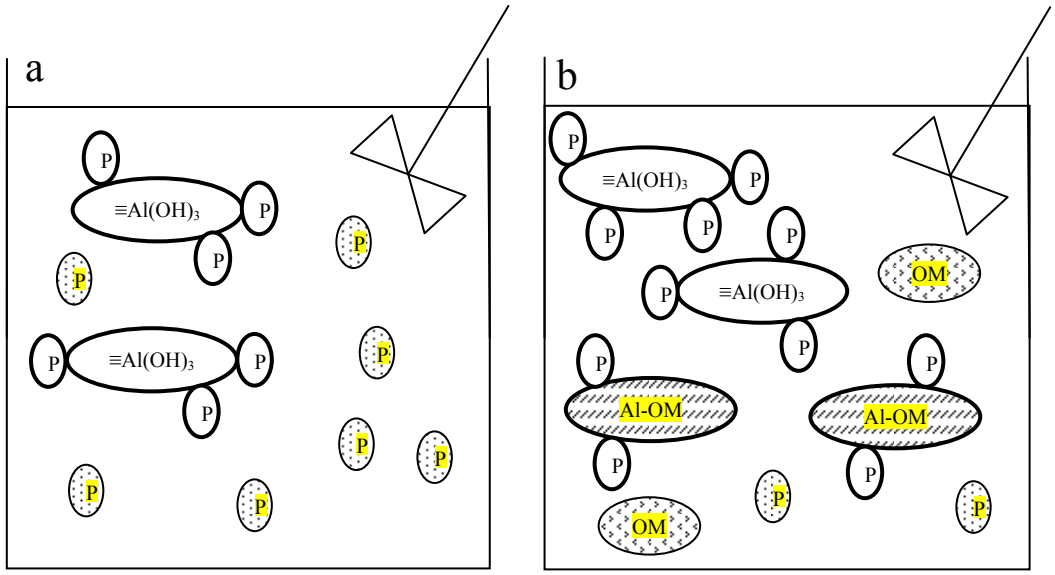

Figure 4-14. Representation of Al, OM, and P interactions in HBM-amended and -unamended batch systems. The reactors display (a) BSM + WTR batch system and (b) BSM + WTR + HBM batch system. The figures explain that HBM amended media exhibited increased P adsorption relative to the media without HBM in batch systems because of increased sequestration of P in an Al-OM-P complex.

via adsorption to the OM itself (Figure 4-14). This would have resulted in greater measured adsorption for the HBM mixtures relative to the non-HBM mixtures.

In the column experiments (Figure 4-15), the Al-OM-P complex may have formed initially but not completely because of reduced reaction time, which was a byproduct of P and OM_P being flushed from the system with throughflow. At the lower WTR concentration of the 2% HBM mixture, the system Al concentration may have been small enough that Al-OM-P complex formation was insufficient to manifest as increased media adsorption. Instead, more influent P exited the column relative to the batch system because flow limited the reaction time with adsorbents. Also, OM_P may have leached from the column (Figure 4-15c), which upon effluent

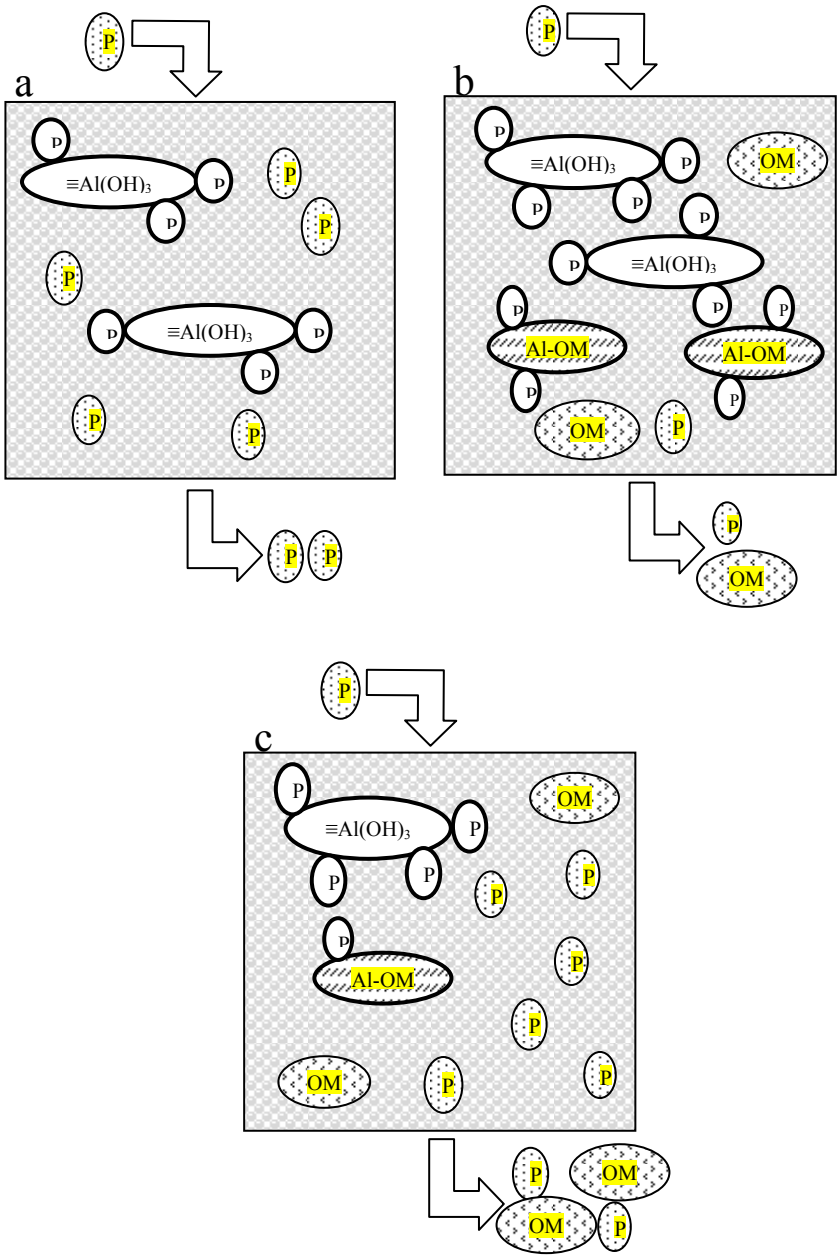

Figure 4-15. Representation of Al, OM, and P interactions in HBM-amended and -unamended column systems. The reactors display (a) BSM + WTR column system, (b) 4% HBM column system, and (c) 2% HBM column system. The figures explain that when HBM amended media exhibited increased P adsorption relative to the media without HBM, it was though sequestration of P in an Al-OM-P complex. The 4% HBM column experienced the formation of this complex, leading to increased adsorption relative to 4% BSM by sequestration of both P and OM_{D-C}. The 2% HBM media did not show increased adsorption relative to 2% BSM column media because the system WTR concentration was insufficient for both P and OM capture under flow conditions.

sample digestion would have been measured as P exiting the system, negatively impacting the measured column media P adsorption. This is supported by Guppy et al. (2005), who explain that the increased P in soil solution upon application of OM amendments is not from reduced adsorption capabilities of the soil or competition for adsorption sites between OM and P, but instead results from additional P supplied to solution by the OM amendments themselves.

Comparatively, the 4% HBM media had greater WTR mass, possibly providing sufficient Al content for Al-OM-P formation and minimal release of P and OM_P (Figure 4-15b). The 4% HBM column was subject to limited reaction time, just as was the 2% HBM column. However, unlike the 2% HBM column, the 4% HBM column showed increased adsorption relative to the non-HBM because the available reactive surface sites provided by the Al-WTR were sufficient to adsorb both P and OM_P from solution. By capturing this OM_P fraction, the column media measured increased adsorption relative to both the 4% BSM column and batch study 4% HBM (Figure 4-16). However, while the occurrence of Al-OM-P complexes in soil solution have been previously reported, little data could be found on formation constants or kinetic impacts (i.e., soil water flow) on the formation and P adsorption capabilities of these compounds. Consequently, further research is necessary to characterize this complex P removal mechanism within the BSM system.

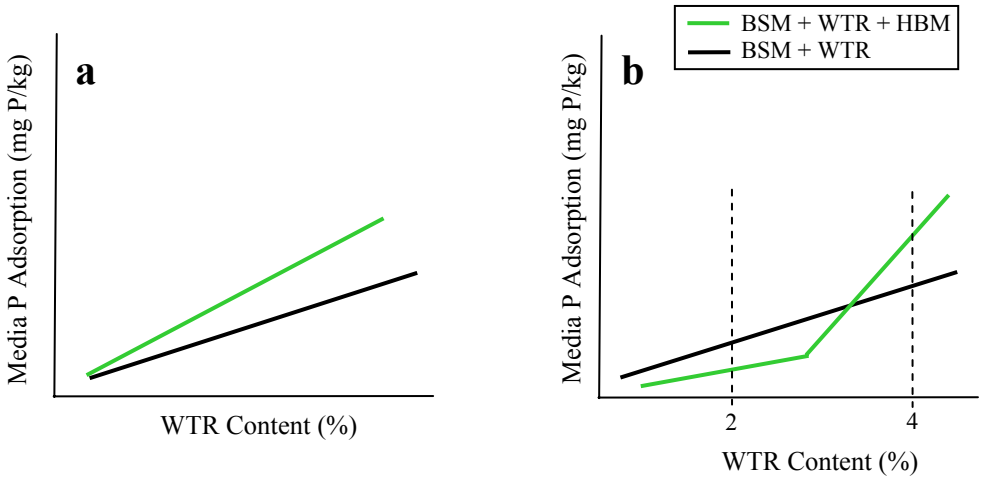

Figure 4-16. Comparison of relative media adsorption capacity trends under (a) batch and (b) continuous flow column conditions, assuming consistent P concentrations in solution, uniform flow conditions, and uniform HBM contents for HBM-amended media.

Similar to both BSM- and LFBSM-amended media, HBM-amended media demonstrated a reduction in media P adsorption under intermittent flow conditions (Figure 4-17). The 4% HBM media showed the smallest % drop in total P adsorption density for intermittent media relative to its continuous flow counterpart among all 3 media tested under both flow regimes (34.6% drop compared to 57.9%, 43.5%, and 81.4% for 4% LFBSM, 4% WTR set I, and 4% WTR set II, respectively).

HBM-amended media did not exhibit elevated turbidity or significant particulate releases as other media did, but problems with clogging were observed, especially during experimental set I. During the first set, both the 2% HBM and 4% HBM media experienced irreversible and complete clogging after increasing the flowrate to 30.5 cm/hr but prior to the increase to 61.0 cm/hr. In the case of both columns, the pumping rate was increased in an attempt to reach the desired flowrate

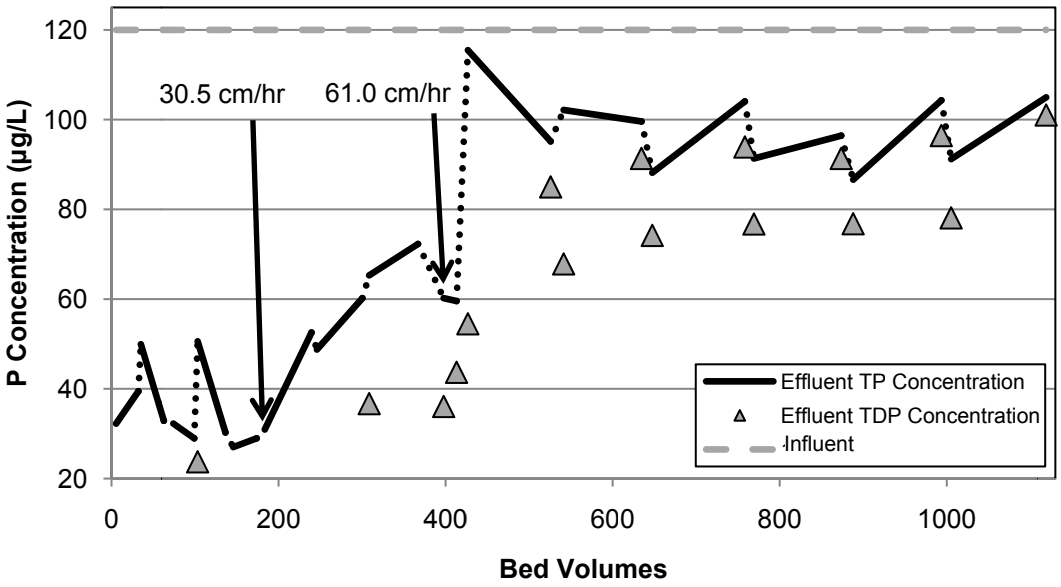

Figure 4-17. Breakthrough curve for intermittently run BSM + 4% WTR + HBM under intermittent flow from set II. Mean influent TP concentration was 120 µg/L and mean pH was 6.63. The column ran 15 cycles (approx. 24 hours each) over a total of 97 days. Labeled arrows indicate increases in column flowrate from an initial rate of 15.2 cm/hr. Total inflow was equivalent to 7.28 m of rain over the entire catchment.

but to no avail. After continually decreasing throughflow even with sustained, elevated pumping rates, the columns were ultimately taken offline prematurely. This may reflect negatively on the calculated media adsorption because the media is not at true equilibrium with the influent. Most of the columns were taken offline prior to breakthrough, though, so the early cessation of these experiments is not extraordinary.

As clogging was observed only with media amended with HBM, it was concluded that this phenomenon was a result of HBM addition. To counteract this and prevent clogging during experimental set II (Figure 4-17) the HBM was not only sieved to < 2 mm but also to > 300 µm to prevent possible clogging by HBM fines material. Regardless, upon attempting to increase the flowrate for this column to 61.0 cm/hr, the desired throughflow was unable to be achieved even with a drastically

increased pumping rate. However, throughflow did not steadily deteriorate over time as observed with the set I columns, and the set II column was allowed to continue at a reduced flowrate (0.75 mL/min; 8.9 cm/hr). Over a short pumping time (approximately 36 hours) the column flowrate gradually increased and reached the target flow. However, it is not known if this is a direct result of removing the HBM fines, or if the intermittent flow regime of the column also played some part in the alleviation of clogged conditions. Regardless, the use of HBM as a soil amendment at the field level is not expected to lead to media clogging because clogging was not observed at 15.2 cm/hr flow, which is the only tested flowrate within the typical bioretention range.

4.5. Column Media Behavior

Overall, media adsorption behavior agreed with that of the batch studies in that increasing WTR content resulted in increasing adsorption capacity (Figure 4-18). However, media P adsorption was generally much lower for column studies than that calculated from batch study isotherms. This is likely caused by the reduced contact time between the P in solution and the media surface. Similar to batch results, HBM addition and decreasing fines content led to increasing P adsorption, although these parameters were only investigated in the presence of WTR. Batch studies suggested a decrease in adsorption with HBM addition and decreasing fines content when no WTR was present.

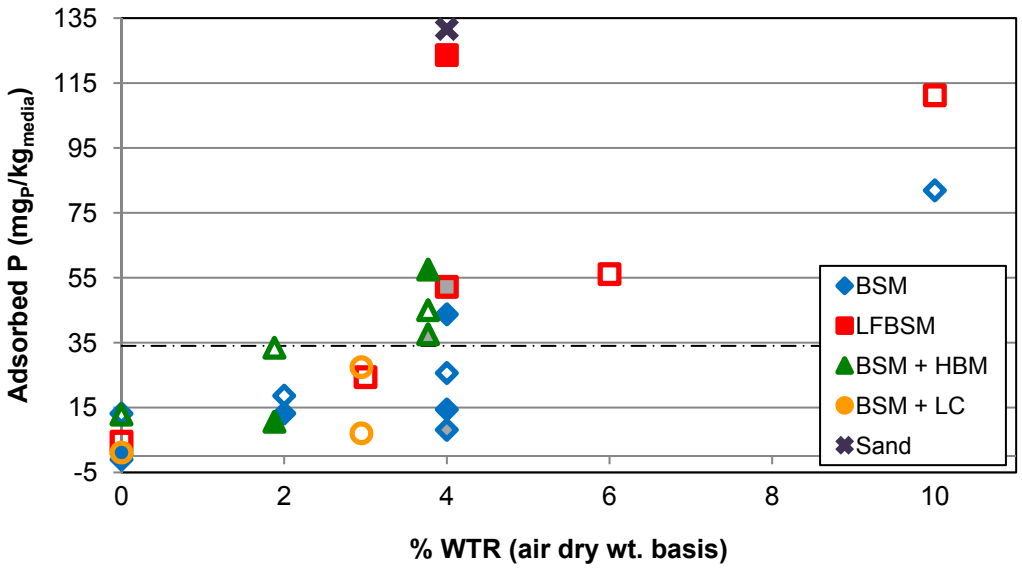

Figure 4-18. Batch and column data detailing P adsorption at equilibrium with 120 µg P/L solution as a function of WTR content (air dry weight basis). Batch adsorption data was calculated from Freundlich isotherms. Open marks represent batch data, closed marks represent data from columns subject to continuous flow, and open grey-filled marks represent intermittent column data. The dotted line represents the media adsorption benchmark of 34 mg P/kg.

LFBSM showed greater P adsorption relative to other batch and column media. Even under intermittent flow, gross media P adsorption was greatest of all 3 media subjected to this flow regime. The even greater adsorption of the sand + 4% WTR media suggests that with the specific media components used in this study fines content and P adsorption are negatively correlated. This relationship may likely exist for other media components as well.

2% HBM media for column studies showed decreased adsorption compared to 2% BSM media, while 4% HBM still exhibited greater media P adsorption than 4% BSM. In conjunction with the behavior of these media mixtures during batch studies, this suggests the formation of an Al-OM-P complex from constituents of the WTR

and HBM, which may yield reduced losses of P and P-containing OM molecules. This complex may have formed within the 2% HBM column but been insufficient to prevent leaching of $OM_{D\text{-}C}$, resulting in a reduced measure of media P adsorption.

The 4% HBM media also was the least impacted by drying during intermittent flow, as evidenced by this media having the smallest decrease in P adsorption relative to its continuous flow counterpart. The development of a characteristic sawtooth pattern in intermittent column effluent P concentrations across all 3 intermittent flow studies also gives support to the hypothesis that "slow" adsorption interactions continue to occur after flow has stopped and "fast" adsorption is no longer taking place.

These preliminary media studies illuminate media behavior under static and dynamic flow conditions. They also give an indication of the ideal BSM mixture for optimal P adsorption and treatment. The performance of such an ideal mixture is not known, however, especially under conditions typical of a bioretention facility.

Chapter 5: Vegetated Column Pollutant Treatment Study

Two vegetated columns were constructed to replicate conditions experienced in a full scale bioretention system. Each column contained a different media, one typical of a standard bioretention cell (control media), and the other consisting of the control mix amended with 5% Al-WTR (experimental media), as described in Section 3.8.3. The column vertical dimensions were of actual bioretention scale (0.9 m), and hydraulic loading was applied at a surface loading rate to again be typical of a bioretention cell (38.5 cm/hr). Across all experiments, influent solution pH was 5.8 ± 0.6, turbidity was ≤ 1.3 NTU, and conductance was 1.3 ± 0.04 mmho/cm. Influent P concentrations averaged 144 ± 79.1 µg/L, with standard runs averaged 117 ± 3.7 µg/L. Cumulatively, the experimental column received 28 m (796 L) of influent, while the control column received 27 m (774 L). This 4% difference was caused by slight variations in flowrate throughout the life of the columns. These surface loading rates are equivalent to approximately 1.3 years worth of rain for the Washington region, assuming a bioretention cell sized at 5% of catchment.

5.1. Vegetation Mortality

Plants were originally purchased from a local nursery in January 2010 to acclimate to the laboratory environment before transplantation to the bioretention column. While they were provided with sufficient light and water, the plants became infested with an unidentified species of winged insect, and despite all best efforts the four individuals died within a matter of weeks.

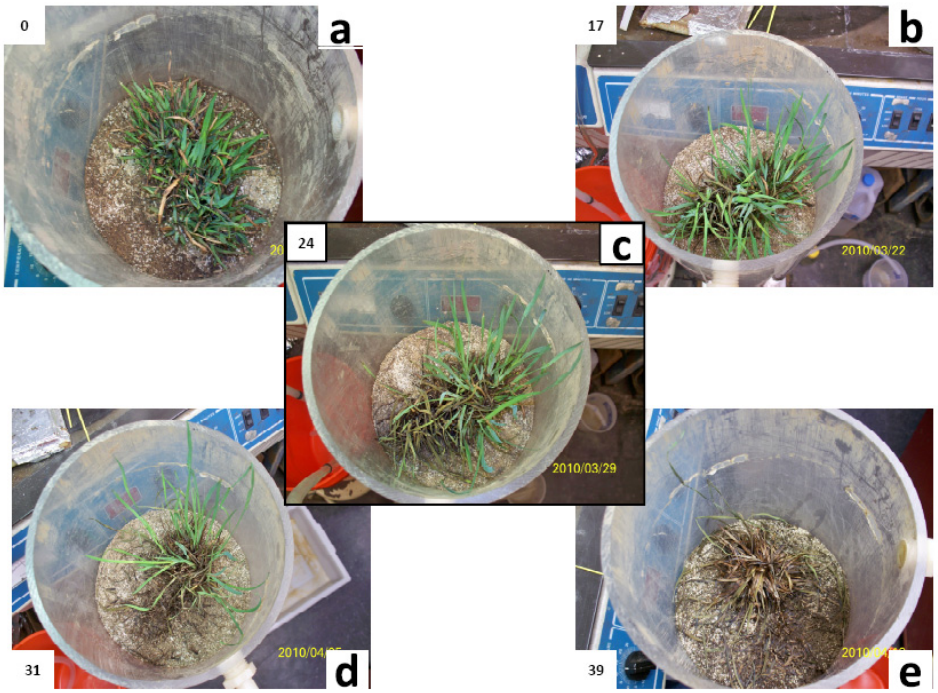

Figure 5-1. Chronosequence of control column *S. angustifolium* development. Numbers in the upper/lower corners identify days of growth after planting.

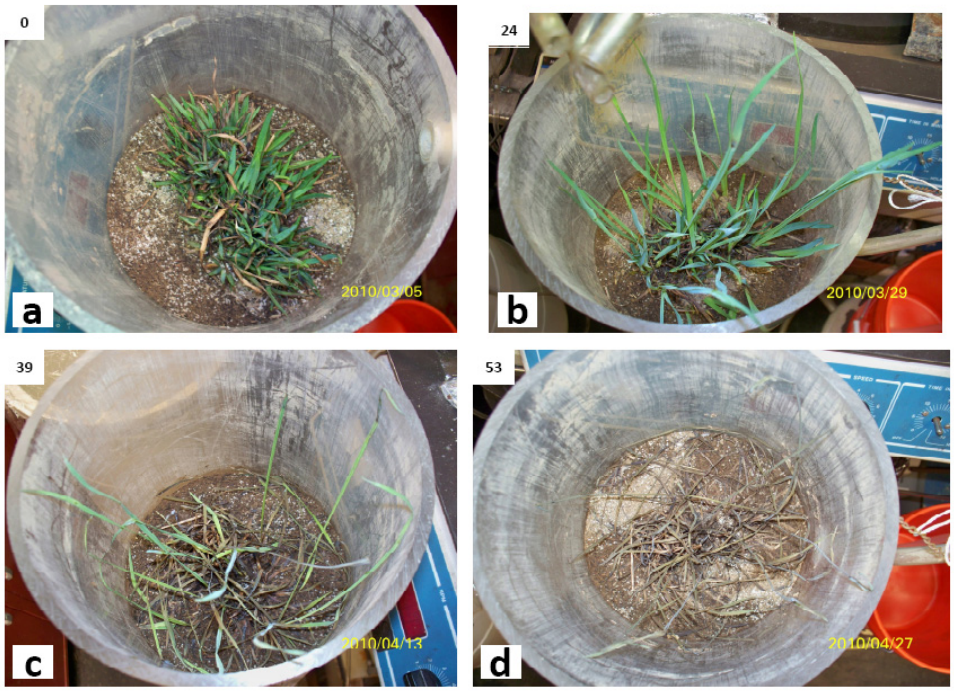

Figure 5-2. Chronosequence of experimental column *S. angustifolium* development. Numbers in the upper corners identify days of growth after planting.

Additional plants were purchased just prior to construction of the columns, and on 5 March, 2010 (day 0) two individual *Sisyrinchium angustifolium* were planted in each bioretention column (Figures 5-1a and 5-2a). Plants in both columns appeared to fare well initially (Figures 5-1b and 5-2b). However, an initial plant in the control column began to show signs of stress around day 24 (Figure 5-1c), becoming brown and languishing. This individual died by day 31 (Figure 5-1d). The second surviving individual in the control column began to show stress almost immediately after the first perished, and was dead by day 39 (Figure 5-1e).

Plants in the experimental column fared better, although ultimately succumbed to the same fate. While initially appearing to thrive (Figure 5-2b), both plants began to show signs of stress around day 39 (Figure 5-2c), beginning to wither and appear brittle, although remaining green in color. Gradually, color faded and both individuals expired around day 53 (Figure 5-2d).

It must be noted that, as had occurred previously, there was an issue with winged insect infestation in both columns. Photographs were attempted, but the small size of this particular species made pictures indistinct. Additionally, plant stress may have been caused by other variables, such as excessive water from large weekly "storms", or light being provided via artificial sources rather than natural sunlight. Regardless, as plants in both columns ultimately perished, it is not believed that WTR or Al phytotoxicity is the cause of their demise.

5.2. General Column Trends

Data for all experimental runs can be seen in Figure 5-3, detailing TP and TDP effluent concentrations for both the experimental and control columns. Influent concentrations differed between runs, but in all cases effluent behavior was similar. The control column discharged P greater than the influent concentration at the beginning of each experiment, but the concentration dropped with continued flow and eventually P removal from the influent was found. Primarily, however, net P was released by the media. This drop in P concentrations led to an exponential decay-shaped curve. TDP followed the same pattern as TP, although the degree of difference between the two (i.e., PP) differed between and within runs. Head buildup never developed in the control column.

The experimental column behaved very differently from the control with respect to P. Effluent TP was much lower, and in most instances the majority of P in the influent was removed. Generally, removal was high at the beginning of flow addition and worsened for the next 15 to 30 minutes, gradually dropping thereafter. This created a pattern of a TP peak around the second or third sample (15 – 30 minutes). This behavior produced a pollutograph with a rising limb and a falling limb that was strongly skewed to the right. The approximately horizontal portion of the falling limb was often not particularly consistent, but fluctuated over a range of about 10 to 15 μg/L. TDP, similar to the control column, started relatively high (approximately 10 to 20 μg/L) and dropped with flow, although in almost all instances effluent TDP concentrations were below detection limit (10 μg/L) within one hour. In several instances the experimental column developed head, but the head

Figure 5-3. Effluent P concentration as a function of cumulative column bed volumes of flow for both the control and experimental columns runs (a) numbers 1-6 and (b) numbers 7-13. Influent P concentration varied by experiment but ranged from 68.4 – 476 µg/L. Mean pH was 5.8. Samples that measured below the method detection limit are estimated as 5 µg/L, and are indicated by open symbols.

remained < 15.2 cm (6 in). Influent EMCs and effluent EMCs for both columns across all runs and pollutants are presented in Table 5-1.

5.3. Standard Condition Experiments

Standard runs (nos. 1 – 5, 8, and 13) where the columns were subjected to a constant flowrate of 38.5 cm/hr (182 mL/min) and concentration of 120 μg P/L are compared for TP, TDP, and PP in Figure 5-4. Initially for the experimental column one can see a 73.6% (17.3 to 4.6 μg/L) drop in effluent PP EMC from the first to the fifth replicate, while TDP EMC remains low and more consistent (6.7 ± 1.5 μg/L; Table 5-1). This shows the stabilization of the column by the fifth replicate as initial soluble materials are flushed, and it is the fifth run (10.4 to 12.9 BV) that is used as a baseline against which other experimental runs are compared. Run 8 (6.3 and 7.5 μg/L TDP and PP, respectively) shows a slight increase in both TDP and PP EMCs relative to run 5 (5.5 μg/L TDP and 4.6 μg/L PP), but a small decrease relative to the previous run 7 (5.0 μg/L TDP and 10.1 μg/L PP). This behavior is believed to show that the column is still returning to a steady state after the elevated flowrate and concentrations encountered in the seventh run. For run 13 (5.0 and 5.3 μg/L TDP and PP, respectively), the experimental column results are nearly identical to those of run 5 (5.5 and 4.6 μg/L TDP and PP, respectively), providing further evidence that this behavior is the typical, stable behavior of the column when subjected to the standard flow and concentration conditions.

Table 5-1. Experimental and control column effluent EMCs and influent EMCs. Influent TDP is not listed as it is the same as TP because all influent P was soluble. Influent NO_2^--N is not listed as it was not a pollutant included in the influent. TP: total phosphorus; TDP: total dissolved phosphorus; PP: particulate-associated phosphorus; NO_3^--N: nitrate nitrogen; NO_2^--N: nitrite nitrogen; TKN: total Kjeldahl nitrogen; TN: total nitrogen.

	Experimental Column							Control Column							Influent			
Test No.	TP (µg/L)	TDP (µg/L)	PP (µg/L)	NO_3^--N (mg/L)	NO_2^--N (µg/L)	TKN (mg/L)	TN (mg/L)	TP (µg/L)	TDP (µg/L)	PP (µg/L)	NO_3^--N (mg/L)	NO_2^--N (µg/L)	TKN (mg/L)	TN (mg/L)	TP (µg/L)	NO_3^--N (mg/L)	TKN (mg/L)	TN (mg/L)
1	25.1	7.8	17.3	0.928	13.2	0.889	1.83	167	127	40.1	0.719	24.1	1.23	1.95	117	0.740	0.980	1.72
2	20.0	8.4	11.6	0.691	6.32	0.468	1.16	156	93.2	62.6	0.618	4.86	0.885	1.51	111	0.703	1.07	1.78
3	19.6	6.8	12.8	0.547	5.08	0.349	0.901	164	97.2	66.6	0.504	6.24	1.08	1.59	120	0.800	1.06	1.86
4	12.1	5.0	7.1	0.493	4.87	0.397	0.895	189	120	68.9	0.533	11.3	1.01	1.55	114	0.743	1.10	1.84
5	10.0	5.5	4.6	0.458	4.98	0.383	0.846	186	117	69.0	0.667	22.7	1.20	1.88	119	0.743	1.03	1.77
6	12.9	5.6	7.3	0.521	4.39	0.541	1.07	220	114	106	0.724	12.3	1.22	1.95	105	0.740	1.09	1.83
7	15.1	5.0	10.1	1.88	6.60	0.712	2.60	273	170	103	2.01	18.8	1.62	3.65	313	2.21	2.60	4.81
8	13.8	6.3	7.5	0.936	3.89	0.709	1.65	180	94.3	86.2	1.02	10.0	1.44	2.47	118	0.700	1.25	1.95
9	23.5	7.4	16.1	2.12	4.82	0.838	2.96	237	126	111	2.26	18.9	1.74	4.02	326	2.37	2.62	4.99
10	16.5	5.0	11.5	0.692	1.00	0.373	1.07	292	177	115	1.05	14.1	1.02	2.09	68.4	0.520	0.809	1.33
11	17.3	5.0	12.3	0.775	1.00	0.327	1.10	640	378	262	0.827	21.0	1.41	2.26	114	1.41	1.03	2.44
12	8.9	5.0	3.9	0.658	1.00	0.327	0.986	427	258	170	0.792	19.1	1.26	2.07	122	0.830	1.12	1.95
13	10.3	5.0	5.3	0.712	1.00	0.281	0.994	322	158	164	0.734	19.2	0.912	1.67	122	0.703	1.04	1.75
Cumulative	16.1	6.1	10.0	0.891	4.80	0.524	1.42	245	144	102	0.978	13.3	1.22	2.22	146	0.880	1.31	2.19

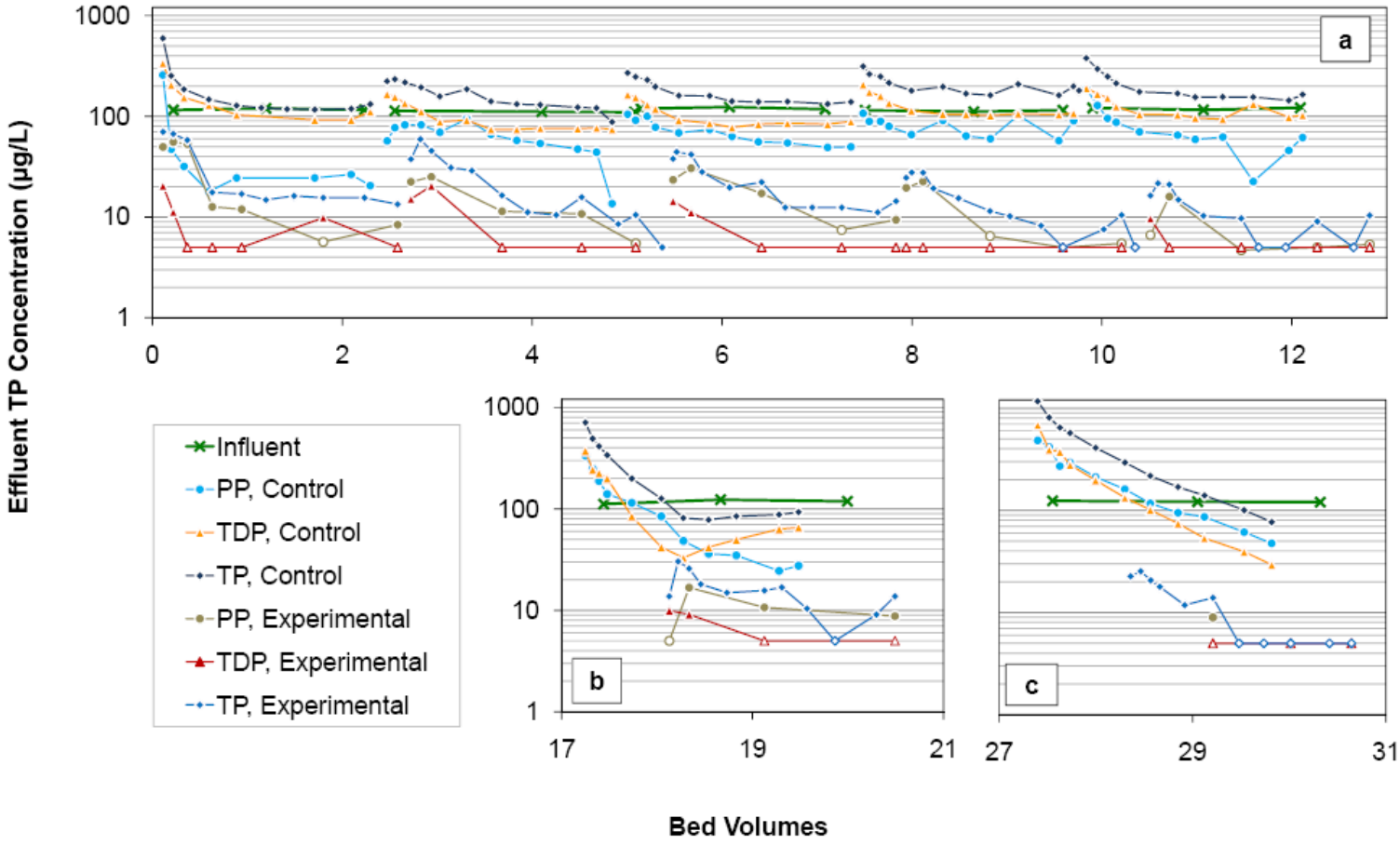

Figure 5-4. Effluent TP concentration for standard condition runs (a) numbers 1-5, (b) number 8, and (c) number 13, as a function of cumulative column bed volumes of flow for both the control and experimental columns. Influent P concentration measured 117 ± 4.4 µg/L. Mean pH was 5.9. Samples that measured below the method detection limit are estimated as 5 µg/L, and are indicated by open symbols.

The control column exhibits very different behavior during the standard runs. After an initial drop in TP effluent EMC from runs 1 to 2 (167 to 156 μg/L), concentrations increased with each experiment (156 to186 μg/L). This shows that the media's adsorption capacity was exhausted during the first two runs. This same pattern of increasing TP EMCs continues with runs 8 (181 μg/L) and 13 (322 μg/L), although the climb in EMC magnitude is not linear because of the varying experimental conditions. This same pattern of consistently increasing effluent EMCs is followed by both TDP and PP, ranging from 93.2 to 158 μg/L TDP and 40.1 to 164 μg/L PP. This increasing release of P must have a source to comply with the law of mass conservation. A proportion of this may be attributed to degradation of the HBM and *S. angustifolium* from the media, as evidenced by the increasing PP effluent EMCs and the turbid, tea-colored column outflow. Also, the increasing P releases from the column are believed to be washout of previously adsorbed P from runs 7 and 9, which both utilized a higher influent P concentration and subsequently were the only experiments to produce net adsorption in the control column (see Section 5.5).

Ultimately, under standard conditions (38.5 cm/hr, 120 μg/L) the experimental column far out performed the control column. The experimental column showed consistent removal of P from solution, with EMCs ranging from 10.0 to 25.1 μg/L, while the control column exported P for all standard runs. Control TP EMCs ranged from 156 to 322 μg/L. Experimental TP effluent EMCs were an 85.0 to 96.8% reduction compared to the control column TP EMCs under standard condition, and the experimental column consistently treated influent via adsorption to maintain

effluent concentrations ≤ 25 μg/L, the EPA recommended limit for freshwater lakes and reservoirs (US EPA, 1986).

5.4. Hydropollutograph Experiments

Experimental runs 6 and 9 were deemed 'hydropollutograph' experiments, whereby the columns were subjected to variable influent flowrate and pollutant concentrations in an attempt to replicate the behavior of an actual runoff event. Run 6 followed a 'standard' run, so column behavior was not impacted by previous non-standard conditions. In both figures, influent concentration is plotted as the mean cumulative BVs of both columns for a given time. A more proper depiction of influent concentration relative to effluent may be seen in Figure 5-5b where concentration is plotted as a function of time for run 9.

One can see from Figure 5-6 that the experimental column shows very little exceptional behavior compared to all other column pollutographs, exhibiting a pollutograph with an initial peak that was skewed to the right and a falling limb that becomes nearly horizontal, but with a slightly fluctuating concentration. The TP effluent EMC was slightly elevated relative to the previous 'standard' run (12.9 vis-à-vis 10.0 μg/L), but this was caused by an increase in effluent PP as the TDP EMC is nearly unchanged (Table 5-1, Figure 5-7a). This additional PP release is likely the result of the increased flowrate experienced by the column for this experiment.
The control column followed previous trends. Peak effluent concentration increased 34.7% relative to the previous experiment (from 378 to 509 μg/L), as did TP (186 to 220 μg/L) and PP (69.0 to 106 μg/L) EMCs, with the highest concentrations found initially. TDP was relatively unchanged (114 vis-à-vis 117 μg/L, 2.82% decrease),

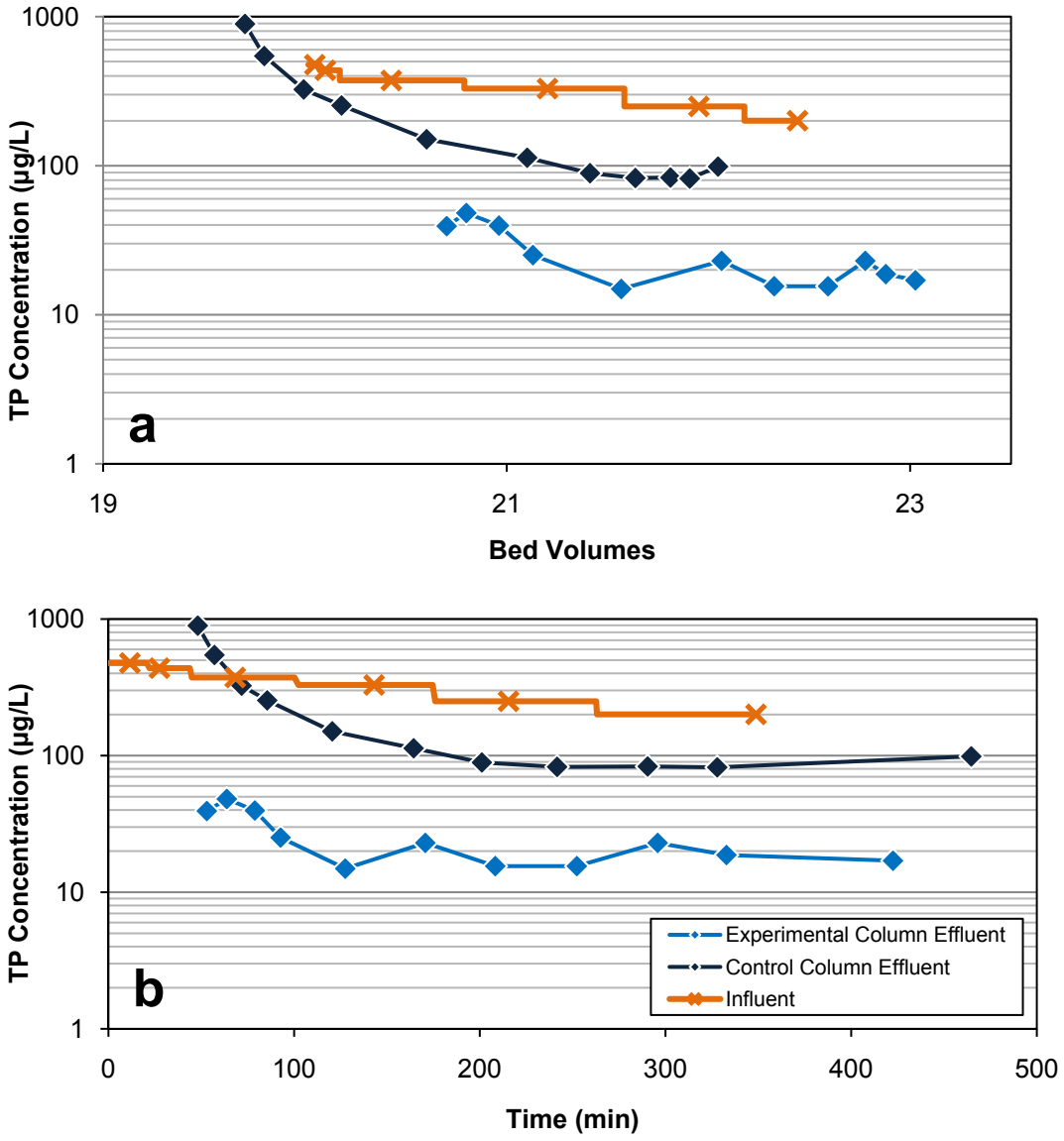

Figure 5-5. Run number 9. Experimental and control column effluent concentrations plotted against (a) column cumulative bed volumes of flow, and (b) run time. Columns were subjected to variable influent flow rates of 50.3 to 345 mL/min, and TP concentrations ranging from 201 to 476 µg /L. Influent solution contained 0.01 M KCl as a background electrolyte and had pH of 5.9 ± 0.7. This experiment also investigated an extended antecedent dry period of 13 days.

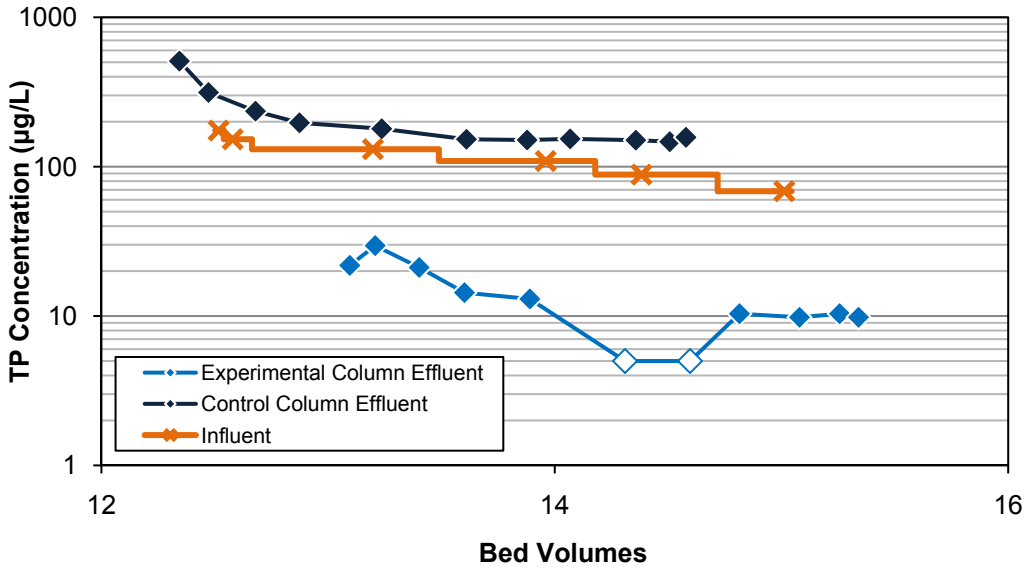

Figure 5-6. Run number 6. Experimental and control column effluent concentrations plotted against column cumulative bed volumes of flow. Columns were subjected to variable influent flow rates of 64 to 327 mL/min, and TP concentrations ranging from 69 to 175 µg/L. Influent solution contained 0.01 M KCl as a background electrolyte and had pH of 5.7 ± 0.5.

and like the experimental column the increased release of P was the result of released PP (Table 5-1, Figure 5-7b). Again, this is attributed to increased inflow rate.

Run 9 (Figure 5-5) subjected the columns to the same inflow rates as run 6, but increased the concentration of each hydropollutograph 'step' by a factor of approximately 2.5 to 476 and 201 µg/L for the initial and final concentrations, from 175 and 68.5 during run 6 (Table 3-8). Additionally, this experiment was also conducted after a doubled antecedent dry period of 13 days. Consequently, the experimental column effluent experienced an increase in both TDP and especially PP relative to run 6 (from 5.6 and 7.3 µg/L to 7.4 and 16.1 µg/L for TDP and PP, respectively) as well as the immediately previous run (6.3 µg/L TDP and 7.5 µg/L PP). TDP did not significantly increase during other experiments when inflow rate

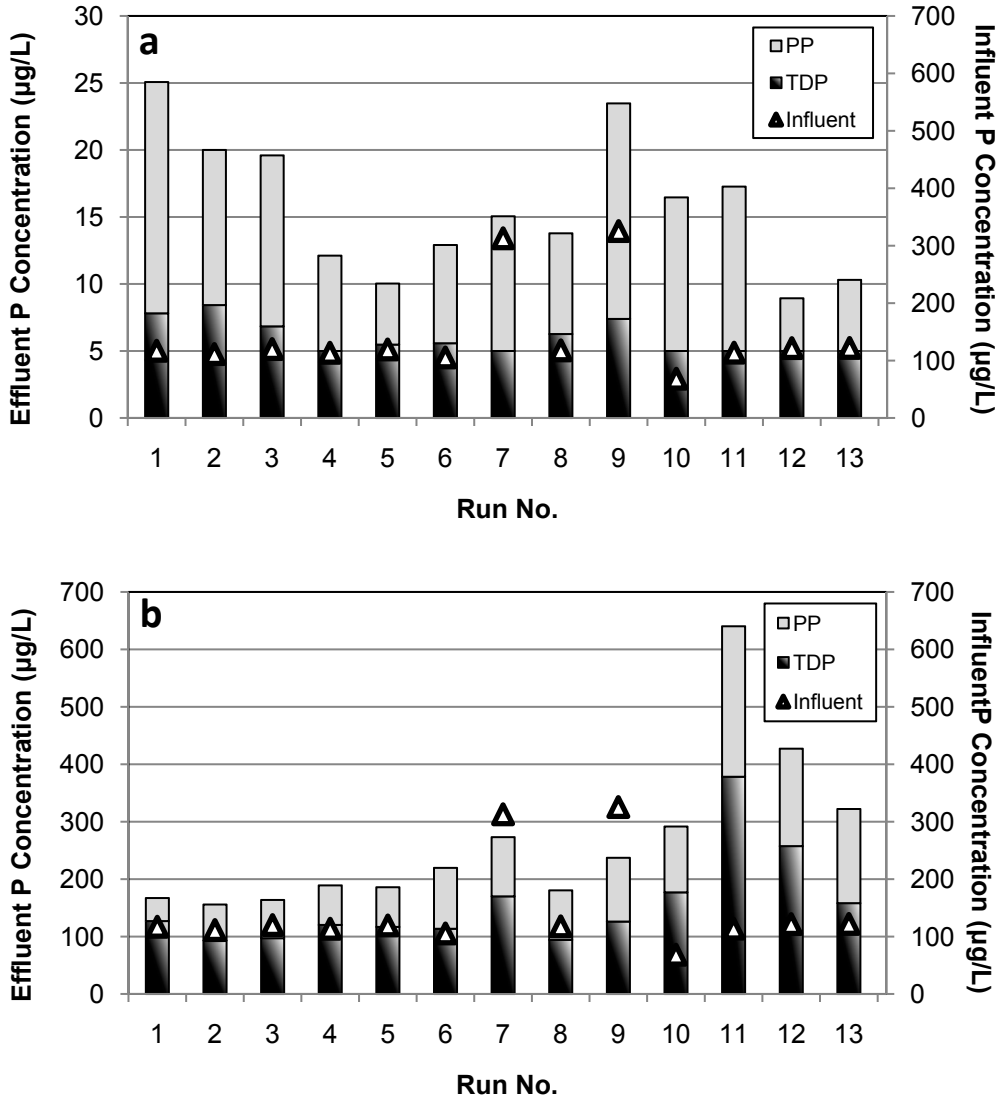

Figure 5-7. Effluent PP and TDP EMCs for the (a) experimental and (b) control columns by run number. Note the differing ordinate axes.

(run 6) or pollutant concentration (run 7) were elevated, which suggests the increased TDP for this run was caused by the combined impact of increasing both variables, leading to decreased reaction time between the media and increased P in solution. Decreased water content of the media after extended drying may also have contributed to the increased TDP concentration by causing some initial limitation in P diffusion. The elevated PP concentration is more convoluted because of the multiple

experimental variables. Elevated PP was experienced for both runs 6 and 7, but both were approximately half the concentration seen in this run (Table 5-1). It is therefore believed that the high PP release observed during this run is the combined result of both an extended dry period and increased flowrate.

Control column run 9 experienced a TP effluent peak (894 μg/L) approximately the same as that of the other elevated concentration run (number 7; 864 μg/L), but had a depressed TP EMC (273 μg/L vis-à-vis 237 μg/L; Figure 5-7b). PP was approximately the same for runs 6, 7, and 9 (106, 103, and 111 μg/L, respectively); it is, in fact, the result of increased TDP releases that led to the elevated effluent TP (Table 5-1). Removal was found to be greater for run 9 than for similar runs, actually showing net adsorption (0.155 mg/kg). It may be that the extended dry period allowed for the oxidation of previously reduced Fe-containing minerals in the media, leading to increased adsorption.

Interestingly, this experiment and the previous run (number 8) also saw an alteration in the TDP column behavior. In previous experiments, column TDP had behaved similar to the experimental column and exhibited a right-skewed pollutograph with an extended, nearly horizontal falling limb. However, these two experiments saw an almost parabolic curve of the effluent TDP (Figure 5-3) which is not explainable. After these two experiments, the column TDP began to show a third type of TDP behavior (see Section 5.5).

Ultimately, it would appear that varying the inflow rate and concentration within a storm event has little impact on the general shape and behavior of the effluent pollutograph for either media. However, varying the magnitude of flow or

concentration elicited distinct responses in media P adsorption behavior, with differing directions for the relationship between either of these variables and media adsorption. Flowrate appears to have a positive correlation with effluent PP concentrations, and increases in antecedent dry time seem to further increase these PP concentrations. Additionally, increased influent concentrations lead to increased effluent TDP concentrations for the control column, and also for the experimental column when these elevated concentrations were coupled with increased flowrate. Also, adsorption was observed for the control media when subjected to elevated concentrations because of the increased concentration gradient between the media surface and bulk solution.

5.5. Additional Investigated Variables

Application of an increased pollutant concentration (~ 2.5 × standard) with a constant flowrate was investigated with experimental run 7 (Figure 5-8). In the experimental column, effluent did not show an elevated TDP EMC relative to run 5 (5.5 and 5.0 μg/L, respectively), but did contain additional PP (4.6 vis-à-vis 10.1 μg/L; 122% increase). The reason for this behavior is not know, although it is possible this additional particulate release was because the column had not returned to a stable condition after the elevated inflow rate it was subjected to in the previous run (number 6; up to 327 mL/min vis-à-vis 182 mL/min for run 7), and these were residual particulate materials being flushed.

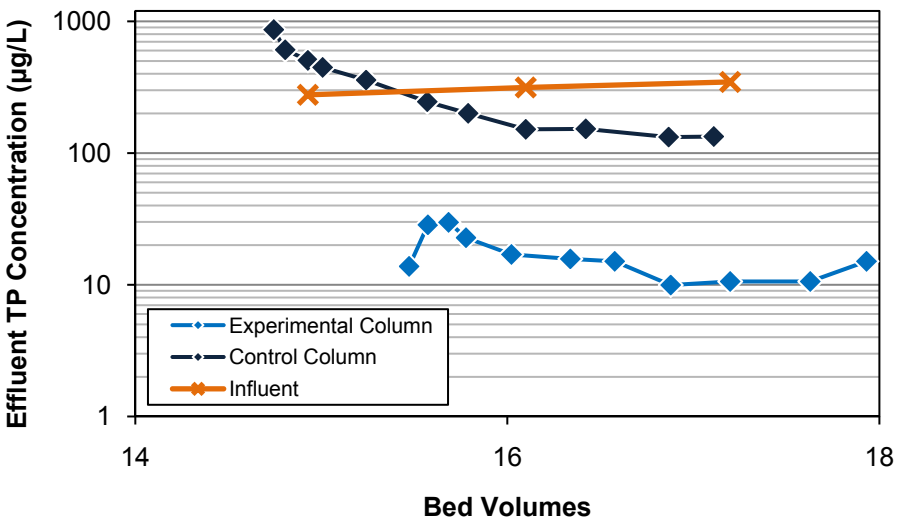

Figure 5-8. Run number 7 showing the effects of elevated influent concentration (313 µg/L) on the media. Experimental and control column effluent concentrations plotted against column cumulative bed volumes of flow. TP concentration was 313 ± 35 µg/L. Influent solution contained 0.01 M KCl as a background electrolyte and had pH of 5.4 ± 1.1

The control column exhibited both elevated TDP and PP releases relative to run 5 (170 µg/L TDP and 103 µg/L PP, up from 69.0 µg/L TDP and 117 µg/L PP during run 5; Table 5-1), although effluent PP was not significantly greater than the previous run (106 µg/L). Elevated TDP is simply throughflow of the influent solution, while PP is believed to again be further washout of particulates dislodged by the elevated flowrate of run 6. Because of the elevated inflow concentration, there was some minimal retention of P by the media (0.062 mg/kg).

Run number 10 (Figure 5-9) investigated the effect of decreased influent concentration on column behavior, applying influent at 60% of the standard concentration (68.4 µg/L). The experimental column behaved mostly as expected, showing effluent TDP below the method detection limit. Elevated PP relative to the

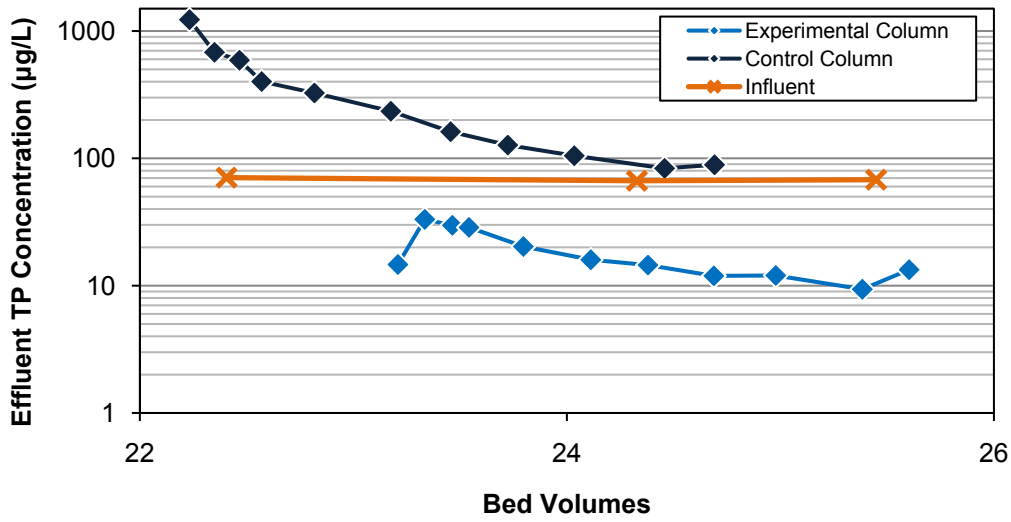

Figure 5-9. Run number 10 showing the effects of decreased influent concentration (68.4 µg/L) on the media. Experimental and control column effluent concentrations plotted against column cumulative bed volumes of flow. TP concentration was 68.4 ± 2.0 µg/L. Influent solution contained 0.01 M KCl as a background electrolyte and had pH of 6.0 ± 0.1.

standard runs was observed (11.5 µg/L vis-à-vis 4.55 µg/L), but again this is believed to be further particulate washout from the elevated flowrates of the previous run (number 9).

The control column showed behavior similar to previous runs, with greatly elevated initial effluent TP concentrations that dropped over the course of the experiment, and unexpectedly this experiment had an increased, not reduced, TP EMC relative to standard run 5 (292 µg/L vis-à-vis 186 µg/L). The PP EMC for this experiment was nearly identical to run number 9 (115 and 111 µg/L, respectively), and so was elevated compared to the standard runs. Again, this was attributed to residual media flushing from the previous experiment. The increased TP was the result of excess release of TDP from the media. It would appear that adsorbed P from run number 9 was partially released during this experiment. This phenomenon will

be discussed in more detail further on. Also, the effluent P profile changed with this experiment from that discussed in Section 6.4. From run 10 through the demobilization of the columns, the column no longer reached a constant effluent concentration but showed continuously dropping P concentrations throughout the duration of the experiment. While the reason for this behavior is not know, it may be that after the elevated influent concentration and double antecedent dry period of run 9 in which column showed net adsorption of P, the column did not reach a steady state but exhibited continued leaching of adsorbed P over the course of several experimental runs until the adsorbed P was flushed from the media.

Runs 11 and 12 (Figure 5-10) were performed to investigate shortened antecedent dry time on the columns. Experiment 11 was a truncated standard run, as was experiment 12, applied to the columns after a dry period of only 3 days. The experimental column acted during run 11 as if its adsorption of P was negatively impacted by the elevated P and inflow conditions encountered during run number 9, showing effective TDP removal but having elevated PP release relative to run 5 (5.0 µg/L TDP and 12.3 µg/L PP EMCs compared to 5.5 µg/L TDP and 4.6 µg/L PP). However, the issue causing this elevated particulate release seemed to be addressed before run 12, because column performance was actually better than previous standard runs, exhibiting both effective TDP removal and reduced PP concentrations (5.0 µg/L TDP and 3.9 µg/L PP EMCs).

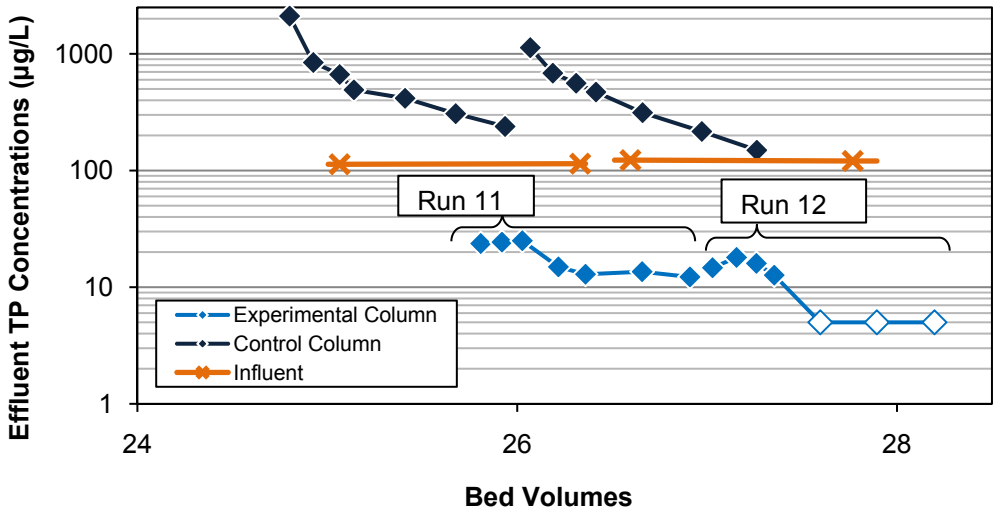

Figure 5-10. Runs number 11 and 12 showing the effects of reduced antecedent dry period (3 days) on the media. Experimental and control column effluent concentrations plotted against column cumulative bed volumes of flow. TP concentration was 118 ± 4.7 µg/L. Influent solution contained 0.01 M KCl as a background electrolyte and had pH of 5.7 ± 0.5.

The control column showed its worst performance during run 11 relative to standard run 5, with high peak release (2.11 mg/L) and elevated TP, TDP, and PP EMCs (640 µg/L, 378 µg/L. and 262 µg/L, respectively; Table 5-1). Performance improved for run 12 (427 µg/L TP, 257 µg/L TDP, and 170 µg/L PP, respectively), but only relative to run 11. It was hypothesized that the relatively high P retention observed for run 9 may be partly explained by newly oxidized Fe components following the extended dry period. If this is the case, the gradual release of large quantities of TDP over the following three experiments (runs 10 to 12) may be the results of the re-reduction of these Fe minerals as the column remains more saturated. However, the elevated PP releases for these three experiments is not explained by this hypothesis.

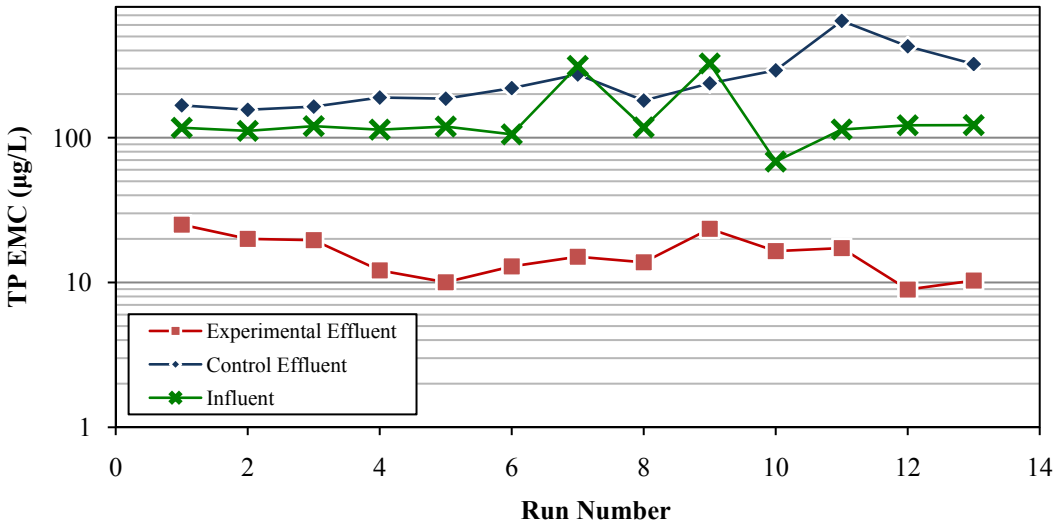

Figure 5-11. Influent and effluent TP EMC of both columns for each run. Influent pH was 5.8 ± 0.6, influent P concentration varied from 68.4 to 572 µg/L, and inflow rate varied from 10.6 to 72.8 cm/hr (50.3 to 344 mL/min).

Control media performance for runs 11 and 12 are somewhat obscured because of previous experiments. Media EMCs continued to decrease from run 11 through 13, and this improvement may be partially a benefit of the shortened drying time between runs 11 and 12. However, because performance improved quite markedly after having a standard antecedent dry time prior to run 13, it is likely that the media was experiencing negative effects due to previous experiments (e.g., leaching of previously sorbed P) and this continued improvement indicates the column media is still working towards reaching a stable state.

The trends in effluent TP EMCs for each column and the effects of influent EMC can be seen in Figure 5-11. A drop in TP EMC from 25.1 to 10.0 µg/L is shown for the experimental column for runs 1 to 5 as the column establishes a steady

state, followed by an increase in EMC from 10.0 to 23.5 μg/L as higher influent concentrations and flow rates are used (runs 6, 7, and 9). Being thereafter subjected to reduced or standard inflow concentrations (approximately 70 to 120 μg/L) and standard inflow rates, the column effluent begins to move toward its original steady state as typified by run 5 (10.0 μg/L TP EMC), showing a final TP EMC for run 13 of 10.3 μg/L. The control column, in comparison, shows a near continuous increase in effluent EMC. Run 1 showed a TP EMC of 167 μg/L and subsequent runs showed ever increasing EMCs until a peak of 640 μg/L was reached during run 11. Thereafter the column showed a slight drop in effluent EMC through run 13 which had an EMC of 322 μg/L. The experimental column clearly performed better under all conditions to which it was subjected, showing removal as opposed to the P export of the control column.

Looking at the entire population of synthetic storm events applied to the columns, the probability of the EMC to exceed a given value may be calculated and plotted, as seen in Figure 5-12. This plot indicates that 95.3% of the influent storms exceeded 68.4 μg/L EMC, while 50% exceeded 118 μg/L, and approximately 12.3% exceeded 313 μg/L.

Statistically, the control column will export TP at all inflow concentrations. 95.3% of TP EMCs exceeded 156 μg/L, 50% exceeded 220 μg/L, and 4.72% exceeded 640 μg/L. This data also appears to exhibit a change point, a distinct point on either side of which the data show different behaviors. For the control column, effluent EMC shows a steady increase as influent concentration increases. It appears that when influent storms exceed the 50% percentile in terms of TP EMC, the control

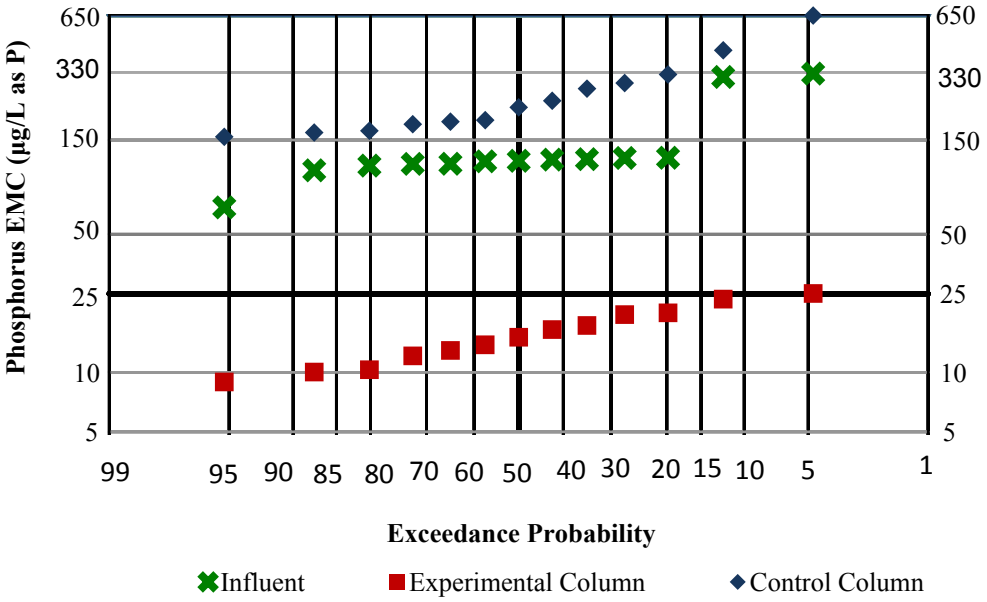

Figure 5-12. Probability plot of influent and effluent TP EMCs. The abscissa indicates the probability that an inflow event will exceed a given P concentration.

column EMC shows a distinctly steeper slope. This may indicate that as influent concentration increases beyond this change point (118 µg/L), there are increasingly greater releases of TP from the column.

The experimental column exhibited much greater P adsorption, showing consistent low TP EMCs. Figure 5-12 indicates that 95.3% of TP EMCs exceeded 8.9 µg/L, 50% exceeded 15.1 µg/L, and only 4.72% exceeded 25.1 µg/L. This indicates that the experimental media possesses the capability to adequately treat P-containing stormwater, reducing the effluent concentration below the EPA recommended limit of 25 µg/L for freshwater lakes for the majority of storms.

These experiments show that increasing influent P concentrations lead to increasing effluent TP and TDP for the control media, but when applied at 38.5 cm/hr (182 mL/min) the experimental column is still able to treat all influent to ≤ 20 µg/L

TP EMC and keep peak effluent concentration ≤ 35 μg/L. However, as stated previously, reduced experimental media performance was observed when both influent flowrate and concentration were increased. The media maintained effluent EMCs at or below the 25 μg/L EPA recommendation regardless of inflow concentration or flowrate. Similarly, reduced influent concentration resulted in reduced effluent TP and TDP concentrations. Also, shortened antecedent dry time produced enhanced removal for the experimental media, just as the extended dry period led to reduced performance. It may therefore be concluded that WTR-amended media P performance should be maximized when subjected to small volume, more frequent storm events. However, this conclusion cannot be supported with minicolumn data as intermittent flow minicolumn experiment showed no correlation between antecedent dry time and P adsorption. However, dry time was not varied significantly throughout the minicolumn experiments, and the impact of antecedent dry time on column P adsorption may have been confounded by other variables such as flowrate increase.

Over the life of the columns, in every instance, WTR amended media far exceeded control media performance with respect to P adsorption. Experimental media treatment also met or surpassed the recommended concentration limit for fresh waters set by the EPA of ≤ 25 μg/L (US EPA, 1986). From all experiments, the control column received 774 L of influent, containing a total mass of 111 mg P. The experimental column received 794 L of influent, containing a total mass of 112 mg P. The mass of P in the effluent was 190 mg and 12.8 mg for the control and experimental columns, respectively. This equates to an 88.5% reduction in P mass in

the stormwater by the experimental column media relative to the influent, and a 93.3% reduction in total effluent mass relative to the control column. These reductions in mass are similar to those observed in some studies for BSM. Davis et al. (2006) reported TP mass reductions ranging from 52 to 96% for laboratory media studies, and field results of 70 – 80%. Hsieh et al. (2007) reported mass TP reductions by two media mixture and column configuration combinations of 63 and 85%. Other studies report much poorer removal of P from the influent. Hatt et al. (2009) reported a 398% increase in effluent TP mass relative to influent at a field site in Australia, and a concomitant increase in SRP mass of 1271%. Similarly, Hunt et al. (2006) reported effluent mass increases at a North Carolina field site relative to influent of 240% and 9.3% for TP and SRP, respectively. This indicates that, similar to our control media, many BSM are poorly suited to removing P from stormwater, and may release P. The use of WTR as a media amendment may be useful to transform a media which poorly adsorbs P to one that reduces effluent P concentrations to within acceptable limits.

Normalized by media mass, the experimental media exhibited adsorption of 3.18 mg P/kg, while the control media exported P (2.38 mg P/kg). This calculated measure of media adsorption for the experimental column media is not representative of the true media adsorption capacity, as oxalate extractions indicate the media capacity is not exhausted (see Chapter 6). Clearly, based on reductions in mass loading, effluent concentration reductions, and calculated media adsorption, the experimental media far out performs the control media at removal of P from the influent. It consistently produced effluent EMCs below 25 μg/L as recommended by

the U.S. EPA, while the control column exported P. Additionally, the reductions in TP mass provided by the experimental column are similar to those reported by others (Davis et al., 2006; Hsieh et al., 2007). This is a vast improvement over the control media, which showed a large export of P (78 mg net). This suggests that the use of WTR as a BSM amendment will produce even greater P adsorption when integrated into a media that shows even moderate ability to bind P.

5.6. Nitrogen Species Removal

Throughout the course of the experiment, mass loading to both columns included 678 mg NO_3^--N, 1.01 g TKN, and no NO_2^-. The control column released 759 mg NO_3^--N, 11.8 mg NO_2^--N, and 951 mg TKN in its effluent. The experimental column, conversely, released 710 mg NO_3^--N, 3.82 mg NO_2^--N, and 417 mg TKN in its effluent. These are 11.9 and 4.72% increases in effluent NO_3^--N mass compared to the influent for the control and experimental columns, respectively. For TKN, mass in the effluent decreased by 5.65 and 58.6% relative to the influent for the control and experimental columns.

Comparatively, mass of effluent TN for the experimental and control columns measured 1.13 and 1.72 g N, respectively, relative to an influent mass of 1.69 g N. This equates to a 32.9% reduction in TN mass loading by the experimental column and a 2.16% increase in mass loading by the control column. This shows that, apart from reductions in TKN mass by the experimental column, treatment of N species by either column was minimal (Table 5-1).

The WTR amended column retained or exported NO_3^- depending on the experiment, but over the course of the entire life of the column all the NO_3^- that entered the column simply flushed out with little additional production (1.1 g N/kg). The same may be said for the control media, although there was greater production of NO_3^- (2.5 g N/kg). Similarly, there was some production of NO_2^- by both columns; 0.1 and 0.4 g N/kg for the experimental and control columns, respectively. This production of oxidized N species from both columns suggests that nitrification is taking place.

Unlike the NOx species, there was some removal of TKN (NH_4^+ + glycine) in both columns. The control column removed 1.7 g N/kg. The removal of TKN is less than the sum of the NOx species produced, suggesting that the NOx are being produced by organic matter in the media. Removal of TKN by the experimental column was much greater than that of the control column, measuring 20.4 g N/kg. This is much greater than the NOx species produced, indicating that the ammonium and/or glycine are being retained by the WTR-containing media. It is likely that the WTR is adsorbing the glycine component of the TKN, because glycine will exist as a zwitterion (pK_{a1} = 2.4, pK_{a2} = 9.8) and at the pH encountered in the column soil system the anionic carboxyl moiety could likely undergo some manner of sorption to the positively charged WTR surface (Lambert, 2008). However, this cannot be conclusively determined as neither NH_4^+ nor organic N were measured individually.

5.7. Leaching

Experimental column effluent was digested and analyzed for Al(III) as described in Section 3.10. All samples analyzed were below the method detection limit of 5 mg/L. However, both EPA and Maryland Department of the Environment have established a drinking water MCL of 50 – 200 μg/L and a criterion continuous concentration (CCC) for freshwater organisms of 87 μg/L. Unfortunately, that renders our results inconclusive with regards to the degree of elemental Al leaching.

As previously discussed, there were also measurable releases of dissolved and particulate materials from both columns. Throughout all the column experiments, WTR-containing media effluent maintained turbidity < 8 NTU, and except for a single sample turbidity was < 2 NTU. The control column, on the contrary, had high effluent turbidity ranging from 2.5 to 155 NTU with a cumulative average of 32.4 ± 20.1 NTU. Turbidity within runs often exhibited the same behavior trends as P species, showing a large initial peak and a near exponential decay with flow. This high turbidity was not exclusively particulate species either. Most samples from the control column remained tea-colored even after filtering, suggesting that the column was leaching dissolved organic matter (DOM). The amount of P that effluent DOM was contributing to TDP was measured by comparing SRP and TDP for the control column. Undigested and filtered samples measured for P by the ascorbic acid method (APHA, 1995) are an operational measure of PO_4(-III). The difference between SRP and TDP is often used as a measure of P_o in solution (Dr. Bruce James, personal communication). For all control column samples, P_o analyzed in this way measured ≤ 10 μg/L, suggesting that the DOM is either not exporting P or the P species are Mo reactive.

It was also observed during ion chromatograph (IC) analysis for anions that a large amount of an unknown ion was leaching from the media, especially the experimental BSM. It was theorized to be sulfate (SO_4^{2-}), and this was confirmed by performing a sample matrix spike. Unfortunately, little SO_4^{2-} data are available, and such large amounts were leached from the WTR-containing media that the initial concentrations exceeded the upper measurement limit of 25 mg SO_4^{2-}/L. Effluent concentrations gradually diminished over time, but the results from runs 1 through 3 were lost due to these circumstances. However, all EMCs that are available ranged from 2.12 to 14.6 mg SO_4^{2-}/L. Including all available results, SO_4^{2-} leaching from each column was measured as 118 and 27.2 mg SO_4^{2-}/kg from the experimental and control columns, respectively.

To account for the lost samples, a media water extraction per Section 3.9 was performed on the WTR-containing media, resulting in a labile media SO_4^{2-} content of 261 mg SO_4^{2-}/kg. It can be assumed this is the content of the media as a whole, and as this concentration is not significantly larger than what was measured during column operation it may be concluded that the experimental column media may be nearly exhausted with respect to SO_4^{2-}. Therefore, SO_4^{2-} leaching should not be of concern, although the possibility of H_2S formation if the media becomes anoxic may lead to nuisance odors. The leaching of SO_4^{2-} is likely to result from the WTR because of the $Al_2(SO_4)_3$ used during drinking water coagulation. The minimal losses from the control media also suggest there is some inherent in the BSM itself. However, studies have previously suggested ligand exchange to be the primary P adsorption process occurring at the WTR surface (Yang et al., 2006), and it is likely

that some of the leaching SO_4^{2-} in this study is the result of the exchange of SO_4^{2-} for PO_4(-III) at the BSM-water interface.

Similar to SO_4^{2-} leaching, an increase in column effluent pH may be an indication of hydroxyl leaching caused by P adsorptive ligand exchange (Yang et al., 2006). The control column exhibited little change in effluent pH across all experiments, averaging 6.3 ± 0.1 for the first run to 5.9 ± 0.1 for the final run, with a mean and median for all samples of 6.1 ± 0.1 and 6.1, respectively. Conversely, the experimental column showed a steady, much more pronounced decrease in effluent pH over time. Effluent pH averaged 7.1 ± 0.3 for the first run to 6.2 ± 0.2 for the last run, with a global mean and median of 6.6 ± 0.3 and 6.5, respectively. While both media showed some buffering of the influent pH and a gradual effluent pH drop with flow, the WTR-containing BSM traversed a pH range twice as great as that of the control column. If hydroxyl ions were in fact being released through ligand exchange, an increase in pH would be expected, suggesting that either ligand exchange for hydroxyl ions is not occurring, or some other process is obscuring this phenomenon. Possibly SO_4^{2-} is being released from residual alum in the media, allowing –OH groups to react with newly exposed Al in the formation of $Al(OH)_3$. Alternatively, it may simply be the leaching or neutralization of pH adjustment chemicals that had been used during the drinking water treatment process, which as they migrate from the media lead to a general decrease in effluent pH.

Chapter 6: Media Oxalate Extractions and Phosphorus Saturation Indices

Oxalate extractions and calculation of the PSI for each media were conducted as per Section 3.10. Additionally, PSI was determined for column media both pre- and post-experiment. For the mesoscale vegetated columns this allowed determination of the degree of media saturation with depth. These data also allowed for a comparison of media adsorptive capacities from batch and column studies, and allowed for the development of media specification requirements for effective P capture.

6.1. Amendment Contributions to Oxalate-extractable Elements

6.1.1. Water Treatment Residual

The addition of increasing WTR content to BSM led to small increases in media P_{ox} and Fe_{ox} contents and much more pronounced increases in Al_{ox} content. For example, in the batch studies 0, 2, 4, and 10% WTR amended BSM showed P_{ox} contents of 4.04, 5.15, 6.30, and 7.39 mmol P_{ox} /kg, respectively. Similarly, Fe_{ox} measured 15.6, 15.2, 17.2, and 22.1 mmol Fe_{ox}/kg, and Al_{ox} measured 10.6, 48.4, 92.9, and 396 mmol Al_{ox}/kg for each mixture, respectively (Table 6-1). These increases were from the WTR itself, as it possesses P_{ox}, Fe_{ox}, and Al_{ox} content greater than the BSM (Table 4-1), and clearly as the WTR content of the mixture increased almost uniformly so did all measured oxalate-extractable contents. A similar general trend of increasing oxalate-extractable content with increasing mixture WTR proportion was also seen among media amended with other components such as HBM and quartz sand, from both batch and minicolumn studies (Tables 6-1 and 6-2).

Table 6-1. Oxalate-extractable P, Fe, and Al contents of BSM mixtures from batch studies. A 0.275 M acid ammonium oxalate extractant was used with pH 3.0 ± 0.1. PSI is defined as per Section 4.5. P_{ox}: oxalate-extractable phosphorus; Al_{ox}: oxalate-extractable aluminum; Fe_{ox}: oxalate-extractable iron; PSI: phosphorus saturation index [$(Al_{ox}+Fe_{ox}):P_{ox}$]; BSM: bioretention soil media; WTR: water treatment residual; LFBSM: low-fines BSM; HBM: hardwood bark mulch; LC: leaf compost; [OM+]: additional organic matter.

	P_{ox}	**Fe_{ox}**	**Al_{ox}**	**PSI**
	mmol/kg			%
BSM	4.04	15.6	10.6	15.4
2% WTR	5.15	15.2	48.4	8.10
4% WTR	6.30	17.2	92.9	5.72
10% WTR	7.39	22.1	396	1.77
LFBSM	1.74	8.86	5.62	12.0
3% WTR	2.55	11.5	66.7	3.26
6% WTR	3.32	11.2	193	1.63
10% WTR	4.60	15.0	338	1.30
BSM + HBM	3.85	17.4	9.35	14.4
2% WTR + HBM	6.88	22.8	54.8	8.87
4% WTR + HBM	5.16	15.4	118	3.87
BSM + LC	5.52	18.5	11.8	18.2
4% WTR + LC	5.59	9.64	62.6	7.74
4% WTR + LC [OM+]	8.79	22.3	53.4	11.6

While the WTR does contribute to an increased P_{ox} measure in the mixtures, the addition of P to the mixture by WTR is nearly two orders of magnitude less than Al_{ox} addition (58.4 mmol P_{ox}/kg vis-à-vis 5.74 mol Al_{ox}/kg) and so a net increase in P adsorption capacity results from amending media with WTR.

6.1.2. Low-fines BSM

LFBSM amended with WTR showed reduced oxalate-extractable elements compared to equivalent WTR-amended BSM mixtures. For example, 4% LFBSM measured 4.86 mmol P_{ox}/kg, 11.2 mmol Fe_{ox}/kg, and 161 mmol Al_{ox}/kg from the set I minicolumn study (Table 6-2). Comparatively, the 4% BSM from the same

Table 6-2. Oxalate-extractable P, Fe, and Al contents of media, initially and after column experimentation. PSI is defined as per Section 4.5. †: Intermittent column flow regime. P_{ox}: oxalate-extractable phosphorus; Al_{ox}: oxalate-extractable aluminum; Fe_{ox}: oxalate-extractable iron; PSI: phosphorus saturation index [$(Al_{ox}+Fe_{ox}):P_{ox}$]; BSM: bioretention soil media; WTR: water treatment residual; LFBSM: low-fines BSM; HBM: hardwood bark mulch; LC: leaf compost; [OM+]: additional organic matter.

	P_{ox}	**Fe_{ox}**	**Al_{ox}**	**Initial PSI**	**Final PSI**
	Initial (Final) content; mmol/kg			(%)	(%)
Experimental Set I:					
BSM	4.02 (4.30)	14.0 (15.0)	12.3 (10.5)	15.3	16.9
BSM + 2% WTR	6.18 (5.51)	17.7 (12.8)	91.7 (70.8)	5.65	6.59
BSM + 4% WTR	6.33 (6.77)	16.7 (12.9)	181 (125)	3.19	4.91
BSM + 2% WTR + HBM	5.04 (6.93)	15.9 (15.4)	119 (99.3)	3.75	6.04
BSM + 4% WTR + HBM	5.95 (6.50)	19.4 (17.3)	217 (196)	2.52	3.05
LFBSM + 4% WTR	4.86 (10.3)	11.2 (14.6)	161 (192)	2.83	5.00
Experimental Set II:					
BSM	4.13 (3.56)	7.85 (11.0)	13.3 (8.82)	19.5	18.0
BSM + 4% WTR	7.75 (8.59)	19.8 (12.9)	101 (164)	6.43	4.86
Sand + 4% WTR	2.35 (5.35)	2.12 (1.04)	222 (148)	1.05	3.58
† BSM + 4% WTR + HBM	5.88 (8.76)	12.8 (17.6)	183 (179)	3.00	4.50
† BSM + 4% WTR	9.24 (6.71)	19.1 (13.4)	228 (202)	3.74	3.10
† LFBSM + 4% WTR	5.26 (7.36)	12.3 (12.3)	218 (182)	2.28	3.80

minicolumn set measured 6.33 mmol P_{ox}/kg, 16.7 mmol Fe_{ox}/kg, and 181 mmol Al_{ox}/kg (Table 6-2). A similar, more exaggerated trend is seen for the WTR amended sand investigated in minicolumn set II where P_{ox} and Fe_{ox} were even less abundant and measured 2.35 mmol P_{ox}/kg and 2.12 mmol Fe_{ox}/kg (Table 6-2). This is logical as the fines in the BSM mixture contain Fe and Al and associated adsorbed P. When the fines content is reduced by the addition of sand to create the LFBSM, these oxalate-extractable media elements will also be reduced.

In a few instances, however, LFBSM and sand amended with WTR measured greater Al_{ox} content compared to analogous WTR-amended BSM mixtures. The amended sand media contained 222 mmol Al_{ox}/kg, greater than the measured Al_{ox}

contents of either 4% amended BSM or LFBSM from minicolumn set I (181 and 161 mmol Al_{ox}/kg, respectively). The continuous and intermittent 4% BSM mixtures from minicolumn set II measured 101 and 228 mmol Al_{ox}/kg, while the intermittent 4% LFBSM media from the same set measured 218 mmol Al_{ox}/kg (Table 6-2). This apparent variability of Al_{ox} contents in media containing the same proportion of WTR is difficult to explain, but may simply be the result of sample variation. T-tests on the mean Al_{ox} contents for the 4% WTR amended BSM, LFBSM, and sand media failed to reject the null hypothesis that these average media Al_{ox} contents were equal ($p > 0.16$), indicating that no two of the amended media have statistically different average Al_{ox} contents.

6.1.3. Organic Amendments

The organic amendments (HBM and LC) both contributed a small amount of Fe_{ox} and Al_{ox} to the overall media mixture. HBM contained 54.4 mmol Fe_{ox}/kg and 12.7 mmol Al_{ox}/kg, while LC contained 39.4 mmol Fe_{ox}/kg and 13.7 mmol Al_{ox}/kg. These differing oxalate extractable metals contents may partially be the cause of the two very different impacts the amendments have on media P adsorption. The major difference between the two based on P performance results because of their respective contributions of P_{ox}. While HBM added no additional P to the overall mixture (3.74 mmol P_{ox}/kg, less than the content of BSM or WTR; Table 4-1), LC added a measureable amount (15.9 mmol P_{ox}/kg). Therefore, while HBM added some Fe and Al with no P and thereby increased the media oxalate ratio and improved adsorption, the addition of P from LC outweighed its minimal Fe and Al contribution and lead to decreased adsorption and a lower oxalate ratio. This can be seen in various media

mixtures. 4% HBM from minicolumn set I had 5.95 mmol P_{ox}/kg, 19.4 mmol Fe_{ox}/kg, and 217 mmol Al_{ox}/kg, resulting in an oxalate ratio of 39.7 (Table 6-2). The same media from the batch studies contained 6.30 mmol P_{ox}/kg, 17.2 mmol Fe_{ox}/kg, and 92.9 mmol Al_{ox}/kg, producing an oxalate ratio of 17.4 (Table 6-1). Comparatively, the BSM + 4% WTR + LC mixture from the batch studies contained 5.59 mmol P_{ox}/kg, 9.64 mmol Fe_{ox}/kg, and 62.6 mmol Al_{ox}/kg, having an oxalate ratio of 12.9. Regardless of the differing Al_{ox} contents, the increase in P_{ox} of the LC-containing media is evident and negatively impacted the mixture's oxalate ratio (Tables 6-1 and 6-2). As oxalate ratio is positively correlated with media P adsorption capacity (see Section 6.2), the reduced P adsorption capacity observed after the addition of LC is explainable.

6.2. Correlation of Oxalate Extraction with P Adsorption

As show in previous work, media P adsorption (e.g., Q_{max}) is correlated with PSI and oxalate extractable Al and Fe (Dayton and Basta, 2005). All media investigated in this study were analyzed for oxalate extractable Al, Fe, and P to quantify their relationship with media P adsorption capacity. The control media from the vegetated column study was included in these analyses. This is because an equilibrium P adsorption capacity could be estimated for the media as it ceased showing adsorption in contact with a 120 μg P/L solution, indicating the media and solution were at equilibrium. The experimental media from the vegetated column study was not included as it was not at equilibrium with the influent and still had available capacity. Because of this, a media adsorption capacity could not be determined.

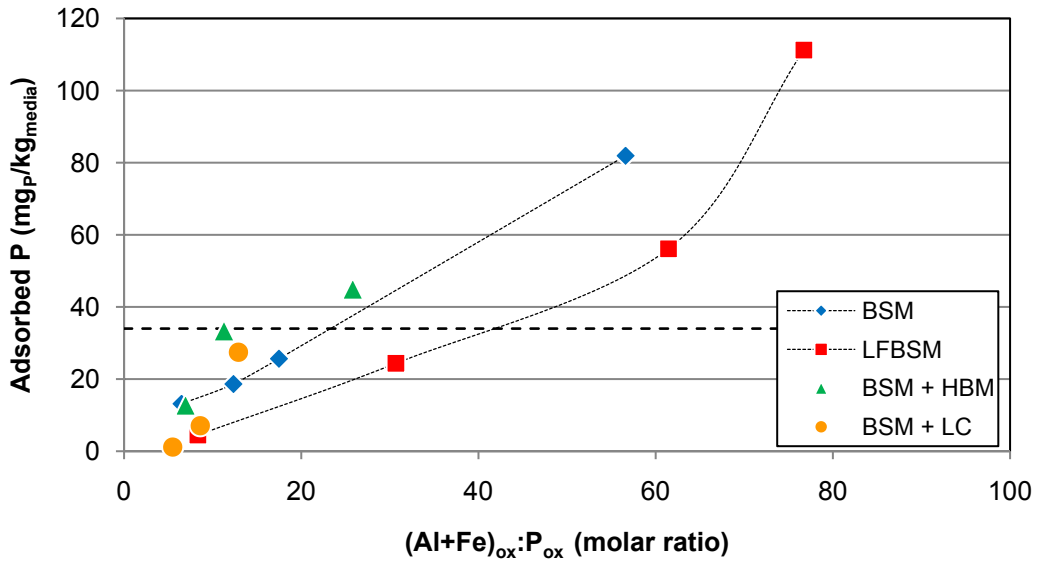

Figure 6-1. Batch adsorption study measured oxalate ratio for each media mixture, and the interpolated media equilibrium adsorption content. The media equilibrium is calculated for a soluble P concentration of 120 µg/L, within a pH range of 4.6 – 7.4. The horizontal dashed line represents the media adsorption benchmark of 34 mg/kg.

In Figures 6-1 to 6-3, points increasing along the abscissa have increasing amorphous Al and Fe content, produced mainly through increasing Al in each mixture caused by greater WTR content. The ordinate axis in all figures is a measure of the equilibrium P adsorption of a mixture with a 120 µg P/L solution. This value was determined by the Freundlich fitted isotherms calculated from the batch adsorption data (Section 4.3) or from the column adsorption studies, as discussed in Sections 4.4 and 5.5.

Figure 6-1 shows the increasing effectiveness of a given media for adsorption of P correlated with increasing $(Al+Fe)_{ox}:P_{ox}$ ratio (Oxalate ratio; PSI^{-1}) for the batch study results. Each mixture of the four amendment types (WTR, LFBSM+WTR, WTR+HBM, WTR+LC) are shown, with each individual point correlating to the expected media P adsorption based on Freundlich isotherms from the batch

adsorption studies and oxalate extractions for a given amendment content (0, 2, 4% WTR, etc.). Under batch conditions, BSM amended with only WTR performed at the threshold requirement (34 mg P/kg) when the oxalate ratio was approximately 23, which correlates to a WTR content of about 5% on an air dry weight basis. Similarly, the LFBSM amended with WTR straddled the threshold with oxalate ratios of 30 and 61, representing a necessary WTR content of between 3% and 6%. BSM amended with both WTR and HBM crossed the threshold between oxalate ratios of 11 and 26, correlating to 2% and 4% WTR. The strong correlation between media P adsorption and oxalate ratio is clear, especially for the BSM and LFBSM media, which exhibit nearly linear relationships.

Figure 6-2 again shows media P adsorption correlated with oxalate ratio, detailing the relationship for column as well as batch studies. The addition of the column data provides a more varied indication of minimum WTR content under conditions invoked by the continuous and intermittent treatments compared to the batch studies (Table 6-1, Figures 6-2). This can be attributed to the fluctuating Al_{ox} content. In some cases, Al_{ox} content for the column media more than doubled that measured for batch media of the same WTR mass. For example, the 4% BSM mixture used for the batch study measured 92.9 mmol Al_{ox}/kg, while media mixed in the same proportions and used for the set I minicolumn study measured 181 mmol Al_{ox}/kg (Tables 6-1 and 6-2). However, even with greater Al_{ox} contents the column data often showed reduced media P adsorption, likely because of reduced contact time between the media and P in solution compared to batch conditions. For example, although 2% BSM from the batch studies had an oxalate ratio of 12.3 and a

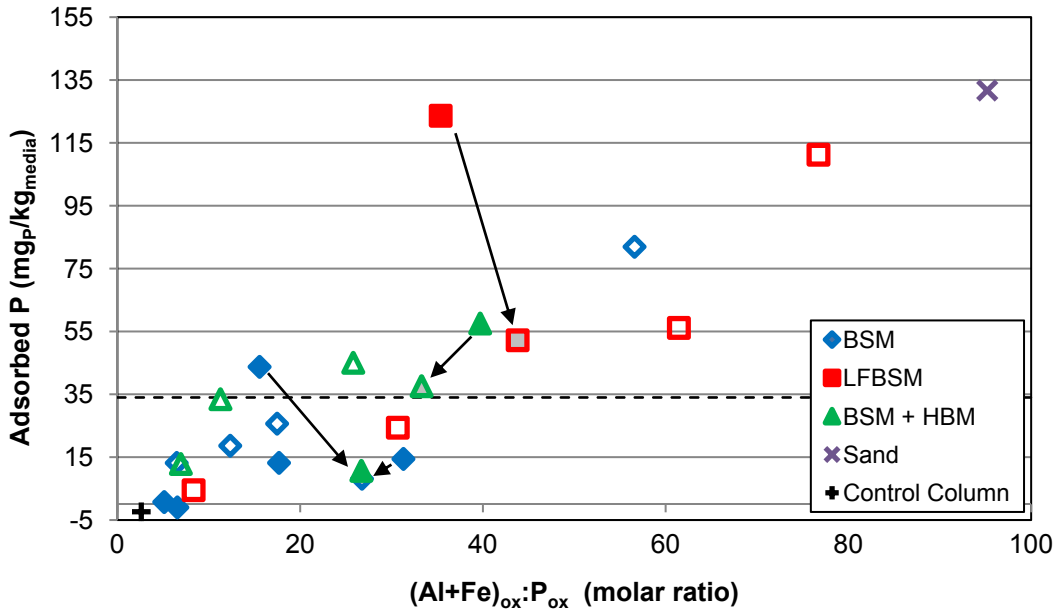

Figure 6-2. Measured oxalate ratio for media from both batch and column studies and the expected or actual TP media equilibrium adsorption capacity. The media equilibrium is for a soluble P concentration of 120 µg/L, within a pH range of 4.6 – 7.4. Open marks represent batch data, closed marks represent data from columns subject to continuous flow, and open grey-filled marks represent intermittent column data, with arrows originating from the equivalent continuous column data. The horizontal dashed line represents the media adsorption benchmark of 34 mg/kg.

P adsorption capacity of 18.6 mg P/kg, from the set I minicolumn study the analogous media had a higher oxalate ratio of 17.7. This high oxalate ratio suggests greater media P adsorption capacity, but measured capacity for the media was only 13.2 mg P/kg. This phenomena was even more pronounced in the intermittent flow columns. For instance, the 4% LFBSM media used in the set I minicolumn study had an oxalate ratio of 35.3 and a media P adsorption capacity of 124 mg P/kg. An identical media mixture used for set II had an oxalate ratio of 43.9, but only had an adsorption capacity under intermittent flow of 52.2 mg P/kg (Table 6-2). In addition to the reduced contact time with flow experienced in the column experiments, the drying of the media subjected to intermittent flow is believed to be the source of this further

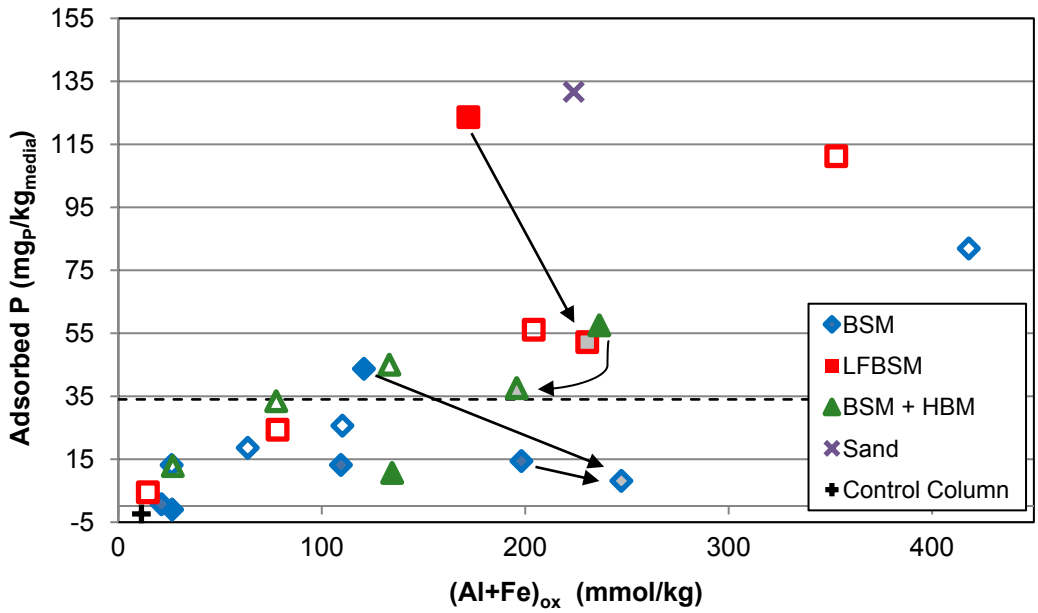

Figure 6-3. Oxalate-extractable Al and Fe for media from both batch and column studies and the expected or actual TP media equilibrium adsorption capacity. The media equilibrium is for a soluble P concentration of 120 µg/L, within a pH range of 4.6 – 7.4. Open marks represent batch data, closed marks represent data from columns subject to continuous flow, and open grey-filled marks represent intermittent column data, with arrows originating from the equivalent continuous column data. The horizontal dashed line represents the media adsorption benchmark of 34 mg/kg.

reduction in media P adsorption capacity. Drying causes the crystallization of WTR, which reduces its surface area and consequently its P adsorption capacity by limiting available adsorption sites (Yang et al., 2008; Agyin-Birikorang and O'Connor, 2009). Even with the complex interactions between flow regime and media adsorption, the strong positive correlation that exists between oxalate ratio and media P adsorption capacity can clearly be seen (Figure 6-2)

Figure 6-3 again shows both media P adsorption capacity for batch and column data on the ordinate axis, but the abscissa expresses the media molar oxalate-extractable Al + Fe content instead of the oxalate ratio. These data also show a general trend of increasing media P adsorption, however the scatter of the data is

much greater, and consequently the correlation between media P adsorption capacity and $(Al+Fe)_{ox}$ is much more poorly defined than the correlation between oxalate ratio and media P adsorption capacity. This figure illustrates the need to include a measure of media P content in a predictor for media P adsorption capacity, such as is done with the PSI or the oxalate ratio.

Along with the variability in measured Al_{ox} contents of the media, a similar observed phenomenon involved the changes in media oxalate-extractable contents from pre- to post-adsorption. It was expected that P_{ox} would increase after experimentation as P adsorbed on media Fe and Al. Similarly, a drop in media Fe_{ox} and/or Al_{ox} was expected due to media drying and crystallization, as well as washout of fines and other media components that contribute to Fe and Al content. However, in a number of instances behavior was contrary to that expected. The 4% LFBSM media from the set I minicolumn study saw an increase of both Fe_{ox} and Al_{ox}, from 11.2 to 14.6 mmol Fe_{ox}/kg and 161 to 192 mmol Al_{ox}/kg. The 4% BSM from minicolumn set II also saw an increase in its Al_{ox} content from 101 to 164 mmol Al_{ox}/kg (Table 6-2). This increase was so large that the oxalate ratio for the media from pre- to post-adsorption actually increased, from 15.6 to 20.6, which suggests increasing capacity for P adsorption. 4% BSM subjected to intermittent flow from minicolumn set II experienced a decrease in P_{ox}, from 9.24 to 6.71 mmol P_{ox}/kg. This also resulted in the media oxalate ratio increasing after adsorption, from 26.7 to 32.3 (Table 6-2).

These decreases in P_{ox} and increases in Fe_{ox} were attributed to poor sample homogenization and sampling variation, as the magnitude of the changes were relatively small (approximately 1 to 3 mmol/kg). However, in the two instances where this occurred for Al_{ox}, the magnitude of the unexpected increase was much greater (31 and 63 mmol/kg). Al-WTR, especially that used in this study, has a very high Al density (5.74 mol Al_{ox}/kg; 6.25 mol Al_{Tot}/kg), so significant variation can result if the media is improperly homogenized, to produce huge swings in measured Al_{ox} content. This high degree of variability for WTR-amended media is further exemplified by the measured Al_{ox} content of the 4% BSM media from the minicolumn set II (Table 6-2). The same media was used in two columns and one each subjected to continuous and intermittent flow. However, a single batch of media was mixed for the construction of both columns and an oxalate extraction was performed on the media on two separate occasions. Table 6-2 shows that the difference in the measured "virgin" media Al_{ox} content was 127 mmol Al_{ox}/kg (101 vis-à-vis 228 mmol Al_{ox}/kg), a factor of approximately 2.3. Additionally, the measured post-adsorption Al_{ox} contents converged somewhat, with the continuous flow media measuring 164 mmol Al_{ox}/kg and the intermittent flow media measuring 202 mmol Al_{ox}/kg, reducing the measured difference to 38 mmol Al_{ox}/kg. These differences may have been more fully understood by analyzing the different media's P adsorption capacity, except each column was subjected to different flow regime treatments, and hence comparison is not valid. Ultimately, the reason for this variation is not known, but because the difference in measured contents converged on

measuring post-adsorption, this phenomenon is attributed to sampling variation. This exemplifies the need to carefully and thoroughly mix amended media when sampling.

Regardless, because Al (hydr)oxides such as the $Al(OH)_3$ in WTR adsorb P, increasing their content in the media will result in greater P adsorption. This held true in general, as seen in Figure 6-2. Specifically, however, even with a greater Al_{ox} content in the column media, in many instances media adsorption capacity was lower than that of batch media because of reduced media/solution contact time. Furthermore, this trend is exacerbated with media subject to an intermittent flow regime, where such columns adsorbed less P per media mass than the same media subjected to continuous flow (Section 4.4), even when the media have similar oxalate ratios. This is because of media drying, as explained in Section 2.2. Therefore, while WTR content has a strong impact on oxalate ratio and P adsorption capacity, the flow conditions to which the media are subject are an important variable to consider when using WTR as a stormwater management amendment. Also, when using the oxalate ratio as a metric, it must be remembered that adsorption to Fe and Al (hydr)oxides is only the dominant P control mechanism under acidic to neutral soil conditions. The oxalate ratio is therefore not expected to be a valid predictor of adsorption capacity under alkaline conditions or in soils with a large Ca content, which can sequester P as Ca-P precipitates, because Ca content and Ca-P interactions are not accounted for using this metric (Kovar and Pierzynski, 2009). Regardless, the use of the oxalate ratio appears to be a fairly reliable and informative metric in predicting the P adsorption capacity of a medium for stormwater treatment.

6.3. Media Capacity Exhaustion with Depth

Changes in media oxalate extractions with depth for the media used in the vegetated columns was investigated. Table 6-3 shows the oxalate-extractable contents for unused media and used media collected at 0-2 cm (surface layer), 11-12 cm (⅛ column length), 21-22 cm (¼ column length), and 43-44 cm (½ column length) depths for the mesoscale vegetated column experiments. Figure 6-4 visually represents media oxalate from Table 6-3. With the control media, little variation is seen in the media with depth or compared to unused media. One minor exception to

Table 6-3. Oxalate extractable contents of control and experimental media from vegetated columns pre- and post-experimentation. 0.275 M acid ammonium oxalate extraction fluid (pH = 3.0 ± 0.1) at 1:40 w/v was used. P_{ox}: oxalate-extractable phosphorus; Al_{ox}: oxalate-extractable aluminum; Fe_{ox}: oxalate-extractable iron; $(Al+Fe)_{ox}$: sum of oxalate-extractable aluminum plus iron; PSI: phosphorus saturation index [$(Al+Fe)_{ox}$:P_{ox}];

Depth (cm)	P_{ox}	Al_{ox}	Fe_{ox}	$(Al+Fe)_{ox}$	PSI (%)	Oxalate Ratio
	(mmol/kg)					
Control						
Unused	4.20	9.74	1.26	11.0	37.9	2.62
0 - 2	2.91	7.44	0.896	8.33	36.3	2.87
11-12	4.94	10.2	1.31	11.5	42.8	2.32
21-22	5.70	11.7	1.59	13.3	42.6	2.34
43-44	4.47	11.0	1.28	12.3	36.4	2.74
Experimental						
Unused	7.88	180	1.30	182	4.32	23.1
0 - 2	13.4	193	1.55	195	6.90	14.5
11-12	9.99	191	1.59	193	5.27	19.3
21-22	8.19	162	1.44	163	5.05	19.9
43-44	7.99	181	1.41	182	4.41	22.8

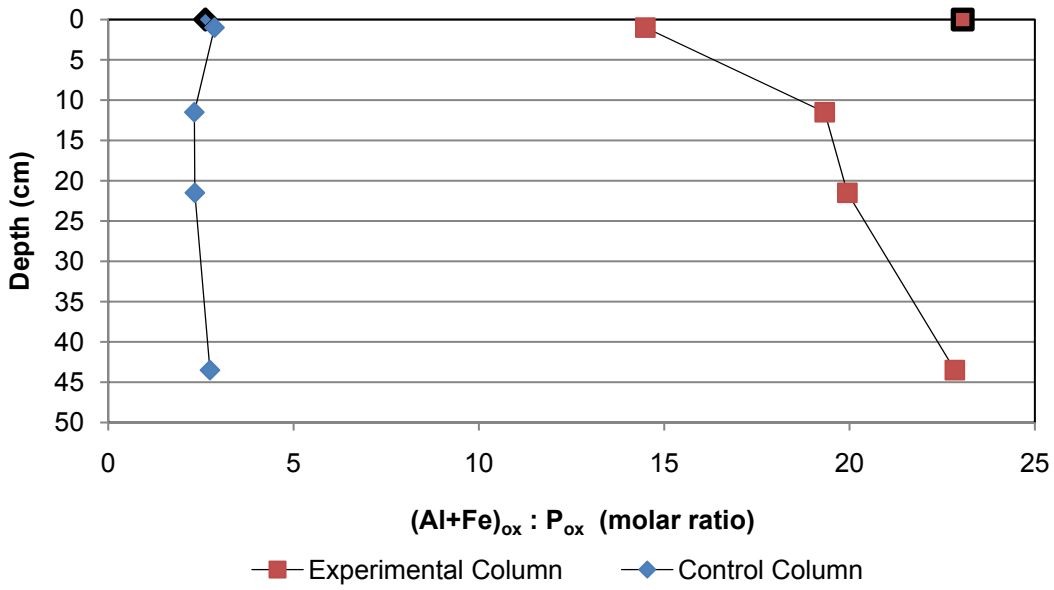

Figure 6-4. Post-adsorption vegetated column oxalate ratios at various depths. 0.275 M acid ammonium oxalate extraction fluid (pH = 3.0 ± 0.1) at 1:40 w/v was used. Marks with black trim represent unused, "virgin" media.

this is the surface layer sample, which showed reduced oxalate-extractable contents for P, Fe, and Al (2.91 mmol P_{ox}/kg, 0.896 mmol Fe_{ox}/kg, and 7.44 mmol Al_{ox}/kg) compared to the unused media (4.20 mmol P_{ox}/kg, 1.26 mmol Fe_{ox}/kg, and 9.74 mmol Al_{ox}/kg) and other depths. This surface portion was observed to have suffered heavily from fines migration, having a clearly greater content of quartz sand relative to other media constituents, and it is believed that this is the reason for the reduced oxalate-extractable contents. Also, the 21-22 cm layer showed a slight increase in all oxalate components (5.70 mmol P_{ox}/kg, 1.59 mmol Fe_{ox}/kg, and 11.7 mmol Al_{ox}/kg) compared to the unused, 11-12 cm layer (4.94 mmol P_{ox}/kg, 1.31 mmol Fe_{ox}/kg, and 10.2 mmol Al_{ox}/kg), and the 43-44 cm layer (4.47 mmol P_{ox}/kg, 1.28 mmol Fe_{ox}/kg, and 11.0 mmol Al_{ox}/kg). This is believed to be caused by heterogeneities in the media, because the slight increase in the Fe_{ox} and Al_{ox} of this layer was accompanied

by a measured increase in P_{ox}. A slight increase in clay or HBM content at that depth in the column media would cause a greater measure of oxalate extractable elements, and explain this occurrence. Because this difference is small and the media at all depths measured nearly identical oxalate ratios, the media being relatively the same throughout is implied, and suggests that the slight increase in oxalate measurements at this depth are not caused by an impurity in the media.

All fresh and unused control media showed very low oxalate ratios, indicating it will be a very poor sink for P and verifying experimental adsorption results (Section 4.4). Agyin-Birikorang and O'Connor (2007) report that the P leachability of a soil greatly increases with a PSI > 10%, which is analogous to an oxalate ratio of < 10. The unused control media has an oxalate ratio of 2.62 (PSI 37.9%), which falls well within this region of P leachability and corroborates the observed poor media P adsorption behavior (-2.38 mg P/kg). The control media is plotted on Figures 6-2 and 6-3, on which it shows behavior consistent with the overall trend in the data, having both a low oxalate ratio and low media P adsorption capacity relative to the other media.

The experimental media, conversely, showed well defined reductions in media capacity near the surface (Figure 6-4, Table 6-3). At 43 – 44 cm (½ column length) the media oxalate extractions measured nearly the same as the unused media (22.8 vis-à-vis 23.1), indicating that P carried into the column by the influent had been nearly completely adsorbed and removed from solution by this depth.

Exhaustion of the surface media may be determined by comparison with the minicolumn post-adsorption oxalate-extractable contents (Tables 6-2 and 6-3, respectively), although the media are not directly comparable because they differ in WTR and fines contents. However, the experimental column surface media sample and minicolumn media having similar WTR and fines contents had approximately the same oxalate-extractable contents post-use. For example, the experimental surface layer measured 7.99 mmol P_{ox}/kg, 1.41 mmol Fe_{ox}/kg, and 181 mmol Al_{ox}/kg. Comparatively, the set II intermittent 4% LFBSM media measured 7.36 mmol P_{ox}/kg, 12.3 mmol Fe_{ox}/kg, and 182 mmol Al_{ox}/kg post-adsorption. Also, the 4% WTR + sand media measured oxalate-extractable contents post-adsorption of 5.35 mmol P_{ox}/kg, 1.04 mmol Fe_{ox}/kg, and 148 mmol Al_{ox}/kg. One can see that the P_{ox} and Al_{ox} for the experimental media are nearly identical to that measured for the LFBSM mixture, while its Fe_{ox} content is more akin to the amended sand mixture. The sand itself should have little to no Fe_{ox} content, and that which was measured is believed to come from the WTR amendment. Consequently, this may indicate that the Fe content of the experimental (and control) media may be crystallized. Also, the similar measurements for the surface layer of the experimental media and these post-adsorption minicolumn experiments may suggest that the experimental media at the surface is in fact exhausted. If such is the case, it may be concluded that the media at greater depths still retain capacity for P adsorption as they have a higher measured oxalate ratio. Therefore, because only the surface layer of the vegetated column has exhausted its capacity, the majority of the experimental media in the column is not exhausted and the media still retains a large proportion of its adsorptive capacity.

The media that has reached capacity for P adsorption is between 2 and 12 cm, or approximately 2.2 to 13% of the media by depth, and nearly half the column (> 44 cm depth) retains most to all of its adsorption capacity. Overall, the experimental column media adsorbed 99.4 of 112 mg P from the influent, compared to the control column which produced 79.0 mg P (see Section 5.5).

A linear regression was performed for media adsorption capacity dependence on the oxalate ratio (Figure 6-2). This regression ($R^2 = 0.7148$) resulted in the equation

$$q = 1.35889 \cdot OR - 0.841644 \quad (6\text{-}1)$$

where q is the media adsorption capacity (mg P/kg), and OR is the oxalate ratio (molar basis). This predicts for the experimental media an adsorption capacity of 30.5 ± 20.3 mg P/kg (± SE) for OR = 23.1. While this is only 90% of the necessary 34 mg P/kg, when the magnitude of the standard error is considered, this suggests the media has a sufficient capacity for P adsorption.

6.4. Recommended Media Specifications and Procedures

Figure 6-3 indicates that a minimum oxalate-extractable Al and Fe content of approximately 150 to 250 mmol/kg is necessary for satisfactory P capture as defined by 120 μg/L soluble P. It must be noted that this is a very coarse predictor of media adsorption, as exemplified by the high degree of variability in the data. The oxalate ratio data presented in Figure 6-2 show a much stronger linear trend and indicate that for any media an oxalate ratio of at least 20 to 40 is necessary for adequate stormwater treatment. This is equivalent to a PSI of no more than 2.5 to 5%. Based on a linear regression ($R^2 = 0.5627$) of percent WTR on media oxalate ratios utilizing

all available data, this is equivalent to 2.6 to 4.3 ± 1.7 % WTR (± SE) for the specific WTR used in this study. Lower WTR contents in this range are more appropriate as P_{ox} content of the unamended media or fines content diminishes. Conversely, unamended media with higher P_{ox} contents or the use of WTR with a lower Al_{ox} content may require higher additions.

WTR-amended media must meet these requirements to perform adequately, but procedures should be followed to correctly prepare the amended BSM for use (Figure 6-5). Al-WTR should be collected dewatered from the drinking water treatment plant. Air dried materials may be used, but those which have aged in the open air for more than 6 months or have been subjected to higher temperatures (> 45°C) may have reduced Al_{ox} contents and reactivity (Agyin-Birikorang and O'Connor, 2009). This same study, however, also implicated such "fresh" Al-WTR (aged < 6 mo.) as having increased risk of Al leaching. Therefore, while reduced reactivity may lead to the need for greater volumes of residual to achieve the desired media P adsorption, this must be counter-balanced with Al leaching potential.

Drinking water plants often produce dewatered sludge as either pellets or large cakes. If possible, the WTR should be fed through an impact crusher, ball mill, grinding mill, or other device well suited for crushing soft materials, especially if the WTR is acquired as cakes. Particles of WTR should be as small as possible to maximize surface area while large enough so as to not migrate within the larger soil matrix or contribute to media clogging. Ostensibly this should be approximately 2 mm. Crushing the WTR is not

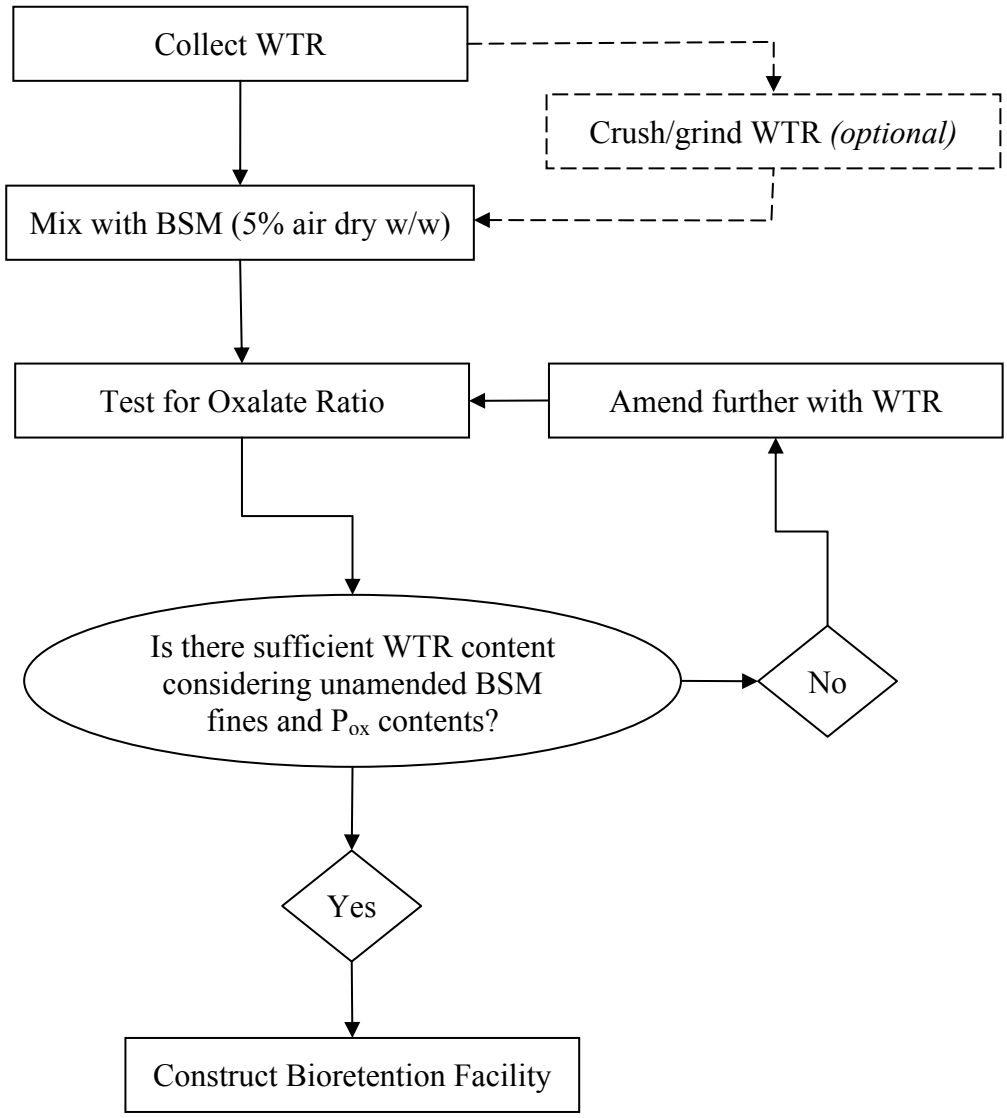

Figure 6-5. Flow chart for amended BSM mixing.

mandatory, however it should improve performance by maximizing the available surface area for P adsorption.

The collected residual must be mixed thoroughly with the BSM. This may be done mechanically such as with a cement mixer or other tumbling device. As explained in Section 4.1, the literature has reported mean WTR Al_{ox} content to be

approximately 70 to 90 g/kg. Therefore, the WTR should be amended at a rate of 5 to 10% of total media mass (air dried weight), trending upwards as fines content or the unamended media P_{ox} content increases. Solids content of the dewatered residual is often obtainable from the source drinking water plant to allow for calculation of the air dry mass equivalent of the moist WTR. After mixing, test the media and determine the oxalate ratio. If necessary, further amend the media. For the period when the BSM is mixed but samples are being analyzed in the laboratory, or in any instance where the amended BSM must sit before installation in the bioretention cell, cover the media with a tarp or other impervious material and attempt to make it as water tight as possible. Prevention of media drying will help to maintain a high oxalate ratio. Once the media meets specifications it should be installed as normal.

Additionally, thought must be given to plant survivorship with WTR-amended facilities. The addition of WTR at the recommended application rates will lead to some stunted plant growth and may cause the death of some individual plants (Oladeji et al., 2007; Mahdy et al., 2009; Lombi et al., 2009; Oladeji et al., 2009). However, healthy plants should not be severely negatively impacted. If plant survivorship is of particular importance and some degree of media performance may be compromised, a 15 – 30 cm (½ - 1 ft.) unamended surface layer may be used for planting. The soil used for this planting layer should have an oxalate ratio of at least 10 to prevent leaching of P to the amended media below.

Retrofitting of established bioretention facilities may be undertaken by rototilling WTR into the soil surface, as surface application of WTR has been shown effective in the agriculture literature. In many agricultural studies (Oladeji et al.,

2007; Agyin-Birikorang et al., 2009; Mahdy et al., 2009; Oladeji et al., 2009), no negative plant effects were reported when surface applying WTR at a rate of approximately 20 – 25 Mg WTR/ha along with a P source (i.e., biosolids, manure, inorganic fertilizer). At 10 – 15 cm depth, this is equivalent to 1 to 1.7% WTR (w/w) assuming a soil bulk density of 1.45 g/cm^3. Amending the soil with WTR at a rate of 5% and to a depth of at least 10 cm (⅓ ft.) should be sufficient to adsorb stormwater P. However, greater application rates and depths will provide greater capacity for P adsorption. During rototilling, established plants may be avoided or non-woody species may be tilled under and the facility replanted with little foreseeable impact on media performance.

Chapter 7: Conclusions and Recommendations

Investigation into the use of Al-WTR as a BSM amendment provided an encouraging indication as to the capability of Al-WTR to control the movement of P through bioretention cells. Batch studies showed only a minimal effect of pH on media P adsorption capacity within the investigated range of both pH and P concentration. Increasing WTR content yielded increasing media P adsorption capacity. Pure $Al(OH)_3$ provided increased P adsorption relative to an equivalent proportion of Al_{ox} provided by WTR. This is believed to be caused by the greater surface area of the $Al(OH)_3$ powder and diffusional limitations of the WTR. Unexpectedly, increasing fines content also yielded increasing media P adsorption capacity. Potential reasons for this behavior are that: sand addition led to a reduction in overall P_{ox} content of the mixture by "diluting" the BSM (PSI > 10%) while maintaining a high Al_{ox} content because the proportion of WTR was kept constant; reduced fines content led to a reduction in competitive adsorption by negatively charged clay particles and P for positively charged WTR reactive sites; and reduced fines content minimized the blocking of WTR micropores by clay particles, helping to maintain a high available WTR surface area. HBM addition (~ 3% dry wt.) yielded increasing media P adsorption capacity in most cases. This is believed to result from the formation of Al-OM-P complexes, which bind P as well as dissolved/colloidal OM. This OM has the capacity to leach from the media and appear as reduced media P adsorption capacity upon effluent digestion. LC addition (~ 5 % wt.) yielded decreased media P adsorption capacity, likely because of P leaching by the LC.

Minicolumn experiments examined the behavior of media under flow conditions. For equivalent media, equilibrium P adsorption capacity generally decreased from: batch > continuous column flow > intermittent column flow. For the investigated media subjected to intermittent flow, the HBM-amended media displayed the least reduction in media P adsorption capacity relative to its continuous flow counterpart. This suggests that the HBM helped to reduce drying and concomitant crystallization of the amended WTR, maintaining a higher amorphous Al content. Also, increased media P adsorption was observed in the intermittent flow column media upon the resumption of flow following dry periods. Media P adsorption rapidly declined thereafter. This suggests that "slow" reactions continue after the cessation of flow, providing some additional reactive surface sites for P adsorption when flow resumes.

Throughout all experiments for the mesoscale vegetated columns, the WTR-amended experimental media showed greatly improved adsorption relative to the control media. Experimental media exhibited a total effluent TP EMC of 16.1 μg/L from an input of 120 μg/L, far superior to the 266 μg/L displayed by the non-WTR-amended control media and sufficient to meet the EPA recommended surface water limit of 25 μg/L.

The vegetated columns generally showed consistent effluent pollutographs throughout all experiments. The experimental media exhibited initial high adsorption which rapidly declined over the course of approximately 15 to 30 minutes. Thereafter, media P adsorption began to improve again, creating a localized peak in P adsorption. Conversely, the control media displayed poor P adsorption initially

which increased with continued flow, creating a exponential-like effluent concentration curve.

Increased flowrate resulted in increased PP releases from both media. The magnitude of these releases were quite different for each column, though, with the experimental column showing EMC increases of 3-8 μg/L relative to the previous run, while the control column increases were 25-36 μg/L. Similarly, increased drying time further exacerbated the release of PP. Total PP EMC for the experimental column measured 10.0 μg/L, while that for the control column measured 102 μg/L.

Increased influent P concentrations led to increased effluent TDP (and concomitantly TP) for the control column. The experimental column only displayed significantly increased effluent TDP when increased influent P concentrations were applied in conjunction with an elevated flowrate. Ultimately, the experimental column total effluent TDP EMC was 6.1 μg/L, while the control column value was 144 μg/L.

Increased drying time, as previously mentioned, induced increased PP release from both columns. However, in the control column it also resulted in decreased effluent TDP, while in the experimental column it resulted in increased effluent TDP. The TDP increase observed in the control column is consistent with the intermittent flow results from the minicolumn experiments, and is attributed to the freeing of surface reactive sites through the occurrence of "slow" reactions during dry periods. Conversely, the reduced P adsorption seen in the experimental column is attributed to media drying, which may have resulted in reduced media adsorptive surface area. Conversely, reduced antecedent dry time resulted in improved P adsorption in the

experimental column. The control column results after reduced antecedent dry time were obscured by the aftereffects of previous runs and no definitive conclusion could be drawn.

Both columns showed minimal releases of NOx, with total effluent EMCs of 0.896 and 0.991 mg NO_3^-+NO_2^-/L for the experimental and control columns, respectively, relative to the influent EMC of 0.880 mg/L. Conversely, there was some removal of TKN from the influent, with the experimental and control columns displaying effluent EMCs of 0.524 and 1.22 mg TKN/L relative to an influent EMC of 1.31 mg/L. The TKN species used were NH_4^+ and organic N as glycine. The removal of TKN from the influent is attributed to the adsorption of glycine to the media, as glycine exists as a zwitterion within the pH range of the experiments.

Some leaching of SO_4^{2-} was observed from the experimental media, attributed to release from the WTR because $Al_2(SO_4)_3 \cdot 14\ H_2O$ was used as a coagulant during its generation. Media SO_4^{2-} density was measured as 261 mg SO_4^{2-}/kg. This is not expected to be environmentally significant or a potential danger to human health, although nuisance odors as a result of H_2S formation may occur if reducing conditions are encountered in the bioretention cell.

Oxalate extractions were used to characterize the media and to develop a metric to predict adsorption performance. Media oxalate ratio [$(Al+Fe)_{ox}$:P_{ox}] was found to positively correlate with media P adsorption capacity. WTR addition improved P adsorption by increasing media measured Al_{ox} content. Sand addition improved media P adsorption by reducing media P_{ox} content while maintaining a high Al_{ox} content via added WTR. HBM improved media P adsorption by contributing

Fe_{ox} to the media mixture along with little to no P_{ox} relative to the BSM. Conversely, LC depressed media P adsorption by contributing increased P_{ox} to the media mixture.

In the vegetated mesocolumn studies, control media exhibited an oxalate ratio of 2.62 (PSI 37.9%). This corroborates the leaching behavior observed in the media, as an oxalate ratio < 10 (PSI > 10%) indicates a media that is at risk of P leaching. Conversely, the experimental media had a measured oxalate ratio of 23.1 (PSI 4.32%). This supports the excellent P adsorption observed in the media. A decreasing oxalate ratio nearer the surface after the 13 experiments also suggests that the P adsorption capacity of the media is not exhausted. A linear regression of media P adsorption capacity on the oxalate ratio ($R^2 = 0.7148$) predicts the P adsorption capacity of the experimental media to be 30.5 ± 20.3 mg P/kg (± SE).

For future use, media amended with WTR are suggested to have an oxalate ratio of at least 20 to 40 (PSI ≤ 2.5 to 5%) to remove sufficient P from influent stormwater. This should be equivalent to approximately 5 to 10% WTR by air dry mass. Oxalate ratios toward the higher end of this range will be required for media with higher fines contents, higher P-content OM amendments (i.e., compost, etc.), and lower Al_{ox}-content WTR.

It is recommended that WTR is collected from the drinking water treatment plant, crushed to approximately 2 mm if possible, and thoroughly mixed with BSM. The WTR will retain maximum adsorption capacity by minimizing ageing and drying prior to and during installation, although very "fresh" WTR has been suggested to be at risk for Al leaching (Agyin-Birikorgan and O'Connor, 2009). Therefore, WTR aged less than one month should not be used, and the risk for Al leaching must be

considered for those residuals aged less than six months. The WTR amended BSM may be installed in the bioretention cell per standard operating procedure. In the end, combining both Al-WTR and an organic amendment such as HBM with an increased nitrogen removal measure such as carefully selected vigorous plant coverage and/or a raised underdrain (anoxic denitrification sump) is theorized to lead to dramatically increased removal efficiency in a bioretention system without sacrificing hydrologic performance. The installation of such a raised underdrain in an amended facility will be ideal to promote N removal by the bioretention cell through denitrification in conjunction with P sequestration. The possible generation of nuisance odors must be considered though. The addition of WTR at the recommended concentrations is also expected to lead to stunted plant growth. An unamended BSM surface layer (15 – 30 cm) may be use to diminish any negative effects on vegetation. However, doing so will reduce the total capacity of the cell for P adsorption.

The retrofitting of established bioretention cells may be undertaken by rototilling WTR into the BSM surface *in situ*. The necessary content of WTR amended to the soil will depend on P treatment goals, but increasing the concentration and depth of amendment will result in improved overall P adsorption. WTR may be applied around vegetation, or non-woody vegetation may be rototilled into the soil along with the WTR and then the bioretention cell replanted with little expected impact on adsorption performance. The surface application of WTR at 5 to 10% (air dry mass) of BSM should be to a depth of 10 to 30 cm (⅓ - 1 ft.). Assuming a BSM bulk density of 1.5 g/cm^3, this is analogous to 7.5 – 45 kg/m^2 (75 - 450 Mg/ha; 1.54 – 9.22 lb/ft^2).

Future research needs are many. It is necessary to attempt to verify these results using different BSM and WTR, possibly one that does not contain a secondary polymer coagulant or that uses a different Al-based coagulant such as polyaluminum chloride (PAC) or polyaluminum chlorosulfate (PACS). Additionally, validation of oxalate extraction as a means of predicting media P adsorption capacity is needed using field core oxalate extractions and monitoring data to verify the robustness of this metric.

Probing into the nature of HBM and the mechanisms by which it interacts with WTR to improve P adsorption in the amended BSM is also of interest. The variable and somewhat inconsistent results between batch and column studies indicate mechanisms are operating which are not fully understood.

An attempt to construct a cell and/or perform a retrofit is necessary to verify the construction specifications outlined. Additionally, this would allow for monitoring to ensure media specifications provide for adequate stormwater P adsorption and verification of plant survivability in a WTR-amended bioretention cell. It may also be beneficial to perform a laboratory or field study to investigate native and local vegetation which provide for maximal nutrient uptake in both WTR-amended and non-amended bioretention cells.

Appendices

Appendix A: Batch Data

Table A-1. Unamended BSM P adsorption isotherm data. Sample mass is adjusted for water content. Volume is the volume of the respective P solution with a 0.01 M KCl background electrolyte. pH_0 is the sample pH before adjustment. pH_i is the adjusted pH before equilibration. pH_f is the sample pH after the 24 hour equilibration period.

	ID	Mass (g)	Vol (mL)	pH_0	pH_i	pH_f	Equilibrium Concentration (mg/L)	Adsorption Capacity (mg P/kg)
0.3 mg P/L solution	Control	-	45	5.39	5.39	5.38	0.320	-
	BK0-1-1	1.787	45	5.86	3.87	4.79	0.075	6.16
	BK0-1-2	1.790	45	5.83	4.08	5.38	0.059	6.55
	BK0-1-3	1.791	45	5.85	4.63	5.68	0.049	6.79
	BK0-1-4	1.788	45	5.85	5.85	5.94	0.042	6.99
	BK0-1-5	1.792	45	5.8	8.63	6.48	0.042	6.96
0.9 mg P/L solution	Control	-	45	5.18	5.18	5.22	0.881	-
	BK0-2-1	1.792	45	5.72	3.77	5.11	0.193	17.28
	BK0-2-2	1.790	45	5.67	4.14	5.65	0.166	17.98
	BK0-2-3	1.789	45	5.74	4.69	5.65	0.152	18.36
	BK0-2-4	1.790	45	5.75	5.75	6.01	0.128	18.96
	BK0-2-5	1.791	45	5.73	8.21	6.29	0.101	19.62
3.0 mg P/L solution	Control	-	45	5.14	5.14	5.08	2.969	-
	BK0-3-1	1.789	45	5.71	3.85	5.23	1.255	43.12
	BK0-3-2	1.789	45	5.61	4.24	5.5	1.130	46.25
	BK0-3-3	1.790	45	5.59	4.43	5.67	1.201	44.45
	BK0-3-4	1.790	45	5.65	5.65	6.1	1.140	45.97
	BK0-3-5	1.788	45	5.66	8.07	6.51	0.828	53.90

Table A-2. BSM + 2% WTR P adsorption isotherm data. Sample mass is adjusted for water content. Volume is the volume of the respective P solution with a 0.01 M KCl background electrolyte. pH_0 is the sample pH before adjustment. pH_i is the adjusted pH before equilibration. pH_f is the sample pH after the 24 hour equilibration period.

ID	Mass (g)	Vol (mL)	pH_0	pH_i	pH_f	Equilibrium Concentration (mg/L)	Adsorption Capacity (mg P/kg)

0.3 mg P/L solution	Control	-	45	5.35	5.35	5.11	0.310	-
	BK0-1-1	1.777	45	5.84	3.93	5.9	0.035	6.96
	BK0-1-2	1.775	45	5.86	4.34	6.08	0.038	6.88
	BK0-1-3	1.776	45	5.86	4.57	6.31	0.026	7.18
	BK0-1-4	1.777	45	5.91	5.91	6.48	0.028	7.13
	BK0-1-5	1.774	45	5.92	8.73	6.6	0.028	7.15
0.9 mg P/L solution	Control	-	45	5.2	5.2	5.23	0.881	-
	BK0-2-1	1.775	45	5.97	4.17	6.23	0.118	19.36
	BK0-2-2	1.776	45	5.84	4.31	6.2	0.104	19.70
	BK0-2-3	1.775	45	5.92	4.61	6.29	0.087	20.13
	BK0-2-4	1.771	45	5.82	5.82	6.51	0.083	20.29
	BK0-2-5	1.773	45	5.79	8.64	6.73	0.110	19.57
3.0 mg P/L solution	Control	-	45	5.14	5.14	5.16	3.112	-
	BK0-3-1	1.774	45	5.79	3.98	5.97	0.895	56.25
	BK0-3-2	1.774	45	5.74	4.22	5.87	0.875	56.76
	BK0-3-3	1.771	45	5.8	4.67	6.48	0.700	61.30
	BK0-3-4	1.775	45	5.75	5.75	6.54	0.744	60.05
	BK0-3-5	1.773	45	5.79	8.29	6.78	0.895	56.28

Table A-3. BSM + 4% WTR P adsorption isotherm data. Sample mass is adjusted for water content. Volume is the volume of the respective P solution with a 0.01 M KCl background electrolyte. pH_0 is the sample pH before adjustment. pH_i is the adjusted pH before equilibration. pH_f is the sample pH after the 24 hour equilibration period.

	ID	Mass (g)	Vol (mL)	pH_0	pH_i	pH_f	Equilibrium Concentration (mg/L)	Adsorption Capacity (mg P/kg)
0.3 mg P/L solution	Control	-	45	5.28	5.28	5.29	0.266	-
	BA4-1-1	1.758	45	5.9	8.9	6.94	0.020	6.31
	BA4-1-2	1.761	45	5.98	5.98	6.47	0.023	6.20
	BA4-1-3	1.759	45	5.94	3.93	5.92	0.024	6.18
	BA4-1-4	1.760	45	5.93	4.2	6.14	0.025	6.17
	BA4-1-5	1.759	45	5.98	4.63	6.59	0.013	6.47
0.9 mg P/L solution	Control	-	45	5.26	5.26	5.24	0.855	-
	BA4-2-1	1.759	45	5.92	3.98	6	0.074	19.97
	BA4-2-2	1.757	45	5.91	4.23	6.29	0.059	20.38
	BA4-2-3	1.757	45	5.91	4.64	6.34	0.064	20.26
	BA4-2-4	1.762	45	5.92	5.92	6.82	0.041	20.79
	BA4-2-5	1.760	45	5.92	8.41	6.66	0.050	20.58

3.0 mg P/L solution	Control	-	45	5.25	5.25	5.26	2.860	-
	BA4-3-1	1.758	45	5.83	3.94	6.06	0.498	60.46
	BA4-3-2	1.760	45	5.81	4.09	6.46	0.289	65.73
	BA4-3-3	1.760	45	5.82	4.59	6.5	0.585	58.16
	BA4-3-4	1.762	45	5.81	5.81	6.43	0.501	60.24
	BA4-3-5	1.758	45	5.81	7.97	6.77	0.545	59.26

Table A-4. BSM + 10% WTR P adsorption isotherm data. Sample mass is adjusted for water content. Volume is the volume of the respective P solution with a 0.01 M KCl background electrolyte. pH_0 is the sample pH before adjustment. pH_i is the adjusted pH before equilibration. pH_f is the sample pH after the 24 hour equilibration period. Highlighted data are those measured below the MDL of 10 µg P/L, and consequently 5 µg P/L was used in media P adsorption capacity calculations

	ID	Mass (g)	Vol (mL)	pH_0	pH_i	pH_f	Equilibrium Concentration (mg/L)	Adsorption Capacity (mg P/kg)
0.3 mg P/L solution	Control	-	45	6.05	6.05	6.03	0.259	-
	BA2-1-1	1.714	45	6.23	3.99	6.86	0.007	6.67
	BA2-1-2	1.712	45	6.25	4.15	6.8	0.007	6.68
	BA2-1-3	1.713	45	6.31	4.68	6.82	0.007	6.67
	BA2-1-4	1.713	45	6.23	6.23	6.98	0.007	6.67
	BA2-1-5	1.712	45	6.3	8.33	7.04	0.002	6.68
0.9 mg P/L solution	Control	-	45	5.8	5.8	5.78	0.856	-
	BA2-2-1	1.713	45	6.12	3.85	6.79	0.010	22.21
	BA2-2-2	1.713	45	6.17	4.27	6.95	0.018	22.03
	BA2-2-3	1.712	45	6.25	4.96	6.91	0.011	22.20
	BA2-2-4	1.714	45	6.25	6.25	7.02	0.012	22.16
	BA2-2-5	1.713	45	6.19	8.58	7.13	0.016	22.06
3.0 mg P/L solution	Control	-	45	5.16	5.16	5.19	2.767	-
	BA2-3-1C	1.710	45	6.06	3.86	6.89	0.049	71.50
	BA2-3-2C	1.713	45	6.02	4.16	6.87	0.093	70.24
	BA2-3-3C	1.712	45	6.03	4.58	7.07	0.076	70.72
	BA2-3-4C	1.714	45	6.02	6.02	7.1	0.088	70.32
	BA2-3-5C	1.712	45	6.04	8.53	7.08	0.075	70.73
9.0 mg P/L solution	Control	-	45	5.1	5.1	5.12	8.646	-
	BA2-4-1	1.716	45	5.9	3.87	6.91	0.547	226.14
	BA2-4-2	1.714	45	5.89	4.29	6.85	0.597	226.34
	BA2-4-3	1.716	45	5.9	4.76	7.08	0.547	226.14
	BA2-4-4	1.713	45	5.96	5.96	7.16	0.648	226.41

BA2-4-5	1.711	45	5.89	7.9	7.37	0.799	226.50

Table A-5. Unamended LFBSM P adsorption isotherm data. Sample mass is adjusted for water content. Volume is the volume of the respective P solution with a 0.01 M KCl background electrolyte. pH_0 is the sample pH before adjustment. pH_i is the adjusted pH before equilibration. pH_f is the sample pH after the 24 hour equilibration period.

	ID	Mass (g)	Vol (mL)	pH_0	pH_i	pH_f	Equilibrium Concentration (mg/L)	Adsorption Capacity (mg P/kg)
0.3 mg P/L solution	Control	-	45	5.28	5.28	5.15	0.306	-
	LF0-1-1	1.801	45	5.56	3.83	4.6	0.217	2.22
	LF0-1-2	1.800	45	5.5	3.98	4.91	0.160	3.66
	LF0-1-3	1.799	45	5.54	4.36	5.06	0.121	4.62
	LF0-1-4	1.800	45	5.53	5.53	5.67	0.102	5.10
	LF0-1-5	1.795	45	5.56	8.92	6.43	0.093	5.36
0.9 mg P/L solution	Control	-	45	5.4	5.4	5.24	0.892	-
	LF0-2-1	1.797	45	5.55	3.98	4.81	0.407	12.13
	LF0-2-2	1.797	45	5.52	4.12	4.78	0.431	11.54
	LF0-2-3	1.799	45	5.55	4.48	5.33	0.384	12.70
	LF0-2-4	1.801	45	5.54	5.54	5.52	0.353	13.45
	LF0-2-5	1.797	45	5.55	8.81	6.12	0.347	13.64
3.0 mg P/L solution	Control	-	45	5.09	5.09	5.16	2.986	-
	LF0-3-1	1.800	45	5.39	3.99	4.82	1.758	30.69
	LF0-3-2	1.798	45	5.44	4.13	4.99	1.825	29.04
	LF0-3-3	1.799	45	5.46	4.45	5.21	1.783	30.07
	LF0-3-4	1.797	45	5.48	5.48	5.75	1.682	32.63
	LF0-3-5	1.800	45	5.45	7.88	6.32	1.657	33.21

Table A-6. LFBSM + 3% WTR P adsorption isotherm data. Sample mass is adjusted for water content. Volume is the volume of the respective P solution with a 0.01 M KCl background electrolyte. pH_0 is the sample pH before adjustment. pH_i is the adjusted pH before equilibration. pH_f is the sample pH after the 24 hour equilibration period.

	ID	Mass (g)	Vol (mL)	pH_0	pH_i	pH_f	Equilibrium Concentration (mg/L)	Adsorption Capacity (mg P/kg)
0.3 mg P/L solution	Control	-	23.5	5.15	5.15	5.12	0.281	-
	LF2-1-1	1.776	45	5.55	4.01	6.31	Sample dropped	
	LF2-1-2	1.778	45	5.54	4.14	6.34	0.018	6.66
	LF2-1-3	1.777	45	5.61	4.36	6.57	0.018	6.68

	LF2-1-4	1.777	45	5.63	5.63	6.53	0.023	6.53
	LF2-1-5	1.775	45	5.61	8.41	6.71	0.039	6.16
0.9 mg P/L solution	Control	-	45	5.13	5.13	5.19	0.843	-
	LF2-2-1	1.778	45	5.55	3.95	6.33	0.047	21.33
	LF2-2-2	1.776	45	5.6	4.13	6.48	0.054	21.36
	LF2-2-3	1.776	45	5.61	4.31	6.47	0.048	21.37
	LF2-2-4	1.778	45	5.6	5.6	6.51	0.079	21.33
	LF2-2-5	1.775	45	5.51	7.84	6.69	0.078	21.38
3.0 mg P/L solution	Control	-	45	5.24	5.24	5.24	3.038	-
	LF2-3-1	1.774	45	5.5	4.05	6.39	0.613	61.53
	LF2-3-2	1.776	45	5.48	4.22	6.47	0.488	64.63
	LF2-3-3	1.777	45	5.52	4.47	6.48	0.606	61.56
	LF2-3-4	1.775	45	5.53	5.53	6.44	0.664	60.21
	LF2-3-5	1.776	45	5.55	7.83	6.86	0.613	61.43

Table A-7. LFBSM + 6% WTR P adsorption isotherm data. Sample mass is adjusted for water content. Volume is the volume of the respective P solution with a 0.01 M KCl background electrolyte. pH_0 is the sample pH before adjustment. pH_i is the adjusted pH before equilibration. pH_f is the sample pH after the 24 hour equilibration period.

	ID	Mass (g)	Vol (mL)	pH_0	pH_i	pH_f	Equilibrium Concentration (mg/L)	Adsorption Capacity (mg P/kg)
0.3 mg P/L solution	Control	-	45	5.25	5.25	5.28	0.326	-
	LF3-3-1	1.755	45	5.77	3.9	6.69	0.014	8.02
	LF3-3-2	1.753	45	5.77	4.15	6.76	0.015	7.98
	LF3-3-3	1.753	45	5.7	4.4	6.89	0.011	8.09
	LF3-3-4	1.752	45	5.85	5.85	6.87	0.012	8.08
	LF3-3-5	1.753	45	5.83	8.44	7	0.012	8.07
0.9 mg P/L solution	Control	-	45	5.21	5.21	5.18	0.844	-
	LF3-2-1	1.753	45	5.71	3.93	6.7	0.018	21.23
	LF3-2-2	1.754	45	5.66	4.1	6.73	0.022	21.11
	LF3-2-3	1.752	45	5.74	4.44	6.84	0.023	21.10
	LF3-2-4	1.754	45	5.9	5.9	6.87	0.027	20.98
	LF3-2-5	1.753	45	5.79	8.93	7.08	0.017	21.24
3.0 mg P/L solution	Control	-	45	5.13	5.13	5.22	3.129	-
	LF3-1-1	1.753	45	5.64	4.07	6.65	0.185	75.58
	LF3-1-2	1.755	45	5.64	4.36	6.84	0.155	76.28
	LF3-1-3	1.753	45	5.74	4.55	6.87	0.209	74.98

LF3-1-4	1.751	45	5.77	5.77	7.02	0.138	76.88
LF3-1-5	1.755	45	5.7	7.83	7	0.269	73.30

Table A-8. BSM + 10% WTR P adsorption isotherm data. Sample mass is adjusted for water content. Volume is the volume of the respective P solution with a 0.01 M KCl background electrolyte. pH_0 is the sample pH before adjustment. pH_i is the adjusted pH before equilibration. pH_f is the sample pH after the 24 hour equilibration period. Highlighted data are those measured below the MDL of 10 µg P/L, and consequently 5 µg P/L was used in media P adsorption capacity calculations

	ID	Mass (g)	Vol (mL)	pH_0	pH_i	pH_f	Equilibrium Concentration (mg/L)	Adsorption Capacity (mg P/kg)
0.3 mg P/L solution	Control	-	45	5.18	5.18	5.26	0.320	-
	LF1-1-1	1.725	45	6.09	3.94	6.92	0.007	8.21
	LF1-1-2	1.722	45	6.04	4.11	6.82	0.008	8.22
	LF1-1-3	1.723	45	6.01	4.55	7.1	0.006	8.22
	LF1-1-4	1.725	45	6.16	6.16	7.01	0.008	8.21
	LF1-1-5	1.720	45	5.93	8.86	7.29	0.009	8.23
0.9 mg P/L solution	Control	-	45	5.25	5.25	5.42	0.895	-
	LF1-2-1	1.721	45	5.91	3.88	6.98	0.010	23.14
	LF1-2-2	1.723	45	5.96	4.23	7.05	0.011	23.08
	LF1-2-3	1.721	45	5.99	4.71	7.13	0.012	23.07
	LF1-2-4	1.721	45	6.1	6.1	7.18	0.011	23.10
	LF1-2-5	1.726	45	6.04	8.65	7.24	0.010	23.08
3.0 mg P/L solution	Control	-	45	5.16	5.16	4.94	2.969	-
	LF1-3-1	1.723	45	5.96	4.13	7.14	0.037	76.59
	LF1-3-2	1.721	45	5.92	4.33	7.17	0.030	76.86
	LF1-3-3	1.720	45	5.99	4.82	7.11	0.043	76.56
	LF1-3-4	1.725	45	5.98	5.98	7.19	0.044	76.31
	LF1-3-5	1.722	45	5.94	8.35	7.29	0.048	76.33
9.0 mg P/L solution	Control	-	45	4.99	4.99	4.93	8.246	-
	LF1-5-1	1.725	45	5.81	3.96	6.82	0.418	204.23
	LF1-5-2	1.724	45	5.84	4.31	6.98	0.401	204.77
	LF1-5-3	1.722	45	5.84	4.58	7.03	0.272	208.38
	LF1-5-4	1.725	45	5.84	5.96	7.08	0.312	206.97
	LF1-5-5	1.725	45	5.81	7.63	7.29	0.418	204.23

Table A-9. BSM + HBM P adsorption isotherm data. Sample mass is adjusted for water content. Volume is the volume of the respective P solution with a 0.01 M KCl background electrolyte. pH_0 is the sample pH before adjustment. pH_i is the adjusted pH before equilibration. pH_f is the sample pH after the 24 hour equilibration period.

	ID	Mass (g)	Vol (mL)	pH_0	pH_i	pH_f	Equilibrium Concentration (mg/L)	Adsorption Capacity (mg P/kg)
0.3 mg P/L solution	Control	-	45	5.24	5.24	5.29	0.376	-
	HM3-1-1	1.755	45	5.81	3.89	5.34	0.074	7.75
	HM3-1-2	1.753	45	5.97	4.1	5.79	0.083	7.52
	HM3-1-3	1.753	45	6.01	4.57	6.04	0.079	7.63
	HM3-1-4	1.755	45	6.15	6.15	6.38	0.078	7.64
	HM3-1-5	1.752	45	5.99	8.47	6.48	0.067	7.94
0.9 mg P/L solution	Control	-	45	5.13	5.13	5.22	0.840	-
	HM3-2-1	1.754	45	5.9	3.97	5.27	0.205	21.54
	HM3-2-2	1.753	45	5.88	4.19	5.82	0.182	21.55
	HM3-2-3	1.755	45	5.87	4.39	5.71	0.159	21.53
	HM3-2-4	1.753	45	5.92	5.92	6.31	0.167	21.55
	HM3-2-5	1.754	45	5.95	8.15	6.45	0.167	21.54
3.0 mg P/L solution	Control	-	45	5.1	5.1	5.19	3.427	-
	HM3-3-1	1.752	45	5.88	3.88	5.46	1.212	56.90
	HM3-3-2	1.751	45	5.8	4.16	5.81	1.073	60.49
	HM3-3-3	1.756	45	5.86	4.35	5.9	1.144	58.50
	HM3-3-4	1.755	45	5.88	5.88	6.25	1.060	60.70
	HM3-3-5	1.754	45	5.81	8.07	6.43	0.911	64.56

Table A-10. BSM + 2% WTR + HBM P adsorption isotherm data. Sample mass is adjusted for water content. Volume is the volume of the respective P solution with a 0.01 M KCl background electrolyte. pH_0 is the sample pH before adjustment. pH_i is the adjusted pH before equilibration. pH_f is the sample pH after the 24 hour equilibration period.

	ID	Mass (g)	Vol (mL)	pH_0	pH_i	pH_f	Equilibrium Concentration (mg/L)	Adsorption Capacity (mg P/kg)
0.3 mg P/L solution	Control	-	45	5.11	5.11	4.95	0.247	-
	HM4-1-1	1.733	45	6.19	3.91	6.08	0.041	5.36
	HM4-1-2	1.732	45	6.24	4.47	6.26	0.023	5.82
	HM4-1-3	1.734	45	6.22	4.81	6.32	0.016	5.99
	HM4-1-4	1.732	45	6.14	6.14	6.43	0.014	6.06
	HM4-1-5	1.730	45	6.19	8.21	6.57	0.020	5.92

0.9 mg P/L solution	Control	-	45	5.05	5.05	4.99	0.849	-
	HM4-2-1	1.732	45	5.8	3.81	5.92	0.040	22.04
	HM4-2-2	1.734	45	5.86	4.19	6.01	0.043	22.02
	HM4-2-3	1.734	45	5.86	4.21	6	0.040	22.02
	HM4-2-4	1.734	45	6.02	6.02	6.45	0.039	22.02
	HM4-2-5	1.731	45	5.95	8.64	6.62	0.059	22.05
3.0 mg P/L solution	Control	-	45	4.93	4.93	5.05	2.769	-
	HM4-3-1	1.732	45	5.75	3.96	6.17	0.231	65.93
	HM4-3-2	1.730	45	5.78	4.09	6.2	0.257	65.35
	HM4-3-3	1.733	45	5.75	4.31	6.38	0.237	65.72
	HM4-3-4	1.730	45	5.87	5.87	6.52	0.427	60.94
	HM4-3-5	1.730	45	5.74	7.85	6.71	0.307	64.01

Table A-11. BSM + 4% WTR + HBM P adsorption isotherm data. Sample mass is adjusted for water content. Volume is the volume of the respective P solution with a 0.01 M KCl background electrolyte. pH_0 is the sample pH before adjustment. pH_i is the adjusted pH before equilibration. pH_f is the sample pH after the 24 hour equilibration period.

	ID	Mass (g)	Vol (mL)	pH_0	pH_i	pH_f	Equilibrium Concentration (mg/L)	Adsorption Capacity (mg P/kg)
0.3 mg P/L solution	Control	-	45	5.2	5.2	5.27	0.305	-
	HM2-1-1	1.733	45	6.03	4.1	6.65	0.017	7.48
	HM2-1-2	1.733	45	5.94	4.32	6.78	0.025	7.27
	HM2-1-3	1.734	45	6.04	4.5	6.83	0.020	7.40
	HM2-1-4	1.734	45	6.16	6.16	6.91	0.021	7.38
	HM2-1-5	1.733	45	6.11	8.5	7.22	0.021	7.38
0.9 mg P/L solution	Control	-	45	5.03	5.03	5.24	0.857	-
	HM2-2-1	1.733	45	5.92	3.99	6.4	0.034	22.24
	HM2-2-2	1.736	45	5.94	4.2	6.71	0.025	22.20
	HM2-2-3	1.734	45	5.96	4.58	6.72	0.045	22.22
	HM2-2-4	1.733	45	5.91	5.91	7.05	0.024	22.24
	HM2-2-5	1.737	45	5.95	8.55	6.95	0.040	22.19
3.0 mg P/L solution	Control	-	45	5.37	5.37	5.39	2.877	-
	HM2-3-1	1.736	45	6.16	4.12	6.43	0.190	69.64
	HM2-3-2	1.735	45	6.24	4.35	6.47	0.281	67.31
	HM2-3-3	1.737	45	6.23	4.56	6.55	0.231	68.55
	HM2-3-4	1.735	45	6.35	6.35	7.1	0.116	71.61
	HM2-3-5	1.735	45	6.27	8.06	7.26	0.248	68.19

Table A-12. BSM + LC P adsorption isotherm data. Sample mass is adjusted for water content. Volume is the volume of the respective P solution with a 0.01 M KCl background electrolyte. pH_0 is the sample pH before adjustment. pH_i is the adjusted pH before equilibration. pH_f is the sample pH after the 24 hour equilibration period.

	ID	Mass (g)	Vol (mL)	pH_0	pH_i	pH_f	Equilibrium Concentration (mg/L)	Adsorption Capacity (mg P/kg)
0.3 mg P/L solution	Control	-	45	5.29	5.29	5.07	0.264	-
	LC2-1-1	1.679	45	6.41	4.23	6.64	0.215	1.30
	LC2-1-2	1.681	45	6.38	4.04	6.6	Outside range	
	LC2-1-3	1.683	45	6.42	4.44	6.69	0.235	0.78
	LC2-1-4	1.679	45	6.54	6.54	6.81	0.157	2.87
	LC2-1-5	1.681	45	6.43	8.08	7.2	0.188	2.04
0.9 mg P/L solution	Control	-	45	5.23	5.23	5.17	0.832	-
	LC2-2-1	1.680	45	6.43	3.91	6.32	0.619	5.69
	LC2-2-2	1.680	45	6.38	4.2	6.58	0.423	10.94
	LC2-2-3	1.682	45	6.46	4.34	6.7	0.450	10.22
	LC2-2-4	1.680	45	6.58	6.58	-	Sample dropped	
	LC2-2-5	1.681	45	6.48	8.57	6.9	0.384	12.00
3.0 mg P/L solution	Control	-	45	5.21	5.21	5.12	2.761	-
	LC2-3-1	1.682	45	6.41	4.06	6.77	1.699	28.41
	LC2-3-2	1.679	45	6.28	4.23	6.4	1.589	31.40
	LC2-3-3	1.682	45	6.34	4.32	6.65	1.782	26.19
	LC2-3-4	1.680	45	6.43	6.43	6.85	1.387	36.81
	LC2-3-5	1.683	45	6.43	8.25	6.89	1.563	32.04

Table A-13. BSM + 4% WTR + LC P adsorption isotherm data. Sample mass is adjusted for water content. Volume is the volume of the respective P solution with a 0.01 M KCl background electrolyte. pH_0 is the sample pH before adjustment. pH_i is the adjusted pH before equilibration. pH_f is the sample pH after the 24 hour equilibration period.

	ID	Mass (g)	Vol (mL)	pH_0	pH_i	pH_f	Equilibrium Concentration (mg/L)	Adsorption Capacity (mg P/kg)
0.3 mg P/L solution	Control	-	45	5.12	5.12	5.03	0.311	-
	LC1-1-1	1.649	45	6.42	3.91	6.41	0.059	6.86
	LC1-1-2	1.650	45	6.36	4.42	6.77	0.057	6.92
	LC1-1-3	1.648	45	6.35	4.35	6.71	0.052	7.05
	LC1-1-4	1.649	45	6.53	6.53	7.03	0.045	7.24
	LC1-1-5	1.648	45	6.45	8.47	7.08	0.045	7.26

0.9 mg P/L solution	Control	-	45	5.14	5.14	5.02	0.865	-
	LC1-2-1	1.647	45	6.2	3.9	6.41	0.082	21.40
	LC1-2-2	1.647	45	6.13	4.67	6.82	0.058	22.06
	LC1-2-3	1.647	45	6.17	4.32	6.88	0.067	21.80
	LC1-2-4	1.652	45	6.39	6.39	6.92	0.071	21.63
	LC1-2-5	1.652	45	6.35	8.42	7.04	0.072	21.62
3.0 mg P/L solution	Control	-	45	5.13	5.13	4.99	2.877	-
	LC1-3-1	1.649	45	6.26	4.28	6.74	0.234	72.11
	LC1-3-2	1.652	45	6.18	3.96	6.96	0.254	71.45
	LC1-3-3	1.647	45	6.17	4.45	6.91	0.281	70.92
	LC1-3-4	1.649	45	6.24	6.24	6.8	0.314	69.93
	LC1-3-5	1.651	45	6.27	8.15	7.07	0.327	69.49

Table A-14. BSM + 4% WTR + LC [OM+] P adsorption isotherm data. Sample mass is adjusted for water content. Volume is the volume of the respective P solution with a 0.01 M KCl background electrolyte. pH_0 is the sample pH before adjustment. pH_i is the adjusted pH before equilibration. pH_f is the sample pH after the 24 hour equilibration period.

	ID	Mass (g)	Vol (mL)	pH_0	pH_i	pH_f	Equilibrium Concentration (mg/L)	Adsorption Capacity (mg P/kg)
0.3 mg P/L solution	Control	-	45	5.23	5.23	5.1	0.281	-
	LC1-1-1	1.492	45	6.91	3.84	6.58	0.125	4.68
	LC1-1-2	1.492	45	6.88	4.16	6.63	0.098	5.50
	LC1-1-3	1.492	45	6.77	4.49	6.88	0.134	4.41
	LC1-1-4	1.492	45	7.17	7.17	7.27	0.096	5.57
	LC1-1-5	1.488	45	6.97	8.72	7.3	0.105	5.30
0.9 mg P/L solution	Control	-	45	5.19	5.19	5.1	0.862	-
	LC1-2-1	1.492	45	6.79	3.75	6.66	0.188	20.33
	LC1-2-2	1.491	45	6.79	4.29	6.77	0.181	20.54
	LC1-2-3	1.490	45	7.8	4.59	6.91	0.271	17.86
	LC1-2-4	1.491	45	6.95	6.95	7.22	0.194	20.15
	LC1-2-5	1.491	45	6.86	8.6	7.31	0.198	20.04
3.0 mg P/L solution	Control	-	45	5.16	5.16	4.96	2.885	-
	LC1-3-1	1.491	45	6.81	3.84	6.65	0.500	71.97
	LC1-3-2	1.491	45	6.77	4.37	6.99	0.287	78.38
	LC1-3-3	1.492	45	6.65	4.52	6.87	0.480	72.53
	LC1-3-4	1.488	45	6.91	6.91	7.21	0.470	73.03
	LC1-3-5	1.491	45	6.94	8.22	7.21	0.540	70.81

Table A-15. BSM + 0.5% $Al(OH)_3$ (WTR Alox equivalent) P adsorption isotherm data. Sample mass is adjusted for water content. Volume is the volume of the respective P solution with a 0.01 M KCl background electrolyte. pH_0 is the sample pH before adjustment. pH_i is the adjusted pH before equilibration. pH_f is the sample pH after the 24 hour equilibration period.

	ID	Mass (g)	Vol (mL)	pH_0	pH_i	pH_f	Equilibrium Concentration (mg/L)	Adsorption Capacity (mg P/kg)
0.3 mg P/L solution	Control	-	45	5.18	5.18	5.13	0.239	-
	AH3-1-1	1.803	45	5.51	3.88	5.06	0.013	5.64
	AH3-1-2	1.801	45	5.52	4.08	5.24	0.012	5.69
	AH3-1-3	1.799	45	5.55	4.41	5.01	0.013	5.67
	AH3-1-4	1.802	45	5.69	5.69	5.61	0.009	5.74
	AH3-1-5	1.799	45	5.65	8.03	6.4	0.015	5.60
0.9 mg P/L solution	Control	-	45	5.28	5.28	5.12	0.837	-
	AH3-2-1	1.802	45	5.39	3.8	5	0.053	19.59
	AH3-2-2	1.802	45	5.45	4.2	4.85	0.036	20.01
	AH3-2-3	1.802	45	5.44	4.5	5.27	0.031	20.13
	AH3-2-4	1.801	45	5.57	5.57	5.62	0.020	20.43
	AH3-2-5	1.801	45	5.43	8.35	6.37	0.043	19.83
3.0 mg P/L solution	Control	-	45	4.95	4.95	4.98	2.960	-
	AH3-2-1	1.802	45	5.42	3.92	4.62	0.203	68.85
	AH3-2-2	1.801	45	5.47	4.09	4.79	0.229	68.22
	AH3-2-3	1.800	45	5.47	4.38	4.57	0.282	66.94
	AH3-2-4	1.803	45	5.48	5.48	5.55	0.143	70.29
	AH3-2-5	1.800	45	5.43	8.23	6.33	0.243	67.93

Table A-16. BSM + 2% $Al(OH)_3$ (WTR Alox equivalent) P adsorption isotherm data. Sample mass is adjusted for water content. Volume is the volume of the respective P solution with a 0.01 M KCl background electrolyte. pH_0 is the sample pH before adjustment. pH_i is the adjusted pH before equilibration. pH_f is the sample pH after the 24 hour equilibration period. Highlighted data are those measured below the MDL of 10 µg P/L, and consequently 5 µg P/L was used in media P adsorption capacity calculations

	ID	Mass (g)	Vol (mL)	pH_0	pH_i	pH_f	Equilibrium Concentration (mg/L)	Adsorption Capacity (mg P/kg)
0.3 mg P/L solution	Control	-	45	5.13	5.13	5.12	0.269	-
	AH2-1-1	1.802	45	5.65	4.26	5.66	0.026	6.07
	AH2-1-2	1.803	45	5.76	4.01	5.36	0.004	6.59

	AH2-1-3	1.798	45	5.79	4.19	5.5	0.002	6.61
	AH2-1-4	1.803	45	5.81	5.81	5.79	0.002	6.59
	AH2-1-5	1.797	45	5.7	7.95	6.27	0.003	6.61
0.9 mg P/L solution	Control	-	45	5.24	5.24	5.15	0.844	-
	AH2-2-1	1.800	45	5.61	3.83	5.16	0.012	20.79
	AH2-2-2	1.801	45	5.69	4.15	5.43	0.006	20.96
	AH2-2-3	1.799	45	5.71	4.62	5.57	0.005	20.98
	AH2-2-4	1.798	45	5.78	5.78	5.69	0.005	20.99
	AH2-2-5	1.799	45	5.62	8.31	6.23	0.006	20.98
3.0 mg P/L solution	Control	-	45	5.11	5.11	5.08	2.720	-
	AH2-3-1	1.802	45	5.55	3.95	5.2	0.017	67.50
	AH2-3-2	1.800	45	5.59	4.22	5.44	0.015	67.64
	AH2-3-3	1.801	45	5.62	4.58	5.53	0.027	67.29
	AH2-3-4	1.801	45	5.72	5.72	5.95	0.007	67.85
	AH2-3-5	1.802	45	5.56	8.13	6.22	0.011	67.66

Table A-17. BSM + 4% $Al(OH)_3$ (WTR Alox equivalent) P adsorption isotherm data. Sample mass is adjusted for water content. Volume is the volume of the respective P solution with a 0.01 M KCl background electrolyte. pH_0 is the sample pH before adjustment. pH_i is the adjusted pH before equilibration. pH_f is the sample pH after the 24 hour equilibration period. Highlighted data are those measured below the MDL of 10 µg P/L, and consequently 5 µg P/L was used in media P adsorption capacity calculations

	ID	Mass (g)	Vol (mL)	pH_0	pH_i	pH_f	Equilibrium Concentration (mg/L)	Adsorption Capacity (mg P/kg)
0.3 mg P/L solution	Control	-	45	5.38	5.38	5.22	0.269	-
	AH1-1-1	1.802	45	5.91	3.99	5.61	0.016	6.32
	AH1-1-2	1.801	45	5.93	4.27	4.93	0.004	6.60
	AH1-1-3	1.802	45	6.05	4.6	5.37	0.003	6.59
	AH1-1-4	1.799	45	6.18	6.18	5.98	0.002	6.60
	AH1-1-5	1.799	45	5.93	8.13	6.43	0.002	6.60
0.9 mg P/L solution	Control	-	45	5.31	5.31	5.33	0.814	-
	AH1-2-1	1.802	45	5.81	3.95	5.06	0.001	20.20
	AH1-2-2	1.803	45	5.9	4.67	5.38	0.002	20.19
	AH1-2-3	1.800	45	5.92	4.3	5.41	0.002	20.22
	AH1-2-4	1.802	45	6.14	6.14	5.94	0.007	20.20
	AH1-2-5	1.801	45	5.87	8.31	6.44	0.003	20.21

3.0 mg P/L solution	Control	-	45	5.3	5.3	5.1	2.960	-
	AH1-3-1	1.802	45	5.76	4.29	5.3	0.002	73.79
	AH1-3-2	1.801	45	5.73	3.96	5.21	0.004	73.83
	AH1-3-3	1.802	45	5.77	4.4	5.61	0.002	73.79
	AH1-3-4	1.802	45	6.06	6.06	5.93	0.002	73.79
	AH1-3-5	1.802	45	5.81	8.19	6.7	0.004	73.79

Appendix B: Minicolumn Data

Table B-1. Unamended BSM media results from the minicolumn experiment, set I. Media mass in the column was 92.58 g. Media was subject to continuous flow of an approximately 120 µg P/L solution. ID is the sample identifier, provided as the date of collection. pH, turbidity, TP, and TDP are the measured effluent sample values. BV is the cumulative bed volumes of flow that had passed through the media at the time of sample collection. Initial Q is the volumetric flowrate before calibration. Calibrated Q is the volumetric flowrate as calibrated prior to sample collection.

ID	pH	Turbidity (NTU)	TP (mg/L)	TDP (mg/L)	BV	Initial Q (mL/min)	Calibrated Q (mL/min)
6/24/2009	5.69	5.6	0.045	0.033	4.8	-	1.327
6/25/2009	5.82	149.0	> 0.25	-	33.9	1.376	1.310
6/26/2009	6.13	62.6	0.251	0.193	59.5	1.277	1.277
6/27/2009	6.13	50.1	0.250	-	97.0	1.266	1.266
6/28/2009	6.01	52.0	0.193		121.5	1.255	1.255
6/29/2009, #1	-	-	-	-	144.5	1.250	1.250
6/29/2009, #2	-	-	0.211	-	150.8	1.250	1.250
6/30/2009	-	-	-	-	172.3	1.042	1.235
7/3/2009	6.39	34.7	0.198	0.139	254.9	1.288	1.288

Table B-2. Unamended BSM media results from the minicolumn experiment, set II. Media mass in the column was 100.7 g. Media was subject to continuous flow of an approximately 120 µg P/L solution. ID is the sample identifier, provided as the date of collection. pH, turbidity, TP, and TDP are the measured effluent sample values. BV is the cumulative bed volumes of flow that had passed through the media at the time of sample collection. Initial Q is the volumetric flowrate before calibration. Calibrated Q is the volumetric flowrate as calibrated prior to sample collection.

ID	pH	Turbidity (NTU)	TP (mg/L)	TDP (mg/L)	BV	Initial Q (mL/min)	Calibrated Q (mL/min)
9/8/2009, #1	5.66	6.8	0.059	-	2.6	-	1.327

9/8/2009, #2	-	-	0.060	-	5.9	1.327	1.327
9/8/2009, #3	-	-	0.070	-	7.8	1.327	1.327
9/8/2009, #4	-	-	0.088	-	12.8	1.327	1.327
9/9/2009, #1	4.54	4.1	0.117	-	34.9	1.261	1.261
9/9/2009, #2	-	-	0.127	-	39.0	1.261	1.261
9/10/2009	6.49	4.0	0.129	0.126	59.7	1.277	1.277

Table B-3. BSM + 2% WTR media results from the minicolumn experiment, set I. Media mass in the column was 86.35 g. Media was subject to continuous flow of an approximately 120 µg P/L solution. ID is the sample identifier, provided as the date of collection. pH, turbidity, TP, and TDP are the measured effluent sample values. BV is the cumulative bed volumes of flow that had passed through the media at the time of sample collection. Initial Q is the volumetric flowrate before calibration. Calibrated Q is the volumetric flowrate as calibrated prior to sample collection.

ID	pH	Turbidity (NTU)	TP (mg/L)	TDP (mg/L)	BV	Initial Q (mL/min)	Calibrated Q (mL/min)
6/24/2009	6.40	5.0	0.046	0.048	4.8	-	1.282
6/25/2009	6.33	25.8	0.100	-	33.5	1.376	1.376
6/26/2009	6.25	33.2	0.116	0.057	60.1	1.316	1.316
6/27/2009	6.11	13.1	0.079	-	99.9	1.382	1.382
6/28/2009	6.22	12.3	0.071	0.071	130.5	1.389	1.357
6/29/2009, #1	6.24	11.2	0.096	0.075	155.5	1.402	1.271
6/29/2009, #2	-	-	0.090	-	162.0	1.402	1.271
6/30/2009	6.39	19.3	0.103	-	184.4	1.339	1.266
7/1/2009	6.53	9.1	0.092	0.092	212.6	1.389	1.261
7/2/2009	6.43	9.8	0.103	-	239.5	1.261	1.261
7/3/2009	6.56	9.6	0.101	0.089	267.4	1.304	1.304
7/4/2009	6.19	10.9	0.112	-	299.9	1.310	1.310
7/5/2009, #1	6.61	24.6	0.118	-	328.7	1.322	1.322
7/5/2009, #2	-	-	0.117	-	332.3	1.322	1.322
7/6/2009, #1	6.41	11.3	0.112	0.097	355.0	1.339	1.339
7/6/2009, #2	-	-	0.107	-	361.3	1.339	1.339
7/7/2009, #1	6.71	32.3	0.109	-	381.6	1.389	1.310
7/7/2009, #2	-	-	0.113	-	389.1	1.389	1.310
7/8/2009	6.40	22.5	0.117	-	412.0	1.351	1.288
7/9/2009, #1	6.44	12.9	0.119	0.104	439.7	1.322	1.322
7/9/2009, #2	-	-	0.117	-	448.4	1.322	1.322
7/10/2009, #1	6.56	20.5	0.111	0.100	467.2	1.345	1.345
7/10/2009, #2	-	-	0.107	-	477.2	1.345	1.345
7/11/2009	6.41	9.8	0.112	-	503.9	1.389	1.345

7/13/2009	6.74	11.5	0.116	-	560.3	1.357	1.250
7/14/2009	6.62	10.0	0.111	0.100	587.2	1.293	1.293
7/15/2009	6.66	13.8	0.102	-	615.1	1.310	1.310
7/16/2009	6.65	8.6	0.103	-	643.3	1.327	1.327
7/17/2009	6.65	26.2	0.111	-	674.0	1.357	1.293
7/18/2009	6.63	12.0	0.113	-	703.8	1.271	1.271
7/19/2009	6.39	9.7	0.102	-	731.8	1.255	1.255
7/20/2009	6.56	26.3	0.114	0.095	759.4	1.351	1.282
7/21/2009	6.49	24.7	0.111	-	785.3	1.277	1.277
7/22/2009, #1	6.44	203.0	> 0.25	0.089	815.2	1.304	2.542
7/22/2009, #2	-	-	0.106	-	824.6	1.304	2.542
7/23/2009, #1	-	-	0.142	-	877.0	3.093	2.679
7/23/2009, #2	6.34	16.2	0.133	-	892.0	3.371	2.703
7/24/2009	6.43	41.4	0.182	0.099	936.3	3.000	2.655
7/25/2009	6.60	5.7	0.116	-	996.7	3.226	2.586
7/26/2009	6.57	31.2	0.153	-	1047.7	2.885	2.564
7/27/2009	6.56	7.5	0.114	0.104	1090.4	2.362	2.564
7/28/2009	6.74	5.8	0.114	0.106	1143.0	2.586	2.564
7/29/2009	6.33	4.5	0.109	-	1199.6	2.564	2.542
7/30/2009	6.52	4.1	0.110	-	1247.0	1.911	2.564
7/31/2009	6.36	3.1	0.113	-	1309.2	3.093	2.679
8/2/2009	6.34	2.9	0.123	-	1446.3	3.261	3.061
8/3/2009	6.57	3.5	0.116	-	1501.1	3.704	2.564
8/5/2009	6.62	5.5	0.119	-	1596.3	2.586	2.752
8/6/2009	6.35	4.2	0.112	-	1662.1	3.333	2.632
8/7/2009	6.32	7.7	0.123	0.097	1713.0	3.061	2.479
8/11/2009	6.68	6.3	0.117	0.116	1933.6	2.564	2.564
8/12/2009	6.54	61.4	0.271	0.114	1990.6	2.469	5.455
8/13/2009	6.67	6.8	0.174	0.120	2083.9	2.597	5.455
8/15/2009	6.89	7.8	0.123	0.106	2212.9	0.312	5.128
8/17/2009	6.51	7.2	0.115	0.115	2403.8	3.822	5.217
8/18/2009	6.50	0.7	0.117	0.116	2493.5	3.947	5.000
8/19/2009	6.52	17.1	0.139	0.102	2553.6	3.015	4.545

Table B-4. BSM + 4% WTR media results from the minicolumn experiment, set I. Media mass in the column was 89.23 g. Media was subject to continuous flow of an approximately 120 µg P/L solution. ID is the sample identifier, provided as the date of collection. pH, turbidity, TP, and TDP are the measured effluent sample values. BV is the cumulative bed volumes of flow that had passed through the media at the time of sample collection. Initial Q is the volumetric flowrate before calibration.

Calibrated Q is the volumetric flowrate as calibrated prior to sample collection.

ID	pH	Turbidity (NTU)	TP (mg/L)	TDP (mg/L)	BV	Initial Q (mL/min)	Calibrated Q (mL/min)
6/24/2009	6.42	4.3	0.019	0.005	4.9	-	1.322
6/25/2009	6.70	22.9	0.072	-	32.5	1.255	1.250
6/26/2009	6.49	44.6	0.102	0.033	56.5	1.136	1.245
6/27/2009	6.60	22.3	0.064	-	91.7	1.154	1.186
6/28/2009	6.73	35.0	0.075	0.044	115.0	1.176	1.255
6/29/2009, #1	6.45	10.5	0.055	0.033	137.3	1.172	1.266
6/29/2009, #2	-	-	0.057	-	143.7	1.172	1.266
6/30/2009	6.50	14.4	0.057	-	165.2	1.240	1.224
7/1/2009	6.53	15.1	0.057	0.042	191.6	1.245	1.230
7/2/2009	6.60	13.5	0.061	-	219.0	1.333	1.333
7/3/2009	6.30	11.7	0.069	0.051	247.4	1.277	1.277
7/4/2009	6.37	16.1	0.081	-	278.9	1.261	1.261
7/5/2009	6.47	13.9	0.076	-	306.4	1.261	1.261
7/6/2009	6.57	8.3	0.071	0.059	331.5	1.271	1.271
7/7/2009	6.74	32.6	0.074	-	356.3	1.261	1.261
7/8/2009	6.58	12.6	0.075	-	385.2	1.240	1.240
7/9/2009	6.55	15.2	0.087	-	411.6	1.277	1.277
7/10/2009	6.57	20.0	0.080	0.059	438.2	1.255	1.255
7/11/2009	6.53	32.7	0.129	-	472.2	1.282	1.282
7/13/2009	6.80	18.9	0.093	-	526.9	1.327	1.327
7/14/2009	6.77	52.2	0.167	0.068	555.8	1.364	1.299
7/15/2009	6.62	14.9	0.090	0.070	582.4	1.240	1.240
7/16/2009	6.64	55.5	0.184	0.066	608.8	1.163	1.339
7/17/2009	6.73	27.3	0.123	0.072	639.1	1.327	1.327
7/18/2009	6.51	8.3	0.093	-	669.7	1.322	1.322
7/19/2009	6.68	9.2	0.092	-	698.5	1.288	1.288
7/20/2009	6.62	22.1	0.095	0.076	723.5	1.163	1.266
7/21/2009	6.52	16.1	0.084	-	748.6	1.083	1.266
7/22/2009, #1	6.44	23.9	0.140	-	776.9	1.119	2.479
7/22/2009, #2	-	-	0.140	-	785.9	1.119	2.479
7/23/2009, #1	-	-	0.108	-	831.9	2.344	2.632
7/23/2009, #2	6.62	16.6	0.113	-	844.8	2.500	2.521
7/24/2009	6.57	9.4	0.113	-	884.3	2.419	2.703
7/25/2009	6.45	5.3	0.099	-	937.9	2.500	2.500
7/26/2009	6.71	46.4	0.178	-	1004.0	2.239	2.542
7/27/2009	6.49	12.6	0.112	0.082	1047.8	2.459	2.459
7/28/2009	6.60	29.5	0.157	0.091	1095.0	2.128	2.609
7/29/2009	6.47	13.2	0.116	0.087	1149.0	2.256	2.703
7/30/2009	6.50	14.9	0.123	0.094	1201.3	2.222	2.564

7/31/2009	6.59	69.5	0.213	0.068	1247.4	1.554	2.564
8/2/2009	6.32	15.7	0.128	-	1361.8	1.402	2.941
8/3/2009	6.67	4.6	0.097	-	1406.3	2.479	2.655
8/5/2009	6.58	16.1	0.131	0.093	1515.5	2.521	2.655
8/6/2009	6.24	0.3	0.091	-	1574.6	2.778	2.679
8/7/2009	6.29	0.2	0.094	0.083	1619.8	2.381	2.857
8/11/2009	6.60	7.5	0.107	0.095	1879.3	2.609	2.609
8/12/2009	6.48	3357.0	5.204	0.072	1939.0	2.553	5.128
8/13/2009	6.53	27.3	0.190	0.100	2023.5	2.113	4.918
8/15/2009	6.51	3.1	0.108	0.109	2233.5	4.878	4.878
8/17/2009	6.60	0.4	0.112	0.101	2429.5	3.488	4.959
8/18/2009	6.46	14.4	0.137	0.100	2504.9	2.643	5.085
8/19/2009	6.55	24.5	0.159	0.092	2573.3	0.538	4.959

Table B-5. BSM + 4% WTR media results from the minicolumn experiment, set II. Media mass in the column was 91.87 g. Media was subject to continuous flow of an approximately 120 µg P/L solution. ID is the sample identifier, provided as the date of collection. pH, turbidity, TP, and TDP are the measured effluent sample values. BV is the cumulative bed volumes of flow that had passed through the media at the time of sample collection. Initial Q is the volumetric flowrate before calibration. Calibrated Q is the volumetric flowrate as calibrated prior to sample collection.

ID	pH	Turbidity (NTU)	TP (mg/L)	TDP (mg/L)	BV	Initial Q (mL/min)	Calibrated Q (mL/min)
9/8/2009	6.91	5.4	0.028	-	5.6	-	1.261
9/9/2009	6.26	4.3	0.045	-	33.7	1.245	1.245
9/10/2009	6.65	4.4	0.053	-	58.2	1.255	1.255
9/11/2009	6.85	3.8	0.064	-	85.4	1.224	1.304
9/14/2009	6.79	2.2	0.066	-	169.7	1.255	1.255
9/15/2009	6.83	2.3	0.071	-	197.5	1.255	1.266
9/16/2009	6.56	2.7	0.071	-	227.3	1.245	1.245
9/18/2009	6.73	3.8	0.068	-	276.8	1.220	1.351
9/19/2009	6.83	3.4	0.064	-	308.4	1.299	1.299
9/20/2009	6.88	3.9	0.068	-	335.8	1.310	1.310
9/21/2009	6.72	4.8	0.066	-	362.7	1.293	1.293
9/23/2009	6.57	4.2	0.072	-	417.9	1.282	1.282
9/24/2009	6.78	5.4	0.076	-	448.6	1.282	1.282
9/25/2009	6.54	3.4	0.075	-	476.3	1.245	1.322
9/28/2009	6.64	3.5	0.074	-	545.2	0.718	1.351
9/29/2009	6.60	3.0	0.081	-	566.9	0.867	1.316
9/30/2009	6.81	3.0	0.079	-	596.9	1.339	1.339

10/1/2009	6.61	3.8	0.075	-	625.1	1.339	1.339
10/2/2009	6.62	4.6	0.070	-	655.6	1.351	1.351
10/5/2009	6.62	5.5	0.081	-	743.3	1.327	1.327
10/6/2009	6.50	85.4	0.233	0.061	775.4	1.339	2.752
10/7/2009	6.54	26.7	0.144	0.092	833.8	2.970	2.679
10/8/2009	6.29	23.0	0.138	0.093	898.6	3.000	2.479
10/9/2009	6.50	9.0	0.109	-	950.3	2.655	2.655
10/12/2009	6.60	10.5	0.101	-	1038.9	0.000	2.521
10/13/2009	6.68	10.4	0.093	-	1071.8	0.144	2.564
10/14/2009	6.60	2.6	0.093	-	1114.6	1.415	2.586
10/15/2009	6.67	23.9	0.140	0.080	1142.3	2.655	1.911
10/16/2009	6.69	3.3	0.117	-	1181.7	0.293	2.679
10/17/2009	6.58	2.2	0.101	0.093	1239.9	2.586	2.752
10/19/2009	6.66	3.7	0.112	-	1351.9	2.500	2.655
10/21/2009	6.59	1.6	0.091	-	1466.2	2.885	2.632
10/22/2009	6.57	1.8	0.095	-	1523.2	2.655	2.655
10/23/2009	6.61	1.8	0.101	-	1579.2	2.609	2.609
10/25/2009	6.69	1.8	0.097	-	1713.7	2.830	2.542
10/26/2009	6.52	1.1	0.096	-	1755.4	2.857	2.679
10/27/2009	6.66	14.7	0.126	0.098	1809.8	1.807	5.128
10/28/2009	6.60	6.8	0.109	0.096	1924.5	5.310	4.286
10/29/2009	6.52	3.3	0.107	0.100	2016.2	5.357	4.082
10/30/2009	6.73	1.6	0.106	0.102	2133.7	6.250	5.455
11/2/2009	6.56	3.6	0.101	-	2372.1	0.259	4.959
11/3/2009	6.58	3.1	0.107	-	2471.9	5.217	5.042
11/4/2009	6.59	2.5	0.109	-	2583.3	3.125	5.263
11/6/2009	6.54	1.2	0.105	-	2797.0	4.800	4.286
11/9/2009	6.42	1.5	0.101	-	3098.5	5.000	3.061
11/10/2009	6.53	1.5	0.096	-	3210.8	5.042	5.128

Table B-6. BSM + 4% WTR media results from the minicolumn experiment, set II. Media mass in the column was 83.30 g. Media was subject to intermittent flow of an approximately 120 μg P/L solution. ID is the sample identifier, provided as the date of collection. pH, turbidity, TP, and TDP are the measured effluent sample values. BV is the cumulative bed volumes of flow that had passed through the media at the time of sample collection. Initial Q is the volumetric flowrate before calibration. Calibrated Q is the volumetric flowrate as calibrated prior to sample collection.

ID	pH	Turbidity (NTU)	TP (mg/L)	TDP (mg/L)	BV	Initial Q (mL/min)	Calibrated Q (mL/min)
9/8/2009	6.77	0.2	0.026	-	5.9	1.327	1.327

9/9/2009	6.02	9.8	0.037	-	38.0	1.796	1.796
9/14/2009	7.18	31.7	0.080	-	41.5	1.676	1.255
9/15/2009	7.04	17.7	0.079	0.054	70.9	1.395	1.435
9/19/2009	7.22	38.2	0.093	-	85.5	2.000	1.304
9/20/2009	7.07	47.1	0.108	0.067	104.0	0.503	0.997
9/24/2009	7.08	57.9	0.144	0.056	110.5	2.419	1.402
9/25/2009	6.88	19.2	0.104	0.076	132.9	1.923	1.796
9/30/2009	6.86	13.5	0.079	0.062	139.5	1.205	1.345
10/1/2009	6.77	6.9	0.102	-	163.9	1.158	1.230
10/6/2009	6.97	42.4	0.123	0.056	177.4	7.895	2.564
10/7/2009	6.66	28.3	0.121	0.074	185.6	2.521	2.344
10/16/2009	6.77	15.8	0.067	0.046	190.3	2.128	2.459
10/17/2009	6.75	14.4	0.118	0.089	244.2	2.500	2.542
10/22/2009	6.74	15.6	0.083	0.061	251.8	2.479	2.479
10/23/2009	6.72	8.4	0.110	-	303.9	2.479	2.479
10/28/2009	6.66	8.9	0.096	0.079	350.3	6.452	5.263
10/29/2009	6.56	11.0	0.121	0.096	446.7	5.172	4.762
11/2/2009	6.72	7.1	0.089	0.073	467.3	5.128	5.505
11/3/2009	6.67	9.4	0.101	0.093	563.2	4.959	5.042
11/12/2009	6.69	16.3	0.101	0.082	575.1	5.357	6.000
11/13/2009	6.71	10.4	0.124	0.098	606.2	6.316	6.186
11/20/2009	6.67	42.0	0.161	0.077	620.3	5.217	6.977
11/21/2009	6.70	7.0	0.116	0.133	734.8	6.122	6.383
12/1/2009	6.55	12.9	0.112	0.084	746.2	5.556	5.263
12/2/2009	6.92		0.153	0.081	801.3	5.217	6.383

Table B-7. BSM + 2% WTR + HBM media results from the minicolumn experiment, set I. Media mass in the column was 87.01 g. Media was subject to continuous flow of an approximately 120 µg P/L solution. ID is the sample identifier, provided as the date of collection. pH, turbidity, TP, and TDP are the measured effluent sample values. BV is the cumulative bed volumes of flow that had passed through the media at the time of sample collection. Initial Q is the volumetric flowrate before calibration. Calibrated Q is the volumetric flowrate as calibrated prior to sample collection.

ID	pH	Turbidity (NTU)	TP (mg/L)	TDP (mg/L)	BV	Initial Q (mL/min)	Calibrated Q (mL/min)
6/24/2009	6.90	2.3	0.025	0.013	4.8	-	1.322
6/25/2009	6.27	19.3	0.064	-	33.1	1.304	1.282
6/26/2009	6.45	31.9	0.093	0.048	57.9	1.200	1.310
6/27/2009	6.53	27.4	0.102	-	92.8	1.060	1.339
6/28/2009	6.38	17.5	0.083	0.063	118.6	1.322	1.322

6/29/2009, #1	6.47	16.1	0.083	0.059	142.6	1.293	1.293
6/29/2009, #2	-	-	0.076	-	149.1	1.293	1.293
6/30/2009	6.69	15.1	0.074	-	170.9	1.224	1.271
7/1/2009	6.55	16.0	0.076	0.059	197.5	1.220	1.310
7/2/2009	6.52	8.9	0.075	-	222.8	1.034	1.271
7/3/2009	6.40	7.1	0.078	0.067	249.9	1.224	1.255
7/4/2009	6.08	6.5	0.087	-	282.7	1.376	1.376
7/5/2009	6.17	11.0	0.087	-	312.3	1.333	1.333
7/6/2009	6.39	23.7	0.088	0.075	339.2	1.310	1.288
7/7/2009	6.56	21.8	0.077	-	363.5	1.271	1.271
7/8/2009	6.33	7.7	0.078	-	392.6	1.240	1.240
7/9/2009	6.32	16.6	0.083	-	420.4	1.415	1.310
7/10/2009	6.68	16.8	0.081	0.074	448.3	1.327	1.327
7/11/2009	6.20	6.2	0.077	-	482.8	1.250	1.250
7/13/2009	6.55	9.0	0.078	-	536.6	1.327	1.327
7/14/2009	6.41	4.2	0.078	-	564.0	1.215	1.261
7/15/2009	6.46	15.2	0.078	-	589.8	1.176	1.316
7/16/2009	6.69	25.4	0.095	-	620.5	1.604	1.250
7/17/2009	6.39	12.9	0.079	-	648.2	1.158	1.293
7/18/2009	6.21	9.1	0.093	-	664.2	0.000	1.266
7/19/2009	6.55	11.6	0.092	-	696.5	1.508	1.316
7/20/2009	6.53	3.6	0.087	-	716.4	0.987	1.277
7/21/2009	6.28	7.2	0.090	-	739.7	0.862	1.351
7/22/2009, #1	6.75	18.6	0.095	-	769.1	1.167	2.752
7/22/2009, #2	-	-	0.094	-	781.2	1.167	2.752
7/23/2009, #1	-	-	0.751	-	820.0	1.442	2.542
7/23/2009, #2	6.42	121.0	> .25	-	832.1	2.239	2.586
7/24/2009	6.50	43.6	0.160	0.091	859.7	0.497	2.941
7/25/2009	6.14	11.1	0.123	-	896.2	1.935	2.542
7/26/2009	6.55	0.3	0.105	-	963.0	2.256	2.500
7/27/2009	6.39	4.4	0.106	0.103	1006.0	2.381	2.655
7/28/2009	6.50	4.3	0.108	0.106	1056.2	2.256	2.521
7/29/2009	6.44	4.3	0.112	-	1113.7	2.679	2.679
7/30/2009	6.43	0.4	0.103	-	1171.3	2.778	2.703
7/31/2009	6.26	3.9	0.112	-	1228.0	2.459	2.586
8/2/2009	6.15	4.1	0.116	-	1351.2	2.344	2.609
8/3/2009	6.51	3.1	0.112	-	1387.6	1.695	2.655
8/5/2009	6.73	16.5	0.123	0.106	1475.0	1.449	1.796

Table B-8. BSM + 4% WTR + HBM media results from the minicolumn experiment, set I. Media mass in the column was 85.67 g. Media was subject to continuous flow of an approximately 120 µg P/L solution. ID is the

sample identifier, provided as the date of collection. pH, turbidity, TP, and TDP are the measured effluent sample values. BV is the cumulative bed volumes of flow that had passed through the media at the time of sample collection. Initial Q is the volumetric flowrate before calibration. Calibrated Q is the volumetric flowrate as calibrated prior to sample collection.

ID	pH	Turbidity (NTU)	TP (mg/L)	TDP (mg/L)	BV	Initial Q (mL/min)	Calibrated Q (mL/min)
6/24/2009	6.87	2.6	0.019	0.013	4.7	-	1.266
6/25/2009	6.76	13.5	0.038	-	34.0	1.456	1.370
6/26/2009	6.67	14.8	0.035	0.017	59.7	1.215	1.370
6/27/2009	6.58	15.5	0.035	-	99.0	1.293	1.293
6/28/2009	6.65	9.8	0.031	0.054	125.9	1.370	1.370
6/29/2009, #1	6.62	9.2	0.035	0.018	150.4	1.310	1.310
6/29/2009, #2	-	-	0.025	-	157.1	1.310	1.310
6/30/2009	6.76	9.4	0.025	-	179.9	1.327	1.327
7/1/2009	6.72	10.9	0.024	0.015	207.6	1.293	1.293
7/2/2009	6.64	8.0	0.029	-	235.6	1.304	1.304
7/3/2009	6.46	5.0	0.025	0.014	263.0	1.224	1.224
7/4/2009	6.31	3.9	0.028	-	293.4	1.220	1.220
7/5/2009	6.29	4.3	0.025	-	319.9	1.195	1.316
7/6/2009	6.33	4.7	0.025	0.023	345.4	1.176	1.261
7/7/2009	6.41	3.6	0.022	-	370.7	1.408	1.304
7/8/2009	6.28	4.8	0.023	-	397.7	1.027	1.327
7/9/2009	6.31	3.7	0.028	-	426.5	1.408	1.310
7/10/2009	6.09	3.8	0.025	0.020	455.7	1.449	1.316
7/11/2009	6.23	0.2	0.022	-	490.5	1.288	1.288
7/13/2009	6.70	18.8	0.025	-	537.4	0.952	1.327
7/14/2009	6.36	3.9	0.031	-	569.2	1.630	1.288
7/15/2009	6.48	0.2	0.027	-	596.2	1.282	1.282
7/16/2009	6.28	4.0	0.032	-	623.1	1.245	1.351
7/17/2009	6.45	5.8	0.030	-	656.0	1.523	1.357
7/18/2009	6.46	3.2	0.034	-	687.8	1.261	1.370
7/19/2009	6.38	5.2	0.032	-	703.8	0.000	1.322
7/20/2009	6.63	6.4	0.028	-	724.1	0.962	1.364
7/21/2009	6.64	26.4	0.032	-	738.9	0.000	1.288
7/22/2009	6.76	2.9	0.057	-	769.9	1.370	2.542
7/22/2009	-	-	0.034	-	779.9	1.370	2.542
7/24/2009	6.59	159.0	0.166	0.025	791.1	0.534	0.293

Table B-9. BSM + 4% WTR + HBM media results from the minicolumn experiment, set II. Media mass in the column was 77.64 g. Media was subject to

intermittent flow of an approximately 120 µg P/L solution. ID is the sample identifier, provided as the date of collection. pH, turbidity, TP, and TDP are the measured effluent sample values. BV is the cumulative bed volumes of flow that had passed through the media at the time of sample collection. Initial Q is the volumetric flowrate before calibration. Calibrated Q is the volumetric flowrate as calibrated prior to sample collection.

ID	pH	Turbidity (NTU)	TP (mg/L)	TDP (mg/L)	BV	Initial Q (mL/min)	Calibrated Q (mL/min)
9/8/2009	6.94	4.2	0.032	-	5.5	1.250	1.250
9/9/2009	4.25	9.6	0.039	-	32.2	1.339	1.339
9/14/2009	7.15	18.4	0.050	-	35.2	1.408	1.266
9/15/2009	6.98	10.9	0.033	-	62.6	1.220	1.224
9/19/2009	6.96	9.8	0.032	-	74.0	0.962	1.345
9/20/2009	6.81	8.2	0.029	-	99.0	1.167	1.299
9/24/2009	6.87	16.4	0.051	0.024	103.1	0.838	1.370
9/25/2009	6.61	5.3	0.030	-	136.4	1.357	1.149
9/30/2009	6.57	6.1	0.027	-	145.6	0.743	1.299
10/1/2009	6.57	3.9	0.029	-	173.7	1.293	1.075
10/6/2009	6.45	5.5	0.031	-	183.5	5.660	2.586
10/7/2009	6.42	2.5	0.053	-	239.4	2.727	2.564
10/16/2009	6.59	7.9	0.049	-	246.0	2.174	2.609
10/17/2009	6.41	3.9	0.060	-	300.4	2.564	2.655
10/22/2009	6.42	14.5	0.065	0.037	308.5	2.752	2.727
10/23/2009	6.37	2.5	0.072	-	366.9	2.830	2.778
10/28/2009	6.45	17.8	0.060	0.036	397.7	3.846	0.746
10/29/2009	6.25	14.7	0.060	0.044	413.1	0.833	1.310
11/2/2009	6.38	27.8	0.115	0.054	426.7	4.615	5.357
11/3/2009	6.18	4.7	0.095	0.085	525.8	5.310	5.505
11/12/2009	6.45	18.4	0.102	0.068	541.3	4.545	5.217
11/13/2009	6.48	4.7	0.100	0.091	634.5	5.660	5.714
11/20/2009	6.57	7.9	0.088	0.074	647.4	4.878	5.714
11/21/2009	6.53	5.1	0.104	0.094	758.3	5.769	5.714
12/1/2009	6.54	8.0	0.091	0.077	769.1	4.511	5.128
12/2/2009	6.54	4.2	0.096	0.091	873.7	5.310	5.263
12/7/2009	6.52	4.3	0.087	0.077	888.0	4.688	6.061
12/8/2009	6.56	3.3	0.104	0.096	993.5	5.172	5.505
12/12/2009	6.46	6.7	0.091	0.078	1005.3	4.959	5.607
12/13/2009	6.57	2.8	0.105	0.101	1119.0	5.357	5.607

Table B-10. LFBSM + 4% WTR media results from the minicolumn experiment, set I. Media mass in the column was 92.44 g. Media was subject to

continuous flow of an approximately 120 µg P/L solution. ID is the sample identifier, provided as the date of collection. pH, turbidity, TP, and TDP are the measured effluent sample values. BV is the cumulative bed volumes of flow that had passed through the media at the time of sample collection. Initial Q is the volumetric flowrate before calibration. Calibrated Q is the volumetric flowrate as calibrated prior to sample collection.

ID	pH	Turbidity (NTU)	TP (mg/L)	TDP (mg/L)	BV	Initial Q (mL/min)	Calibrated Q (mL/min)
6/24/2009	6.82	2.3	0.015	0.036	4.8	-	1.339
6/25/2009	6.79	9.3	0.037	-	32.7	1.240	1.310
6/26/2009	6.73	9.4	0.031	0.019	59.2	1.376	1.376
6/27/2009	6.48	7.8	0.036	-	98.5	1.271	1.271
6/28/2009	6.75	4.5	0.018	0.022	124.1	1.261	1.261
6/29/2009, #1	6.71	5.9	0.026	0.018	147.5	1.310	1.310
6/29/2009, #2	-	-	0.016	-	154.3	1.310	1.310
6/30/2009	6.76	5.5	0.016	-	177.1	1.327	1.327
7/1/2009	6.76	4.2	0.018	0.010	204.8	1.288	1.288
7/2/2009	6.77	4.2	0.020	-	232.0	1.255	1.255
7/3/2009	6.54	3.2	0.015	0.010	259.5	1.271	1.271
7/4/2009	6.19	4.6	0.018	-	290.6	1.224	1.224
7/5/2009	6.46	4.2	0.017	-	317.5	1.240	1.240
7/6/2009	6.75	3.5	0.016	0.016	342.4	1.190	1.327
7/7/2009	6.78	7.2	0.014	-	367.7	1.316	1.316
7/8/2009	6.63	5.1	0.014	-	397.4	1.271	1.271
7/9/2009	6.57	3.9	0.013	-	424.4	1.293	1.293
7/10/2009	6.40	4.1	0.014	0.014	452.2	1.322	1.322
7/11/2009	6.38	6.1	0.016	-	487.0	1.299	1.299
7/13/2009	6.62	5.3	0.017	-	540.2	1.245	1.245
7/14/2009	6.64	3.5	0.022	-	566.7	1.190	1.316
7/15/2009	6.72	8.2	0.018	-	593.5	1.250	1.250
7/16/2009	6.54	4.4	0.017	-	621.3	1.357	1.339
7/17/2009	6.70	5.6	0.017	-	650.9	1.250	1.250
7/18/2009	6.40	5.1	0.021	-	679.6	1.124	1.316
7/19/2009	6.39	4.1	0.017	-	695.2	0.000	1.339
7/20/2009	6.63	5.6	0.019	-	717.3	1.111	1.299
7/21/2009	6.27	7.4	0.020	-	743.2	1.091	1.266
7/22/2009, #1	6.57	2.5	0.021	-	772.7	1.014	2.679
7/22/2009, #2	-	-	0.023	-	781.0	1.014	2.679
7/23/2009, #1	-	-	0.045	-	820.2	1.415	3.093
7/23/2009, #2	6.62	15.3	0.049	-	828.7	0.000	2.500
7/24/2009	6.62	3.9	0.047	-	871.3	2.609	2.679
7/25/2009	6.55	6.3	0.047	-	914.6	1.639	2.586

7/26/2009	6.66	0.2	0.047	-	991.7	2.970	2.586
7/27/2009	6.54	5.2	0.061	0.057	1040.7	3.030	2.679
7/28/2009	6.59	0.5	0.065	-	1098.2	2.970	2.609
7/29/2009	6.54	0.5	0.063	-	1159.4	2.941	2.679
7/30/2009	6.33	0.2	0.064	-	1214.0	2.439	3.191
7/31/2009	6.45	3.2	0.057	-	1250.5	0.000	2.586
8/2/2009	6.33	3.8	0.071	-	1353.6	1.351	2.679
8/3/2009	6.68	3.5	0.068	-	1386.7	1.215	2.970
8/5/2009	6.67	7.6	0.059	-	1485.0	0.000	2.703
8/6/2009	6.35	0.4	0.066	-	1545.9	2.913	2.586
8/7/2009	6.37	0.2	0.068	0.059	1592.8	2.609	3.061
8/11/2009	6.53	0.3	0.080	-	1878.8	2.703	2.703
8/12/2009	6.44	0.3	0.085	0.078	1935.7	2.326	5.455
8/13/2009	6.52	0.5	0.093	-	2030.4	2.655	5.263
8/15/2009	6.36	0.2	0.085	-	2192.0	1.662	5.128
8/17/2009	6.48	0.2	0.091	-	2406.8	2.941	5.042
8/18/2009	6.53	8.0	0.070	-	2460.9	0.000	6.061
8/19/2009	6.58	5.7	0.075	0.064	2528.8	0.612	2.885

Table B-11. LFBSM + 4% WTR media results from the minicolumn experiment, set II. Media mass in the column was 90.48 g. Media was subject to intermittent flow of an approximately 120 µg P/L solution. ID is the sample identifier, provided as the date of collection. pH, turbidity, TP, and TDP are the measured effluent sample values. BV is the cumulative bed volumes of flow that had passed through the media at the time of sample collection. Initial Q is the volumetric flowrate before calibration. Calibrated Q is the volumetric flowrate as calibrated prior to sample collection.

ID	pH	Turbidity (NTU)	TP (mg/L)	TDP (mg/L)	BV	Initial Q (mL/min)	Calibrated Q (mL/min)
9/8/2009	6.99	4.2	0.022	-	5.3	1.266	1.266
9/9/2009	6.77	16.1	0.040	-	34.3	1.515	1.515
9/14/2009	7.15	23.3	0.052	-	37.3	1.442	1.357
9/15/2009	7.01	9.6	0.030	-	57.3	1.293	1.304
9/19/2009	7.05	15.4	0.043	0.017	70.8	1.796	1.316
9/20/2009	7.11	10.0	0.027	-	90.3	0.616	1.948
9/24/2009	7.12	19.5	0.049	0.015	98.4	2.174	0.785
9/25/2009	6.89	8.3	0.039	-	127.1	1.176	1.200
9/30/2009	6.90	11.9	0.036	0.017	138.6	2.752	1.261
10/1/2009	6.98	4.7	0.033	-	159.4	0.811	1.210
10/6/2009	6.93	9.6	0.034	-	169.5	6.000	2.500
10/7/2009	6.58	3.4	0.053	-	223.0	2.586	2.308

10/16/2009	6.86	10.4	0.037	0.014	227.9	2.143	2.586
10/17/2009	6.81	4.9	0.054	-	284.6	2.632	2.703
10/22/2009	6.73	9.0	0.034	0.020	292.6	2.609	2.632
10/23/2009	6.87	3.7	0.060	-	348.1	2.655	2.679
10/28/2009	6.67	3.6	0.042	0.037	392.7	4.724	1.130
10/29/2009	6.52	5.1	0.078	0.067	494.9	5.128	6.122
11/2/2009	6.51	3.5	0.044	-	515.5	5.357	5.172
11/3/2009	6.56	2.2	0.073	-	609.9	5.217	5.263
11/12/2009	6.74	5.9	0.050	0.042	625.2	4.317	5.941
11/13/2009	6.75	2.0	0.075	-	710.8	4.959	5.085
11/20/2009	6.67	3.0	0.079	-	722.7	4.918	5.263
11/21/2009	6.73	1.8	0.049	-	820.3	5.085	5.042
12/1/2009	6.71	3.6	0.061	0.056	830.5	4.800	5.263
12/2/2009	6.81	2.8	0.077	-	939.8	5.556	5.405
12/7/2009	6.70	1.4	0.053	-	957.2	7.229	5.882
12/8/2009	6.77	0.8	0.084	-	1067.6	5.660	5.455
12/12/2009	6.63	4.6	0.058	0.048	1079.4	5.505	3.750
12/13/2009	6.69	5.0	0.098	0.087	1193.2	5.607	5.455

Table B-12. Sand + 4% WTR media results from the minicolumn experiment, set II. Media mass in the column was 85.93 g. Media was subject to continuous flow of an approximately 120 µg P/L solution. ID is the sample identifier, provided as the date of collection. pH, turbidity, TP, and TDP are the measured effluent sample values. BV is the cumulative bed volumes of flow that had passed through the media at the time of sample collection. Initial Q is the volumetric flowrate before calibration. Calibrated Q is the volumetric flowrate as calibrated prior to sample collection.

ID	pH	Turbidity (NTU)	TP (mg/L)	TDP (mg/L)	BV	Initial Q (mL/min)	Calibrated Q (mL/min)
9/8/2009	7.69	0.2	0.007	-	5.6	-	1.271
9/9/2009	7.48	1.0	0.009	-	33.8	1.240	1.240
9/10/2009	7.18	1.2	0.009	-	58.1	1.240	1.240
9/11/2009	7.41	1.5	0.009	-	85.3	1.250	1.299
9/14/2009	7.26	0.3	0.010	-	170.2	1.277	1.277
9/15/2009	7.23	0.3	0.011	-	197.5	1.190	1.255
9/16/2009	6.80	0.3	0.009	-	222.9	1.245	1.245
9/18/2009	7.05	0.5	0.009	-	277.0	1.235	1.327
9/19/2009	7.25	0.6	0.015	-	308.6	1.316	1.316
9/20/2009	7.16	0.3	0.015	-	336.1	1.304	1.304
9/21/2009	6.84	0.3	0.013	-	363.0	1.304	1.304
9/23/2009	6.96	0.3	0.015	-	418.6	1.288	1.288

9/24/2009	6.92	0.2	0.017	-	449.0	1.250	1.250
9/25/2009	6.82	0.3	0.020	-	475.9	1.210	1.288
9/28/2009	6.86	0.2	0.024	-	553.8	1.010	1.288
9/29/2009	7.03	0.3	0.015	-	573.4	0.711	1.316
9/30/2009	6.93	1.0	0.027	-	603.1	1.322	1.322
10/1/2009	6.83	0.3	0.028	-	631.1	1.316	1.316
10/2/2009	6.78	0.7	0.026	-	660.7	1.316	1.316
10/5/2009	6.78	0.9	0.029	-	746.7	1.310	1.310
10/6/2009	6.72	0.5	0.041	-	777.3	1.299	2.500
10/7/2009	6.69	0.9	0.060	-	829.3	2.479	2.479
10/8/2009	6.44	0.4	0.048	-	886.4	2.439	2.632
10/9/2009	6.49	0.2	0.052	-	938.4	2.586	2.586
10/12/2009	6.79	0.6	0.060	-	1086.1	1.899	2.479
10/13/2009	6.67	0.7	0.068	-	1142.4	2.206	2.632
10/14/2009	6.71	0.3	0.072	-	1191.4	2.174	2.542
10/15/2009	6.81	0.4	0.075	-	1236.7	1.657	1.744
10/16/2009	6.75	0.8	0.061	-	1270.0	0.337	2.521
10/17/2009	6.76	0.6	0.078	-	1324.4	2.326	2.586
10/19/2009	6.68	0.4	0.091	-	1439.3	2.679	2.655
10/21/2009	6.67	0.3	0.066	-	1553.8	2.778	2.542
10/22/2009	6.65	0.4	0.062	-	1608.5	2.500	2.586
10/23/2009	6.65	0.5	0.079	-	1663.0	2.632	2.564
10/25/2009	6.75	0.8	0.077	-	1792.2	2.564	2.830
10/26/2009	6.73	0.2	0.071	-	1831.7	2.362	2.609
10/27/2009	6.55	1.8	0.090	-	1892.0	5.310	5.357
10/28/2009	6.72	0.5	0.095	-	2005.5	5.172	5.042
10/29/2009	6.65	0.3	0.099	-	2107.9	4.380	5.941
10/30/2009	6.64	1.2	0.096	-	2217.5	5.217	5.128
11/2/2009	6.60	0.5	0.089	-	2500.5	4.511	5.455
11/3/2009	6.72	1.0	0.089	-	2598.3	1.700	5.085
11/4/2009	6.45	0.4	0.096	-	2711.7	4.196	4.138
11/6/2009	6.53	0.3	0.091	-	2921.5	1.519	4.138
11/9/2009	6.51	0.5	0.086	-	3150.7	4.196	5.128
11/10/2009	6.49	0.6	0.088	-	3292.2	5.042	5.128

Table B-13. Influent solution measurements from the minicolumn experiment, set I. ID is the sample identifier, provided as the date of collection. pH, turbidity, and TP are the measured influent sample values.

ID	pH	Turbidity (NTU)	TP (mg/L)
6/24/2009	6.47	0.5	0.108
6/25/2009	6.08	0.3	0.123

6/26/2009	5.99	0.8	0.114
6/27/2009	6.12	1.6	0.112
6/28/2009	6.19	0.1	0.110
6/29/2009, #1	6.24	0.1	0.118
6/29/2009, #2	-	-	0.109
6/30/2009	6.41	0.2	0.108
7/1/2009	6.24	0.3	0.109
7/2/2009	6.33	4.0	0.141
7/3/2009	6.39	0.2	0.133
7/4/2009	6.39	0.2	0.138
7/5/2009	6.31	0.2	0.141
7/6/2009	6.35	0.3	0.146
7/7/2009	6.47	0.2	0.138
7/8/2009	6.68	7.7	0.143
7/9/2009	6.40	3.3	0.140
7/10/2009	6.61	3.2	0.130
7/11/2009	6.36	3.5	0.124
7/13/2009	6.70	7.1	0.119
7/14/2009	6.69	0.2	0.121
7/15/2009	6.57	0.2	0.120
7/16/2009	6.56	0.3	0.119
7/17/2009	6.76	0.1	0.121
7/18/2009	6.77	0.3	0.122
7/19/2009	6.68	7.3	0.120
7/20/2009	6.73	0.5	0.124
7/21/2009	6.55	9.1	0.124
7/22/2009, #1	6.57	0.5	0.122
7/22/2009, #2	-	-	0.121
7/23/2009, #1	-	-	0.122
7/23/2009, #2	6.67	0.2	0.124
7/24/2009	6.65	4.6	0.120
7/25/2009	6.89	0.2	0.124
7/26/2009	6.71	0.1	0.120
7/27/2009	6.55	0.1	0.120
7/28/2009	6.66	0.3	0.120
7/29/2009	6.63	0.3	0.120
7/30/2009	6.56	0.1	0.116
7/31/2009	6.53	0.4	0.126
8/2/2009	7.77	0.1	0.123
8/3/2009	6.74	0.3	0.129
8/5/2009	6.52	0.4	0.120
8/6/2009	7.23	0.1	0.129
8/7/2009	7.04	0.2	0.119

8/11/2009	6.58	0.1	0.131
8/12/2009	6.74	0.1	0.123
8/13/2009	6.51	0.1	0.128
8/15/2009	6.56	0.3	0.121
8/17/2009	6.54	2.0	0.121
8/18/2009	6.40	4.2	0.122
8/19/2009	6.61	0.4	0.117

Table B-14. Influent solution measurements from the minicolumn experiment, set II. ID is the sample identifier, provided as the date of collection. pH, turbidity, and TP are the measured influent sample values.

ID	pH	Turbidity (NTU)	TP (mg/L)
9/8/2009	5.81	0.3	0.123
9/9/2009	4.40	1.6	0.123
9/10/2009	6.53	1.3	0.126
9/11/2009	6.81	1.0	0.122
9/14/2009	6.27	0.4	0.121
9/15/2009	6.46	1.1	0.123
9/16/2009	6.14	1.8	0.126
9/18/2009	6.49	0.9	0.123
9/19/2009	5.88	0.4	0.123
9/20/2009	6.48	0.3	0.121
9/21/2009	6.57	0.7	0.126
9/23/2009	6.27	0.5	0.121
9/24/2009	6.59	1.9	0.121
9/25/2009	6.58	0.3	0.123
9/28/2009	6.71	0.3	0.122
9/29/2009	6.70	0.5	0.120
9/30/2009	6.60	0.4	0.123
10/1/2009	6.59	0.4	0.125
10/2/2009	6.50	0.4	0.120
10/5/2009	6.56	0.5	0.125
10/6/2009	6.45	0.3	0.122
10/7/2009	6.54	0.9	0.122
10/8/2009	6.22	0.7	0.118
10/9/2009	6.57	0.6	0.119
10/12/2009	6.88	0.3	0.121
10/13/2009	6.75	0.5	0.121
10/14/2009	6.60	0.3	0.123
10/15/2009	6.80	0.3	0.117
10/16/2009	6.64	0.8	0.115

10/17/2009	6.62	0.5	0.119
10/19/2009	8.23	1.0	0.115
10/21/2009	6.48	0.2	0.112
10/22/2009	6.64	0.5	0.117
10/23/2009	6.62	0.7	0.119
10/25/2009	6.82	0.9	0.119
10/26/2009	6.58	0.4	0.120
10/27/2009	6.57	3.0	0.118
10/28/2009	6.74	0.7	0.119
10/29/2009	6.54	0.2	0.118
10/30/2009	6.64	0.6	0.113
11/2/2009	6.62	0.3	0.117
11/3/2009	6.39	0.2	0.117
11/4/2009	6.49	1.2	0.121
11/6/2009	6.45	0.6	0.114
11/9/2009	7.47	1.9	0.115
11/10/2009	6.42	0.4	0.114
11/12/2009	7.78	0.6	0.119
11/13/2009	6.62	1.3	0.117
11/20/2009	8.27	0.7	0.117
11/21/2009	6.61	1.1	0.121
12/1/2009	9.06	0.9	0.117
12/2/2009	6.53	0.7	0.116
12/7/2009	6.59	0.2	0.118
12/8/2009	6.66	0.3	0.117
12/12/2009	6.55	0.5	0.118
12/13/2009	6.71	1.0	0.119

Appendix C: Vegetated Column Flow Data

Table C-1. Influent flow measurements of both vegetated columns for run 1. Sample ID is provided if a sample was taken concurrently with measured flow. Runtime is the time of the measurement taken relative to the commencement of inflow. Exp. Flow and Ctrl. Flow are the measured flowrates at a given time for the experimental and control column, respectively. V_e In and V_c In are the cumulative volume of influent applied to the experimental and control columns, respectively.

Sample ID	Runtime (min)	Exp. Flow (mL/min)	V_e In (mL)	Ctrl. Flow (mL/min)	V_c In (mL)
	0	190.5	-	181.8	-
0	11	-	2166.3	-	2031.3

	106	203.4	20874.9	187.5	19573.9
3	181	-	36002.0	-	33528.2
	220	200.0	43868.1	184.6	40784.4
	299	203.4	59802.0	187.5	55483.0
5.5	323	-	64683.4	-	59983.0

Table C-2. Effluent flow measurements of both vegetated columns for run 1. Sample ID is provided if a sample was taken concurrently with measured flow. Runtime is the time of the measurement taken relative to the commencement of inflow. Flow is the measured flowrate at a given time. Cum. V is the cumulative volume of effluent that the column produced. †: Volume of effluent collected between column runs.

Experimental Column				**Control Column**			
Sample ID	Runtime (min)	Flow (mL/min)	Cum. V (mL)	Sample ID	Runtime (min)	Flow (mL/min)	Cum. V (mL)
	22	150.0	1650.0		27	136.4	1840.9
0	30	162.2	2898.6	0	34	157.9	2870.8
0.3	44	240.0	5713.8	0.3	48	166.7	5142.7
0.7	64	142.9	9542.4	0.7	69	166.7	8642.7
1	84	181.8	12789.1	1	90	176.5	12245.7
1.3	103	193.5	16355.1	1.3	108	176.5	15422.2
2	147	171.4	24384.6	2	151	176.5	23010.4
2.7	184	187.5	31024.8	2.7	189	176.5	29716.3
3.3	225	187.5	38712.3	3.3	229	176.5	36775.1
4	268	181.8	46652.6	4	273	166.7	44324.1
5	330	181.8	57925.3	5	331	176.5	54275.1
	344	62.5	59635.6		351	27.9	56318.9
6	579	0	66979.3	6	579	0	59500.3
		† ~ 0.6 L	67579.3			† ~ 1.1 L	60600.3

Table C-3. Influent flow measurements of both vegetated columns for run 2. Sample ID is provided if a sample was taken concurrently with measured flow. Runtime is the time of the measurement taken relative to the commencement of inflow. Exp. Flow and Ctrl. Flow are the measured flowrates at a given time for the experimental and control column, respectively. V_e In and V_c In are the cumulative volume of influent applied to the experimental and control columns, respectively.

Sample ID	Runtime (min)	Exp. Flow (mL/min)	V_e In (mL)	Ctrl. Flow (mL/min)	V_c In (mL)
	0	187.5	-	171.4	-
0	15	-	2881.7	-	2629.0

	56	196.7	10758.2	179.1	9814.9
	65	187.5	12487.2	166.7	11370.9
	69	200.0	13262.2	179.1	12062.4
	81	184.6	15569.9	-	14165.6
	115	184.6	21846.8	171.4	20124.7
3	185	-	34769.9	-	32301.2
	200	184.6	37539.1	176.5	34910.4
	333	184.6	62093.0	-	-
	334	157.9	62264.2	176.5	58557.5
5.5	339	190.5	63135.1	-	59439.8
	347	-	64659.0	-	60851.6
	355	-	66182.8	-	62263.4

Table C-4. Effluent flow measurements of both vegetated columns for run 2. Sample ID is provided if a sample was taken concurrently with measured flow. Runtime is the time of the measurement taken relative to the commencement of inflow. Flow is the measured flowrate at a given time. Cum. V is the cumulative volume of effluent that the column produced. †: Volume of effluent collected between column runs.

Experimental Column				**Control Column**			
Sample ID	Runtime (min)	Flow (mL/min)	Cum. V (mL)	Sample ID	Runtime (min)	Flow (mL/min)	Cum. V (mL)
	26	157.9	2052.6		27	150.0	2025.0
0	35	187.5	3606.9	0	36	176.5	3494.1
0.25	46	176.5	5608.7	0.25	48	176.5	5611.8
0.5	61	222.2	8598.9	0.5	63	187.5	8341.5
0.75	85	222.2	13932.3	0.75	86	200.0	12797.8
1	92	230.8	15517.7	1	94	187.5	14347.8
1.3	111	206.9	19675.6	1.3	113	187.5	17910.3
	134	176.5	24084.3		136	157.9	21882.3
	143	176.5	25672.5		145	162.2	23322.6
2	154	230.8	27912.3	2	155	222.2	25244.5
	157	166.7	28508.5		158	150.0	25802.8
	182	187.5	32935.6		192	171.4	31267.1
2.7	191	250.0	34904.3	2.7	195	222.2	31857.6
	194	187.5	35560.6		195	162.2	31857.6
	212	166.7	38748.1		213	176.5	34905.3
	228	176.5	41493.2		228	176.5	37552.4
3.3	234	230.8	42714.9	3.3	235	206.9	38894.1
	238	187.5	43551.4		238	162.2	39447.7
	263	176.5	48101.1		263	171.4	43617.6
4	271	206.9	49634.5	4	272	206.9	45320.1

	289	171.4	53039.5		289	166.7	48495.4
	326	157.9	59131.9		326	171.4	54750.1
5	329	193.5	59659.1	5	330	214.3	55521.6
	345	139.5	62323.8		345	171.4	58414.4
	357	146.3	64039.0		357	150.0	60343.0
6	359	230.8	64416.1	6	359	200.0	60693.0
	367	139.5	65897.4		369	65.2	62019.1
7	446	5.9	71642.3	7	451	5.6	64922.5
		† ~ 0.7 L	72322.3			† ~ 0.9 L	65817.5

Table C-5. Influent flow measurements of both vegetated columns for run 3. Sample ID is provided if a sample was taken concurrently with measured flow. Runtime is the time of the measurement taken relative to the commencement of inflow. Exp. Flow and Ctrl. Flow are the measured flowrates at a given time for the experimental and control column, respectively. V_e In and V_c In are the cumulative volume of influent applied to the experimental and control columns, respectively.

Sample ID	Runtime (min)	Exp. Flow (mL/min)	V_e In (mL)	Ctrl. Flow (mL/min)	V_c In (mL)
	0	193.5	-	193.5	-
	2	179.1	372.7	179.1	372.7
	5	-	914.0	-	914.0
0	16	-	2899.1	-	2899.1
	143	181.8	25817.7	181.8	25817.7
3	191	-	35234.0	-	35234.0
6	338	210.5	64071.3	210.5	64071.3

Table C-6. Effluent flow measurements of both vegetated columns for run 3. Sample ID is provided if a sample was taken concurrently with measured flow. Runtime is the time of the measurement taken relative to the commencement of inflow. Flow is the measured flowrate at a given time. Cum. V is the cumulative volume of effluent that the column produced. †: Volume of effluent collected between column runs.

Experimental Column				**Control Column**			
Sample ID	Runtime (min)	Flow (mL/min)	Cum. V (mL)	Sample ID	Runtime (min)	Flow (mL/min)	Cum. V (mL)
	31	11.9	184.5		24.0	55.6	666.7
	37	25.5	296.8		27.0	133.3	950.0
	40	136.4	539.7		28.0	187.5	1110.4
0	52	150.0	2257.9		32.0	200.0	1885.4
	53	181.8	2423.8	0	39.0	222.2	3363.2

0.25	57	222.2	3231.8		47.0	181.8	4979.4
	65	230.8	5043.8	0.25	50.0	181.8	5524.8
0.5	74	250.0	7207.3		58.0	187.5	7002.1
	80	250.0	8707.3	0.5	67.0	193.5	8716.8
0.75	86	250.0	10207.3		72.0	181.8	9655.2
	95	230.8	12370.7	0.75	79.0	181.8	10927.9
1	103	193.5	14068.0		88.0	176.5	12540.2
	115	187.5	16354.3	1	93.0	181.8	13436.0
1.3	122	193.5	17688.0		110.0	187.5	16575.2
	141	187.5	21307.9	1.3	114.0	181.8	17313.8
2	168	193.5	26452.1		140.0	187.5	22114.9
	181	187.5	28928.9	2	160.0	176.5	25754.6
2.6	202	187.5	32866.4		180.0	181.8	29337.5
	225	181.8	37113.6	2.6	194.0	176.5	31845.6
3.3	242	187.5	40252.8		219.0	181.8	36324.2
	261	181.8	43761.3	3.3	234.0	181.8	39051.4
4	286	181.8	48306.7		260.0	176.5	43709.2
	321	171.4	54488.6	4	279.0	171.4	47014.2
5	343	162.2	58158.1		319.0	181.8	54079.2
	354	61.9	59390.2	5	340.0	187.5	57957.0
6	467	4.5	63138.0		352.0	52.6	59397.8
	546	2.6	63416.5	6	535.0	1.2	64321.6
		† ~ 1.0 L	64416.5			† ~ 1.1 L	65421.6

Table C-7. Influent flow measurements of both vegetated columns for run 4. Sample ID is provided if a sample was taken concurrently with measured flow. Runtime is the time of the measurement taken relative to the commencement of inflow. Exp. Flow and Ctrl. Flow are the measured flowrates at a given time for the experimental and control column, respectively. V_e In and V_c In are the cumulative volume of influent applied to the experimental and control columns, respectively.

Sample ID	Runtime (min)	Exp. Flow (mL/min)	V_e In (mL)	Ctrl. Flow (mL/min)	V_c In (mL)
	0	181.8	-	184.6	-
	2	184.6	366.4	184.6	369.2
	4	174.5	725.6	173.3	727.1
0	29	-	5137.9	-	5124.7
	71	178.4	12550.6	178.5	12512.5
	119	177.1	21084.0	175.3	21003.2
	186	174.0	32846.2	174.6	32725.1
3	188	-	33196.0	-	32725.1
	221	175.8	38967.9	172.4	38452.0

	231	174.6	40720.2	173.5	40181.5
	233	178.3	41069.4	177.2	40528.4
	298	179.2	52687.0	177.5	52057.5
	340	177.7	60181.6	177.2	59507.1
6	355	-	62847.0	-	62165.1

Table C-8. Effluent flow measurements of both vegetated columns for run 4. Sample ID is provided if a sample was taken concurrently with measured flow. Runtime is the time of the measurement taken relative to the commencement of inflow. Flow is the measured flowrate at a given time. Cum. V is the cumulative volume of effluent that the column produced. †: Volume of effluent collected between column runs.

Experimental Column				**Control Column**			
Sample ID	Runtime (min)	Flow (mL/min)	Cum. V (mL)	Sample ID	Runtime (min)	Flow (mL/min)	Cum. V (mL)
	34	3.3	55.6		22	8.7	95.4
	35	117.6	116.0		26	163.4	439.5
0	44	193.5	1516.4	0	36	193.5	2224.2
0.25	52	187.5	3040.6		39	193.7	2805.2
	56	181.8	3779.2	0.25	45	179.3	3924.2
0.5	68	205.5	6103.4		53	177.9	5353.0
	76	201.5	7731.5	0.5	62	184.3	6982.9
0.75	82	198.3	8931.0		66	176.8	7705.0
	90	204.3	10541.6	0.75	75	175.7	9291.2
1	96	203.0	11763.4		83	182.0	10721.9
	110	189.3	14509.5	1	91	180.5	12171.7
1.3	117	183.5	15814.6		105	180.8	14700.3
	140	175.5	19943.5	1.3	109	180.8	15423.5
2	165	182.1	24414.0		139	182.7	20876.5
	173	173.6	25837.0	2	156	184.4	23997.3
2.6	197	158.3	29820.1		169	184.4	26395.1
	218	172.8	33296.9	2.6	191	173.9	30337.0
3.3	247	173.6	38320.0		219	177.4	35255.5
	261	176.0	40766.9	3.3	229	172.0	37002.7
4	280	197.3	44312.9		252	174.9	40992.0
	302	193.9	48616.4	4	272	184.3	44583.5
5	337	197.9	55473.1		303	189.0	50368.9
6	371	87.2	60319.3	5	332	177.1	55677.7
	374	57.1	60535.8	6	374	13.8	59687.7
	474	6.0	63692.7		377	22.8	59742.5
7	546	3.2	64024.3		484	2.9	61113.7
		† ~ 725 mL	64024.3	7	548	0.0	61205.3

† ~ 855 mL 61205.3

Table C-9. Influent flow measurements of both vegetated columns for run 5. Sample ID is provided if a sample was taken concurrently with measured flow. Runtime is the time of the measurement taken relative to the commencement of inflow. Exp. Flow and Ctrl. Flow are the measured flowrates at a given time for the experimental and control column, respectively. V_e In and V_c In are the cumulative volume of influent applied to the experimental and control columns, respectively.

Sample ID	Runtime (min)	Exp. Flow (mL/min)	V_e In (mL)	Ctrl. Flow (mL/min)	V_c In (mL)
	0	185.8	-	180.8	-
	2	185.1	370.9	179.0	359.8
0	9	-	2476.3	-	1622.5
	14	165.8	3353.6	-	2524.4
	16	181.1	3700.5	181.7	2885.1
	39	185.2	7912.9	182.9	7078.8
	53	186.5	10514.5	182.6	9637.4
	80	185.7	15539.0	183.9	14585.2
	95	175.6	18248.5	184.9	17351.0
	98	192.5	18775.2	-	17907.6
	105	185.1	20122.7	186.2	19206.5
	127	183.9	24182.1	184.0	23278.8
	170	183.8	32088.3	183.2	31173.6
3	194	-	36459.6	-	35562.2
	204	180.5	38281.0	182.5	37390.7
	239	177.6	44547.2	179.4	43724.6
	284	177.3	52532.5	181.1	51835.3
	287	178.1	53065.5	180.3	52377.3
	319	175.8	58728.2	178.4	58115.7
	339	179.5	62281.8	177.2	61671.3
6	341	-	62640.8	-	62025.7

Table C-10. Effluent flow measurements of both vegetated columns for run 5. Sample ID is provided if a sample was taken concurrently with measured flow. Runtime is the time of the measurement taken relative to the commencement of inflow. Flow is the measured flowrate at a given time. Cum. V is the cumulative volume of effluent that the column produced. †: Volume of effluent collected between column runs.

Experimental Column **Control Column**

Sample ID	Runtime (min)	Flow (mL/min)	Cum. V (mL)	Sample ID	Runtime (min)	Flow (mL/min)	Cum. V (mL)
	28	167.6	2346.4		23	33.8	388.9
	29	198.9	2529.6		26	149.1	274.3
0	37	212.6	4175.9		27	199.1	448.4
	45	176.2	5731.0	0	34	237.6	1977.1
0.25	48	178.3	6262.7		42	191.8	3694.8
	57	178.3	7867.2	0.25	49	184.3	5011.2
0.5	65	190.8	9343.5		56	182.3	6294.2
	72	193.2	10687.6	0.5	64	189.2	7780.1
0.75	78	189.7	11836.2		71	176.8	9060.9
	87	202.1	13599.2	0.75	77	179.6	10130.0
1	91	203.0	14409.3		86	167.4	11691.5
1.3	113	181.8	18642.1	1	90	184.1	12394.5
	124	182.7	20647.0	1.3	112	188.2	16490.0
2	168	195.9	28975.9		123	190.1	18570.7
	185	189.7	32253.4	2	167	188.6	26902.9
2.6	193	180.8	33735.3		183	195.6	29976.4
	225	178.4	39482.3	2.6	192	193.0	31724.9
3.3	234	179.6	41093.3		224	177.8	37657.1
	256	184.8	45101.4	3.3	233	173.4	39237.5
4	281	185.7	49732.5		255	177.6	43098.8
	308	190.7	54813.3	4	280	178.9	47555.8
5	335	166.9	59641.0		307	180.3	52405.5
	346	157.0	61422.6	5	334	178.9	57255.1
	351	125.1	62127.7		345	133.7	58974.6
	354	77.0	62430.9		349	77.2	59396.4
6	389	15.7	64054.2		353	57.2	59665.2
		† ~ 1.8 L	65859.2	6	395	7.7	61029.3
						† ~ 1.2 L	62286.3

Table C-11. Influent flow measurements of both vegetated columns for run 6. Sample ID is provided if a sample was taken concurrently with measured flow. Runtime is the time of the measurement taken relative to the commencement of inflow. Exp. Flow and Ctrl. Flow are the measured flowrates at a given time for the experimental and control column, respectively. V_e In and V_c In are the cumulative volume of influent applied to the experimental and control columns, respectively.

	Experimental Column			**Control Column**		
Sample ID	Runtime (min)	Exp. Flow (mL/min)	V_e In (mL)	Runtime (min)	Ctrl. Flow (mL/min)	V_c In (mL)
	0.0	0.0	-	0.0	0.0	-

	1.8	65.7	59.1	3.2	63.6	101.9
	3.6	-	178.1	3.6	-	128.3
	9.3	64.3	518.3	11.2	60.4	596.2
Step 2	16.8	-	1002.8	16.8	-	937.4
	19.0	246.5	1536.5	20.8	192.8	1706.3
	28.6	241.4	3876.5	24.4	229.2	2467.7
0	29.4	-	4077.7	29.4	-	3612.6
Step 3	40.0	-	6631.9	40.0	-	6038.5
	45.2	328.2	8328.8	46.6	325.5	8194.0
	60.4	334.2	13388.0	59.9	322.7	12504.1
	75.3	332.8	18325.0	74.7	318.7	17248.4
Step 4	97.0	-	25562.9	97.0	-	24350.7
	108.9	266.9	28730.2	108.5	261.3	27364.0
	117.9	240.8	31141.2	115.9	233.3	29288.6
	130.1	240.9	34083.5	126.4	231.4	31724.5
	152.0	241.8	39353.6	151.6	231.7	37552.4
Step 5	181.9	-	46600.7	181.9	-	44588.5
	185.7	142.9	47134.0	185.9	145.3	45162.4
3	199.0	-	49050.6	199.0	-	47007.5
	209.2	143.9	50515.6	209.8	135.3	48520.5
	226.4	149.4	52979.0	224.4	151.7	50489.9
	254.0	152.6	57151.8	254.2	153.0	55032.9
Step 6	274.9	-	60344.0	274.9	-	58205.1
	279.5	61.1	60622.9	279.1	60.9	58457.9
	302.5	60.0	62014.8	298.9	59.3	59650.4
	328.8	58.8	63581.0	325.2	58.4	61198.4
	329.7	88.1	63631.0	328.8	-	61422.0
	336.0	65.0	64193.2	334.0	65.2	61727.5
	359.6	63.5	65708.3	359.1	64.0	63344.8
6	366.2	-	66126.6	366.2	-	63800.2

Table C-12. Effluent flow measurements of both vegetated columns for run 6. Sample ID is provided if a sample was taken concurrently with measured flow. Runtime is the time of the measurement taken relative to the commencement of inflow. Flow is the measured flowrate at a given time. Cum. V is the cumulative volume of effluent that the column produced. †: Volume of effluent collected between column runs.

Experimental Column				**Control Column**			
Sample ID	Runtime (min)	Flow (mL/min)	Cum. V (mL)	Sample ID	Runtime (min)	Flow (mL/min)	Cum. V (mL)
	39.0	193.4	3770.5		37.0	249.4	4613.5

0	45.8	-	5319.8	0	41.8	-	5958.9
	51.6	264.6	6655.3		48.0	315.3	7720.1
0.25	57.3	283.6	8223.3	0.25	53.0	313.3	9284.3
	68.8	328.8	11737.1		65.9	328.2	13424.0
0.5	73.3	346.6	13257.3	0.5	69.7	324.9	14664.1
	82.1	345.4	16290.8		79.1	319.5	17703.3
0.75	88.4	330.9	18432.6	0.75	85.5	307.2	19693.1
1	107.1	128.4	22716.2	1	103.4	235.0	24550.6
1.3	123.3	264.8	25914.3	1.3	122.9	231.3	29105.0
	132.4	251.4	28249.9		129.2	233.6	30561.6
	156.8	241.2	34258.6		152.5	235.6	36030.8
2	167.1	249.1	36795.5	2	164.3	232.7	38789.9
	179.6	235.3	39810.7		176.5	226.4	41594.6
	195.3	125.0	42648.0		191.9	120.3	44264.2
2.7	207.2	142.8	44234.4	2.7	203.9	122.6	45723.5
	234.6	147.9	48221.6		231.4	135.5	49263.8
3.3	245.7	150.8	49882.2	3.3	241.1	150.6	50651.4
	262.5	155.3	52451.3		259.2	146.3	53351.1
	284.6	115.0	55438.0		280.9	114.4	56173.1
4	294.6	147.6	56750.8	4	297.0	131.5	58158.3
	325.5	56.4	59904.2		319.0	57.0	60224.4
5	349.0	65.6	61336.8	5	351.1	55.7	62037.3
	364.1	60.9	62291.7		360.5	59.7	62578.7
6	382.6	69.1	63494.7	6	382.5	0	63892.1
	385.8	51.1	63683.1		386.3	0	63892.1
		† ~ 2.6 L	66233.1		390.0	13.3	63916.5
						† ~ 1.7 L	65581.5

Table C-13. Influent flow measurements of both vegetated columns for run 7. Sample ID is provided if a sample was taken concurrently with measured flow. Runtime is the time of the measurement taken relative to the commencement of inflow. Exp. Flow and Ctrl. Flow are the measured flowrates at a given time for the experimental and control column, respectively. V_e In and V_c In are the cumulative volume of influent applied to the experimental and control columns, respectively.

Experimental Column				**Control Column**			
Sample ID	Runtime (min)	Exp. Flow (mL/min)	V_e In (mL)	Sample ID	Runtime (min)	Ctrl. Flow (mL/min)	V_c In (mL)
	3.03	178.4	539.9		4.92	182.4	898.3
0	15.24	-	2696.4		6.01	179.4	1095.6
	27.64	174.8	4886.3	0	15.24	-	2733.9

	66.45	177.0	11712.4		25.05	175.6	4476.4
	97.48	176.3	17194.2		69.57	169.0	12146.0
	103.65	177.9	18286.2		95.42	166.9	16487.4
	132.03	175.7	23303.3		101.38	178.8	17483.1
	139.98	177.4	24706.9		129.25	170.4	22349.5
	170.33	174.5	30047.1		138.25	177.9	23883.4
	174.27	175.2	30734.7		168.40	169.0	29112.5
3	183.13	-	32288.0		172.10	177.8	29737.8
	197.52	191.2	34807.7	3	183.13	-	31733.6
	250.48	190.6	44919.9		199.43	184.0	34682.0
	280.57	192.4	50680.8		236.32	178.0	41358.1
	313.43	191.5	56990.3		252.92	195.1	44313.1
6	346.08	-	63254.6		278.58	192.1	49282.4
	352.48	192.2	64482.5		311.65	190.1	55601.0
				6	346.08	-	62089.2
					350.85	186.8	62987.4
					352.48	-	63292.4

Table C-14. Effluent flow measurements of both vegetated columns for run 7. Sample ID is provided if a sample was taken concurrently with measured flow. Runtime is the time of the measurement taken relative to the commencement of inflow. Flow is the measured flowrate at a given time. Cum. V is the cumulative volume of effluent that the column produced. †: Volume of effluent collected between column runs.

Experimental Column				**Control Column**			
Sample ID	Runtime (min)	Flow (mL/min)	Cum. V (mL)	Sample ID	Runtime (min)	Flow (mL/min)	Cum. V (mL)
	18.4	4.0	36.6		22.4	86.6	970.6
0	29.6	111.9	687.3	0	34.1	192.6	2606.7
0.25	47.7	178.4	3307.8	0.25	42.6	181.1	4191.9
0.5	63.8	179.8	6191.4	0.5	60.4	175.6	7358.0
0.75	77.4	178.5	8621.6	0.75	72.3	169.7	9413.0
1	91.9	176.0	11206.3	1	88.7	164.5	12165.0
1.3	113.1	177.8	14950.5	1.3	108.0	177.8	15468.2
	127.1	177.5	17437.2		125.7	155.7	18408.5
2	158.2	190.3	23158.9	2	157.1	199.5	23997.9
	177.5	174.7	26671.7		176.1	175.5	27551.3
2.7	192.7	177.6	29345.8	2.7	188.3	175.0	29692.4
	202.1	189.9	31081.9		201.0	175.5	31912.3
	224.8	190.7	35401.0		223.4	188.4	35987.7

3.3	234.0	190.7	37151.8	3.3	232.9	177.6	37726.2
	256.6	191.3	41461.2		255.4	190.5	41873.4
4	276.8	200.6	45435.4	4	275.4	231.0	46085.0
	294.9	195.1	49003.5		293.5	196.9	49965.1
5	333.5	197.9	56595.2	5	332.4	197.7	57633.7
	357.3	168.1	60944.5		356.0	173.0	62016.7
	364.4	84.0	61841.7		362.6	55.5	62764.8
	370.8	53.0	62277.8		369.0	29.6	63036.4
	378.4	36.0	62616.0		375.6	18.7	63195.8
6	432.6	31.0	64434.9	6	439.5	4.3	63931.3
	451.5	7.2	64794.9			† ~ 1.1 L	64981.3
		† ~ 1.2 L	65949.9				

Table C-15. Influent flow measurements of both vegetated columns for run 8. Sample ID is provided if a sample was taken concurrently with measured flow. Runtime is the time of the measurement taken relative to the commencement of inflow. Exp. Flow and Ctrl. Flow are the measured flowrates at a given time for the experimental and control column, respectively. V_e In and V_c In are the cumulative volume of influent applied to the experimental and control columns, respectively.

	Experimental Column			**Control Column**		
Sample ID	Runtime (min)	Exp. Flow (mL/min)	V_e In (mL)	Runtime (min)	Ctrl. Flow (mL/min)	V_c In (mL)
	1.981	179.6	355.8	4.368	179.0	782.0
0	9.18616667	-	1677.0	9.18617	-	1647.3
	61.1	187.1	11196.3	63.05	180.2	11321.4
	93.8666667	187.4	17332.4	92.2167	164.6	16349.2
	108.316667	188.6	20049.2	99.8	186.6	17597.4
	128.233333	187.1	23790.9	126.583	176.1	22453.9
	139.266667	188.1	25861.2	136.967	185.0	24281.9
	161.066667	185.5	29933.9	159.117	171.0	28224.1
	167.283333	187.1	31092.1	164.55	185.2	29153.0
3	194.983333	-	36270.5	194.983	-	34713.9
	200.933333	186.8	37382.8	198.55	180.2	35365.6
	234.4	187.9	43653.0	232.65	174.6	41415.5
	240.25	191.4	44752.5	238.217	200.2	42387.5
	287.55	190.7	53790.7	295.95	192.7	53729.6
	331.55	190.6	62179.6	329.667	191.9	60213.1
6	342.466667	-	64260.0	342.467	-	62669.5

Table C-16. Effluent flow measurements of both vegetated columns for run 8. Sample ID is provided if a sample was taken concurrently with measured flow. Runtime is the time of the measurement taken relative to the commencement of inflow. Flow is the measured flowrate at a given time. Cum. V is the cumulative volume of effluent that the column produced. †: Volume of effluent collected between column runs.

Experimental Column				**Control Column**			
Sample ID	Runtime (min)	Flow (mL/min)	Cum. V (mL)	Sample ID	Runtime (min)	Flow (mL/min)	Cum. V (mL)
	14.9	11.7	86.8		18.7	9.5	103.2
	19.4	37.4	198.1		22.9	113.1	358.9
0	47.6	205.8	3619.5	0	37.9	184.4	2590.7
0.25	59.3	199.8	5992.0	0.25	48.6	180.5	4552.0
	64.4	200.9	7017.1	0.5	58.4	176.5	6292.0
0.5	74.1	209.4	9000.1		65.6	171.1	7549.1
	82.4	203.8	10718.5	0.75	71.2	168.7	8509.3
0.75	89.5	210.3	12185.1		81.4	166.2	10214.6
1	109.7	217.7	16511.6	1	88.5	160.4	11365.9
	114.4	214.1	17540.6	1.3	110.8	182.0	15180.4
1.3	122.8	197.1	19253.8		115.6	179.6	16063.3
	142.2	198.0	23095.8		141.1	175.2	20586.6
2	176.9	-	29427.5	2	156.3	168.1	23181.3
	188.0	166.8	31439.7		171.6	190.2	25937.6
2.7	204.0	173.9	34176.8	2.7	189.3	180.7	29204.7
	226.4	172.8	38057.2		211.6	174.1	33162.9
3.3	242.9	180.1	40971.9	3.3	227.8	181.7	36047.2
	254.4	173.2	43000.4		253.3	200.7	40924.9
	268.3	183.4	45472.3	4	266.8	188.4	43545.0
4	286.0	170.4	48599.9		303.7	195.3	50625.2
	304.8	186.2	51954.7	5	327.3	190.1	55169.3
5	347.1	187.1	59847.1		353.1	97.4	58877.7
	354.2	165.9	61103.3		357.2	46.4	59172.5
	358.2	183.7	61805.5		359.7	35.9	59276.0
	367.8	58.6	62970.6		364.6	23.6	59422.9
	372.0	48.3	63196.0	6	439.8	3.9	60459.7
	375.2	40.8	63337.1			† ~ 1.0 L	61409.7
6	425.3	20.7	64878.6				
		† ~1.4 L	66268.6				

Table C-17. Influent flow measurements of both vegetated columns for run 9. Sample ID is provided if a sample was taken concurrently with measured flow. Runtime is the time of the measurement taken relative to the commencement of inflow. Exp. Flow and Ctrl. Flow are the measured flowrates at a given time for the experimental and control column, respectively. V_e In and V_c In are the cumulative volume of influent applied to the experimental and control columns, respectively.

Experimental Column				Control Column			
Sample ID	Runtime (min)	Exp. Flow (mL/min)	V_e In (mL)	Sample ID	Runtime (min)	Ctrl. Flow (mL/min)	V_c In (mL)
	0	11.9			2.5	63.5	157.2
	7.4	61.3	87.3		16.4	55.0	984.5
	11.6	71.9	344.4	Step 1 End	20.6	-	1212.3
	15.0	70.5	589.8	Step 2 Begin	22.1	-	-
	16.9	18.4	724.9		25.8	239.8	2114.2
Step 1 End	20.6	-	792.3		41.2	241.5	5803.5
Step 2 Begin	22.1	-	-	Step 2 End	43.8	-	6447.5
	27.4	232.0	2032.2	Step 3 Begin	44.9	-	-
	43.4	231.6	5741.2		49.8	344.1	8116.5
Step 2 End	43.8	-	5837.7		67.0	338.3	14014.0
Step 3 Begin	44.9	-	-		88.7	346.9	21443.1
	51.3	343.7	8026.1	Step 3 End	100.2	-	25432.7
	68.3	347.4	13906.8	Step 4 Begin	102.3	-	-
	87.5	349.0	20610.3		105.7	305.0	26454.3
Step 3 End	100.2	-	25037.3		107.9	278.3	27135.4
Step 4 Begin	102.3	-	-		141.5	283.4	36562.8
	104.3	293.1	25608.8		171.8	280.5	45115.7
	107.9	266.1	26673.8	Step 4 End	174.6	-	45905.8
	143.1	271.4	36128.4	Step 5 Begin	176.0	-	-
	169.9	269.8	43394.2		178.1	162.6	46241.8
Step 4 End	174.6	-	44658.0		183.7	151.4	47165.7
Step 5 Begin	176.0	-	-		213.0	148.6	51557.0
	180.1	171.6	45364.3		258.3	149.5	58298.7
	183.7	152.4	45987.7	Step 5 End	262.7	-	58966.6
	215.5	148.4	50760.7	Step 6 Begin	263.1	-	-
	256.1	149.0	56801.5		269.5	68.8	59410.4
Step 5 End	262.7	-	57790.0		314.6	66.8	62462.7
Step 6 Begin	263.1	-	-		348.7	-	64746.1
	268.2	68.5	58141.5				
	315.9	66.8	61366.8				
	348.7	-	63557.5				

Table C-18. Effluent flow measurements of both vegetated columns for run 9. Sample ID is provided if a sample was taken concurrently with measured flow. Runtime is the time of the measurement taken relative to the commencement of inflow. Flow is the measured flowrate at a given time. Cum. V is the cumulative volume of effluent that the column produced. †: Volume of effluent collected between column runs.

Experimental Column				**Control Column**			
Sample ID	Runtime (min)	Flow (mL/min)	Cum. V (mL)	Sample ID	Runtime (min)	Flow (mL/min)	Cum. V (mL)
	30.1	79.2	1190.0		35.5	135.2	2399.1
	36.6	5.4	1465.6		37.8	188.6	2779.7
	46.1	220.5	2544.4	0	48.1	200.2	4775.6
0	53.0	231.3	4091.9	0.25	57.1	351.1	7256.4
	56.0	230.0	4776.1		65.0	345.2	10001.0
0.25	63.8	241.4	6614.6	0.5	71.7	-	12323.8
	69.9	275.5	8212.8		76.8	346.4	14099.0
0.5	78.9	305.8	10804.4	0.75	85.5	364.3	17184.7
	83.0	307.1	12086.3		98.0	317.5	21423.0
0.75	92.7	329.9	15170.1	1	100.2	314.8	22139.5
	98.8	328.8	17156.9		115.4	279.1	26652.9
1	107.0	321.2	19832.6	1.3	120.6	291.7	28117.8
	114.6	332.0	22314.9		143.9	289.6	34899.2
1.3	127.5	316.3	26512.8	2	164.4	309.1	41035.8
	144.8	302.9	31848.0		189.4	182.3	47187.0
2	170.7	-	39411.3	2.7	201.1	145.7	49105.7
	172.6	281.2	39975.9		233.2	141.1	53710.3
	190.8	131.8	43726.8	3.3	241.6	151.8	54940.3
2.7	208.3	146.5	46168.6		274.1	59.7	58371.3
	234.6	160.1	50190.3	4	290.4	-	59448.0
3.3	252.3	166.3	53081.5		297.6	72.3	59919.8
	276.0	96.8	56205.4		319.7	63.1	61421.2
4	295.8	-	57871.2	5	327.9	-	61926.9
	300.1	71.7	58237.8		336.0	61.0	62428.5
	324.7	69.4	59967.2		350.0	58.0	63263.9
5	332.9	-	60508.0		357.8	48.4	63677.2
	337.5	62.5	60815.8		365.1	30.4	63964.0
	351.3	60.5	61666.0	6	464.7	-	65563.9
	359.5	58.2	62150.8		519.0	1.7	66435.7
	367.1	45.1	62542.2			† ~ 1.0 L	67385.7
6	422.5	-	64315.2				
	427.4	18.9	64470.3				

† ~ 1.5 L 66005.3

Table C-19. Influent flow measurements of both vegetated columns for run 10. Sample ID is provided if a sample was taken concurrently with measured flow. Runtime is the time of the measurement taken relative to the commencement of inflow. Exp. Flow and Ctrl. Flow are the measured flowrates at a given time for the experimental and control column, respectively. V_e In and V_c In are the cumulative volume of influent applied to the experimental and control columns, respectively.

	Experimental Column			**Control Column**		
Sample ID	Runtime (min)	Exp. Flow (mL/min)	V_e In (mL)	Runtime (min)	Ctrl. Flow (mL/min)	V_c In (mL)
	2.9	179.9	530.0	4.9	184.6	908.6
0	19.2	-	3476.6	19.2	-	3573.1
	33.6	181.7	6063.5	35.3	187.5	6554.5
	67.5	185.1	12284.4	70.0	186.3	13048.9
	93.3	184.5	17049.9	94.9	188.6	17716.0
	126.8	186.0	23261.8	128.7	189.6	24108.0
	168.3	186.1	30982.8	166.0	189.2	31176.1
3	191.1	-	35194.0	191.1	-	35892.1
	207.7	183.5	38268.4	205.9	187.6	38683.3
	246.3	184.4	45364.5	248.0	187.5	46575.8
	292.6	184.5	53909.3	294.5	186.6	55276.7
6	335.6	-	61841.0	335.6	-	62942.6
	343.7	-	63348.0	343.7	-	64466.5

Table C-20. Effluent flow measurements of both vegetated columns for run 10. Sample ID is provided if a sample was taken concurrently with measured flow. Runtime is the time of the measurement taken relative to the commencement of inflow. Flow is the measured flowrate at a given time. Cum. V is the cumulative volume of effluent that the column produced. †: Volume of effluent collected between column runs.

Experimental Column				**Control Column**			
Sample ID	Runtime (min)	Flow (mL/min)	Cum. V (mL)	Sample ID	Runtime (min)	Flow (mL/min)	Cum. V (mL)
	10.7	62.8	335.9		20.5	120.7	1238.3
	27.6	130.2	1966.8		22.5	161.9	1519.6
0	34.7	-	3049.3	0	30.5	202.0	2964.0
	41.0	177.3	4023.0		39.9	177.5	4763.0
0.25	53.5	189.0	6312.2	0.25	46.7	188.2	6003.2

	59.9	183.4	7510.0		54.7	179.9	7466.5
0.5	71.9	174.7	9661.5	0.5	63.0	196.9	9030.3
	79.0	175.7	10890.9		74.1	187.7	11174.4
0.75	83.5	175.3	11680.7	0.75	77.1	183.5	11722.0
	91.3	173.3	13052.1		85.6	185.9	13292.0
1	98.2	180.1	14268.3	1	89.1	191.0	13954.7
	112.1	174.4	16722.8		103.6	194.0	16739.6
1.3	120.8	183.8	18289.6	1.3	110.7	195.5	18132.0
	132.9	178.8	20483.1		131.3	179.3	21992.7
2	163.8	208.3	26469.4	2	157.1	241.3	27411.1
	170.4	198.2	27793.6		161.9	203.7	28478.9
	189.2	197.4	31514.8		190.4	187.3	34057.0
2.7	198.8	196.3	33414.1	2.7	193.7	191.8	34673.1
	211.6	195.3	35913.7		210.2	181.7	37757.3
	221.2	192.0	37769.6		220.1	186.6	39592.3
3.3	240.4	186.6	41413.8	3.3	230.9	190.5	41612.6
	259.3	172.1	44794.5		258.2	191.6	46834.8
4	282.4	185.6	48935.0	4	273.0	193.7	49686.5
	311.9	187.1	54424.4		313.1	185.7	57294.2
5	338.9	184.6	59440.1	5	331.0	188.6	60653.7
	348.5	161.8	61114.3		347.3	164.5	63517.1
	379.2	26.7	64003.3		379.2	7.0	66254.0
6	439.9	-	65124.4	6	490.0	-	66722.9
	444.0	10.2	65200.3		526.8	1.5	66878.6
		† ~1.2 L	66405.3			† ~ 1.0 L	67693.6

Table C-21. Influent flow measurements of both vegetated columns for run 11. Sample ID is provided if a sample was taken concurrently with measured flow. Runtime is the time of the measurement taken relative to the commencement of inflow. Exp. Flow and Ctrl. Flow are the measured flowrates at a given time for the experimental and control column, respectively. V_e In and V_c In are the cumulative volume of influent applied to the experimental and control columns, respectively.

	Experimental Column			**Control Column**		
Sample ID	Runtime (min)	Exp. Flow (mL/min)	V_e In (mL)	Runtime (min)	Ctrl. Flow (mL/min)	V_c In (mL)
	2.6	172.0	441.2	5.9	172.7	1022.7
	6.6	183.5	1137.5	6.6	185.2	1141.6
0	9.0	-	1578.2	9.0	-	1587.2
	41.2	185.6	7524.3	39.4	188.1	7267.8
	79.5	185.9	14631.6	77.7	188.8	14473.2
	122.7	185.4	22651.4	119.4	188.7	22349.8

	152.5	185.0	28180.5	150.8	188.8	28273.6
3	170.9	-	31572.9	170.9	-	32065.3
	172.8	-	31930.7	172.8	-	32430.3

Table C-22. Effluent flow measurements of both vegetated columns for run 11. Sample ID is provided if a sample was taken concurrently with measured flow. Runtime is the time of the measurement taken relative to the commencement of inflow. Flow is the measured flowrate at a given time. Cum. V is the cumulative volume of effluent that the column produced. †: Volume of effluent collected between column runs.

Experimental Column				**Control Column**			
Sample ID	Runtime (min)	Flow (mL/min)	Cum. V (mL)	Sample ID	Runtime (min)	Flow (mL/min)	Cum. V (mL)
	27.5	158.7	2180.7		18.8	63.5	595.3
	30.3	188.1	2669.0		21.1	175.5	875.5
0	37.3	200.8	4033.3	0	26.5	-	1872.4
	45.2	171.2	5506.0		29.3	191.8	2374.3
0.25	53.6	168.4	6926.8		34.4	190.1	3361.4
	58.1	174.9	7690.6	0.25	43.8	181.6	5108.2
0.5	69.5	177.0	9707.9		54.8	191.6	7151.6
	74.3	177.3	10552.3	0.5	62.9	189.7	8705.5
0.75	81.9	175.0	11894.1		66.9	185.2	9449.0
	94.2	183.0	14090.3	0.75	73.3	190.5	10654.2
1	97.1	183.2	14630.5		83.1	183.0	12481.4
	113.2	187.5	17611.6	1	93.1	175.5	14271.0
1.3	117.1	186.7	18335.1		101.5	185.5	15793.1
	147.1	188.3	23972.7	1.3	111.6	180.5	17637.9
2	158.1	192.0	26061.0		133.8	187.0	21716.3
	177.1	151.2	29321.5	2	148.9	189.0	24551.6
	182.6	119.9	30067.1		156.6	182.5	25985.1
	198.2	38.1	31301.0		181.2	73.5	29139.1
3	249.9	-	32591.2		191.9	22.2	29649.5
	253.5	11.9	32680.8	3	334.4	-	31294.1
		~1.3 L	34000.8		383.4	0.9	31859.1
						~ 0.6 L	32496.1

Table C-23. Influent flow measurements of both vegetated columns for run 12. Sample ID is provided if a sample was taken concurrently with measured flow. Runtime is the time of the measurement taken relative to the commencement of inflow. Exp. Flow and Ctrl. Flow are the

measured flowrates at a given time for the experimental and control column, respectively. V_e In and V_c In are the cumulative volume of influent applied to the experimental and control columns, respectively.

	Experimental Column			Control Column		
Sample ID	Runtime (min)	Exp. Flow (mL/min)	V_e In (mL)	Runtime (min)	Ctrl. Flow (mL/min)	V_c In (mL)
	3.6	181.1	645.2	1.9	183.1	355.4
0	11.4	-	2087.8	11.4	-	2124.2
	45.1	186.6	8276.9	43.3	190.4	8076.3
	74.5	186.0	13754.3	69.8	190.6	13123.9
	120.1	184.5	22197.3	118.0	188.0	22249.8
	144.9	185.3	26786.6	143.1	190.5	26999.3
3	167.1	-	30906.2	164.8	186.0	31074.2
	169.8	184.7	31393.5	167.1	-	31517.4
	171.7	-	31750.5	171.7	-	32366.6

Table C-24. Effluent flow measurements of both vegetated columns for run 12. Sample ID is provided if a sample was taken concurrently with measured flow. Runtime is the time of the measurement taken relative to the commencement of inflow. Flow is the measured flowrate at a given time. Cum. V is the cumulative volume of effluent that the column produced. †: Volume of effluent collected between column runs.

	Experimental Column				Control Column		
Sample ID	Runtime (min)	Flow (mL/min)	Cum. V (mL)	Sample ID	Runtime (min)	Flow (mL/min)	Cum. V (mL)
	9.7	11.0	53.6		17.8	115.6	1026.7
	27.1	16.7	293.1		19.0	171.6	1200.6
	28.3	192.6	423.8	0	24.5	203.8	2232.1
0	34.6	-	1670.5		29.6	187.5	3226.6
	36.5	205.5	2045.3		33.6	189.7	3996.3
	41.7	193.4	3082.3	0.25	40.7	186.0	5314.5
0.25	51.9	171.4	4954.9	0.5	57.6	189.2	8497.5
	58.9	174.4	6153.7		64.1	193.4	9740.7
0.5	67.5	173.9	7660.0	0.75	72.0	180.5	11204.8
0.75	81.2	182.0	10097.9		83.0	189.9	13247.7
	86.7	176.8	11078.6	1	85.6	185.9	13745.6
1	96.2	182.7	12795.4		97.3	184.3	15911.0
	108.4	182.0	15023.1	1.3	106.2	189.8	17569.2
1.3	115.9	183.2	16386.2		122.8	181.1	20653.5
	123.9	183.9	17857.4		138.4	198.3	23610.0
	139.4	197.6	20816.8	2	149.0	189.0	25662.8

2	155.6	-	24113.7		162.0	201.4	28190.6
	157.4	210.3	24480.8		175.8	155.6	30662.9
	161.0	193.8	25198.1		182.1	58.1	31337.7
	174.8	182.9	27800.2		188.4	29.1	31612.2
	179.9	134.3	28614.4	3	290.7	-	33170.7
	199.0	34.9	30228.0		364.7	1.4	34299.2
3	256.8	-	31981.7			† ~ 0.8 L	35082.2
	276.8	25.7	32586.2				
		† ~1.1 L	33731.2				

Table C-25. Influent flow measurements of both vegetated columns for run 13. Sample ID is provided if a sample was taken concurrently with measured flow. Runtime is the time of the measurement taken relative to the commencement of inflow. Exp. Flow and Ctrl. Flow are the measured flowrates at a given time for the experimental and control column, respectively. V_e In and V_c In are the cumulative volume of influent applied to the experimental and control columns, respectively.

	Experimental Column			**Control Column**		
Sample ID	Runtime (min)	Exp. Flow (mL/min)	V_e In (mL)	Runtime (min)	Ctrl. Flow (mL/min)	V_c In (mL)
	3.2	196.6	619.4	1.6	198.6	310.6
	4.0	183.9	784.8	4.0	179.0	768.9
0	22.6	-	4209.3	22.6	-	4182.8
	45.1	183.5	8333.3	41.4	187.2	7622.6
	78.7	180.5	14441.4	77.0	184.7	14236.9
	102.8	181.5	18808.8	101.0	185.5	18682.4
	136.0	185.2	24896.5	134.2	189.6	24900.2
	174.4	182.4	31955.7	172.6	185.6	32110.7
3	185.7	-	34010.1	185.7	-	34532.4
	204.4	181.7	37420.8	202.6	184.6	37660.6
	241.0	180.5	44046.8	239.2	184.4	44415.9
	274.2	181.9	50060.6	272.4	185.2	50553.0
	304.2	179.2	55474.3	302.3	182.7	56058.2
	332.5	178.4	60543.6	330.8	183.0	61259.3
6	347.6	-	63239.5	347.6	-	64308.3
	349.2	179.0	63528.4	347.2	180.0	64241.7
	350.5	-	63764.1	350.5	-	64835.8

Table C-26. Effluent flow measurements of both vegetated columns for run 13. Sample ID is provided if a sample was taken concurrently with measured flow. Runtime is the time of the measurement taken relative

to the commencement of inflow. Flow is the measured flowrate at a given time. Cum. V is the cumulative volume of effluent that the column produced. †: Volume of effluent collected between column runs.

Experimental Column				Control Column			
Sample ID	Runtime (min)	Flow (mL/min)	Cum. V (mL)	Sample ID	Runtime (min)	Flow (mL/min)	Cum. V (mL)
	10.2	66.0	337.4		16.4	11.0	90.4
	26.5	6.7	928.1		17.7	81.1	149.9
	28.2	177.5	1084.3		19.9	151.5	411.2
	30.5	190.4	1506.6		21.0	187.1	591.4
0	35.5	-	2442.3	0	26.5	-	1612.3
	39.5	178.9	3184.1		29.4	186.0	2157.9
	49.3	155.2	4818.7		34.4	181.3	3073.3
0.25	51.6	-	5179.3	0.25	43.1	-	4690.4
	53.8	165.4	5532.0		48.0	191.2	5615.4
	59.1	171.6	6422.1		52.7	191.6	6505.5
0.5	67.4	-	7835.1	0.5	58.2	-	7550.5
	69.7	166.2	8212.3		60.1	189.5	7928.4
	74.2	174.7	8987.9		66.9	178.7	9174.3
0.75	81.3	-	10239.3	0.75	73.2	-	10301.0
	83.3	177.8	10585.9		75.3	181.8	10688.6
	89.1	183.0	11635.3	1	87.4	-	12908.2
1	96.1	-	12912.2		90.1	184.0	13399.1
	98.8	180.1	13390.3		97.3	182.3	14721.1
	111.3	179.7	15641.9	1.3	110.3	189.8	17133.3
1.3	118.4	179.1	16915.6		130.5	179.6	20867.3
	138.1	175.5	20411.3	2	153.1	186.2	24989.3
2	160.8	-	24512.8		161.8	188.4	26628.2
	163.0	185.9	24904.3		183.1	188.4	30643.9
	170.9	174.4	26330.2	2.7	189.3	-	31799.0
	184.4	174.9	28684.7		191.3	187.3	32171.5
2.7	200.3	179.6	31514.9		207.3	181.7	35126.0
	212.5	178.9	33702.3		219.0	186.0	37286.2
	221.8	178.5	35352.4	3.3	229.5	186.2	39243.7
3.3	237.5	178.8	38171.7		250.2	180.6	43031.2
	251.2	173.0	40578.2	4	268.3	-	46316.2
4	278.5	177.9	45365.0		270.4	182.7	46703.8
	288.2	174.2	47064.1		280.7	182.3	48577.6
	299.7	178.8	49096.8		298.6	181.5	51836.6
	310.5	174.6	51010.8		309.5	171.0	53757.6
	323.4	176.0	53277.9		322.4	177.8	56013.0
5	337.6	171.9	55744.9	5	327.8	-	56975.6

	345.6	173.0	57118.7		334.0	183.2	58103.7
	356.0	139.4	58743.4		344.6	179.1	60026.9
	365.4	64.9	59705.6		354.9	158.5	61754.5
	371.1	44.9	60019.7		363.3	36.2	62574.0
	384.5	18.4	60444.4		369.4	22.9	62753.9
6	485.4	-	61647.0		373.2	18.0	62831.6
	499.0	5.4	61808.3	6	530.1	-	64340.9
		† ~1.2 L	62998.3		570.3	1.3	64727.4
						† ~ 0.8 L	65527.4

Appendix D: Vegetated Column Contaminant Data

Table D-1. Influent characteristics for vegetated column run 1. N.D.: Not detected.

Sample ID	pH	Turbidity (NTU)	Conductance (mmhos)	TP (µg P/L)	TDP (µg P/L)	NO_3^- (mg N/L)	NO_2^- (µg N/L)	TKN (mg N/L)	SO_4^{2-} (mg SO_4^{2-}/L)
0	6.42	0.2	-	115.3	-	0.74	< 2	0.93	n.d.
3	6.22	0.4	-	119.9	-	0.74	< 2	0.93	n.d.
5.5	6.24	0.5	-	116.0	-	-	< 2	1.07	-

Table D-2. Effluent characteristics for experimental vegetated column run 1.

Sample ID	pH	Turbidity (NTU)	Conductance (mmhos)	TP (µg P/L)	TDP (µg P/L)	NO_3^- (mg N/L)	NO_2^- (µg N/L)	TKN (mg N/L)	SO_4^{2-} (mg SO_4^{2-}/L)
0	7.37	0.2	-	70.0	20.4	2.00	> 25	1.68	> 25
0.3	6.14	6.3	-	66.8	11.3	-	-	-	-
0.7	7.26	0.2	-	58.0	< 10.0	-	-	-	-
1	-	-	-	-	-	0.76	9.2	-	> 25
1.3	7.19	1.0	-	17.6	< 10.0	-	-	-	-
2	7.27	1.2	-	16.9	< 10.0	0.82	10.7	-	> 25
2.7	7.21	1.0	-	14.8	-	-	-	-	-
3.3	7.17	0.9	-	16.2	-	-	-	-	-
4	7.19	0.7	-	15.5	9.8	0.78	14.6	0.47	> 25
5	7.15	0.8	-	15.5	-	-	-	-	-
6	7.22	0.7	-	13.4	< 10.0	-	21.5	0.33	-

Table D-3. Effluent characteristics for control vegetated column run 1.

Sample ID	pH	Turbidity (NTU)	Conductance (mmhos)	TP (µg P/L)	TDP (µg P/L)	NO_3^- (mg N/L)	NO_2^- (µg N/L)	TKN (mg N/L)	SO_4^{2-} (mg SO_4^{2-}/L)
0	6.53	155	-	593.0	336.4	0.53	> 25	2.15	16.1
0.3	6.31	20.8	-	251.7	204.5	-	-	-	-
0.7	6.36	8.1	-	185.4	153.7	-	-	-	-
1	-	-	-	-	-	0.79	23.1	-	30.5
1.3	6.28	3.2	-	147.0	129.2	-	-	-	
2	6.36	2.6	-	127.9	103.4	0.74	23.1	0.65	12.8
2.7	6.36	2.5	-	121.2	-	-	-	-	-
3.3	6.17	3.1	-	117.9	-	-	-	-	-
4	6.18	4.8	-	116.6	92.1	0.73	25.4	-	3.1
5	6.24	8.7	-	118.6	92.1	-	-	-	-
6	6.24	2.6	-	131.8	111.3	-	> 25	0.65	-

Table D-4. Influent characteristics for vegetated column run 2. N.D.: Not detected.

Sample ID	pH	Turbidity (NTU)	Conductance (mmhos)	TP (µg P/L)	TDP (µg P/L)	NO_3^- (mg N/L)	NO_2^- (µg N/L)	TKN (mg N/L)	SO_4^{2-} (mg SO_4^{2-}/L)
0	5.68	0.3	-	113.1	-	0.69	< 2	1.03	n.d.
3	6.1	1.2	-	111.2	-	0.60	< 2	0.98	n.d.
5.5	6.03	0.3	-	109.8	-	0.82	< 2	1.21	n.d.

Table D-5. Effluent characteristics for experimental vegetated column run 2.

Sample ID	pH	Turbidity (NTU)	Conductance (mmhos)	TP (µg P/L)	TDP (µg P/L)	NO_3^- (mg N/L)	NO_2^- (µg N/L)	TKN (mg N/L)	SO_4^{2-} (mg SO_4^{2-}/L)
0	7.02	1.2	-	37.5	15.1	0.22	2.0	0.79	> 25
0.25	7.09	1.9	-	59.2	-	-	-	-	-
0.5	7.16	1.4	-	45.4	20.3	0.45	2.4	-	> 25
0.75	7.05	1.4	-	30.9	-	-	-	-	-
1	-	-	-	-	0.7	3.28	-	-	> 25
1.3	7.04	0.8	-	28.9	-	-	-	-	-
2	7.09	1.3	-	16.4	< 10.0	0.58	5.8	0.42	> 25
2.7	7.01	0.7	-	11.1	-	-	-	-	-
3.3	7.04	0.7	-	10.5	-	-	-	-	-
4	7.05	0.6	-	15.7	< 10.0	1.01	8.0	-	> 25
5	6.98	0.7	-	8.5	-	-	-	-	-
6	7.1	0.4	-	10.5	< 10.0	0.71	10.1	0.33	> 25
7	7.29	1.2	-	< 10.0	-	-	-	-	-

Table D-6. Effluent characteristics for control vegetated column run 2.

Sample ID	pH	Turbidity (NTU)	Conductance (mmhos)	TP (µg P/L)	TDP (µg P/L)	NO_3^- (mg N/L)	NO_2^- (µg N/L)	TKN (mg N/L)	SO_4^{2-} (mg SO_4^{2-}/L)
0	6.29	12.5	-	222.9	166.0	0.29	4.6	1.49	2.7
0.25	6.16	18.0	-	232.6	155.6	-	-	-	-
0.5	6.1	21.5	-	216.4	134.2	0.46	4.6	-	4.0
0.75	6.1	23.0	-	193.8	111.6	-	-	-	-
1	-	-	-	-	-	0.55	5.0	-	1.8

1.3	6.13	22.2	-	157.5	88.3	-	-	-	-
2	6.11	35.3	-	186.0	91.5	0.72	4.6	0.84	0.9
2.7	6.17	24.8	-	140.1	74.1	-	-	-	-
3.3	6.12	25.9	-	131.7	74.1	-	-	-	-
4	6.17	25.7	-	129.7	76.0	0.68	4.6	-	0.5
5	6.12	28.5	-	122.6	75.4	-	-	-	-
6	6.33	23.8	-	120.7	76.6	0.67	5.8	0.56	0.5
7	6.46	8.5	-	87.6	74.1	-	-	-	-

Table D-7. Influent characteristics for vegetated column run 3. N.D.: Not detected.

Sample ID	pH	Turbidity (NTU)	Conductance (mmhos)	TP (µg P/L)	TDP (µg P/L)	NO_3^- (mg N/L)	NO_2^- (µg N/L)	TKN (mg N/L)	SO_4^{2-} (mg SO_4^{2-}/L)
0	6.28	0.5	-	119.0	-	0.92	< 2	1.03	n.d.
3	4.32	0.4	-	123.5	-	0.72	< 2	1.12	n.d.
5.5	6.14	0.5	-	117.7	-	0.76	< 2	1.03	n.d.

Table D-8. Effluent characteristics for experimental vegetated column run 3.

Sample ID	pH	Turbidity (NTU)	Conductance (mmhos)	TP (µg P/L)	TDP (µg P/L)	NO_3^- (mg N/L)	NO_2^- (µg N/L)	TKN (mg N/L)	SO_4^{2-} (mg SO_4^{2-}/L)
0	6.83	1.2	-	37.8	14.4	0.30	< 2	0.09	> 25
0.25	6.83	1.4	-	44.3	-	-	-	-	-
0.5	6.89	1.0	-	41.7	11.1	0.48	2.3	-	> 25

0.75	6.92	1.0	-	28.0	-	-	-	-	-
1	-	-	-	-	-	0.58	3.6	-	> 25
1.3	6.91	0.9	-	19.6	-	-	-	-	-
2	6.9	0.7	-	22.2	< 10.0	0.54	6.5	0.51	24.1
2.7	6.88	0.8	-	12.4	-	-	-	-	-
3.3	6.9	0.7	-	12.4	-	-	-	-	-
4	6.88	0.6	-	12.4	< 10.0	0.59	6.5	-	13.2
5	6.86	1.5	-	11.1	-	-	-	-	-
6	7.19	1.1	-	14.4	< 10.0	0.61	5.2	0.28	12.9

Table D-9. Effluent characteristics for control vegetated column run 3. N.D.: Not detected.

Sample ID	pH	Turbidity (NTU)	Conductance (mmhos)	TP (µg P/L)	TDP (µg P/L)	NO_3^- (mg N/L)	NO_2^- (µg N/L)	TKN (mg N/L)	SO_4^{2-} (mg SO_4^{2-}/L)
0	6.06	38.8	-	269.1	164.1	0.37	10.2	1.45	0.6
0.25	6.08	32.0	-	245.4	154.0	-	-	-	-
0.5	6.11	33.6	-	230.0	130.0	0.48	7.3	-	1.0
0.75	6.06	26.1	-	196.4	118.4	-	-	-	-
1	-	-	-	-	-	0.53	7.3	-	0.5
1.3	6.12	25.7	-	160.1	91.5	-	-	-	-
2	6.16	25.3	-	159.4	85.5	0.50	6.5	1.21	n.d.
2.7	6.12	22.5	-	140.6	77.4	-	-	-	-
3.3	6.06	24.9	-	139.2	83.5	-	-	-	-
4	6.08	23.9	-	139.9	85.5	0.55	5.2	-	n.d.
5	6.2	31.9	-	132.5	83.5	-	-	-	-
6	6.51	25.6	-	138.6	88.9	0.49	4.0	0.61	n.d.

Table D-10. Influent characteristics for vegetated column run 4. N.D.: Not detected.

Sample ID	pH	Turbidity (NTU)	Conductance (mmhos)	TP (µg P/L)	TDP (µg P/L)	NO_3^- (mg N/L)	NO_2^- (µg N/L)	TKN (mg N/L)	SO_4^{2-} (mg SO_4^{2-}/L)
0	6.26	0.5	-	114.9	-	0.79	< 2	1.12	n.d.
3	3.88	0.5	-	111.0	-	0.73	< 2	1.07	n.d.
6	6.17	1.3	-	114.9	-	0.71	< 2	-	n.d.

Table D-11. Effluent characteristics for experimental vegetated column run 4.

Sample ID	pH	Turbidity (NTU)	Conductance (mmhos)	TP (µg P/L)	TDP (µg P/L)	NO_3^- (mg N/L)	NO_2^- (µg N/L)	TKN (mg N/L)	SO_4^{2-} (mg SO_4^{2-}/L)
0	6.68	0.8	-	24.5	< 10.0	0.12	< 2	0.28	25.1
0.25	6.68	1.1	-	27.7	-	-	-	-	-
0.5	6.66	1.0	1.69	27.5	< 10.0	0.39	2.1	-	27.3
0.75	6.65	0.8	-	19.3	-	-	-	-	-
1	-	-	-	-	-	0.48	3.7	-	21.7
1.3	6.63	0.8	1.52	15.4	-	-	-	-	-
2	6.78	1.0	1.46	11.5	< 10.0	0.48	6.6	0.47	15.0
2.7	6.73	0.7	-	10.2	-	-	-	-	-
3.3	6.79	1.0	1.43	8.2	-	-	-	-	-
4	6.79	0.5	1.42	< 10.0	< 10.0	0.54	5.4	-	9.8
5	6.70	0.8	1.40	7.6	-	-	-	-	-
6	6.79	1.0	1.37	10.5	< 10.0	0.61	5.0	0.37	7.5
7	7.01	1.7	1.41	< 10.0	-	-	-	-	-

Table D-12. Effluent characteristics for control vegetated column run 4.

Sample ID	pH	Turbidity (NTU)	Conductance (mmhos)	TP (µg P/L)	TDP (µg P/L)	NO_3^- (mg N/L)	NO_2^- (µg N/L)	TKN (mg N/L)	SO_4^{2-} (mg SO_4^{2-}/L)
0	6.1	47.5	-	313.1	206.3	0.36	17.5	1.45	1.1
0.25	6.03	35.2	-	262.4	173.5	-	-	-	-
0.5	5.98	37.1	1.45	248.0	159.1	0.60	14.2	-	0.6
0.75	5.98	32.4	-	214.5	135.1	-	-	-	-
1	-	-	-	-	-	0.53	11.7	-	0.6
1.3	6	31.0	1.32	179.3	113.6	-	-	-	-
2	6.12	34.8	1.26	196.2	104.9	0.52	10.4	1.03	0.4
2.7	6.07	32.2	-	168.3	104.5	-	-	-	-
3.3	6.14	31.2	1.29	161.8	101.9	-	-	-	-
4	6.12	38.2	1.3	208.3	105.9	0.54	11.2	-	0.4
5	6.04	31.7	1.31	161.1	103.9	-	-	-	-
6	6.18	36.3	1.28	197.2	106.9	0.59	8.3	0.70	0.4
7	6.72	33.7	1.31	180.2	-	-	-	-	-

Table D-13. Influent characteristics for vegetated column run 5. N.D.: Not detected.

Sample ID	pH	Turbidity (NTU)	Conductance (mmhos)	TP (µg P/L)	TDP (µg P/L)	NO_3^- (mg N/L)	NO_2^- (µg N/L)	TKN (mg N/L)	SO_4^{2-} (mg SO_4^{2-}/L)
0	6.29	0.3	1.32	120.9	-	0.77	< 2	0.70	n.d.
3	6.06	0.3	1.31	115.7	-	0.73	< 2	1.17	n.d.
6	6.01	0.8	1.31	121.5	-	0.73	< 2	1.21	n.d.

Table D-14. Effluent characteristics for experimental vegetated column run 5.

Sample ID	pH	Turbidity (NTU)	Conductance (mmhos)	TP (µg P/L)	TDP (µg P/L)	NO_3^- (mg N/L)	NO_2^- (µg N/L)	TKN (mg N/L)	SO_4^{2-} (mg SO_4^{2-}/L)
0	6.64	1.1	1.53	16.3	9.7	0.09	< 2	0.47	15.8
0.25	6.64	1.2	1.56	21.6	-	-	-	-	-
0.5	6.66	0.7	1.55	20.9	< 10.0	0.40	2.1	-	15.4
0.75	6.59	0.9	1.53	14.9	-	-	-	-	-
1	-	-	-	-	-	0.47	3.8	-	12.7
1.3	6.63	1.1	1.48	10.3	-	-	-	-	-
2	6.62	0.6	1.41	9.7	< 10.0	0.50	6.2	0.37	8.9
2.7	6.68	0.5	1.38	< 10.0	-	-	-	-	-
3.3	6.65	0.6	1.38	< 10.0	-	-	-	-	-
4	6.68	0.7	1.37	9.0	< 10.0	0.52	6.2	-	5.9
5	6.64	0.5	1.34	< 10.0		-	-	-	-
6	6.74	0.6	1.36	10.3	< 10.0	0.55	6.2	0.33	5.1

Table D-15. Effluent characteristics for control vegetated column run 5. N.D.: Not detected.

Sample ID	pH	Turbidity (NTU)	Conductance (mmhos)	TP (µg P/L)	TDP (µg P/L)	NO_3^- (mg N/L)	NO_2^- (µg N/L)	TKN (mg N/L)	SO_4^{2-} (mg SO_4^{2-}/L)
0	6.11	57.6	1.58	378.1	191.0	1.01	34.3	2.29	0.7
0.25	6.09	50.0	1.47	294.7	166.6	-	-	-	-
0.5	6.13	38.2	1.41	247.3	152.0	0.92	18.8	-	0.5
0.75	6.05	33.3	1.39	211.9	124.8	-	-	-	-

1	-	-	-	-	-	0.73	20.8	-	0.4
1.3	6.03	30.4	1.33	174.6	104.6	-	-	-	-
2	6.1	31.7	1.31	168.5	103.7	0.59	11.9	0.89	0.4
2.7	6.07	28.8	1.28	155.0	96.0	-	-	-	-
3.3	6.02	29.7	1.29	155.6	93.4	-	-	-	-
4	6.08	25.9	1.28	155.3	132.8	0.57	39.1	-	n.d.
5	6.2	26.9	1.31	143.8	98.0	-	-	-	-
6	6.41	31.1	1.28	163.9	102.4	0.59	9.0	0.83	n.d.

Table D-16. Influent characteristics for vegetated column run 6. N.D.: Not detected.

Sample ID	pH	Turbidity (NTU)	Conductance (mmhos)	TP (µg P/L)	TDP (µg P/L)	NO_3^- (mg N/L)	NO_2^- (µg N/L)	TKN (mg N/L)	SO_4^{2-} (mg SO_4^{2-}/L)
Step 1	-	-	-	174.5	-	-	-	-	-
Step 2	5.14	0.4	1.34	152.5	-	1.01	< 2	1.35	n.d.
Step 3	-	-	-	130.9	-	-	-	-	-
Step 4	-	-	-	109.1	-	-	-	-	-
Step 5	6.08	0.7	1.36	88.5	-	0.56	< 2	0.93	n.d.
Step 6	5.99	0.5	1.36	68.5	-	0.43	< 2	0.67	n.d.

Table D-17. Effluent characteristics for experimental vegetated column run 6.

Sample ID	pH	Turbidity (NTU)	Conductance (mmhos)	TP (µg P/L)	TDP (µg P/L)	NO_3^- (mg N/L)	NO_2^- (µg N/L)	TKN (mg N/L)	SO_4^{2-} (mg SO_4^{2-}/L)

0	6.53	1.7	1.66	21.8	9.1	0.21	< 2	0.51	11.8
0.25	6.5	1.5	1.62	29.6	-	-	-	-	-
0.5	6.56	1.1	1.55	21.1	< 10.0	0.77	2.9	-	9.3
0.75	6.52	0.8	1.51	14.3	-	-	-	-	-
1	-	-	-	-	-	0.75	3.4	-	7.1
1.3	6.57	1.0	1.49	13.0	-	-	-	-	-
2	6.59	0.6	1.42	< 10.0	< 10.0	0.59	6.2	0.65	5.3
2.7	6.59	0.8	1.40	< 10.0	-	-	-	-	-
3.3	6.65	0.8	1.42	10.4	-	-	-	-	-
4	6.5	1.1	1.34	9.8	< 10.0	0.42	7.0	-	4.4
5	6.56	0.8	1.35	10.4	-	-	-	-	-
6	6.7	1.4	1.45	9.8	< 10.0	0.23	2.9	0.37	4.8

Table D-18. Effluent characteristics for control vegetated column run 6. N.D.: Not detected.

Sample ID	pH	Turbidity (NTU)	Conductance (mmhos)	TP (µg P/L)	TDP (µg P/L)	NO_3^- (mg N/L)	NO_2^- (µg N/L)	TKN (mg N/L)	SO_4^{2-} (mg SO_4^{2-}/L)
0	6.1	61.7	1.64	509.3	247.7	1.15	23.6	2.01	0.4
0.25	6.06	43.0	1.52	313.7	150.2	-	-	-	-
0.5	6	28.0	1.44	235.3	127.9	0.92	12.3	-	n.d.
0.75	5.96	22.9	1.37	196.6	105.2	-	-	-	-
1	-	-	-	-	-	0.80	10.6	-	n.d.
1.3	6.06	31.1	1.38	179.4	85.3	-	-	-	-
2	5.94	24.5	1.34	152.5	81.2	0.62	10.6	0.84	n.d.
2.7	6.19	29.3	1.34	150.9	76.0	-	-	-	-
3.3	6.24	33.1	1.32	153.5	88.6	-	-	-	-

4	6.01	28.1	1.29	150.5	88.5	0.44	8.2	-	n.d.
5	6.19	34.6	1.3	146.9	84.6	-	-	-	-
6	6.35	35.3	1.31	157.2	94.5	0.33	8.6	0.75	n.d.

Table D-19. Influent characteristics for vegetated column run 7. N.D.: Not detected.

Sample ID	pH	Turbidity (NTU)	Conductance (mmhos)	TP (µg P/L)	TDP (µg P/L)	NO_3^- (mg N/L)	NO_2^- (µg N/L)	TKN (mg N/L)	SO_4^{2-} (mg SO_4^{2-}/L)
0	6.08	0.4	1.29	277.0	-	2.18	< 2	2.38	n.d.
3	5.86	0.4	1.31	315.1	-	2.14	< 2	2.52	n.d.
6	4.14	0.3	1.36	346.8	-	2.31	< 2	2.90	n.d.

Table D-20. Effluent characteristics for experimental vegetated column run 7.

Sample ID	pH	Turbidity (NTU)	Conductance (mmhos)	TP (µg P/L)	TDP (µg P/L)	NO_3^- (mg N/L)	NO_2^- (µg N/L)	TKN (mg N/L)	SO_4^{2-} (mg SO_4^{2-}/L)
0	6.43	0.9	1.49	13.8	< 10.0	0.18	< 2	0.37	8.9
0.25	6.48	1.6	1.61	28.5	-	-	-	-	-
0.5	6.43	0.9	1.53	29.8	< 10.0	1.94	2.5	-	8.6
0.75	6.39	1.3	1.52	22.8	-	-	-	-	-
1	-	-	-	-	-	1.91	3.8	-	7.7
1.3	6.42	1.0	1.46	17.0	-	-	-	-	-
2	6.54	0.6	1.40	15.7	< 10.0	1.87	6.6	0.65	5.7
2.7	6.38	0.6	1.36	15.1	-	-	-	-	-

3.3	6.45	0.9	1.36	10.0	-	-	-	-	-
4	6.37	0.5	1.34	10.6	< 10.0	1.99	7.8	-	3.8
5	6.62	0.5	1.35	10.6	-	-	-	-	-
6	6.95	1.3	1.32	15.1	< 10.0	2.17	10.2	0.98	3.2

Table D-21. Effluent characteristics for control vegetated column run 7. N.D.: Not detected.

Sample ID	pH	Turbidity (NTU)	Conductance (mmhos)	TP (µg P/L)	TDP (µg P/L)	NO_3^- (mg N/L)	NO_2^- (µg N/L)	TKN (mg N/L)	SO_4^{2-} (mg SO_4^{2-}/L)
0	6.17	71.7	1.66	864.3	527.8	1.57	25.2	2.52	n.d.
0.25	6.11	57.0	1.53	608.1	358.4	-	-	-	-
0.5	6.08	37.7	1.45	505.5	289.7	1.94	21.2	-	n.d.
0.75	6.11	32.3	1.41	446.9	257.3	-	-	-	-
1	-	-	-	-	-	1.89	20.4	-	n.d.
1.3	6.02	26.6	1.35	358.4	218.1	-	-	-	-
2	5.92	26.4	1.32	245.2	151.9	1.95	20.0	1.40	n.d.
2.7	6.07	24.7	1.31	200.2	110.5	-	-	-	-
3.3	6.18	19.3	1.29	151.5	95.8	-	-	-	-
4	6.05	17.2	1.29	152.6	99.9	2.00	15.5	-	n.d.
5	6	16.9	1.29	132.3	117.6	-	-	-	-
6	6.41	21.1	1.32	133.5	83.4	2.49	17.5	1.37	n.d.

Table D-22. Influent characteristics for vegetated column run 8. N.D.: Not detected.

Sample ID	pH	Turbidity (NTU)	Conductance (mmhos)	TP (µg P/L)	TDP (µg P/L)	NO_3^- (mg N/L)	NO_2^- (µg N/L)	TKN (mg N/L)	SO_4^{2-} (mg SO_4^{2-}/L)
0	5.76	0.4	1.27	111.5	-	0.69	< 2	1.31	n.d.
3	5.69	0.6	1.27	123.1	-	0.68	< 2	1.40	n.d.
6	5.72	0.4	1.28	118.6	-	0.73	< 2	1.04	n.d.

Table D-23. Effluent characteristics for experimental vegetated column run 8.

Sample ID	pH	Turbidity (NTU)	Conductance (mmhos)	TP (µg P/L)	TDP (µg P/L)	NO_3^- (mg N/L)	NO_2^- (µg N/L)	TKN (mg N/L)	SO_4^{2-} (mg SO_4^{2-}/L)
0	6.28	0.9	1.46	13.8	9.9	0.44	2.1	0.75	5.8
0.25	6.38	1.5	1.57	30.4	-	-	-	-	-
0.5	6.45	1.5	1.52	25.9	9.1	3.00	2.5	-	6.3
0.75	6.43	1.3	1.46	18.1	-	-	-	-	-
1	-	-	-	-	-	1.15	2.1	-	5.3
1.3	6.36	1.5	1.36	14.9	-	-	-	-	-
2	6.45	1.1	1.35	15.7	< 10.0	0.63	4.2	0.84	3.8
2.7	6.39	0.9	1.33	16.8	-	-	-	-	-
3.3	6.4	0.9	1.33	10.4	-	-	-	-	-
4	6.41	1.7	1.48	< 10.0	-	0.67	5.0	-	2.7
5	6.46	0.9	1.32	9.1	-	-	-	-	-
6	-	-	-	13.8	< 10.0	0.65	5.4	0.47	2.3

Table D-24. Effluent characteristics for control vegetated column run 8. N.D.: Not detected.

Sample ID	pH	Turbidity (NTU)	Conductance (mmhos)	TP (µg P/L)	TDP (µg P/L)	NO_3^- (mg N/L)	NO_2^- (µg N/L)	TKN (mg N/L)	SO_4^{2-} (mg SO_4^{2-}/L)
0	6.13	66.6	1.58	708.8	373.6	2.68	15.9	2.80	n.d.
0.25	6.04	47.2	1.5	492.4	243.7	-	-	-	-
0.5	6.15	35.2	1.44	413.8	225.6	2.09	14.3	-	n.d.
0.75	6.07	29.0	1.35	339.1	199.2	-	-	-	-
1	-	-	-	-	-	1.16	12.7	-	n.d.
1.3	5.99	25.5	1.29	199.2	84.5	-	-	-	-
2	6.06	21.7	1.28	126.4	41.9	0.77	9.8	1.07	n.d.
2.7	5.97	18.1	1.29	81.3	32.9	-	-	-	-
3.3	6.14	15.7	1.26	78.0	42.0	-	-	-	-
4	6.18	16.1	1.28	84.5	49.7	0.69	7.4	-	n.d.
5	6.13	13.1	1.27	87.7	63.2	-	-	-	-
6	-	-	-	93.1	65.6	0.69	8.2	1.10	n.d.

Table D-25. Influent characteristics for vegetated column run 9. N.D.: Not detected.

Sample ID	pH	Turbidity (NTU)	Conductance (mmhos)	TP (µg P/L)	TDP (µg P/L)	NO_3^- (mg N/L)	NO_2^- (µg N/L)	TKN (mg N/L)	SO_4^{2-} (mg SO_4^{2-}/L)
Step 1	5.92	-	-	476.3	-	3.44	-	-	n.d.
Step 2	6.06	0.5	1.35	436.8	-	3.20	< 2	3.03	n.d.
Step 3	6.05	-	-	373.4	-	2.66	-	-	n.d.
Step 4	4.55	-	-	329.3	-	2.48	-	-	n.d.
Step 5	6.28	0.9	1.35	249.9	-	1.81	< 2	2.24	n.d.
Step 6	6.23	1.1	1.36	200.5	-	1.46	< 2	1.73	n.d.

Table D-26. Effluent characteristics for experimental vegetated column run 9.

Sample ID	pH	Turbidity (NTU)	Conductance (mmhos)	TP (µg P/L)	TDP (µg P/L)	NO_3^- (mg N/L)	NO_2^- (µg N/L)	TKN (mg N/L)	SO_4^{2-} (mg SO_4^{2-}/L)
0	6.12	1.5	1.62	39.3	10.4	0.54	< 2	0.56	6.8
0.25	6.29	1.8	1.65	48.2	-	-	-	-	-
0.5	6.39	1.8	1.59	39.6	11.7	3.14	1.7	-	6.0
0.75	6.26	1.2	1.49	25.1	-	-	-	-	-
1	-	-	-	-	-	2.56	2.9	-	4.6
1.3	6.25	1.1	1.41	14.9	-	-	-	-	-
2	6.42	1.1	1.35	23.0	< 10.0	2.29	5.6	1.21	3.2
2.7	6.37	1.4	1.37	15.5	-	-	-	-	-
3.3	6.41	1.2	1.36	15.5	-	-	-	-	-
4	6.52	1.1	1.35	23.0	< 10.0	1.80	8.3	-	2.8
5	6.58	1.4	1.45	18.7	-	-	-	-	-
6	6.67	1.4	1.39	17.0	< 10.0	1.76	9.5	0.47	3.4

Table D-27. Effluent characteristics for control vegetated column run 9. N.D.: Not detected.

Sample ID	pH	Turbidity (NTU)	Conductance (mmhos)	TP (µg P/L)	TDP (µg P/L)	NO_3^- (mg N/L)	NO_2^- (µg N/L)	TKN (mg N/L)	SO_4^{2-} (mg SO_4^{2-}/L)
0	6.07	72.8	1.69	894.2	466.9	2.50	19.2	2.61	n.d.
0.25	5.93	58.6	1.56	544.8	284.5	-	-	-	-
0.5	5.96	30.3	1.42	325.0	302.4	2.65	13.4	-	n.d.
0.75	5.94	25.7	1.38	253.8	137.3	-	-	-	-
1	-	-	-	-	-	2.56	14.9	-	n.d.

1.3	6.03	33.2	1.37	150.6	77.0	-	-	-	-
2	6.01	24.0	1.31	113.2	40.3	2.25	16.1	1.49	n.d.
2.7	6.17	26.2	1.32	89.1	28.3	-	-	-	-
3.3	6.11	27.6	1.31	82.7	27.7	-	-	-	-
4	6.23	24.0	1.36	83.3	29.9	1.80	24.7	-	n.d.
5	6.06	26.7	1.34	82.1	33.5	-	-	-	-
6	6.22	25.4	1.33	98.7	41.5	1.50	36.4	0.84	n.d.

Table D-28. Influent characteristics for vegetated column run 10. N.D.: Not detected.

Sample ID	pH	Turbidity (NTU)	Conductance (mmhos)	TP (µg P/L)	TDP (µg P/L)	NO_3^- (mg N/L)	NO_2^- (µg N/L)	TKN (mg N/L)	SO_4^{2-} (mg SO_4^{2-}/L)
0	6.04	0.8	1.23	70.6	-	0.51	< 2	0.75	n.d.
3	5.96	-	1.23	66.6	-	0.51	< 2	0.84	n.d.
6	5.92	0.6	1.28	68.0	-	0.54	< 2	0.84	n.d.

Table D-29. Effluent characteristics for experimental vegetated column run 10.

Sample ID	pH	Turbidity (NTU)	Conductance (mmhos)	TP (µg P/L)	TDP (µg P/L)	NO_3^- (mg N/L)	NO_2^- (µg N/L)	TKN (mg N/L)	SO_4^{2-} (mg SO_4^{2-}/L)	SRP (µg P/L)
0	6.31	2.0	1.41	14.7	< 10.0	0.32	< 2	0.37	4.5	< 10.0
0.25	6.28	1.6	1.40	33.2	-	-	-	-	-	-
0.5	6.4	0.9	1.38	29.8	< 10.0	1.93	< 2	-	4.1	< 10.0
0.75	6.29	1.6	1.35	28.7	-	-	-	-	-	-
1	-	-	-	-	-	1.22	< 2	-	3.6	-

1.3	6.34	-	1.31	20.3	-	-	-	-	-	-
2	6.32	0.7	1.31	16.0	< 10.0	0.60	< 2	0.37	2.9	< 10.0
2.7	6.35	0.8	1.29	14.5	-	-	-	-	-	-
3.3	6.27	0.9	1.27	11.9	-	-	-	-	-	-
4	6.3	0.6	1.29	12.0	< 10.0	0.45	< 2	-	2.0	< 10.0
5	6.31	1.5	1.28	9.4	-	-	-	-	-	-
6	6.49	0.8	1.32	13.3	< 10.0	0.40	< 2	0.37	1.9	< 10.0

Table D-30. Effluent characteristics for control vegetated column run 10. N.D.: Not detected.

Sample ID	pH	Turbidity (NTU)	Conductance (mmhos)	TP (µg P/L)	TDP (µg P/L)	NO_3^- (mg N/L)	NO_2^- (µg N/L)	TKN (mg N/L)	SO_4^{2-} (mg SO_4^{2-}/L)	SRP (µg P/L)
0	6.05	63.1	1.53	1228.1	790.3	3.65	17.1	2.43	n.d.	782.1
0.25	6.02	50.0	1.38	680.9	338.8	-	-	-	-	-
0.5	6.03	39.9	1.33	589.8	306.6	1.92	17.5	-	n.d.	307.9
0.75	6.12	30.4	1.3	400.9	280.1	-	-	-	-	-
1	-	-	-	-	-	1.47	18.4	-	n.d.	-
1.3	6.03	-	1.27	326.0	212.8	-	-	-	-	-
2	6.06	21.3	1.23	234.4	146.5	0.65	15.1	0.65	n.d.	141.1
2.7	5.93	20.6	1.23	161.9	100.1	-	-	-	-	-
3.3	6.05	18.0	1.23	127.2	74.4	-	-	-	-	-
4	5.9	15.6	1.27	104.8	56.4	0.49	9.4	-	n.d.	52.0
5	5.97	17.7	1.28	83.4	51.9	-	-	-	-	-
6	5.83	14.4	1.29	89.0	33.8	0.43	13.5	0.56	n.d.	29.5

Table D-31. Influent characteristics for vegetated column run 11. N.D.: Not detected.

Sample ID	pH	Turbidity (NTU)	Conductance (mmhos)	TP (µg P/L)	TDP (µg P/L)	NO_3^- (mg N/L)	NO_2^- (µg N/L)	TKN (mg N/L)	SO_4^{2-} (mg SO_4^{2-}/L)
0	5.21	0.3	1.28	113.1	-	1.90	< 2	1.03	n.d.
3	6.15	0.4	1.28	114.5	-	0.92	< 2	1.03	n.d.

Table D-32. Effluent characteristics for experimental vegetated column run 11.

Sample ID	pH	Turbidity (NTU)	Conductance (mmhos)	TP (µg P/L)	TDP (µg P/L)	NO_3^- (mg N/L)	NO_2^- (µg N/L)	TKN (mg N/L)	SO_4^{2-} (mg SO_4^{2-}/L)
0	6.15	1.4	1.49	23.7	< 10.0	0.24	< 2	0.33	4.0
0.25	6.14	1.0	1.48	24.3	-	-	-	-	-
0.5	6.27	1.2	1.45	25.0	< 10.0	1.06	< 2	-	3.5
0.75	-	-	-	-	-	1.01	< 2	-	3.4
1	6.11	0.8	1.38	14.9	-	-	-	-	-
1.3	6.21	0.6	1.36	12.9	-	-	-	-	-
2	6.3	0.9	1.34	13.6	< 10.0	0.86	< 2	-	2.5
3	6.37	1.4	1.35	12.2	< 10.0	0.72	< 2	0.33	2.4

Table D-33. Effluent characteristics for control vegetated column run 11. N.D.: Not detected.

Sample ID	pH	Turbidity (NTU)	Conductance (mmhos)	TP (µg P/L)	TDP (µg P/L)	NO_3^- (mg N/L)	NO_2^- (µg N/L)	TKN (mg N/L)	SO_4^{2-} (mg SO_4^{2-}/L)
0	6.01	89.3	1.55	2108.4	890.1	0.91	21.2	2.05	n.d.
0.25	5.89	65.1	1.44	843.4	453.7	-	-	-	-
0.5	5.9	49.6	1.38	665.7	475.5	0.84	18.4	-	n.d.
0.75	-	-	-	-	-	0.76	18.4	-	n.d.

1	5.9	38.6	1.32	491.1	310.3	-	-	-	-
1.3	5.83	32.0	1.3	416.3	238.6	-	-	-	-
2	5.91	23.8	1.3	307.2	257.3	0.90	17.5	-	n.d.
3	6.27	24.7	1.28	238.6	294.7	0.67	35.7	0.75	n.d.

Table D-34. Influent characteristics for vegetated column run 12. N.D.: Not detected.

Sample ID	pH	Turbidity (NTU)	Conductance (mmhos)	TP (µg P/L)	TDP (µg P/L)	NO_3^- (mg N/L)	NO_2^- (µg N/L)	TKN (mg N/L)	SO_4^{2-} (mg SO_4^{2-}/L)
0	5.42	0.6	1.28	122.8	-	0.74	< 2	1.12	n.d.
3	6.18	0.4	1.33	120.8	-	0.92	< 2		n.d.

Table D-35. Effluent characteristics for experimental vegetated column run 12.

Sample ID	pH	Turbidity (NTU)	Conductance (mmhos)	TP (µg P/L)	TDP (µg P/L)	NO_3^- (mg N/L)	NO_2^- (µg N/L)	TKN (mg N/L)	SO_4^{2-} (mg SO_4^{2-}/L)
0	6.09	1.4	1.38	14.7	< 10.0	0.10	< 2	0.37	3.3
0.25	6.06	0.8	1.42	18.0	-	-	-	-	-
0.5	6.13	0.7	1.39	16.0	< 10.0	0.99	< 2	-	2.7
0.75	6.14	0.9	1.39	12.7	-	-	-	-	-
1	-	-	-	-	-	0.80	< 2	-	2.6
1.3	6.11	0.4	1.36	< 10.0	-	-	-	-	-
2	6.14	0.6	1.35	< 10.0	< 10.0	0.65	< 2	-	2.2
3	6.39	0.5	1.36	< 10.0	< 10.0	0.60	< 2	0.28	2.0

Table D-36. Effluent characteristics for control vegetated column run 12. N.D.: Not detected.

Sample ID	pH	Turbidity (NTU)	Conductance (mmhos)	TP (µg P/L)	TDP (µg P/L)	NO_3^- (mg N/L)	NO_2^- (µg N/L)	TKN (mg N/L)	SO_4^{2-} (mg SO_4^{2-}/L)
0	5.94	96.3	1.44	1130.5	591.0	1.02	14.3	1.68	n.d.
0.25	6.04	65.0	1.45	683.6	387.4	-	-	-	-
0.5	6.18	51.2	1.39	560.2	347.3	1.05	18.8	-	n.d.
0.75	6.18	40.4	1.34	470.7	313.4	-	-	-	-
1	-	-	-	-	-	0.75	18.8	-	2.8
1.3	6.16	29.4	1.31	313.4	214.9	-	-	-	-
2	6.13	24.8	1.3	216.3	144.0	0.69	16.7	-	0.2
3	6.24	23.0	1.34	149.3	83.0	0.55	28.6	0.84	n.d.

Table D-37. Influent characteristics for vegetated column run 13. N.D.: Not detected.

Sample ID	pH	Turbidity (NTU)	Conductance (mmhos)	TP (µg P/L)	TDP (µg P/L)	NO_3^- (mg N/L)	NO_2^- (µg N/L)	TKN (mg N/L)	SO_4^{2-} (mg SO_4^{2-}/L)
0	6.36	0.3	1.31	123.8	-	0.69	< 2	1.03	n.d.
3	6.14	0.4	1.30	121.8	-	0.69	< 2	0.98	n.d.
6	6.12	0.5	1.33	120.4	-	0.73	< 2	1.12	n.d.

Table D-35. Effluent characteristics for experimental vegetated column run 12.

Sample ID	pH	Turbidity (NTU)	Conductance (mmhos)	TP (µg P/L)	TDP (µg P/L)	NO_3^- (mg N/L)	NO_2^- (µg N/L)	TKN (mg N/L)	SO_4^{2-} (mg SO_4^{2-}/L)
0	6.14	1.4	1.49	22.7	-	0.18	< 2	0.56	3.4
0.25	6.17	1.0	1.44	25.3	-	-	-	-	-
0.5	6.21	1.0	1.45	20.7	-	1.13	< 2	-	2.9
0.75	6.15	0.7	1.43	17.9	-	-	-	-	-
1	-	-	-	-	-	0.79	< 2	-	2.7
1.3	6.14	0.6	1.38	11.8	-	-	-	-	-
2	6.19	0.5	1.35	14.0	< 10.0	0.71	< 2	0.19	2.2
2.7	6.14	0.5	1.34	< 10.0	-	-	-	-	-
3.3	6.09	0.4	1.35	< 10.0	-	-	-	-	-
4	6.15	0.5	1.35	< 10.0	< 10.0	0.72	< 2	-	1.5
5	6.26	0.6	1.35	< 10.0	-	-	-	-	-
6	6.37	0.7	1.37	< 10.0	< 10.0	0.69	< 2	0.23	1.5

Table D-39. Effluent characteristics for control vegetated column run 13. N.D.: Not detected.

Sample ID	pH	Turbidity (NTU)	Conductance (mmhos)	TP (µg P/L)	TDP (µg P/L)	NO_3^- (mg N/L)	NO_2^- (µg N/L)	TKN (mg N/L)	SO_4^{2-} (mg SO_4^{2-}/L)
0	5.97	97.0	1.57	1169.4	685.9	0.98	20.0	2.15	0.2
0.25	5.92	60.4	1.49	809.8	391.5	-	-	-	-
0.5	5.9	50.2	1.42	645.7	374.8	0.74	21.9	-	0.5
0.75	5.92	41.8	1.39	572.5	278.1	-	-	-	-
1	-	-	-	-	-	0.75	23.1	-	0.2
1.3	5.96	31.6	1.35	409.5	197.4	-	-	-	-

2	5.91	29.8	1.32	294.4	133.2	0.64	20.4	0.65	0.4
2.7	5.99	25.4	1.32	218.3	101.3	-	-	-	-
3.3	5.96	20.7	1.31	169.2	74.4	-	-	-	-
4	5.83	21.0	1.32	139.9	53.5	0.73	14.6		n.d.
5	5.75	19.1	1.33	100.6	39.4	-	-	-	-
6	6.26	15.7	1.37	76.9	29.4	0.77	20.8	0.51	0.3

Appendix E: Media Oxalate Extraction Data

Table E-1. Oxalate extractions for batch media and media components. Mass is sample mass adjusted for water content.

Id	Mass (g)	Volume (mL)	P Concentration (mg/L)	P_{ox} (mg/kg)	P_{ox} (mmol/kg)	Fe Concentration (mg/L)	Fe_{ox} (mg/kg)	Fe_{ox} (mmol/kg)	Al Concentration (mg/L)	Al_{ox} (mg/kg)	Al_{ox} (mmol/kg)	PSI (%)	Oxalate Ratio
OX-BSM1	1.000	40	0.152	118.8	3.83	20.9	830.2	14.9	6.60	264.1	9.79	15.6	6.43
OX-BSM2	1.000	40	0.110	84.7	2.74	21.1	836.8	15.0	6.97	278.8	10.3	10.8	9.25
OX-BSM3	0.996	40	0.218	171.8	5.55	23.7	945.8	16.9	7.84	314.8	11.7	19.4	5.16
OX-WTR1	0.232	40	0.575	1970.7	63.6	22.1	3784.7	67.8	853.9	147,264.5	5458.3	1.15	86.8
OX-WTR2	0.231	40	0.534	1836.9	59.3	21.9	3765.4	67.4	891.8	154,566.0	5728.9	1.02	97.7
OX-WTR3	0.231	40	0.470	1613.7	52.1	20.2	3463.8	62.0	827.2	143,013.8	5300.7	0.97	102.9
WTR1	0.394	40	1.421	2880.8	93.0	27.2	2747.1	49.2	1596.0	161,969.0	6003.3	1.54	65.1
WTR2	0.395	40	1.380	2795.4	90.3	26.5	2678.9	48.0	1606.0	162,845.8	6035.8	1.48	67.4
WTR3	0.394	40	1.264	2564.6	82.8	23.2	2343.9	42.0	1585.5	161,081.6	5970.4	1.38	72.6
WTR4	0.396	40	1.305	2635.2	85.1	23.8	2396.0	42.9	1571.0	158,854.6	5887.9	1.43	69.7
WTR5	0.395	40	1.305	2642.4	85.3	22.2	2242.9	40.2	1585.5	160,756.1	5958.3	1.42	70.3
WTR6	0.395	40	1.247	2521.6	81.4	23.4	2359.3	42.2	1477.5	149,639.5	5546.3	1.46	68.6
WTR7	0.395	40	1.264	2554.2	82.5	22.1	2225.7	39.9	1428.0	144,501.0	5355.9	1.53	65.4

WTR8	0.394	40	1.443	2926.9	94.5	23.9	2419.3	43.3	1566.5	159,105.1	5897.1	1.59	62.9
HBM1-1	1.000	40	0.161	125.0	4.03	93.3	3730.0	66.8	10.0	399.8	14.8	4.94	20.2
HBM1-2	1.003	40	0.154	119.4	3.86	91.8	3661.0	65.6	10.0	398.8	14.8	4.80	20.8
HBM1-3	0.956	40	0.134	108.2	3.50	87.8	3671.5	65.7	9.07	379.6	14.1	4.38	22.8
HBM2-1	0.836	40	0.106	101.1	3.27	67.2	3213.0	57.5	7.56	361.9	13.4	4.60	21.7
HBM3-1	0.998	40	0.155	120.5	3.89	59.6	2386.8	42.7	7.63	305.8	11.3	7.19	13.9
HBM3-2	1.004	40	0.159	122.8	3.97	58.8	2342.6	41.9	7.00	279.0	10.3	7.58	13.2
HBM3-3	1.005	40	0.149	114.5	3.70	57.1	2270.6	40.7	6.91	275.0	10.2	7.27	13.8
LC-1	0.995	40	0.588	469.0	15.1	58.9	2365.8	42.4	9.14	367.5	13.6	27.0	3.70
LC-2	1.005	40	0.616	486.5	15.7	50.8	2019.9	36.2	8.99	357.7	13.3	31.8	3.15
LC-3	0.977	40	0.639	519.8	16.8	54.3	2221.1	39.8	9.35	382.6	14.2	31.1	3.21
2% BSM	0.990	40	0.201	159.5	5.15	21.1	846.6	15.2	32.4	1306.6	48.4	8.10	12.3
4% BSM	0.975	40	0.242	195.1	6.30	23.6	961.6	17.2	61.1	2506.5	92.9	5.72	17.5
10% BSM	0.954	40	0.276	228.7	7.39	29.6	1233.3	22.1	254.7	10682.2	395.9	1.77	56.6
LFBSM	1.003	40	0.069	53.8	1.74	12.5	494.6	8.86	3.80	151.5	5.62	12.0	8.33
3% LFBSM	0.992	40	0.099	79.0	2.55	16.0	643.6	11.5	44.7	1799.8	66.7	3.26	30.7
6% LFBSM	0.972	40	0.126	102.9	3.32	15.2	622.8	11.2	126.5	5207.4	193.0	1.63	61.4
10% LFBSM	0.957	40	0.172	142.4	4.60	20.1	839.6	15.0	218.0	9115.2	337.9	1.30	76.7
BSM+HBM	0.983	40	0.147	119.3	3.85	23.9	970.7	17.4	6.20	252.2	9.35	14.4	6.94
2% HBM	1.003	40	0.268	213.1	6.88	32.0	1275.4	22.8	37.1	1477.6	54.8	8.87	11.3
4% HBM	0.972	40	0.198	159.8	5.16	21.1	859.4	15.4	77.3	3178.1	117.8	3.87	25.8
BSM+LC	1.003	40	0.215	170.9	5.52	26.0	1035.1	18.5	7.96	317.5	11.8	18.2	5.49
4% LC	1.003	40	0.218	173.2	5.59	13.6	538.6	9.64	42.3	1687.7	62.6	7.74	12.9
4% LC [OM+]	1.003	40	0.343	272.3	8.79	31.3	1244.0	22.3	36.1	1439.7	53.4	11.6	8.60
4% AH	0.990	40	0.253	203.2	6.56	27.9	1123.7	20.1	66.2	2676.2	99.2	5.50	18.2

Table E-2. Oxalate extractions for fresh minicolumn media. Mass is sample mass adjusted for water content.

Id	Mass (g)	Vol. (mL)	Concentration (mg/L)	P_{ox} (mg/kg)	P_{ox} (mmol/kg)	Fe Concentration (mg/L)	Fe_{ox} (mg/kg)	Fe_{ox} (mmol/kg)	Al Concentration (mg/L)	Al_{ox} (mg/kg)	Al_{ox} (mmol/kg)	PSI (%)	Oxalate Ratio
Set I													
BSM-1	0.995	40	0.123	96.1	3.10	18.4	732.1	13.1	7.14	287.0	10.6	13.1	7.65
BSM-2	1.002	40	0.175	137.3	4.43	18.7	740.7	13.3	8.80	351.3	13.0	16.9	5.93
BSM-3	0.998	40	0.178	140.3	4.53	22.1	880.2	15.8	8.97	359.2	13.3	15.6	6.42
2% WTR-1	1.003	40	0.247	195.5	6.31	23.4	933.2	16.7	60.1	2398.0	88.9	5.98	16.7
2% WTR-2	1.001	40	0.220	174.4	5.63	22.6	902.0	16.2	71.5	2858.9	106.0	4.61	21.7
2% WTR-3	1.005	40	0.259	204.7	6.61	28.4	1130.8	20.2	54.4	2163.7	80.2	6.58	15.2
4% WTR-1	0.998	40	0.248	197.1	6.36	23.0	919.9	16.5	124.1	4971.0	184.2	3.17	31.5
4% WTR-2	1.000	40	0.225	178.3	5.76	23.0	917.6	16.4	125.0	4998.6	185.3	2.85	35.0
4% WTR-3	1.006	40	0.269	212.6	6.87	24.0	955.0	17.1	118.7	4716.2	174.8	3.58	28.0
2% HBM-1	1.004	40	0.230	182.0	5.88	21.4	850.8	15.2	71.7	2856.5	105.9	4.85	20.6
2% HBM-2	1.004	40	0.181	142.3	4.59	25.2	1005.2	18.0	96.3	3835.5	142.2	2.87	34.9
2% HBM-3	1.004	40	0.183	144.0	4.65	20.3	807.9	14.5	73.1	2913.0	108.0	3.80	26.3
4% HBM-1	1.008	40	0.237	185.6	5.99	27.4	1079.1	19.3	150.4	5967.3	221.2	2.49	40.1
4% HBM-2	1.004	40	0.274	216.1	6.98	28.6	1132.1	20.3	148.3	5912.6	219.1	2.91	34.3
4% HBM-3	1.004	40	0.193	151.6	4.89	26.1	1034.4	18.5	142.7	5686.7	210.8	2.13	46.9
4% LFBSM-1	1.000	40	0.176	139.4	4.50	15.9	635.8	11.4	89.6	3584.5	132.9	3.12	32.0
4% LFBSM-2	1.002	40	0.196	155.0	5.00	15.8	630.8	11.3	105.6	4215.3	156.2	2.99	33.5
4% LFBSM-3	1.003	40	0.199	157.4	5.08	15.3	608.3	10.9	130.9	5219.3	193.5	2.49	40.2
Set II													
BSM-1	0.998	40	0.178	141.5	4.57	14.4	573.3	10.3	9.62	385.4	14.3	18.6	5.37
BSM-2	0.998	40	0.151	119.7	3.87	10.9	432.1	7.74	8.76	351.2	13.0	18.6	5.37
BSM-3	1.004	40	0.155	122.8	3.96	7.9	310.0	5.55	8.58	341.8	12.7	21.8	4.60

4% WTR-1	1.000	40	0.385	303.3	9.79	31.2	1242.9	22.3	120.9	2321.7	86.1	9.04	11.1
4% WTR-2	1.002	40	0.276	215.9	6.97	26.7	1063.1	19.0	153.7	2946.9	109.2	5.44	18.4
4% WTR-3	1.002	40	0.258	201.3	6.50	25.2	1003.1	18.0	151.3	2900.6	107.5	5.18	19.3
4% Sand-1	1.009	40	0.092	68.5	2.21	2.7	104.9	1.88	141.2	5595.1	207.4	1.06	94.6
4% Sand-2	0.990	40	0.136	104.8	3.38	4.0	158.5	2.84	194.0	7834.1	290.4	1.15	86.7
4% Sand-3	0.998	40	0.062	45.1	1.46	2.4	91.5	1.64	112.7	4514.9	167.3	0.863	116
4% HBM-1 (Int.)	1.007	40	0.228	177.3	5.73	18.5	725.9	13.0	113.6	4511.4	167.2	3.18	31.5
4% HBM-2 (Int.)	1.009	40	0.270	210.5	6.80	19.0	743.1	13.3	143.9	5704.6	211.4	3.02	33.1
4% HBM-3 (Int.)	1.010	40	0.205	158.7	5.12	17.1	667.4	12.0	116.1	4598.3	170.4	2.81	35.6
4% WTR-1 (Int.)	1.007	40	0.272	211.2	6.82	22.0	870.6	15.6	143.1	5681.1	210.6	3.02	33.2
4% WTR-2 (Int.)	1.015	40	0.481	374.3	12.1	32.8	1287.8	23.1	178.8	7043.7	261.1	4.25	23.5
4% WTR-3 (Int.)	1.012	40	0.351	272.7	8.81	26.3	1033.7	18.5	145.4	5744.3	212.9	3.81	26.3
4% LFBSM-1 (Int.)	1.007	40	0.154	118.0	3.81	15.2	599.1	10.7	141.3	5615.1	208.1	1.74	57.4
4% LFBSM-2 (Int.)	0.996	40	0.207	161.4	5.21	15.7	627.7	11.2	147.5	5922.7	219.5	2.26	44.3
4% LFBSM-3 (Int.)	1.006	40	0.269	209.5	6.76	21.1	836.3	15.0	153.9	6119.2	226.8	2.80	35.7

Table E-3. Oxalate extractions for minicolumn media post adsorption experiments. Mass is sample mass adjusted for water content.

Id	Mass (g)	Vol. (mL)	Concentration (mg/L)	P_{ox} (mg/kg)	P_{ox} (mmol/kg)	Fe Concentration (mg/L)	Fe_{ox} (mg/kg)	Fe_{ox} (mmol/kg)	Al Concentration (mg/L)	Al_{ox} (mg/kg)	Al_{ox} (mmol/kg)	PSI (%)	Oxalate Ratio
						Set I							
BSM-1	1.085	40	0.163	116.9	3.77	23.4	859.2	15.4	7.36	271.2	10.1	14.8	6.74
BSM-2	1.008	40	0.174	134.5	4.34	21.1	834.4	14.9	7.27	288.4	10.7	16.9	5.90
BSM-3	1.010	40	0.192	148.5	4.80	20.7	819.0	14.7	7.30	289.4	10.7	18.9	5.29
2% WTR-1	1.027	40	0.229	177.4	5.73	18.7	726.3	13.0	47.3	1842.1	68.3	7.05	14.2
2% WTR-2	1.002	40	0.197	156.2	5.04	17.3	689.6	12.3	47.1	1880.2	69.7	6.15	16.3
2% WTR-3	0.990	40	0.222	178.2	5.75	17.9	723.5	13.0	49.7	2005.6	74.3	6.59	15.2

4% WTR-1	0.995	40	0.242	193.0	6.23	16.2	650.7	11.7	77.6	3117.8	115.6	4.90	20.4
4% WTR-2	1.005	40	0.282	223.4	7.21	19.4	771.0	13.8	84.9	3379.4	125.3	5.19	19.3
4% WTR-3	1.002	40	0.268	212.8	6.87	18.4	735.1	13.2	90.8	3622.5	134.3	4.66	21.5
2% HBM-1	1.004	40	0.265	208.1	6.72	19.3	767.8	13.7	74.9	2983.8	110.6	5.40	18.5
2% HBM-2	1.005	40	0.320	250.9	8.10	25.0	991.2	17.7	68.1	2709.7	100.4	6.85	14.6
2% HBM-3	1.001	40	0.236	185.1	5.98	20.7	826.1	14.8	58.6	2343.7	86.9	5.88	17.0
4% HBM-1	1.029	40	0.338	260.0	8.40	24.6	951.1	17.0	117.2	4554.6	168.8	4.52	22.1
4% HBM-2	1.027	40	0.217	166.5	5.37	23.8	918.4	16.4	139.8	5444.1	201.8	2.46	40.6
4% HBM-3	1.022	40	0.230	177.7	5.74	26.3	1020.9	18.3	149.4	5849.9	216.8	2.44	41.0
4% LFBSM-1	1.019	40	0.429	335.6	10.8	22.1	867.4	15.5	135.4	5315.5	197.0	5.10	19.6
4% LFBSM-2	1.005	40	0.389	308.6	9.96	21.2	844.6	15.1	108.4	4315.5	160.0	5.69	17.6
4% LFBSM-3	0.997	40	0.394	314.9	10.2	18.1	726.3	13.0	147.1	5898.3	218.6	4.39	22.8
						Set II							
BSM-1	1.005	40	0.148	114.3	3.69	16.5	649.3	11.6	6.43	255.9	9.49	17.5	5.72
BSM-2	1.005	40	0.153	118.0	3.81	16.1	632.2	11.3	7.32	291.3	10.8	17.2	5.80
BSM-3	0.997	40	0.127	98.5	3.18	14.3	563.2	10.1	4.14	166.2	6.16	19.6	5.11
4% WTR-1	0.998	40	0.297	234.6	7.58	18.5	732.7	13.1	111.2	4455.9	165.2	4.25	23.5
4% WTR-2	1.008	40	0.374	293.4	9.48	19.2	751.2	13.5	104.9	4160.9	154.2	5.65	17.7
4% WTR-3	1.003	40	0.343	269.8	8.71	17.3	682.6	12.2	116.0	4625.6	171.4	4.74	21.1
4% Sand-1	1.000	40	0.223	174.9	5.65	1.6	56.0	1.0	102.5	4099.7	152.0	3.69	27.1
4% Sand-2	1.005	40	0.211	164.0	5.30	1.7	59.2	1.1	96.5	3843.1	142.4	3.69	27.1
4% Sand-3	0.996	40	0.201	158.0	5.10	1.7	58.3	1.0	100.9	4052.0	150.2	3.37	29.6
4% HBM-1 (Int.)	1.001	40	0.410	322.9	10.4	26.1	1037.2	18.6	142.5	5695.1	211.1	4.54	22.0
4% HBM-2 (Int.)	0.999	40	0.351	276.2	8.92	25.5	1017.2	18.2	110.6	4428.1	164.1	4.89	20.4
4% HBM-3 (Int.)	1.005	40	0.276	215.0	6.94	22.6	897.7	16.1	109.4	4352.9	161.3	3.91	25.6
4% WTR-1 (Int.)	1.003	40	0.283	223.8	7.23	18.4	729.2	13.1	153.4	6116.2	226.7	3.01	33.2

4% WTR-2 (Int.)	0.996	40	0.249	197.7	6.38	19.0	758.0	13.6	123.5	4963.4	184.0	3.23	30.9
4% WTR-3 (Int.)	0.996	40	0.254	202.0	6.52	19.1	762.5	13.7	130.5	5239.1	194.2	3.14	31.9
4% LFBSM-1 (Int.)	0.994	40	0.301	237.6	7.67	18.4	737.3	13.2	122.5	4928.6	182.7	3.92	25.5
4% LFBSM-2 (Int.)	0.992	40	0.304	240.2	7.75	16.6	666.5	11.9	129.2	5209.6	193.1	3.78	26.4
4% LFBSM-3 (Int.)	0.999	40	0.263	205.7	6.64	16.4	651.2	11.7	115.2	4611.6	170.9	3.64	27.5

Table E-4. Oxalate extractions for vegetated column media both unused and post-adsorption at various depths. Mass is sample mass adjusted for water content.

	Id	Mass (g)	Vol. (mL)	Concentration (mg/L)	P_{ox} (mg/kg)	P_{ox} (mmol/kg)	Fe Concentration (mg/L)	Fe_{ox} (mg/kg)	Fe_{ox} (mmol/kg)	Al Concentration (mg/L)	Al_{ox} (mg/kg)	Al_{ox} (mmol/kg)	PSI (%)	Oxalate Ratio
Control Column	(0-2 cm)-1	0.997	40	84.0	67.2	2.71	1.03	41.5	0.743	5.22	209.2	7.75	31.9	3.13
	(0-2 cm)-2	1.001	40	94.9	75.7	3.07	1.26	50.1	0.898	3.74	149.4	5.54	47.6	2.10
	(0-2 cm)-3	1.001	40	91.0	72.6	2.94	1.46	58.5	1.05	6.08	243.2	9.01	29.2	3.42
	(11-12 cm)-1	0.997	40	113.3	90.7	3.66	1.51	60.4	1.08	5.42	217.3	8.06	40.0	2.50
	(11-12 cm)-2	0.998	40	186.5	149.4	6.02	2.10	84.0	1.50	7.56	303.2	11.2	47.3	2.12
	(11-12 cm)-3	1.004	40	159.6	127.0	5.15	1.88	75.1	1.34	7.61	303.0	11.2	41.0	2.44
	(21-22 cm)-1	1.002	40	200.9	160.2	6.49	2.42	96.8	1.73	8.46	337.6	12.5	45.5	2.20
	(21-22 cm)-2	1.008	40	145.0	114.9	4.68	1.90	75.2	1.35	7.18	285.0	10.6	39.3	2.54
	(21-22 cm)-3	0.997	40	184.1	147.5	5.94	2.34	93.8	1.68	8.16	327.3	12.1	43.0	2.32
	(43-44 cm)-1	1.004	40	145.6	115.8	4.70	1.81	72.0	1.29	7.68	305.8	11.3	37.3	2.68
	(43-44 cm)-2	1.001	40	122.5	97.7	3.95	1.71	68.4	1.23	7.20	287.7	10.7	33.3	3.01
	(43-44 cm)-3	1.013	40	147.4	116.2	4.76	1.89	74.4	1.33	7.49	295.8	11.0	38.7	2.58
	Unused-1	1.011	40	163.3	129.0	5.27	2.02	79.8	1.43	7.01	277.2	10.3	45.1	2.22

	Unused-2	1.003	40	109.8	87.4	3.55	1.48	59.0	1.06	6.19	246.9	9.15	34.7	2.88
	Unused-3	1.002	40	116.8	93.1	3.77	1.80	71.9	1.29	6.61	264.1	9.79	34.0	2.94
Experimental Column	(0-2 cm)-1	1.002	40	449.2	358.3	14.5	2.27	90.5	1.62	137.3	5478.0	203.0	7.09	14.1
	(0-2 cm)-2	1.001	40	373.4	298.3	12.1	2.08	83.0	1.49	127.0	5074.2	188.1	6.36	15.7
	(0-2 cm)-3	0.997	40	425.2	340.9	13.7	2.13	85.6	1.53	126.5	5074.9	188.1	7.24	13.8
	(11-12 cm)-1	1.000	40	259.2	207.2	8.37	1.98	79.1	1.42	132.3	5291.5	196.1	4.24	23.6
	(11-12 cm)-2	1.001	40	287.1	229.3	9.27	2.24	89.4	1.60	140.0	5593.1	207.3	4.44	22.5
	(11-12 cm)-3	1.023	40	381.5	298.0	12.3	2.50	97.7	1.75	118.0	4611.7	170.9	7.13	14.0
	(21-22 cm)-1	0.994	40	256.6	206.3	8.28	1.79	72.0	1.29	104.8	4216.5	156.3	5.26	19.0
	(21-22 cm)-2	1.009	40	268.8	212.9	8.68	2.03	80.5	1.44	104.9	4158.6	154.1	5.58	17.9
	(21-22 cm)-3	0.999	40	235.6	188.4	7.61	2.20	88.1	1.58	118.1	4728.2	175.2	4.30	23.2
	(43-44 cm)-1	1.006	40	239.1	190.0	7.72	2.09	83.2	1.49	122.2	4859.3	180.1	4.25	23.5
	(43-44 cm)-2	0.997	40	263.1	210.9	8.50	1.89	75.7	1.36	111.7	4482.8	166.2	5.07	19.7
	(43-44 cm)-3	1.001	40	240.0	191.6	7.75	1.93	77.1	1.38	133.0	5311.7	196.9	3.91	25.6
	Unused-1	1.006	40	282.8	224.7	9.13	1.99	79.2	1.42	131.7	5236.3	194.1	4.67	21.4
	Unused-2	1.006	40	235.6	187.2	7.61	1.75	69.6	1.25	120.8	4804.0	178.1	4.24	23.6
	Unused-3	1.010	40	213.8	169.2	6.90	1.75	69.1	1.24	115.0	4557.4	168.9	4.06	24.7

Appendix F: Electron Microscope Media Images

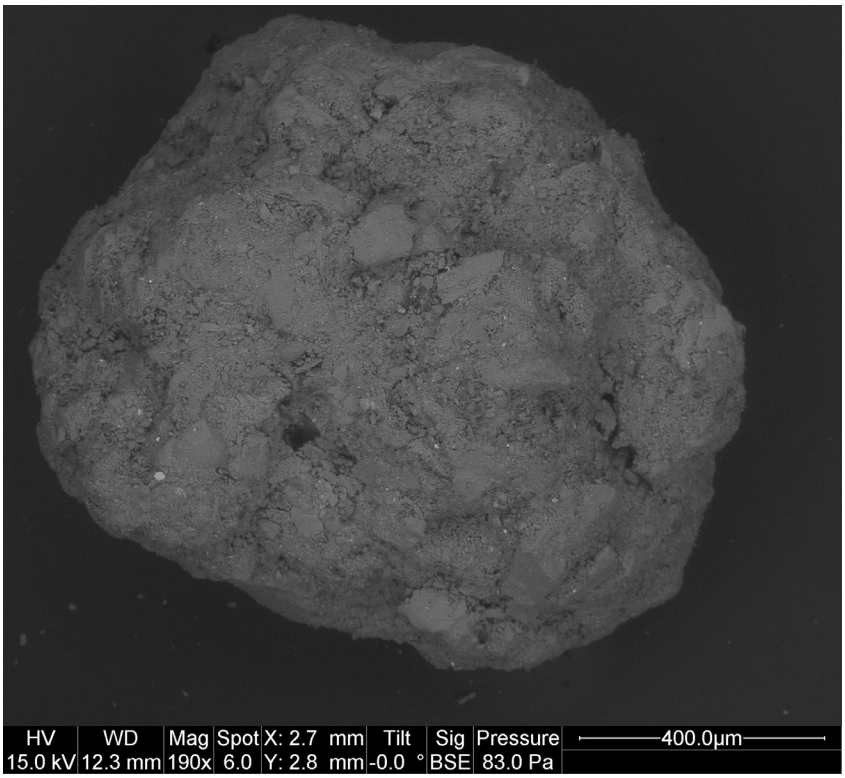

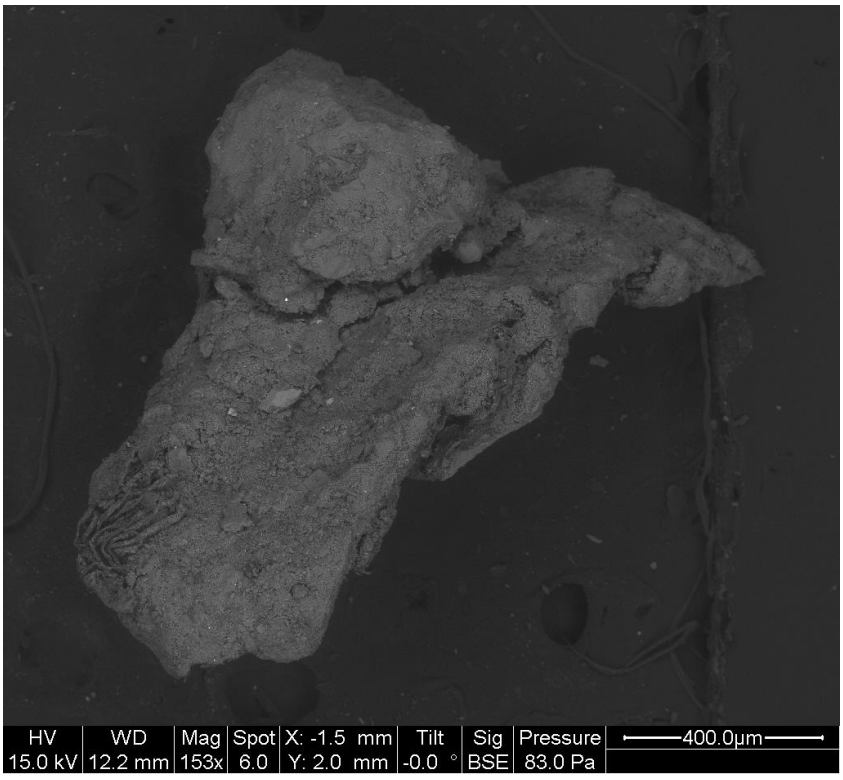

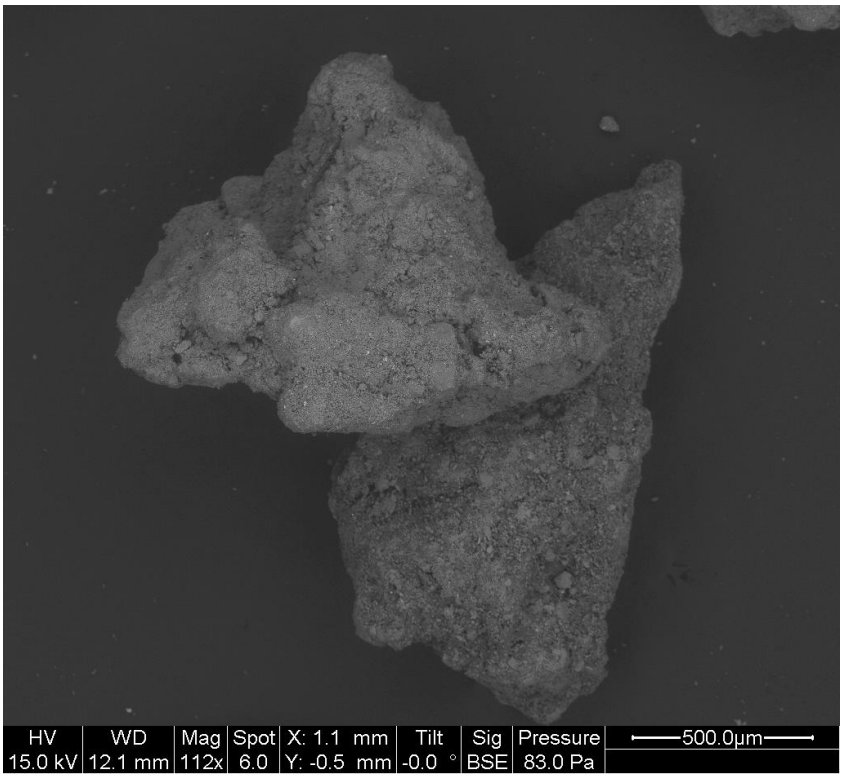
HV
15.0 kV
WD
12.1 mm
Mag
112x
Spot
6.0
X: 1.1 mm
Y: -0.5 mm
Tilt
-0.0 °
Sig
BSE
Pressure
83.0 Pa
500.0µm

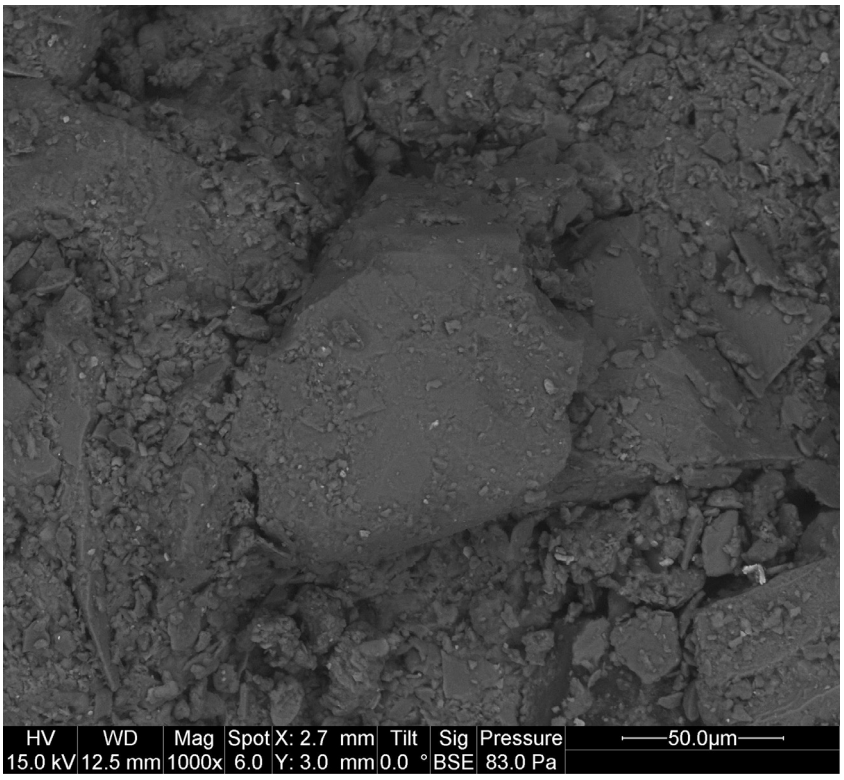
HV
15.0 kV
WD
12.5 mm
Mag
1000x
Spot
6.0
X: 2.7 mm
Y: 3.0 mm
Tilt
0.0 °
Sig
BSE
Pressure
83.0 Pa
50.0µm

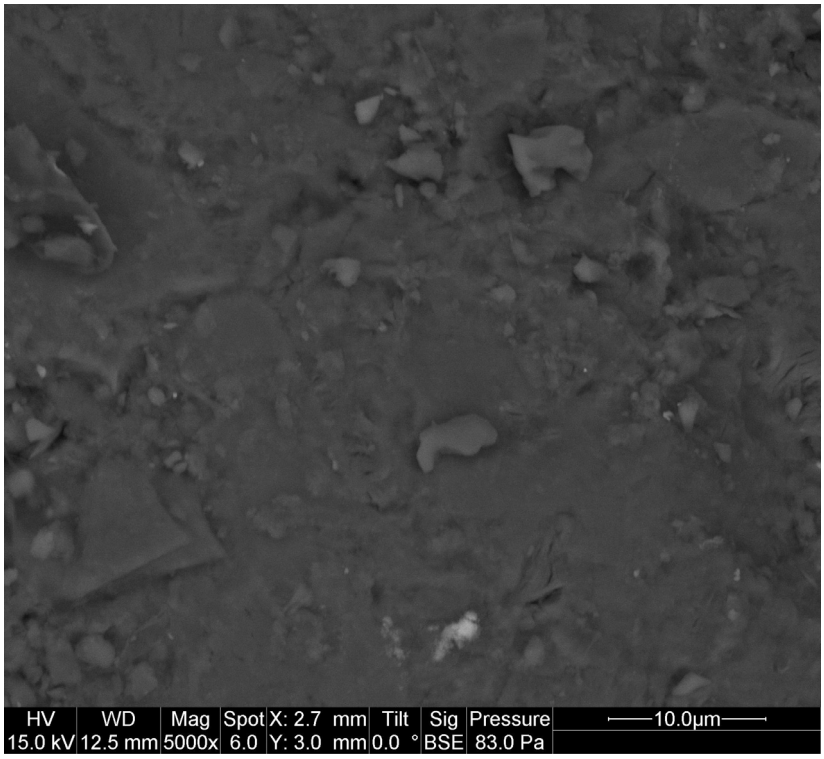

Figure F-1. Electron microscope images (6 frames) of BSM grains from an unused, "fresh" BSM + 4% WTR + HBM mixture. Media was dried at 103°C for 2 hours and sieved to between 300 and 590 µm prior to imaging.

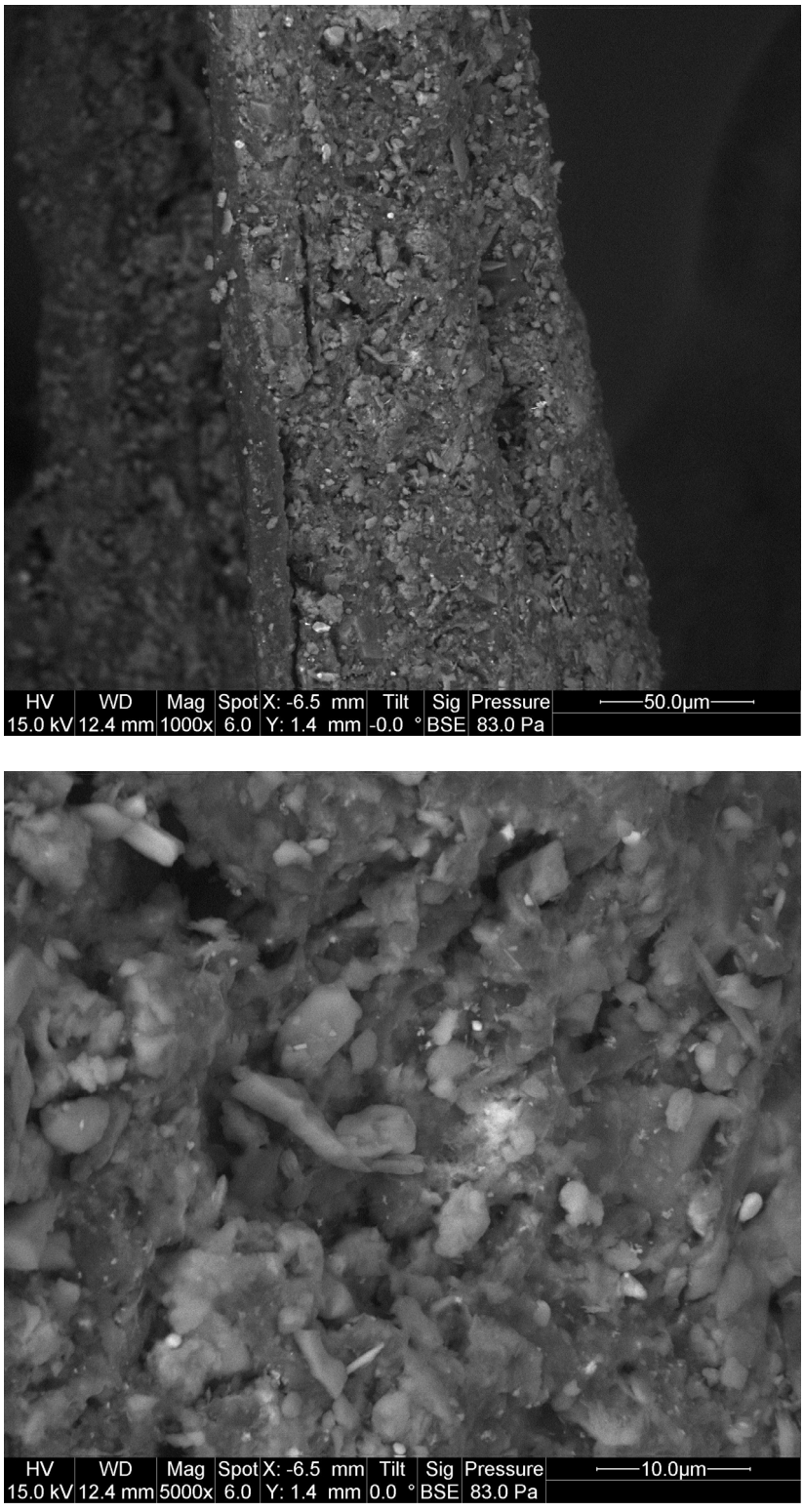

Figure F-2. Electron microscope images (2 frames) of HBM particles from an unused, "fresh" BSM + 4% WTR + HBM mixture. Media was dried at 103°C for 2 hours and sieved to between 300 and 590 µm prior to imaging.

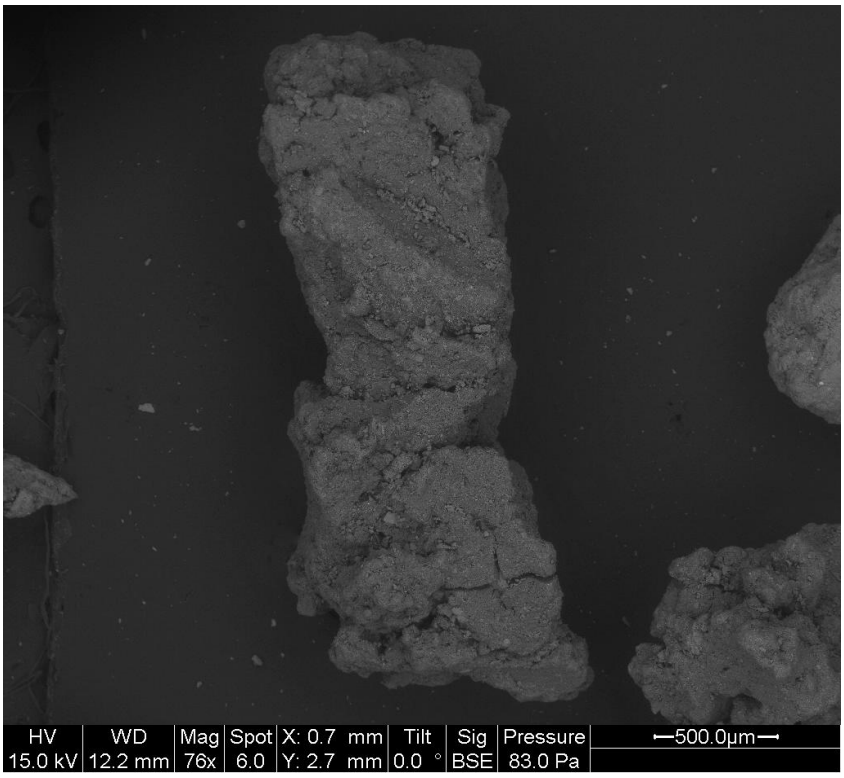
HV
15.0 kV
WD
12.2 mm
Mag
76x
Spot
6.0
X: 0.7 mm
Y: 2.7 mm
Tilt
0.0 °
Sig
BSE
Pressure
83.0 Pa
500.0µm

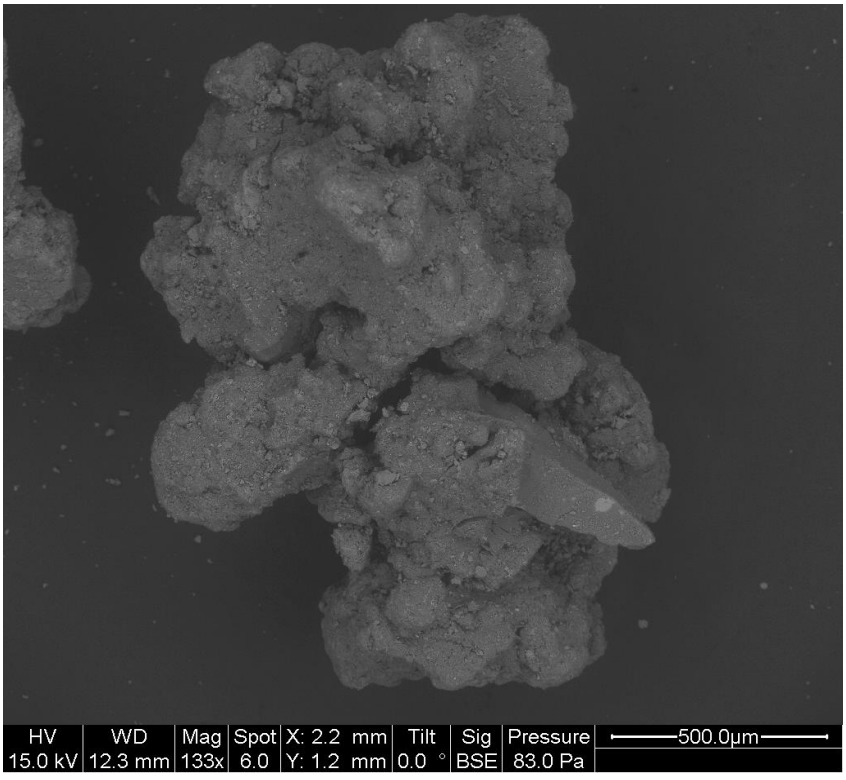
HV
15.0 kV
WD
12.3 mm
Mag
133x
Spot
6.0
X: 2.2 mm
Y: 1.2 mm
Tilt
0.0 °
Sig
BSE
Pressure
83.0 Pa
500.0µm

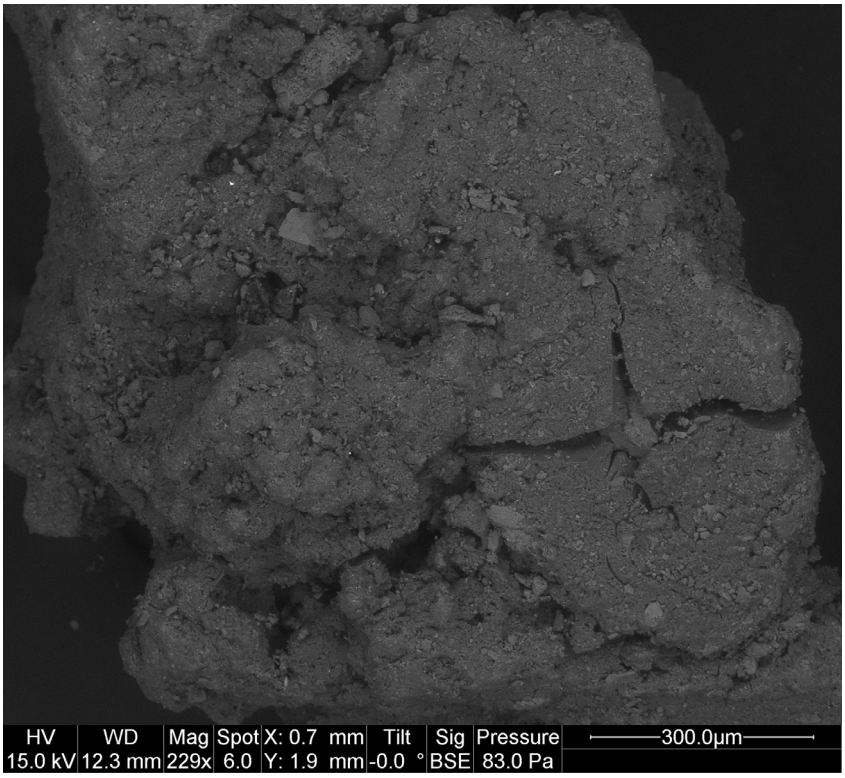
HV
15.0 kV
WD
12.3 mm
Mag
229x
Spot
6.0
X: 0.7 mm
Y: 1.9 mm
Tilt
-0.0 °
Sig
BSE
Pressure
83.0 Pa
300.0µm

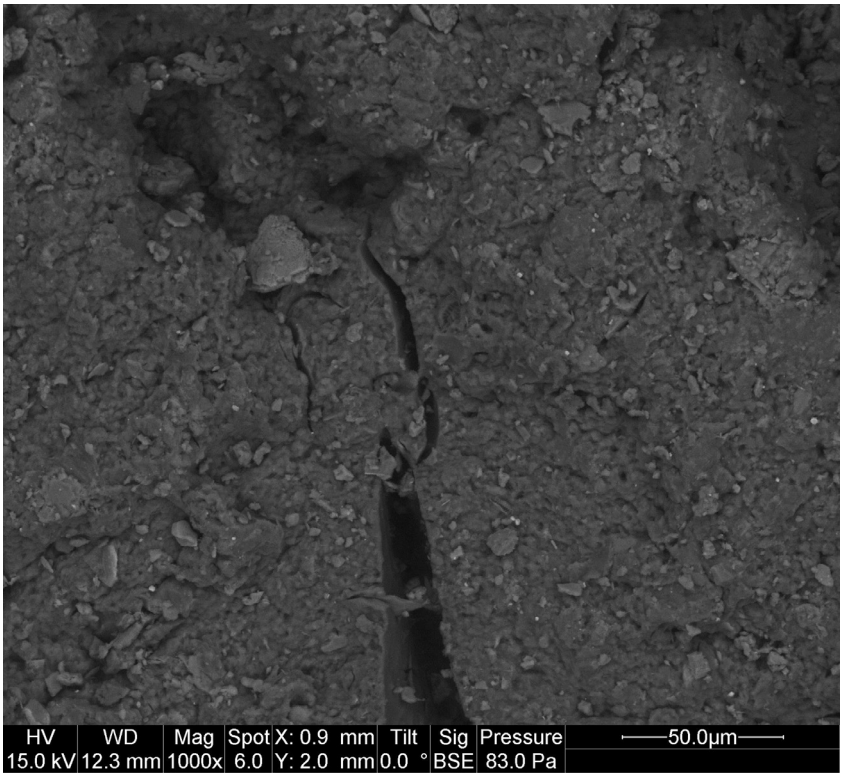
HV
15.0 kV
WD
12.3 mm
Mag
1000x
Spot
6.0
X: 0.9 mm
Y: 2.0 mm
Tilt
0.0 °
Sig
BSE
Pressure
83.0 Pa
50.0µm

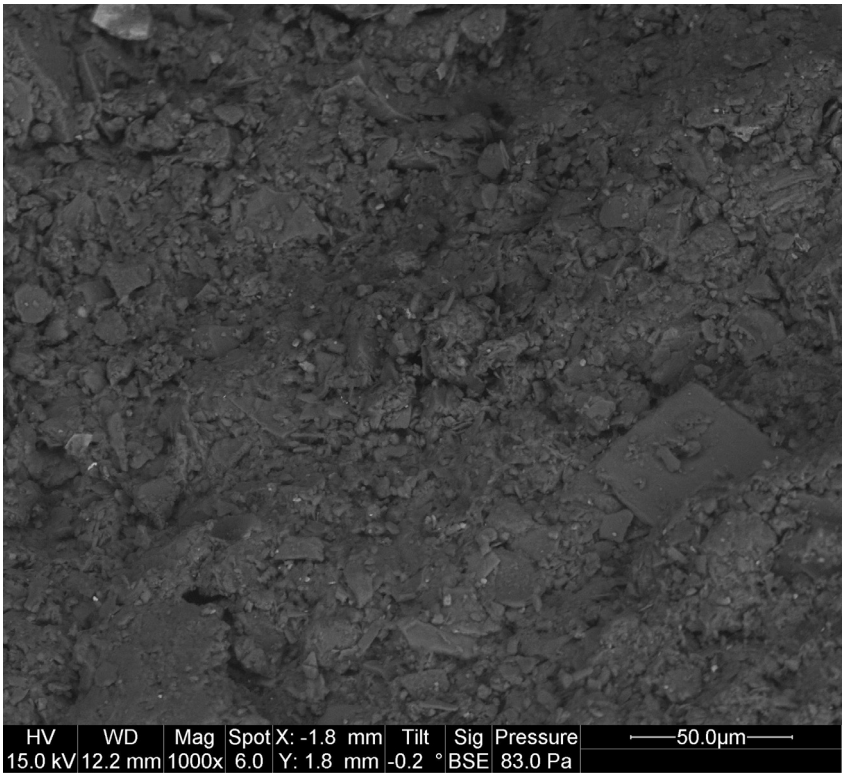
HV
15.0 kV
WD
12.2 mm
Mag
1000x
Spot
6.0
X: -1.8 mm
Y: 1.8 mm
Tilt
-0.2 °
Sig
BSE
Pressure
83.0 Pa
50.0µm

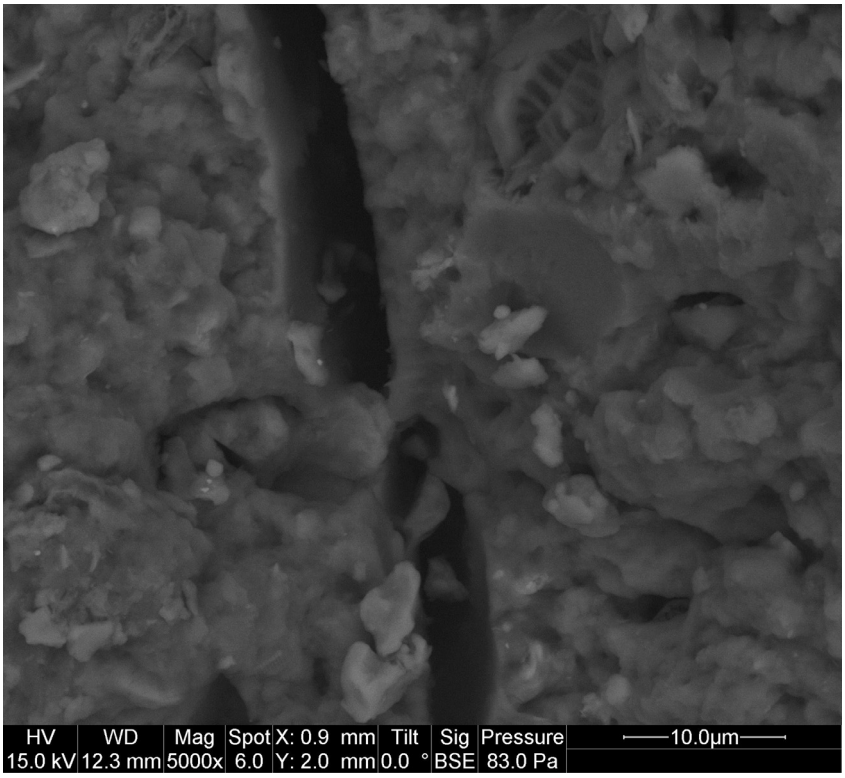
HV
15.0 kV
WD
12.3 mm
Mag
5000x
Spot
6.0
X: 0.9 mm
Y: 2.0 mm
Tilt
0.0 °
Sig
BSE
Pressure
83.0 Pa
10.0µm

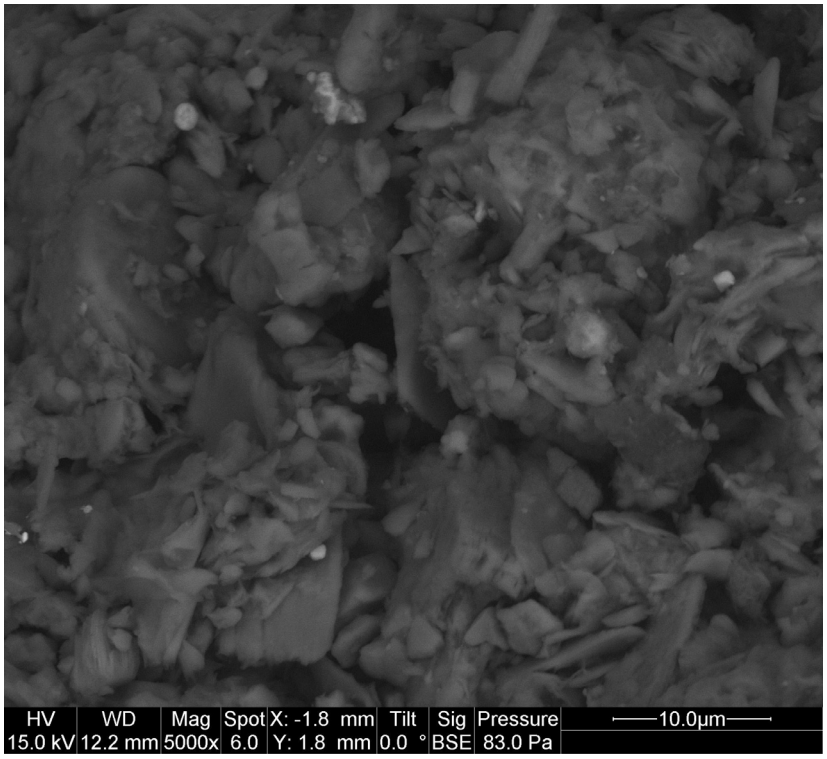

Figure F-3. Electron microscope images (7 frames) of WTR particles from an unused, "fresh" BSM + 4% WTR + HBM mixture. Media was dried at 103°C for 2 hours and sieved to between 300 and 590 µm prior to imaging.

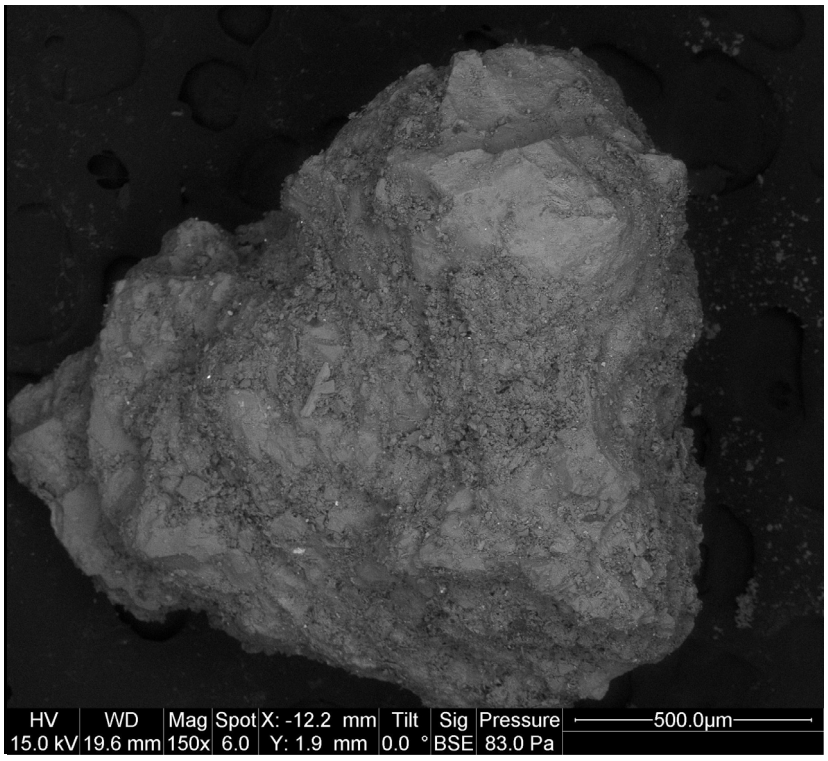

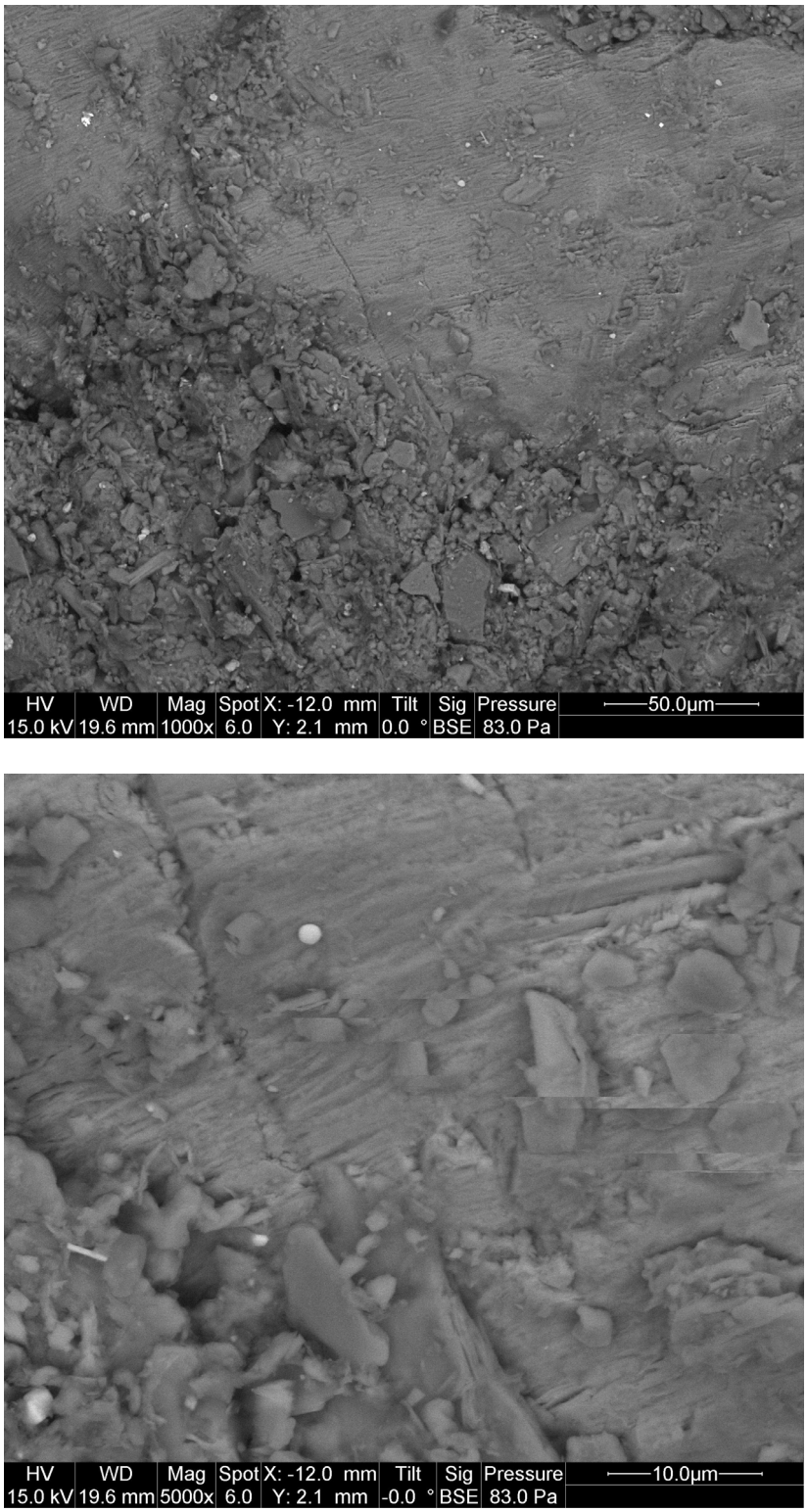

Figure F-4. Electron microscope images (3 frames) of BSM grains post-adsorption from a BSM + 4% WTR + HBM mixture subject to continuous flow. Media was dried at 103°C for 2 hours and sieved to between 300 and 590 µm prior to imaging.


HV
15.0 kV
WD
20.4 mm
Mag
97x
Spot
6.0
X: -16.2 mm
Y: 5.3 mm
Tilt
0.0 °
Sig
BSE
Pressure
83.0 Pa
500.0µm

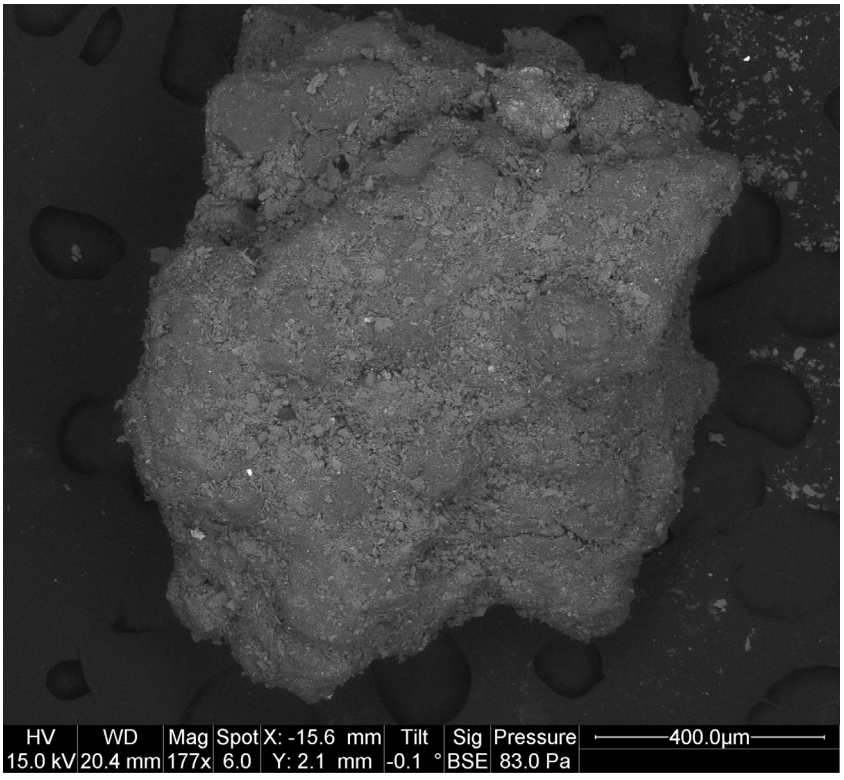
HV
15.0 kV
WD
20.4 mm
Mag
177x
Spot
6.0
X: -15.6 mm
Y: 2.1 mm
Tilt
-0.1 °
Sig
BSE
Pressure
83.0 Pa
400.0µm

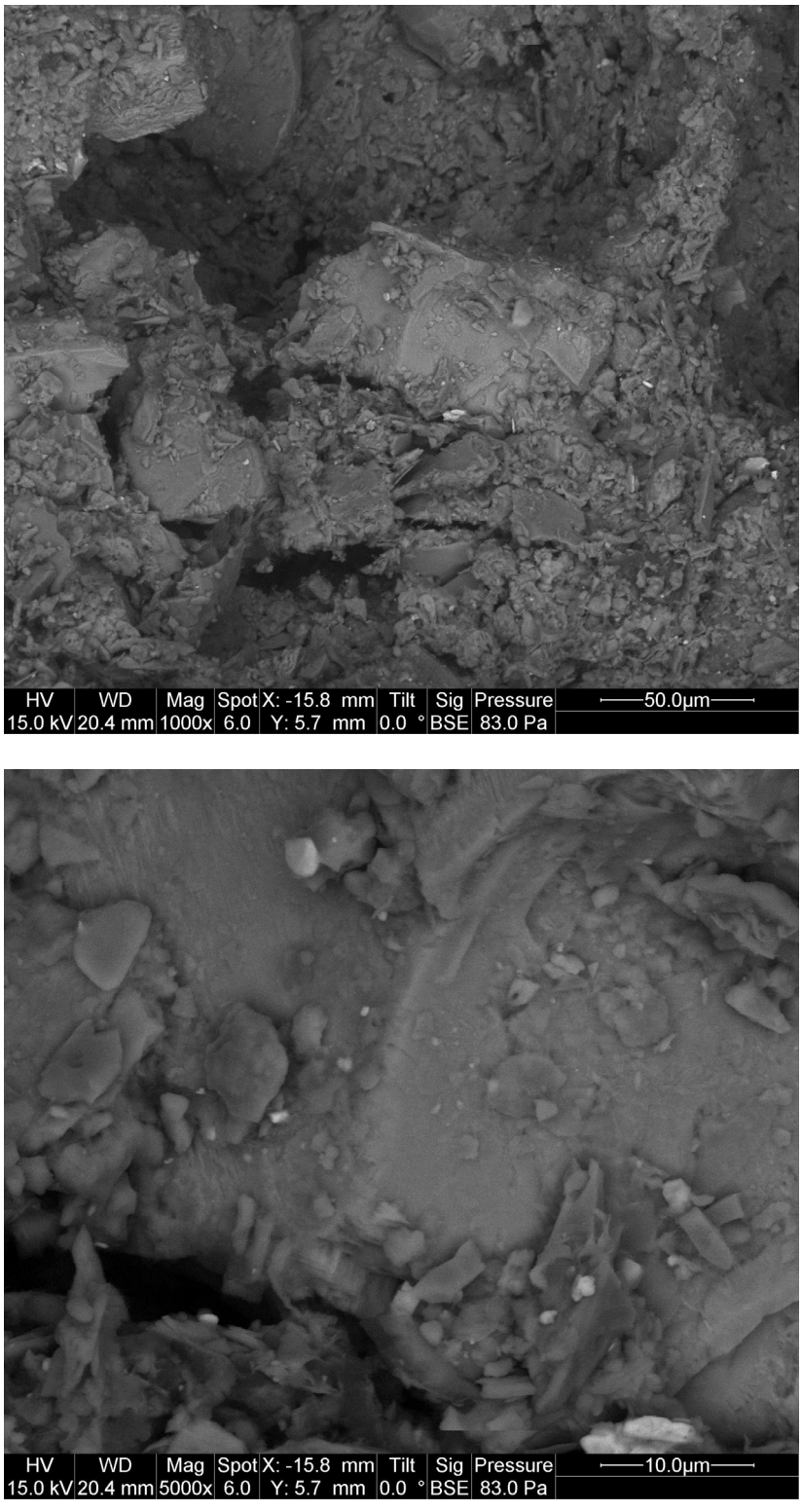

Figure F-5. Electron microscope images (4 frames) of WTR particles post-adsorption from a BSM + 4% WTR + HBM mixture subject to continuous flow. Media was dried at 103°C for 2 hours and sieved to between 300 and 590 µm prior to imaging.

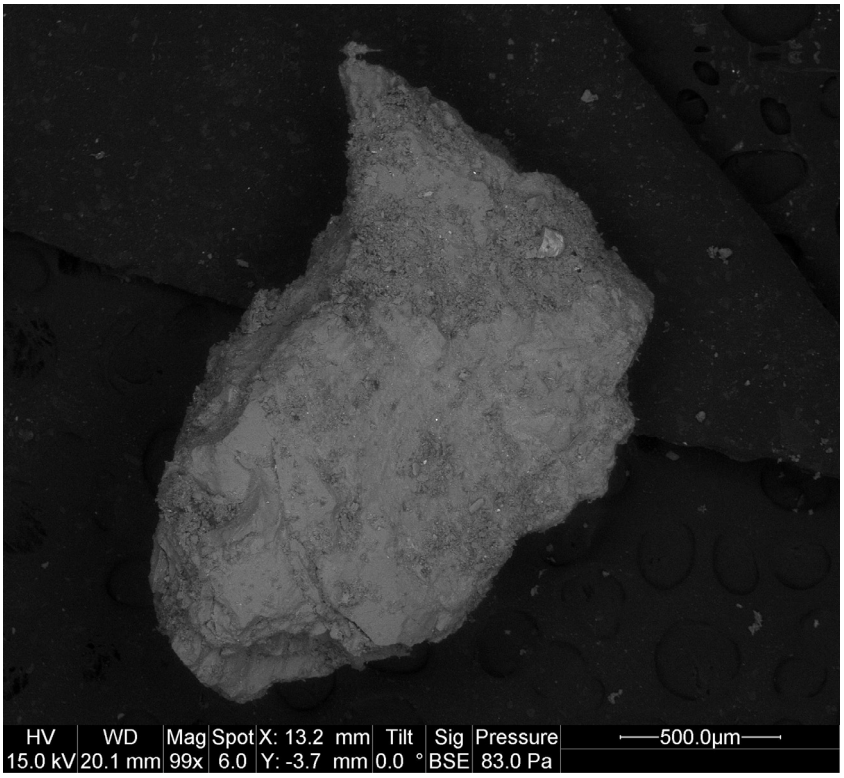
HV
15.0 kV
WD
20.1 mm
Mag
99x
Spot
6.0
X: 13.2 mm
Y: -3.7 mm
Tilt
0.0 °
Sig
BSE
Pressure
83.0 Pa
500.0µm

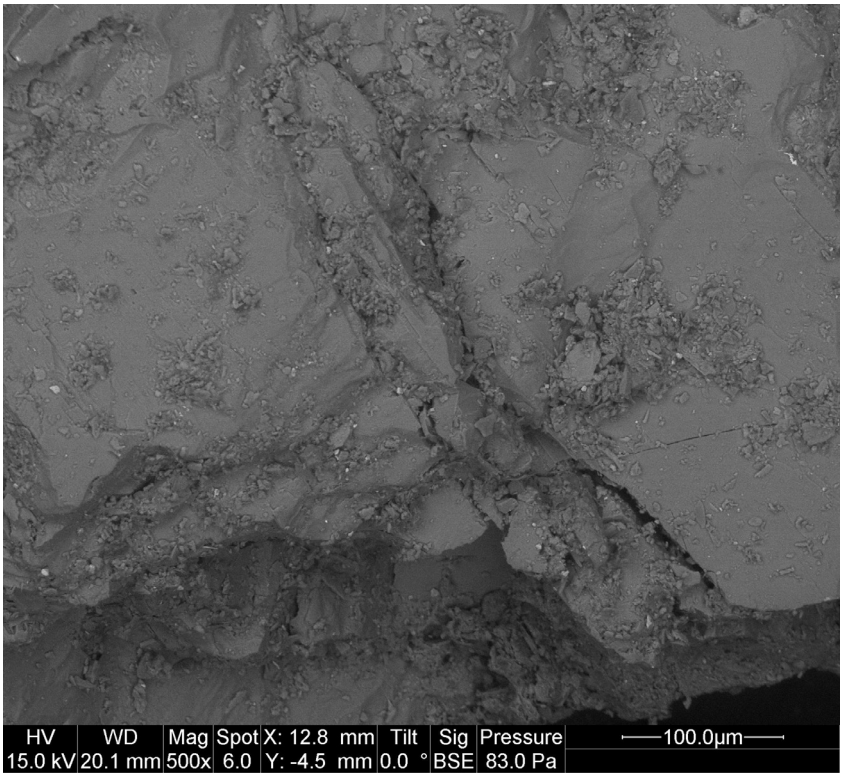
HV
15.0 kV
WD
20.1 mm
Mag
500x
Spot
6.0
X: 12.8 mm
Y: -4.5 mm
Tilt
0.0 °
Sig
BSE
Pressure
83.0 Pa
100.0µm

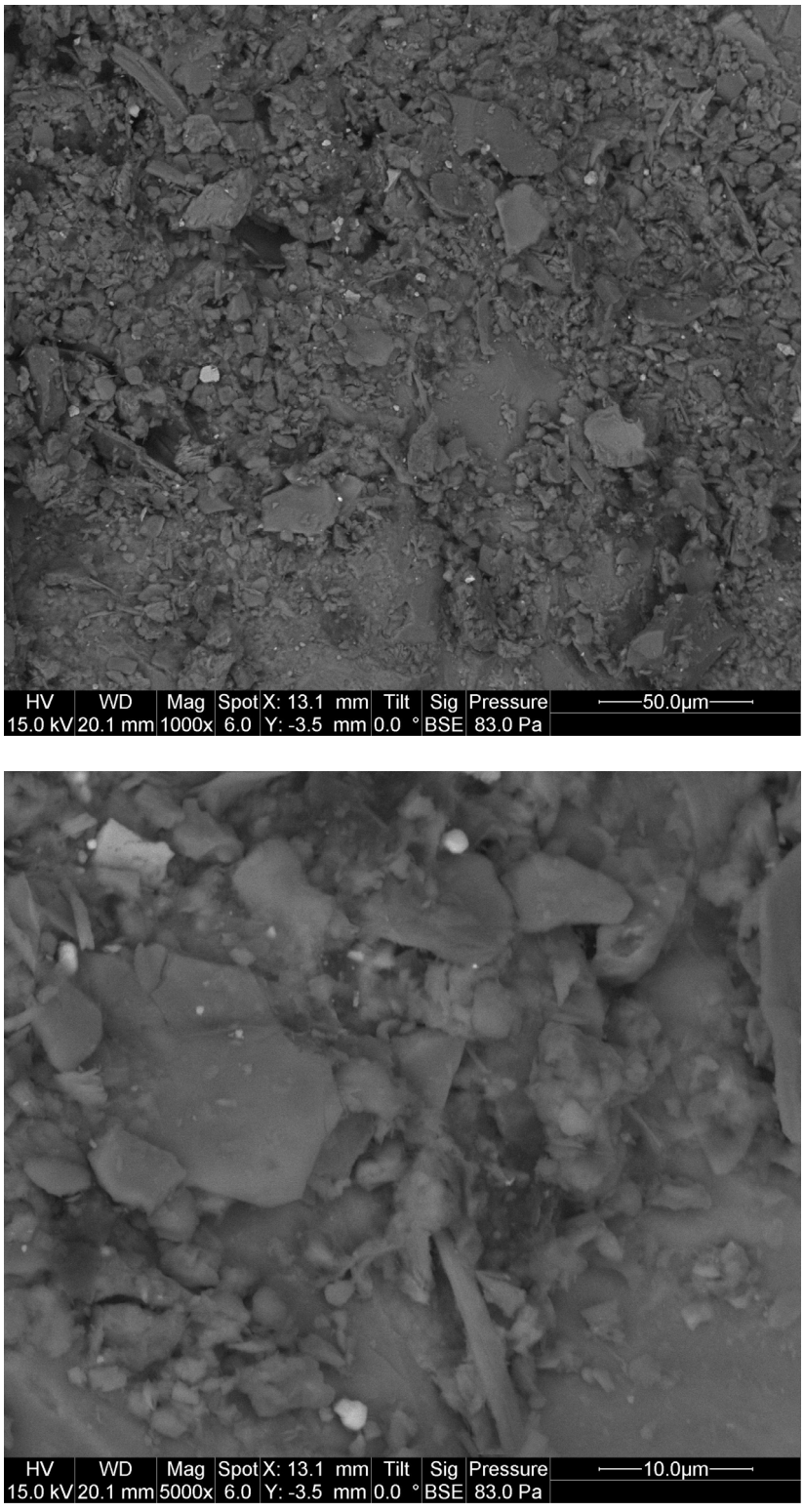

Figure F-6. Electron microscope images (4 frames) of BSM grains post-adsorption from a BSM + 4% WTR + HBM mixture subject to intermittent flow. Media was dried at 103°C for 2 hours and sieved to between 300 and 590 µm prior to imaging.

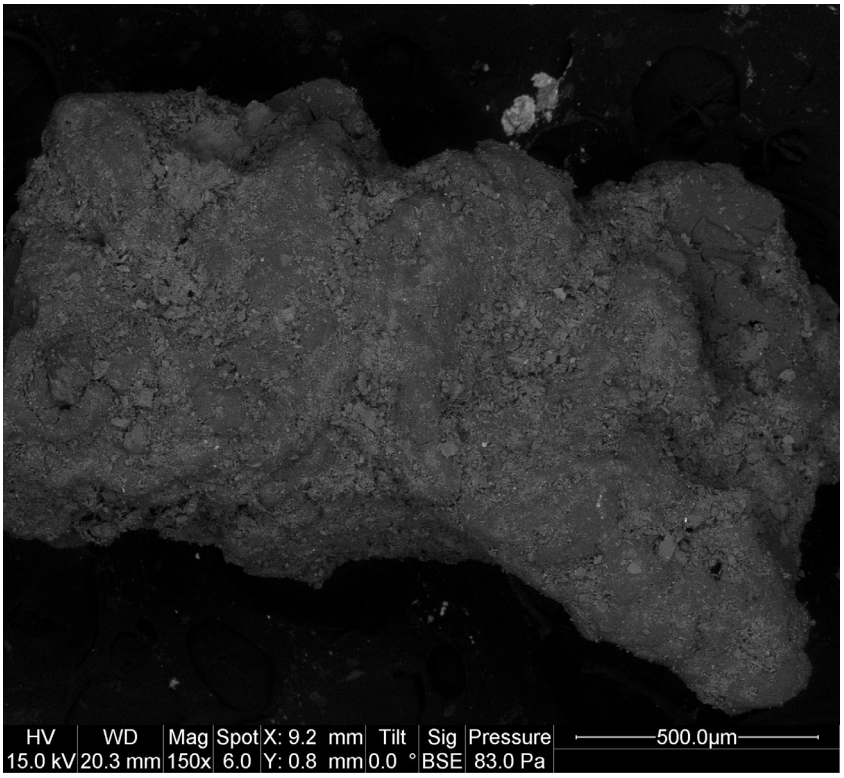
HV
15.0 kV
WD
20.3 mm
Mag
150x
Spot
6.0
X: 9.2 mm
Y: 0.8 mm
Tilt
0.0 °
Sig
BSE
Pressure
83.0 Pa
500.0µm

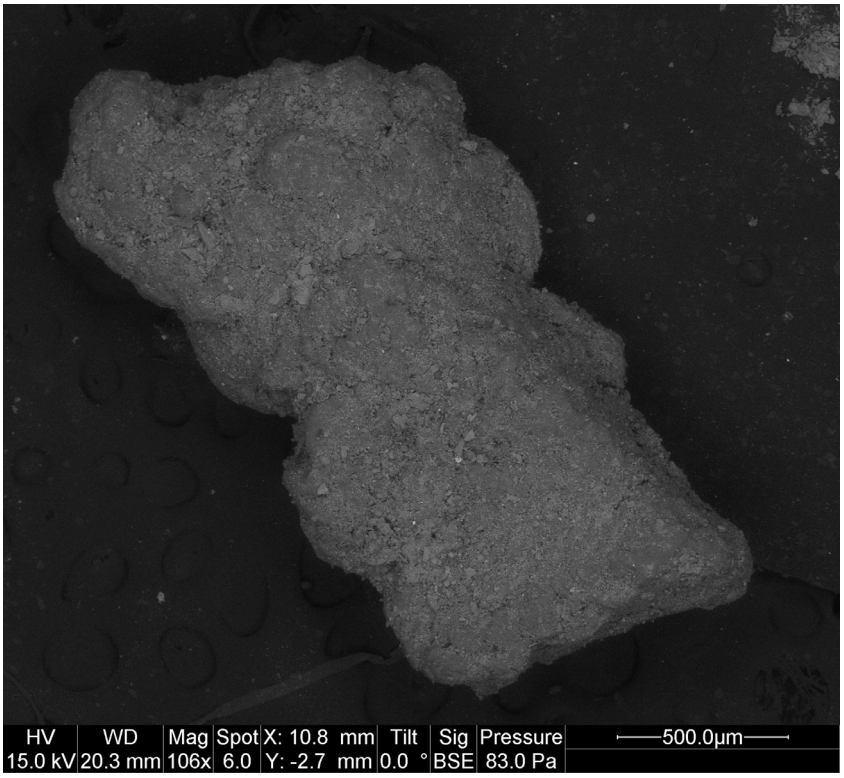
HV
15.0 kV
WD
20.3 mm
Mag
106x
Spot
6.0
X: 10.8 mm
Y: -2.7 mm
Tilt
0.0 °
Sig
BSE
Pressure
83.0 Pa
500.0µm

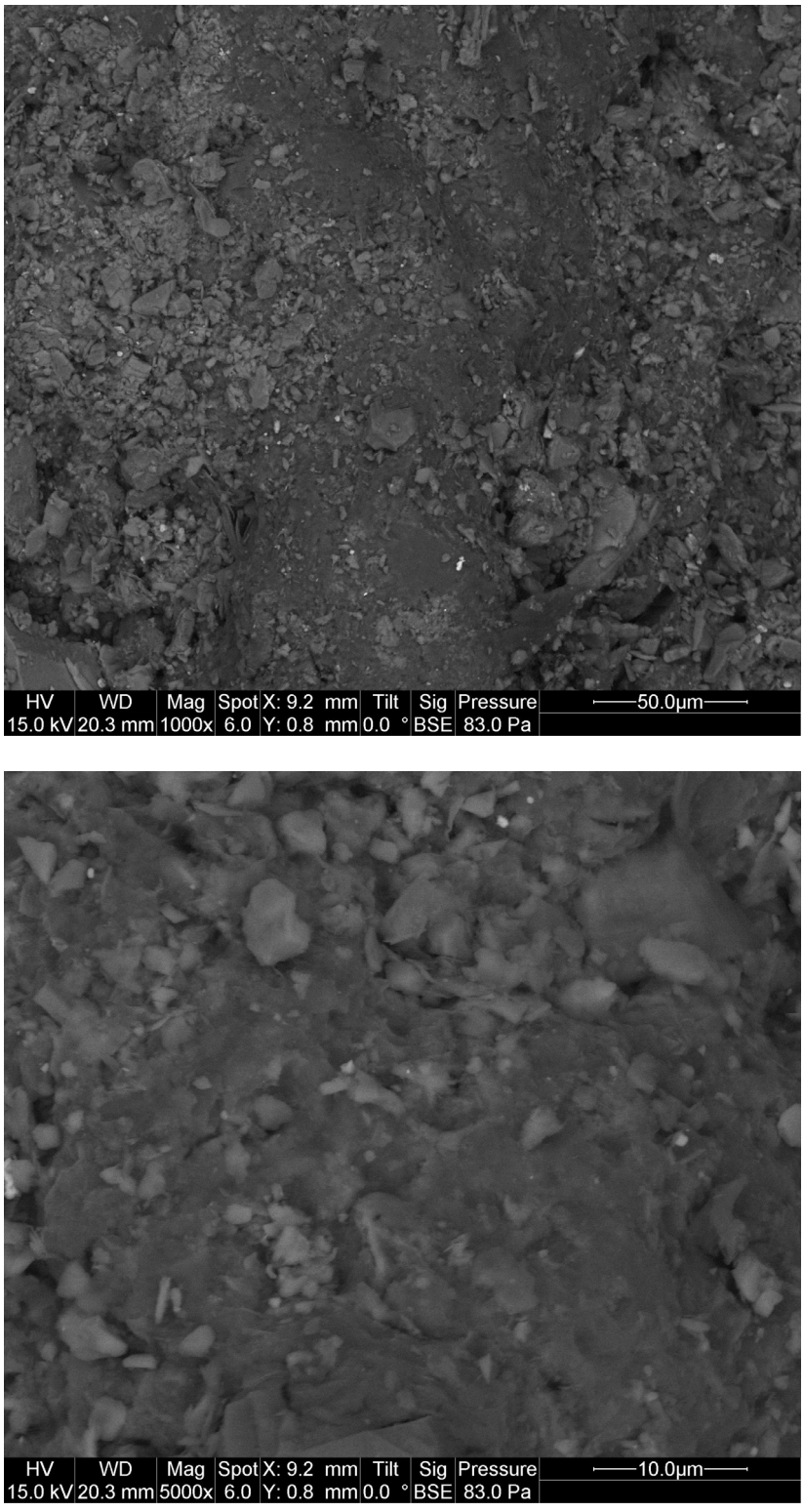

Figure F-7. Electron microscope images (4 frames) of WTR particles post-adsorption from a BSM + 4% WTR + HBM mixture subject to intermittent flow. Media was dried at 103°C for 2 hours and sieved to between 300 and 590 µm prior to imaging.

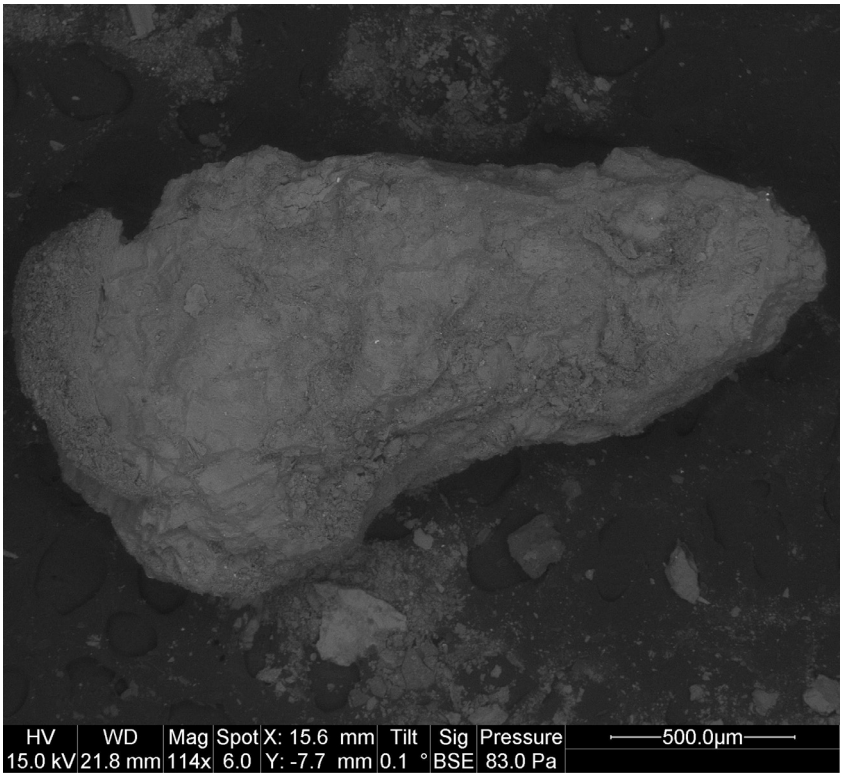
HV
15.0 kV
WD
21.8 mm
Mag
114x
Spot
6.0
X: 15.6 mm
Y: -7.7 mm
Tilt
0.1 °
Sig
BSE
Pressure
83.0 Pa
500.0µm

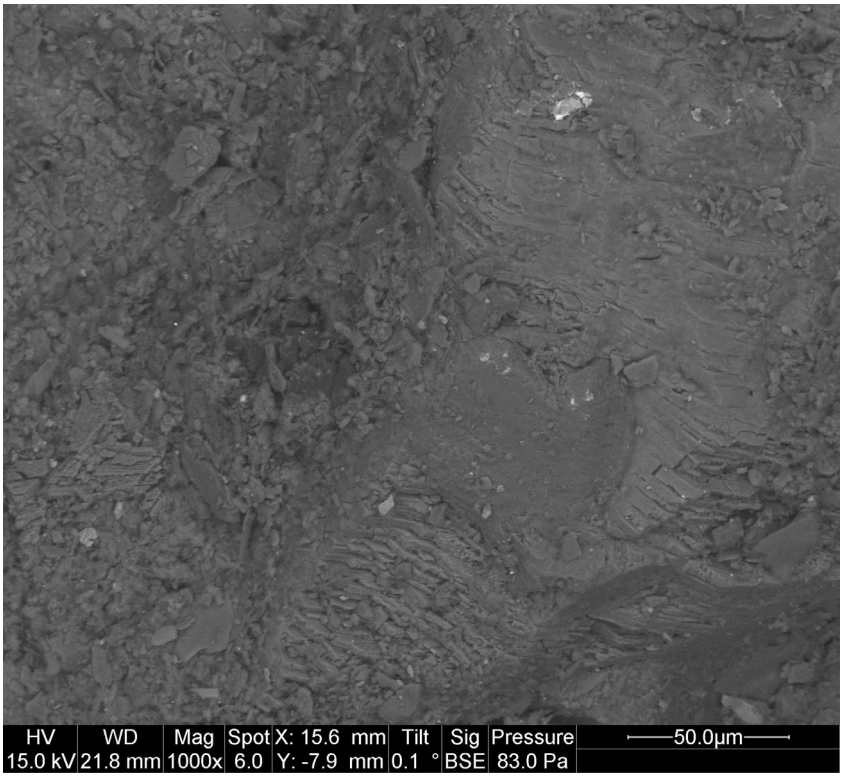
HV
15.0 kV
WD
21.8 mm
Mag
1000x
Spot
6.0
X: 15.6 mm
Y: -7.9 mm
Tilt
0.1 °
Sig
BSE
Pressure
83.0 Pa
50.0µm

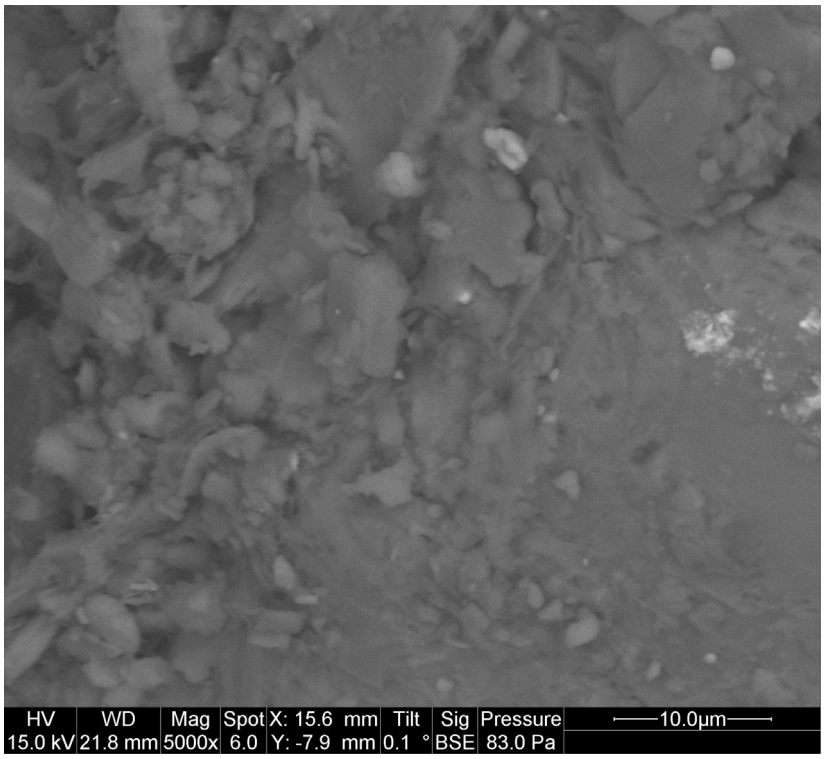

Figure F-8. Electron microscope images (3 frames) of soil grains (i.e., BSM grains) post-adsorption from a LFBSM + 4% WTR mixture subject to intermittent flow. Media was dried at 103°C for 2 hours and sieved to between 300 and 590 µm prior to imaging.

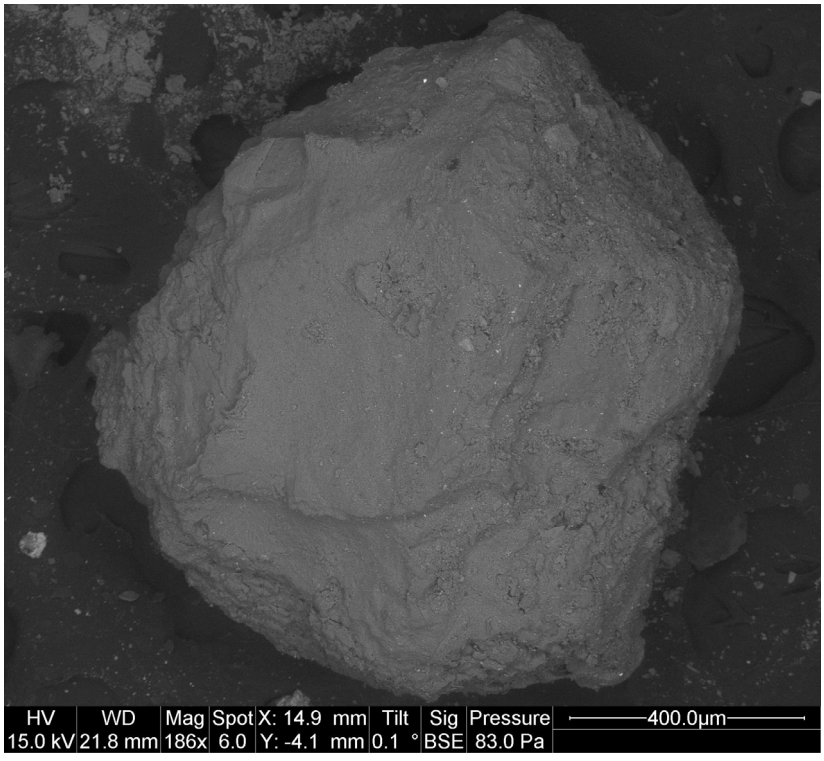

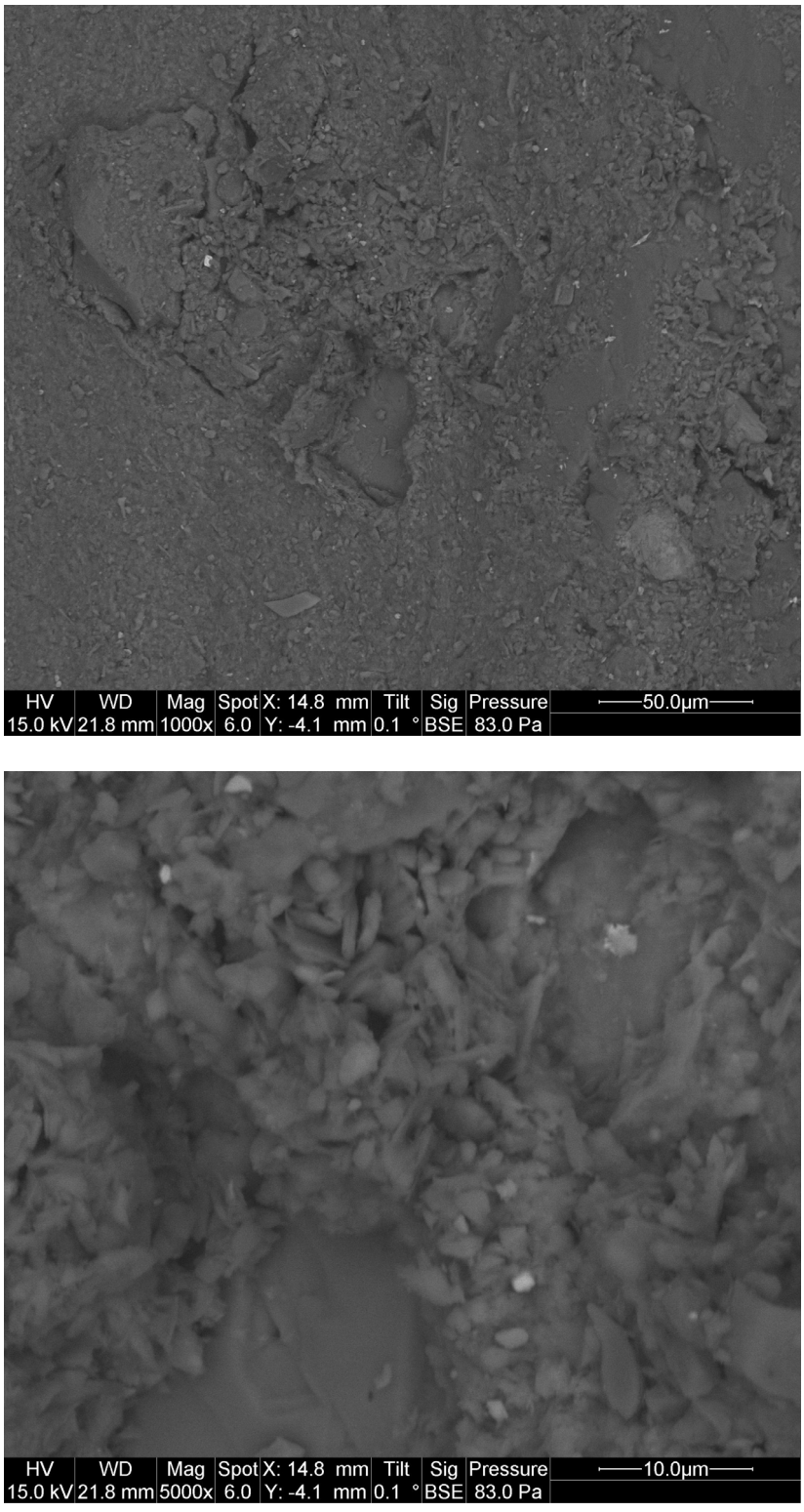

Figure F-9. Electron microscope images (3 frames) of quartz sand grains post-adsorption from a LFBSM + 4% WTR mixture subject to intermittent flow. Media was dried at 103°C for 2 hours and sieved to between 300 and 590 µm prior to imaging.

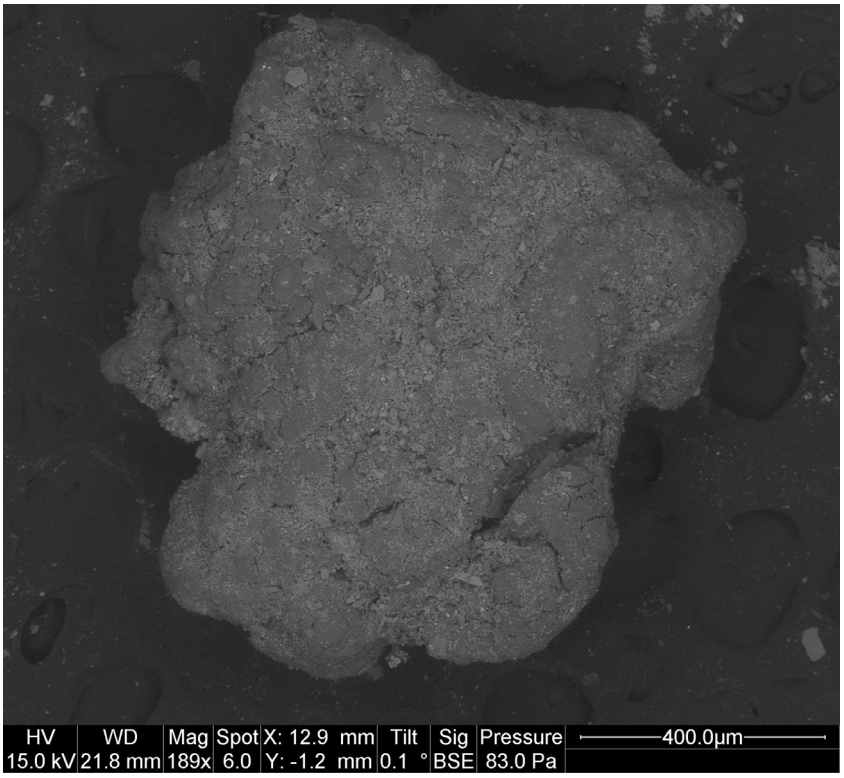
HV
15.0 kV
WD
21.8 mm
Mag
189x
Spot
6.0
X: 12.9 mm
Y: -1.2 mm
Tilt
0.1 °
Sig
BSE
Pressure
83.0 Pa
400.0µm

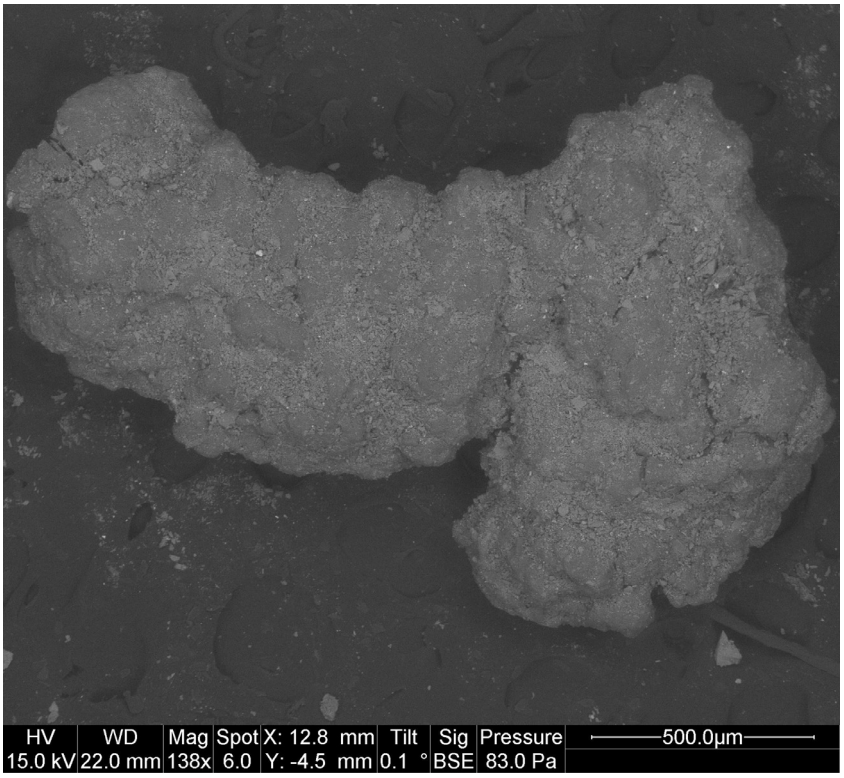
HV
15.0 kV
WD
22.0 mm
Mag
138x
Spot
6.0
X: 12.8 mm
Y: -4.5 mm
Tilt
0.1 °
Sig
BSE
Pressure
83.0 Pa
500.0µm

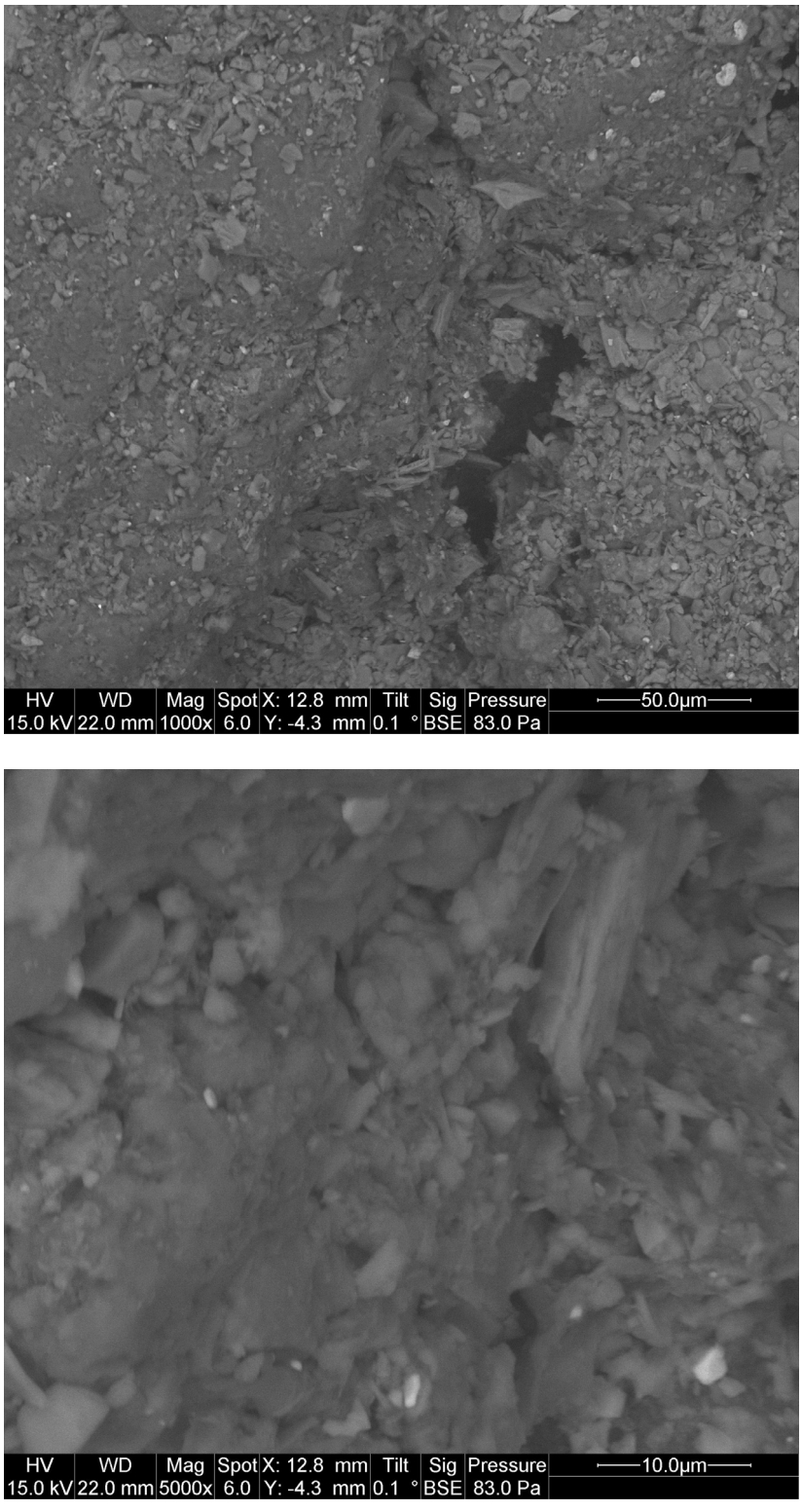

Figure F-10. Electron microscope images (4 frames) of WTR particles post-adsorption from a LFBSM + 4% WTR mixture subject to intermittent flow. Media was dried at 103°C for 2 hours and sieved to between 300 and 590 µm prior to imaging.

Citations

Agyin-Birikorang, S., O'Connor, G. A. (2007). "Lability of drinking water treatment residuals (WTR) immobilized phosphorus: Aging and pH effects." *J. Environ. Qual.*, 36, 1076-1085.

Agyin-Birikorang, S., O'Connor, G. A. (2009). "Aging effects on reactivity of an aluminum-based drinking-water treatment residual as a soil amendment" *Sci. Tot. Environ.*, 407, 826-834.

Agyin-Birikorang, S., Oladeji, O. O., O'Connor, G. A., Obreza, T. A., Capece, J. C. (2009). "Efficacy of drinking-water treatment residuals in controlling off-site phosphorus losses: A field study in Florida." *J. Environ. Qual.*, 38, 1076-1085.

American Public Health Association (APHA), American Water Works Association, Water Environment Federation. (1992). *Standard Methods for the Examination of Water and Wastewater, 18th Ed.*, Washington, DC.

Ann, Y., Reddy, K. R., Delfino, J. J. (2000). "Influence of chemical amendments on phosphorus immobilization in soils from a constructed wetland." *Ecol. Eng.*, 14, 157-167.

Antikainen, R., Haapanen, R., Rekolainen, S. (2004). "Flows of nitrogen and phosphorus in Finland – The forest industry and use of wood fuels." *J. Clean. Prod.*, 12, 191-934.

Arai, Y., Sparks, D. L. (2007). "Phosphate reaction dynamics in soils and soil components: A multiscale approach." *Adv. Agron.* 94, 135-179.

Baptista, M. S., Vasconcelos, M. T. S. D., Cabral, J. P., Freitas, M. C., Pacheco, A. M. G. (2008). "Copper, nickel, and lead in lichen and tree bark transplants over different periods of time." *Environ. Poll.*, 151, 408-413.

Beauchamp, C. J., Camire, C., Chalifour, F.-P. (2006). "Use of bark and combined paper sludge for the revegetation of bark-covered land." *J. Environ. Eng. Sci.*, 5, 253-261.

Blecken, G.-T., Zinger, Y., Deletic, A., Fletcher, T. D., Viklander, M. (2009). "Influence of intermittent wetting and drying conditions on heavy metal removal by stormwater biofilters." *Water Res.*, 43, 4590-4598.

Borggaard, O. K., Jorgensen, S. S., Moberg, J. P., Raben-Lange, B. (1990). "Influence of organic matter on phosphate adsorption by aluminium and iron oxides in sandy soils." *J. Soil Sci.*, 41, 443-449.

Borggaard, O. K., Raben-Lange, B., Gimsing, A. L., Strobel, B. W. (2005). "Influence of humic substances on phosphate adsorption by aluminum and iron oxides." *Geoderma*, 127, 270-279.

Bratieres, K., Fletcher, T. D., Deletic, A., Zinger, Y. (2008). "Nutrient and sediment removal by stormwater biofilters: A large-scale design optimisation study." *Water Res.,* 42(14), 3930-3940.

Byard, R., Lewis, K. C., Montagnini, F. (1996). "Leaf litter decomposition and mulch performance from mixed and monospecific plantations of native tree species in Costa Rica." *Agric. Ecosyst. Environ.*, 58, 145-155.

Dalal, R. C. (1977). "Soil organic phosphorus." *Adv. Agron.*, 29, 83-117.

Darke, A. K., Walbridge, M. R. (2000). "Al and Fe biogeochemistry in a floodplain forest: Implications for P retention." *Biogeochemsitry*, 51, 1-32.

Davis, A. P. (2008). "Field performance of bioretention: Hydrology impacts." *J. Hydrol. Eng.*, 13(2), 90-95.

Davis, A. P., Shokouhian, M., Sharma, H., Minami, C. (2001). "Laboratory study of biological retention for urban stormwater management." *Water Environ. Res.*, 73(5), 5-14.

Dayton, E. A., Basta, N. T. (2005). "A method for determining the phosphorus sorption capacity and amorphous aluminum of aluminum-based drinking water treatment residuals." *J. Environ. Qual.*, 34, 1112-1119.

Dietz, M. E., Clausen, J. C. (2005). "A field evaluation of rain garden flow and pollution treatment." *Water Air Soil Pollut.*, 167, 123-138.

Dietz, M. E., Clausen, J. C. (2006). "Saturation to improve pollutant retention in a rain garden." *Environ. Sci. Technol.,* 40(4), 1335-1340.

Dodds, W. K., Bouska, W. W., Eitzmann, J. L., Pilger, T. J., Pitts, K. L., Riley, A. J., Schloesser, J. T., Thornbrugh, D. J. (2009). "Eutrophication of U.S. freshwaters: Analysis of potential economic damages." *Environ. Sci. Technol.*, 43(1), 12-19.

Dolfing, J., Chardon, W. J., Japenga, J. (1999). "Association between colloidal iron, aluminum, phosphorus, and humic acids." *Soil Sci.* 164, 171-179.

Duncan, H. P. (1999). *Urban Stormwater Quality: A Statistical Overview*. Cooperative Research Centre for Catchment Hydrology, Report 99/3.

Elliott, H. A., O'Connor, G. A., Lu, P., Brinton, S. (2002). "Influence of water treatment residuals on phosphorus solubility and leaching." *J. Environ. Qual.*, 31, 1362-1369.

Gerke, J., Hermann, R. (1992). "Adsorption of orthophosphate to humic-Fe-complexes and to amorphous Fe-oxide." *Z. Pflanz. Bodenkunde.* 155, 233-236.

Goldberg, S. (1989). "Interaction of aluminum and iron oxides and clay minerals and their effect on soil physical properties: A review." *Comm. Soil Sci. Plan.* 20, 1181-1207.

Goldberg, S., Sposito, G. (1985). "On the mechanism of specific phosphate adsorption by hydroxylated mineral surfaces: A review." *Commun. Soil Sci. Plan.*, 16(8), 801-821.

Gressel, N., McColl, J. G., Preston, C. M., Newman, R. H., Powers, R. F. (1996). "Linkages between phosphorus transformations and carbon decomposition in a forest soil." *Biogeochemistry*, 33, 97-123

Guan, X.-H., Shang, C., Chen, G.-H. (2006). "Competitive adsorption of organic matter with phosphate on aluminum hydroxide." *J. Colloid Interface Sci.*, 296, 51-58.

Guppy, C. N., Menzies, N. W., Moody, P. W., Blamey, F. P. C. (2005). "Competitive sorption reactions between phosphorus and organic matter in soil: a review." *Aust. J. Soil Res.* 43, 189-202.

Hatt, B. E., Fletcher, T. D., Deletic, A. (2009). "Pollutant removal performance of field-scale stormwater biofiltration systems." *Water Sci. Technol.* 59, 1567-1576.

Hens, M., Merckx, R. (2001). "Functional characterization of colloidal phosphorus species in the soil solution of sandy soils." *Environ. Sci. Technol.* 35, 493-500.

Hsieh, C. H., Davis, A. P. (2005). "Evaluation and optimization of bioretention media for treatment of urban storm water runoff." *J. Environ. Eng.*, 131(11), 1521-1531.

Hsieh, C. H., Davis, A. P., Needelman, B. A. (2007a). "Bioretention column studies of phosphorus removal from urban stormwater runoff." *Water Environ. Res.,* 79(2), 177-184.

Hsieh, C. H., Davis, A. P., Needelman, B. A. (2007b). "Nitrogen removal from urban stormwater runoff through layered bioretention columns." *Water Environ. Res.,* 79(12), 2404-2411.

Hunt, W. F., Jarrett, A. R., Smith, J. T., Sharkey, L. J. (2006). "Evaluating bioretention hydrology and nutrient removal at three field sites in North Carolina." *J. Irrig. Drain. Eng*., 132(6), 600-608.

Kang, J., Hesterberg, D., Osmond, D. L. (2009). "Soil organic matter effects on phosphorus sorption: A path analysis." *Soil Sci. Soc. Am. J.*, 73(2), 360-366.

Kim, H., Seagren, E.A., Davis, A.P. (2003). "Engineered bioretention for removal of nitrate from stormwater runoff." *Water Environ. Res.*, 75, 355-367.

Kleinman, P. J. A., Bryant, R. B., Reid, W. S., Sharpley, A. N. (2000). "Using soil phosphorus behavior to identify environmental thresholds." *Soil Sci.* 165, 943-950.

Kovar, J. L., Pierzynski, G.M., eds. (2009). "Methods of phosphorus analysis for soils, sediments, residuals, and waters." Southern Cooperative Series Bulletin 408, Southern Extension–Research Activity–17 (SERA 17). <http://www.sera17.ext.vt.edu/Documents/P_Methods2ndEdition2009.pdf>

Kreeb, L. B. (2003). "Hydrologic efficiency and design sensitivity of bioretention facilities." Honors Research Thesis, Univ. of Maryland, College Park, Md.

Lambert, J.-F. (2008). "Adsorption and polymerization of amino acids on mineral surfaces: A review." *Orig. Life Evol. Biosph.* 38, 211-242.

Li, H., Davis, A. P. (2008a). "Heavy metal capture and accumulation in bioretention media." *Environ. Sci. Technol.*, 42(14), 5247-5253.

Li, H., Davis, A. P. (2008b). "Urban particle capture in bioretention media. I: Laboratory and field studies." *J. Environ. Eng.*, 134(6), 409-418.

Li, H., Davis, A. (2009). "Water quality improvement through reductions of pollutant loads using bioretention." *J. Environ. Eng.* 135, 567-576.

Lijklema, L. (1980). "Interaction of orthophosphate with iron(III) and aluminum hydroxides." *Env. Sci. Technol.*, 14(5), 537-541.

Lombi, E., Stevens, D. P., McLaughlin, M. J. (2010). "Effect of water treatment residuals on soil phosphorus, copper, and aluminum availability and toxicity." *Environ. Poll.* 158, 2110-2116.

Lucas, W. C., Greenway, M. (2007). "Nutrient retention in vegetated and nonvegetated bioretention mesocosms." *J. Irrig. Drain. Eng.*, 134(5), 613-623.

Maestre, A., Pitt, R. (2005). "The national stormwater quality database, ver. 1.1: A compilation and analysis of NPDES stormwater monitoring information." Accessed 14 June, 2010. <http://unix.eng.ua.edu/~rpitt/Research/ms4/Paper/Mainms4paper.html>

Mahdy, A. M., Elkhatib, E. A., Fathi, N. O., Lin, Z.-Q. (2009). "Effects of co-application of biosolids and water treatment residuals on corn growth and bioavailable phosphorus and aluminum in alkaline soils in Egypt." *J. Environ. Qual.*, 38, 1501-1510.

Makris, K. C., El-Shall, H., Harris, W. G., O'Connor, G. A., Obreza, T. A. (2004). "Intraparticle phosphorus diffusion in a drinking water treatment residual at room temperature." *J. Colloid Interface Sci.*, 277, 417-423.

Maryland Department of the Environment (MDE). 2000. *Stormwater Design Manual: Volumes I and II*, Baltimore, MD.

McGechan, M. B., Lewis, D. R. (2002). "Sorption of phosphorus by soil, part 1: Principles, equations, and models." *Biosyst. Eng.*, 82, 1-24.

McGill, W. B., Cole, C. V. (1981). "Comparative aspects of cycling of organic C, N, and P through soil organic matter." *Geoderma*, 26(4), 267-286.

McKeague, J. A., Day, J.H. (1966). "Dithionite- and oxalate-extractable Fe and Al as aids in differentiating various classes of soils." *Can. J. Soil Sci.*, 46, 13-22.

McKeague, J. A., Day, J.H. (1993). "Ammonium oxalate extraction of amorphous iron and aluminum." p. 241. In M.R. Carter (ed.) Soil sampling and methods of analysis. Lewis Publ., Boca Raton, FL.

Metropolitan Washington Council of Governments (MWCOG). (1983). *Pollutant removal capability of urban best management practices in the Washington Metropolitan Area: Final report*, Washington, DC.

Murphy, J., Riley, J. P. (1962). "A modified single solution method for the determination of phosphate in natural water." *Anal. Chim. Acta*, 27, 31-36.

Nair, P. S., Logan, T. J., Sharpley, A. N., Sommers, L. E., Tabatabai, M. A., Yuan, T. L. (1984). Ínterlaboratory comparison of a standardized phosphorus adsorption procedure." *J. Environ. Qual.*, 13(4), 591-595.

Oladeji, O. O., O'Connor, G. A., Sartain, J. B., Nair, V. D. (2007). "Controlled application rate of water treatment residual for agronomic and environmental benefits." *J. Environ. Qual.*, 36, 1715-1724.

Oladeji, O. O., Sartain, J. B., O'Connor, G. A. (2009). "Land application of aluminum water treatment residual: Aluminum phytoavailability and forage yield." *Comm. Soil Sci. Plan.*, 40, 1483-1498.

Read, J., Wevill, T., Fletcher, T. D., Deletic, A. (2008). "Variation among plant species in pollutant removal from stormwater in biofiltration systems." *Water Res.,* 42, 893-902.

Saarela, K.-E., Harju, L., Rajander, J., Lill, J.-O., Heselius, S.-J., Lindroos, A., Mattsson, K. (2005). "Elemental analysis of pine bark and wood in an environmental study." *Sci. Tot. Environ.*, 343, 231-241.

Sardans, J., Penuelas, J., Ogaya, R. (2008). "Drought-induced changes in C and N stoichiometry in a *Quercus ilex* Mediterranean forest." *For. Sci.*, 54(5), 513-517.

Saunders, W. M. H. (1965). "Phosphate retention by New Zealand soils and its relationship to free sesquioxides, organic matter, and other soil properties." *New Zeal. J. Agr. Res.*, 8, 30-57.

Schindler, D.W., Hecky, R. E., Findlay, D. L., Stainton, M. P., Parker, B. R., Paterson, M. J., Beaty, K. G., Lyng, M., Kasian, S. E. M. (2008). "Eutrophication of lakes cannot be controlled by reducing nitrogen input: Results of a 37-year whole-ecosystem experiment." *P. Natl. Acad. Sci. USA*, 105(32), 11254–11258.

Sharpley, A. N., Daniel, T., Sims, T., Lemunyon, J., Stevens, R., Parry, R. (2003). *Agricultural Phosphorus and Eutrophication, 2nd Edition,* United States Department of Agriculture, Agricultural Research Service, ARS-149, University Park, PA.

Sinha, M. K. (1971). "Organo-metallic phosphates I. Interaction of phosphorus compounds with humic substances." *Plant Soil*. 35, 471-484.

Smolders, A. J. P., Lucassen, E. C. H. E. T., Bobbink, R., Roelofs, J. G. M., Lamers, L. P. M. (2010). "How nitrate leaching from agricultural lands provokes phosphate eutrophication in groundwater fed wetlands: The sulfur bridge." *Biogeochemistry*, 98, 1-7.

Sotero-Santos, R. B., Rocha, O., Povinelli, J. (2005). "Evaluation of water treatment sludges toxicity using the *Daphnia* bioassay." *Water Res.*, 39, 3909-3917.

Sposito, G., Skipper, N. T., Sutton, R., Park, S.-H., Soper, A. K., Greathouse, J. A. (1999). "Surface geochemistry of the clay minerals." *P. Natl. Acad. Sci. USA*. 96, 3358-3364.

Stumm, W., Morgan, J. J. (1996). *Aquatic Chemistry: Chemical Equilibria and Rates in Natural Waters*, John Wiley and Sons, Inc., New York, NY.

Styles, D., Coxon, C. (2006). "Laboratory drying of organic-matter rich soils: Phosphorus solubility effects, influence of soil characteristics, and consequences for environmental interpretation." *Geoderma*, 136, 120-135.

U.S. Environmental Protection Agency (US EPA). (1983). *Results of the Nationwide Urban Runoff Program: Volume 1 - Final Report*, Washington, DC.

U.S. Environmental Protection Agency (US EPA). (1986). *Quality Criteria for Water*, 440/5-86-001, Washington, DC.

Wolf, A. M., Baker, D. E. (1990). "Colorimetric method for phosphorus measurement in ammonium oxalate soil extracts." *Commun. Soil Sci. Plan.*, 21(19/20), 2257-2263.

Worsfold, P. J., Gimbert, L. J., Mankasingh, U., Omaka, O. N., Hanrahan, G., Gardolinski, P. C. F. C., Haygarth, P. M., Turner, B. L., Keith-Roach, M. J., McKelvie, I. D. (2005). "Sampling, sample treatment and quality assurance issues for the determination of phosphorus species in natural waters and soils." *Talanta*, 66, 273-293.

Yang, Y., Zhao, Y. Q., Babatunde, A. O., Wang, L., Ren, Y. X., Han, Y. (2006). "Characteristics and mechanisms of phosphate adsorption on dewatered alum sludge." *Sep. Purif. Technol.*, 51, 193-200.

Yang, Y., Zhao, Y. Q., Kearney, P. (2008). "Influence of ageing on the structure and phosphate adsorption capacity of dewatered alum sludge." *Chem. Eng. J*, 145, 276-284.

Yarie, J., Van Cleve, K. (1996). "Effects of carbon, fertilizer, and drought on foliar chemistry of tree species in interior Alaska." *Ecol. Appl.*, 6(3), 815-827.

Zhang, W., Brown, G. O., Storm, D. E., Zhang, H. (2008). "Fly-ash-amended sand as filter media in bioretention cells to improve phosphorus removal." *Water Environ. Res.*, 80(6), 507-516.

Zhao, X., Zhong, X., Bao, H., Li, H., Li, G., Tuo, D., Lin, Q., Brookes, P. C. (2007). "Relating soil P concentrations at which P movement occurs to soil properties in Chinese agricultural soils." *Geoderma*, 142, 237-244.

Zinger, Y., Deletic, A., Fletcher, T.D. (2007). "The effect of various intermittent dry–wet cycles on nitrogen removal capacity in biofilter systems." Rainwater & Urban Design, Sydney, NSW, Australia.